Hster

Digital Seismic Data Acquisition and Processing as Applied to Seismic Networks in the Rio Grande Rift and on Mount Erebus, Antarctica

Michael Skov
Department of Geoscience
New Mexico Institute of Mining and Technology
Socorro, NM 87801

Submitted in partial fulfillment of the requirements for the Degree, Master of Science in Geophysics from the Department of Geoscience, New Mexico Institute of Mining and technology.

January 7, 1994

Abstract

The recent creation of digital data acquisition systems for the Socorro and Mount Erebus seismic networks is an important development. While both networks were digitally recorded in the past, these installations are the first permanent digital recording systems used by either of the seismic networks. Digital data from these systems will help resolve subsurface structures in Mount Erebus and within the Rio Grande Rift.

While the digital acquisition systems are too young to have recorded the volume of data necessary to yield new scientific results, the systems have been operated long enough to provide information about their operational characteristics. This document is intended to provide a first examination of the behavior of the IASPEI seismic data logger and to provide operational information.

The data logging systems make use of MS-DOS based personal computers and Sun UNIX workstations. The operational information in this document was written to provide the information necessary to successfully operate the systems, however, familiarity with both MS-DOS and UNIX is assumed.

Table of Contents

Introduction

The availability of personal computer based, triggered seismic data loggers has greatly enhanced the ability to quickly and inexpensively install digital event recorders. One such system is based on a software package assembled by W. H. K. Lee and D. Tottingham for the International Association of Seismology and Physics of the Earth's Interior (IASPEI)(Lee, 1992b). The system uses low-cost, commercially available hardware and can be installed for just a few thousand dollars.

Cost is clearly not the only issue; successful operation is the most important result. Two IASPEI systems have been installed in conjunction with research projects currently underway by New Mexico Institute of Mining and Technology researchers. One system is currently monitoring local and teleseismic signals near Socorro, New Mexico, the second system is recording seismic activity associated with Mount Erebus, an active volcano on Ross Island, Antarctica.

The Socorro seismic network currently consists of seven vertical-component seismometers located in the Rio Grande Rift. The current network was installed between August 1982 and February 1983, (Sanford, personal communication, 1993) with the data logger added in 1991. Data is recorded both by the PC digital data logger and on paper records.

Seismic events in the Socorro region are remarkable in their relatively common inclusion of reflected phases (Sanford et. al., 1977; Hartse, 1991;

Balch, 1992). These phases are the result of interactions between propagating seismic waves and a thin magma body located approximately 19km beneath the surface of the central rift. Such phases are best observed in small events, $M_d \lesssim 1.0$ (Sanford, personal communication, 1993) hence it is important that a local event data logger consistently record weak events in this region.

Mount Erebus has long been an important site for seismic monitoring. Seismometers were first deployed on Mount Erebus in 1973 (Kyle et al., 1982). The current Erebus seismic network was installed during the 1980-81 field season (Rowe and Kienle, 1986) during a multi-national effort known as the International Mount Erebus Seismic Study (IMESS). Seismic data from the current network was originally telemetered to Scott Base (New Zealand) where it was continuously recorded by a frequency modulated, multi-track tape recorder. During the 1992-93 field season, the radio receivers were moved to McMurdo Station (U.S.) and the tape recorder was replaced by an IASPEI event recorder. (Skov and Kyle, 1993)

An excellent opportunity to examine the operational behavior of the IASPEI system was provided by the installation of the two systems into environments which have been studied using data gathered by other recording devices. Essential questions include: Does the system reliably record the data required for the scientific investigation? Does the system efficiently reject noise? How adaptable is the system to changing requirements? Can the system be operated with only a minimum of human intervention?

Acquisition alone does not necessarily yield a useful system. The acquired data must be transferred to a computing facility and converted into a format suitable for assessment and analysis. The process of preparing the data for analysis varies depending on the characteristics of the seismic network. The Socorro network requires little more than a relatively simple transfer of data

from the PC data logger to a UNIX workstation. Once moved to the workstation, the data is converted to the Lamont ah (adhoc) file format. The data is then displayed on screen, providing the user with the opportunity to categorize the event, or to delete false and/or unwanted triggers.

Because of its remote location, the Erebus system requires much more effort. The ability to transfer data via internet from McMurdo Station to the United States became possible in December, 1992 when the STARS communication system went online. Using the STARS system, the data can be transmitted to the U.S. on a daily basis. Once in Socorro, the data is handled in a manner similar to that from the Socorro Network.

Finally, at least some rudimentary analysis, for monitoring the gross features of the seismicity and evaluating the health of the network, should occur before the data is archived. P and S picks can be made from the currently available data formats using **xpick** software from the Seismology Lab of the Geophysical Institute, University of Alaska, Fairbanks. During the course of this study, **xpick** was also modified to interact with the hypocenter location program, **seismos** (Hartse, 1991). Using this system, preliminary Socorro network hypocenter locations may be obtained and archived with the seismic data. An accurate velocity model for Mount Erebus suitable for use with **seismos** has not yet been determined, thus no Erebus hypocenters have yet been determined through this interface since the digital data logger was installed.

The IASPEI Seismic Data Logger

The IASPEI seismic data logger is a compilation of software tools assembled into a library known as the International Association of Seismology and Physics of the Earth's Interior (IASPEI) Software Library. The package is available from the Seismological Society of America, El Cerrito, California 94530, and consists of both the data acquisition software and several tools for processing and analyzing the data. The systems employed in Socorro and Antarctica use only the data acquisition software, subsequent assessment and analysis is performed using various tools written for UNIX workstations.

XDETECT Overview

The principal data acquisition software, XDETECT, is a triggered event recorder designed for local seismic event recording. XDETECT uses a trigger algorithm designed by Eaton, Lee, and Stewart (Lee, 1992). This algorithm operates on the first difference, the short term average of the first differences, and the long-term average of the short term averages. Ratios of these averages are used to evaluate the data stream for suspected seismic events. Once such an event is detected, the system records the data stream. The system buffers the data stream, allowing the recording to begin a few seconds before event detection. Data continues to be recorded until the the trigger is lost, or until a maximum recording time has been reached. The critical ratio values for event detection and continuation, as well as the pre-event recording time and

the maximum recording time are all user-definable, making the system quite versatile in this respect. However, severe limitations on the configuration of the short and long-term averages can hamper operation. Specifically, a fast algorithm is used which constrains the number of samples used in the calculation of the averages to exactly a power of two. This limitation severely quantizes the possible configurations, particularly if lengthy long-term averages are desired.

The IASPEI software has other current configuration limitations which should be considered before installation. Perhaps the most important concern is the restriction to only one compatible analog-to-digital converter. Only data acquisition boards from Data Translation can be used with the IASPEI system. While these boards generally perform well, several problems have occurred as a result of imperfections in the Data Translation boards. The most severe problem encountered is related to timing errors within the board; the clock on one board produced a drift of nearly 10 minutes per day, yielding significant errors in digitization rates. The IASPEI software keeps time by counting samples, therefore the timing error propagates to event time stamping. Unfortunately, difficulties in obtaining a replacement board from Data Translation forced the deployment of the system in Antarctica based on the faulty board.

Another problem appears to be related to the multiplex operation of the Data Translation board. On rare occasions, the IASPEI system recorded data on the wrong channel; the system has shifted the recording such that data intended for channel zero of the data acquisition board was recorded on channel one, channel one was recorded on channel two, et cetera. This problem was observed on both the Socorro, and the Erebus systems. The incorrect recording can be difficult to detect on casual inspection unless an easily recognizable

signal such as a time code is recorded along with the seismic data. While not understood completely, this problem may be the result of insufficient memory allocated to data acquisition buffers. Thankfully, this condition can be removed by restarting XDETECT.

The basic operation of the system is relatively simple. The output from the discriminators is connected to the Data Translation terminal board. The acquisition board samples the analog inputs at a user definable frequency, buffers the data and makes it available to the XDETECT program. XDETECT then continuously evaluates the data stream using a user-configurable trigger algorithm.

XDETECT Control Parameters

Each time XDETECT is started on the PC, a control file named xdetect.inp is loaded. This file contains most of the information needed to control the trigger algorithm. The instructions included in xdetect.inp are grouped into four parts. The first set of instructions controls general system operations such as memory buffer size. The second portion of the control file includes instructions to control the trigger algorithm. Following the trigger control instructions is a small set of instructions related to event file storage. The final portion of the control file contains a seismic station list and instructions governing individual recording channels.

```
# FILE: xdetect.inp (W. Lee, 12/9/91)
# *** Erebus Network (M. Skov, 16/NOV/92)
# *** ***
# *** HIGH WIND CONFIGURATION

EventAlertBell= ON;
Autotrigger= ON;
AutoLocation= OFF;
Autoreboot= ON, Time= 00:00:00;
```

ChannelGain= 1; # must change so input signal is +- 10 volts
ClockSource= INTERNAL;
TriggerSource= INTERNAL;

ChannelBlocksize= 256; # must change if DigitizationRate is changed
DigitizationRate= 100.0; # must change for your network

PreEventTime= 20.0; # changed 9-JAN-93 by M. Skov
MinEventTime= 30.0; # changed 23-NOV-92 by M. Skov
MaxEventTime= 120.0; # changed 16-NOV-92 by M. Skov

TriggerTimeLimit= 10; # changed by M. Skov 20-NOV-92
CriticalNu= 1; # changed by S. Doherty 15-JUN-93

STAverageWindow= 64; # changed 08-MAY-93 by S. Doherty
LTAverageWindow= 8192; # changed 08-MAY-93 by S. Doherty
LTALowerBound= 10; # added 16-NOV-92 by M. Skov

CriticalAlpha= 1; # changed 16-NOV-92 by M. Skov
TriggerConfirmationCount=20; # changed 16-NOV-92 by M. Skov
CriticalBeta= 2; # changed 16-NOV-92 by M. Skov

EventContinuationCount= 20; # changed 16-NOV-92 by M. Skov
CriticalGamma= 2; # changed 26-DEC-92 by M. Skov

CriticalMu= 1; # changed 26-DEC-92 by M. Skov
CriticalPhi= 4;
HalfspaceVelocity = 6.0;

AuthorityCode = 101; # must change
NetworkName= "EREBUS";
NetworkNodeId= "MP, IY#2"; # must change
PathName= "C:\xdt204\event1";

Station definitions -
#

#
Ch= 0, StName=CLCK, Component= V, Trigger= OFF, Display= ON, Gain =1;
Ch= 1, StName= E1Z, Component= V, Trigger= OFF, Display= OFF, Gain =4;
Ch= 2, StName=MACZ, Component= V, Trigger= OFF, Display= ON, Gain =4;
Ch= 3, StName=BOMB, Component= V, Trigger= OFF, Display= ON, Gain =4;
Ch= 4, StName= TCS, Component= V, Trigger= OFF, Display= ON, Gain =4;
Ch= 5, StName= APK, Component= V, Trigger= OFF, Display= ON, Gain =4;
Ch= 6, StName=HOSR, Component= V, Trigger= ON, Display= ON, Gain =4;
Ch= 7, StName=MCMZ, Component= V, Trigger= OFF, Display= ON, Gain =1;
Ch= 8, StName=NONE, Component= V, Trigger= OFF, Display= OFF, Gain =1;

```
Ch= 9, StName= E1Z, Component= V, Trigger= OFF, Display= OFF, Gain =1;
Ch= 10, StName=MACZ, Component= V, Trigger= OFF, Display= ON, Gain =1;
Ch= 11, StName=BOMB, Component= V, Trigger= OFF, Display= ON, Gain =1;
Ch= 12, StName= TCS, Component= V, Trigger= OFF, Display= ON, Gain =1;
Ch= 13, StName= APK, Component= V, Trigger= OFF, Display= ON, Gain =1;
Ch= 14, StName=HOSR, Component= V, Trigger= OFF, Display= ON, Gain =1;
Ch= 15, StName=NONE, Component= V, Trigger= OFF, Display= OFF, Gain =1;
```

Source Listing 1 – Sample XDETECT.INP control file

Eight instructions are used to control general system performance. **EventAlertBell** controls the audible event alarm. The trigger algorithm can be turned off by setting **Autotrigger** = OFF. If the system detects a seismic event, it will perform a simple location using a homogeneous half-space velocity model if **AutoLocation** is turned on. The autoreboot feature of the system provides an easy way to perform daily bookkeeping and to reset the system. The autoreboot feature is controlled by the **Autoreboot** flag and the **Time** command. Midnight was selected for the reboot time to facilitate grouping of events by date.

ChannelGain sets the gain for the analog to digital converter. A gain of n yields $\pm \frac{10}{n}$ volts full scale. The gain value applies to all channels, and must be set to a value of 1, 2, 4 or 8. Both the **ClockSource** and the **TriggerSource** flags must be set to INTERNAL, future releases of XDETECT may allow for external clocks and triggers. The **ChannelBlocksize** parameter is not completely documented, however it determines the size of the buffers used by XDETECT. The **ChannelBlocksize** must be set to a value equal to a power of two, and can not be larger than 32,768 ÷ number of channels. Finally, the **DigitizationRate** is the approximate number of samples recorded per second.

Several commands provide near complete control over the behavior of the trigger algorithm. **PreEventTime** sets the amount of pre-trigger data to be

recorded. **MinEventTime** sets the minimum number of seconds to record, while **MaxEventTime** limits the length of the event file. The use of **MaxEventTime** can reduce the amount of spurious data recorded during noisy periods.

TriggerTimeLimit controls the number of seconds to hold a seismic event trigger on a given channel. **CriticalNu** sets the minimum number of stations required to trigger before the system begins recording. **CriticalNu** stations must meet the trigger requirements in less than **TriggerTimeLimit** seconds, or the event will not be recorded.

STAverageWindow and **LTAverageWindow** control the number of samples averaged to produce the short and long term averages respectively. The short term average is a running average of **STAverageWindow** first differences, while the long term average is a running average of **LTAverageWindow** short term averages. Both **STAverageWindow** and **LTAverageWindow** must be set to values of a power of two. While not documented in the IASPEI software manuals, the **LTALowerBound** sets the minimum value of the long term average. The minimum value must be large enough to avoid division my small numbers, yet small enough not to saturate the system's integer arithmetic.

CriticalAlpha sets the critical value used to determine an "alpha trigger". The alpha value is the ratio of the first difference to the long term average. If the alpha value exceeds **CriticalAlpha**, the system confirms the trigger with the beta comparison. Beta is the ratio of the short term and long term averages, if this value exceeds **CriticalBeta** for at least **TriggerConfirmationCount** samples, then that channel is triggered.

Once an event is declared, and recording begins, the system begins to monitor the event. Unless **CriticalMu** stations provide gamma values in

excess of **CriticalGamma** for at least **EventContinuationCount** samples, the trigger is lost, and recording stops. Gamma, like Beta is the ratio of the short and long term averages. The system is prevented from recording less than **MinEventTime** seconds, or more than **MaxEventTime** seconds.

If the **AutoLocate** feature is activated, the system will use **CriticalPhi** and the **HalfspaceVelocity** to compute event location. **CriticalPhi** is the fewest number of stations which must have triggered before the system will attempt to locate the event. The **HalfspaceVelocity** contains an approximate velocity for the region in kilometers per second. The ability of the system to correctly trigger on the first motion of an event is questionable, so the autolocation feature has not been used with the Socorro or Mount Erebus installations.

The third section of the control file sets four variables associated with the recording of event files. **AuthorityCode** is recorded in the SUDS format event file and could be used to distinguish the data from data recorded by other systems. At the present time, the **AuthorityCode** has been left at 101, however obtaining a code for the Socorro and Erebus networks could be useful if data exchanges were planned. In November of 1993, the Erebus network was given an authority code of 415001. The **NetworkName** variable simply provides an easy way to identify the data. **NetworkNodeId** provides the ability to uniquely name event files should two systems be installed for the same network. **PathName** contains the DOS path name to the directory where event files should be stored.

The station definition portion of the control file contains important information regarding the display and triggering status of individual stations. Each of the 16 channels recorded must have its own command line. If fewer than 16 channels are required, then the number of channels identified must

be a power of two. **StName** is a three or four letter station name, unused channels should be named NONE. **Component** describes the orientation of the seismometer. **Trigger** is used to control the triggering status of a channel. If a particular station is noisy, or not functioning, then **Trigger** should be set to OFF. **Display** allows for the selection of which channels will be displayed on the default XDETECT screen. All channels can be viewed by issuing the appropriate runtime command. **Gain** can be used to overrule the global gain setting. This can be useful if some field stations have different gain settings or operational behavior.

A second control file is also loaded each time XDETECT begins execution. This file, named STATION.@@@, is a binary file which contains information about the seismic stations. Because the file is binary in type, it can not be directly edited, however a program called STPARSE accompanies the IASPEI library. STPARSE converts a correctly formatted ascii file into the binary file STATION.@@@. Some information in the XDETECT.INP file is duplicated in the STATION.@@@, duplicate information must match exactly!!!

```
# FILE: station.sta
#
# Station list for Erebus Network
#
#
# Translate into "stations.@@@" via "stparse".
#

# 0 CLOCK (CLOCK)
Network= EREBUS, StName= CLCK, Component= V, InstrumentType= 202,
Azimuth= 0, Incidence= 0, StLatitude= 0.0, StLongitude= 0.0,
Elevation= 0, StDelay= 0, Enclosure= '_', Annotation= 0, RecorderType= '_',
RockClass= '_', RockType= 0, SiteCondition= '_', SensorType= v,
SensorGain= 1, Polarity= n;

# 1 E1Z (E1Z)
Network= EREBUS, StName=E1Zh, Component=V, InstrumentType= 202,
Azimuth= 0, Incidence= 0, StLatitude= 00.0000, StLongitude= -000.0000,
Elevation= 0000, StDelay= 0, Enclosure= 's', Annotation= 0, RecorderType= '_',
```

RockClass= '_', RockType= 0, SiteCondition= '_', SensorType= v,
SensorGain= 1, Polarity= n;

# 2 MACZ (MACZ) 00.0000S 000.0000W
Network= EREBUS, StName=MACZh, Component= V, InstrumentType= 202,
Azimuth= 0, Incidence= 0, StLatitude= 00.0000, StLongitude= -000.0000,
Elevation= 0000, StDelay= 0, Enclosure= 's', Annotation= 0, RecorderType= '_',
RockClass= '_', RockType= 0, SiteCondition= '_', SensorType= v,
SensorGain= 1, Polarity= n;

# 3 BOMB (BOMB) 00.0000S 000.0000W 0000
Network= EREBUS, StName=BOMBh, Component= V, InstrumentType= 202,
Azimuth= 0, Incidence= 0, StLatitude= 00.0000, StLongitude= -000.0000,
Elevation= 0000, StDelay= 0, Enclosure= 's', Annotation= 0, RecorderType= '_',
RockClass= '_', RockType= 0, SiteCondition= '_', SensorType= v,
SensorGain= 1, Polarity= n;

# 4 TCS (TCS) 00.0000S 000.0000W 0000
Network= EREBUS, StName= TCSh, Component= V, InstrumentType= 202,
Azimuth= 0, Incidence= 0, StLatitude= 00.0000, StLongitude= -000.0000,
Elevation= 0000, StDelay= 0, Enclosure= 's', Annotation= 0, RecorderType= '_',
RockClass= '_', RockType= 0, SiteCondition= '_', SensorType= v,
SensorGain= 1, Polarity= n;

# 5 APK (APK) 00.0000S 000.0000W 0000
Network= EREBUS, StName= APKh, Component= V, InstrumentType= 202,
Azimuth= 0, Incidence= 0, StLatitude= 00.0000, StLongitude= -000.0000,
Elevation= 0000, StDelay= 0, Enclosure= 's', Annotation= 0, RecorderType= '_',
RockClass= '_', RockType= 0, SiteCondition= '_', SensorType= v,
SensorGain= 1, Polarity= n;

# 6 HOSR (HOSR) 00.0000S 000.0000W 0000
Network= EREBUS, StName=HOSRh, Component= V, InstrumentType= 202,
Azimuth= 0, Incidence= 0, StLatitude= 00.0000, StLongitude= -000.0000,
Elevation= 0000, StDelay= 0, Enclosure= 's', Annotation= 0, RecorderType= '_',
RockClass= '_', RockType= 0, SiteCondition= '_', SensorType= v,
SensorGain= 1, Polarity= n;

# 7 MCMZ (MCMZ)
Network= EREBUS, StName=MCMZ, Component= V, InstrumentType= 202,
Azimuth= 0, Incidence= 0, StLatitude= 00.0000, StLongitude= -000.0000,
Elevation= 0000, StDelay= 0, Enclosure= 's', Annotation= 0, RecorderType= '_',
RockClass= '_', RockType= 0, SiteCondition= '_', SensorType= v,
SensorGain= 1, Polarity= n;

# 8 NONE (NONE)
Network= EREBUS, StName=NONE, Component= V, InstrumentType= 202,
Azimuth= 0, Incidence= 0, StLatitude= 00.0000, StLongitude= -000.0000,
Elevation= 0000, StDelay= 0, Enclosure= 'v', Annotation= 0, RecorderType= '_',
RockClass= '_', RockType= 0, SiteCondition= '_', SensorType= v,
SensorGain= 1, Polarity= n;

# 9 E1Z (E1Z)
Network= EREBUS, StName=E1Zl, Component= V, InstrumentType= 202,
Azimuth= 0, Incidence= 0, StLatitude= 00.0000, StLongitude= -000.0000,
Elevation= 0000, StDelay= 0, Enclosure= 's', Annotation= 0, RecorderType= '_',

```
RockClass= '_', RockType= 0, SiteCondition= '_', SensorType= v,
SensorGain= 1, Polarity= n;

# 10 MACZ (MACZ)
Network= EREBUS, StName=MACZl, Component= V, InstrumentType= 202,
Azimuth= 0, Incidence= 0, StLatitude= 00.0000, StLongitude= -000.0000,
Elevation= 0000, StDelay= 0, Enclosure= 's', Annotation= 0, RecorderType= '_',
RockClass= '_', RockType= 0, SiteCondition= '_', SensorType= v,
SensorGain= 1, Polarity= n;

# 11 BOMB (BOMB)
Network= EREBUS, StName=BOMBl, Component= V, InstrumentType= 202,
Azimuth= 0, Incidence= 0, StLatitude= 00.0000, StLongitude= -000.0000,
Elevation= 0000, StDelay= 0, Enclosure= 's', Annotation= 0, RecorderType= '_',
RockClass= '_', RockType= 0, SiteCondition= '_', SensorType= v,
SensorGain= 1, Polarity= n;

# 12 TCS (TCS)
Network= EREBUS, StName=TCSl, Component= V, InstrumentType= 202,
Azimuth= 0, Incidence= 0, StLatitude= 00.0000, StLongitude= -000.0000,
Elevation= 0000, StDelay= 0, Enclosure= 's', Annotation= 0, RecorderType= '_',
RockClass= '_', RockType= 0, SiteCondition= '_', SensorType= v,
SensorGain= 1, Polarity= n;

# 13 APK (APK)
Network= EREBUS, StName=APKl, Component= V, InstrumentType= 202,
Azimuth= 0, Incidence= 0, StLatitude= 00.0000, StLongitude= -000.0000,
Elevation= 0000, StDelay= 0, Enclosure= 's', Annotation= 0, RecorderType= '_',
RockClass= '_', RockType= 0, SiteCondition= '_', SensorType= v,
SensorGain= 1, Polarity= n;

# 14 HOSR (HOSR)
Network= EREBUS, StName=HOSRl, Component= V, InstrumentType= 202,
Azimuth= 0, Incidence= 0, StLatitude= 00.0000, StLongitude= -000.0000,
Elevation= 0000, StDelay= 0, Enclosure= 's', Annotation= 0, RecorderType= '_',
RockClass= '_', RockType= 0, SiteCondition= '_', SensorType= v,
SensorGain= 1, Polarity= n;

# 15 NONE (NONE)
Network= EREBUS, StName=NONE, Component= V, InstrumentType= 202,
Azimuth= 0, Incidence= 0, StLatitude= 00.0000, StLongitude= -000.0000,
Elevation= 0000, StDelay= 0, Enclosure= 's', Annotation= 0, RecorderType= '_',
RockClass= '_', RockType= 0, SiteCondition= '_', SensorType= v,
SensorGain= 1, Polarity= n;
```

Source Listing 2 – Sample STATION.STA control file

The STATION.@@@ file is created by editing an ascii file, normally named STATION.STA. The STATION.STA file is converted to STATION.@@@ by issuing the command STPARSE STATION.STA STATION.@@@. Included

in the STATION.STA file is important information about the seismic station sites. This information is appended to each event file as part of the SUDS data structure. The information in this file is not presently used, however it is included for completeness. The structure of the STATION.STA file is simple and well documented in the IASPEI manuals and will not be repeated here.

Trigger Configuration and Operation

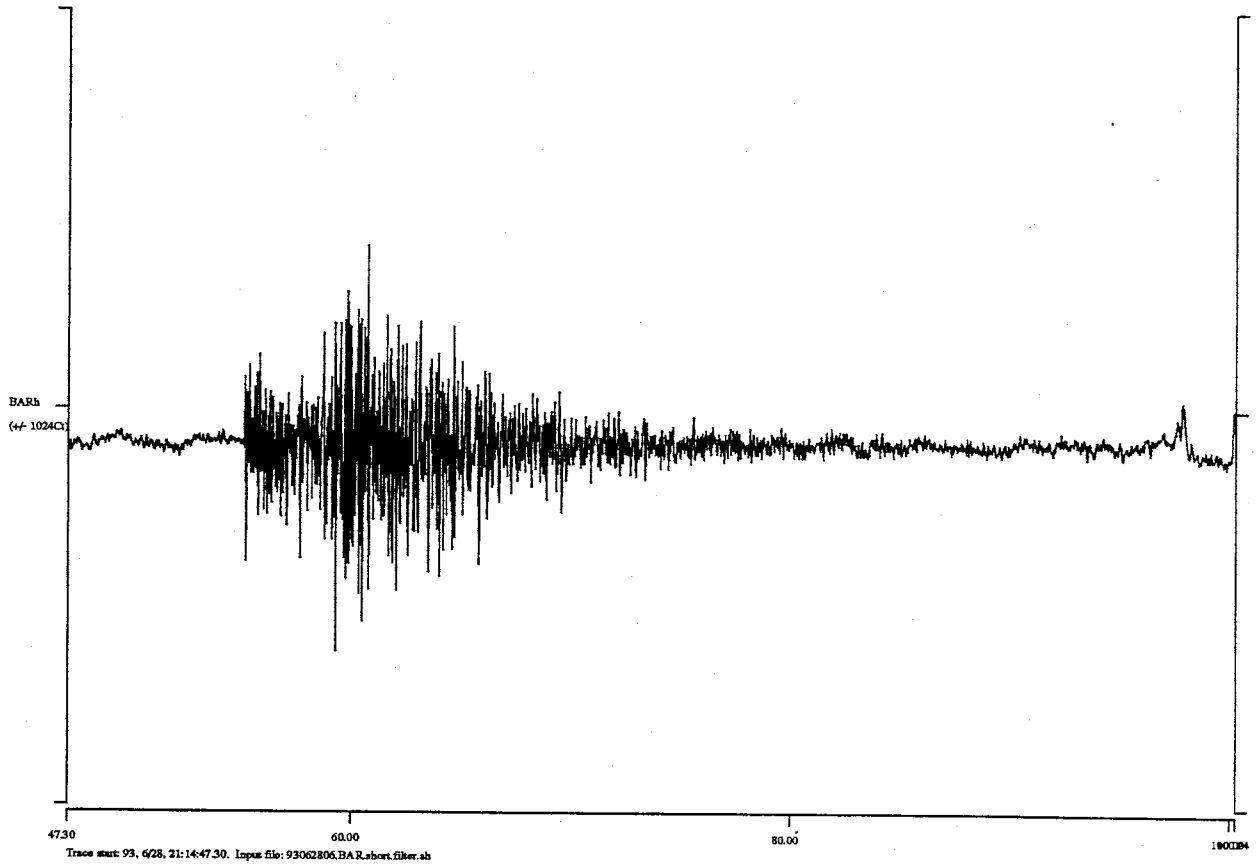

Figure 1 – Local earthquake time series from station BAR recorded by the Socorro acquisition system on June 28, 1993

Once the system is installed, the tedious task of configuring the trigger algorithm must be completed. A thorough knowledge of the trigger algorithm will assist the process of configuration. The simplest way to understand the trigger algorithm is to initially consider only one channel. Figure 1 shows the time series from station BAR of a typical event from the Socorro region as recorded by the IASPEI system.

The basic idea behind this trigger algorithm is quite simple, however, the implementation is more complex. Equations 1 – 3 show the basic averaging calculations performed by the trigger system, as functions of the sample number, n.

$$first\ difference_n = |sample_n - sample_{n-1}| \tag{1}$$

$$STA_n = \frac{\sum_{j=n-STAverageWindow}^{n} (first\ difference_j)}{STAverageWindow} \tag{2}$$

$$LTA_n = \frac{\sum_{j=n-LTAverageWindow}^{n} (STA_j)}{LTAverageWindow} \tag{3}$$

Unfortunately, this simple system could computationally overwhelm the early personal computers around which the IASPEI system was designed. The following equations show much more of the complexity required to operate this algorithm on simple personal computers.

$$first\ difference = |sample_n - sample_{n-1}| \tag{4}$$

$$STA = STA + (first\ difference - STA) >> sta\_shift \tag{5}$$

$$where\ >>\ is\ the\ bit-wise\ shift\ right\ operator$$

$$LTA = LTA + (STA - LTA) >> lta\_shift \tag{6}$$

$$sta\_shift = Log_2(STAverageWindow) \tag{7}$$

$$lta\_shift = Log_2(LTAverageWindow) \tag{8}$$

While these equations are much simpler to implement on a computer, and execute much faster than a straight forward implementation of (1) - (3), they can produce several undesirable side effects.

Perhaps the most obvious effect is the influence of the shift right operation. Each bit-wise shift right operation has the effect of dividing by two. In equation 5, the value of the first difference minus the current STA value is bit-wise right shifted sta_shift times, effectively dividing by 2^{sta_shift}. Similarly, in equation 6, the value of the current STA minus the current LTA is right shifted lta_shift times. Normally the use of the shift operation would not hinder the operation of the trigger, however, 16 bit integers are used to store the values of STA and LTA. Repeated shift operations reduce the dynamic range of the variable, effectively limiting its maximum value. For example, suppose a system is installed which records data at the rate of 100 samples per second, and an LTAverageWindow of approximately 80 seconds is desired. Under this situation, an LTAverageWindow of 8192 would be chosen, ($8192 \approx 100$ *samples per second times* 80 *seconds*). This LTAverageWindow would require 13 shift right operations in equation 6 ($8192 = 2^{13}$). Thirteen shift right operations would limit the maximum LTA to 7 ($2^{16-13} - 1$).

Despite the limitations imposed by integer arithmetic, careful selection of averaging windows can produce satisfactory results. Figure 2 shows trigger performance for the June 28, 1993 event shown in figure 1. Notice the sharp increase in α and β following the P-arrival, within a few seconds the long term average rises, and α and β fall back to pre-trigger levels. This response limits the duration of the trigger, and could help reduce false triggers during noisy periods, however, it also has the effect of limiting the duration of recording for true events. Less than ten seconds after the initiation of a trigger, the trigger

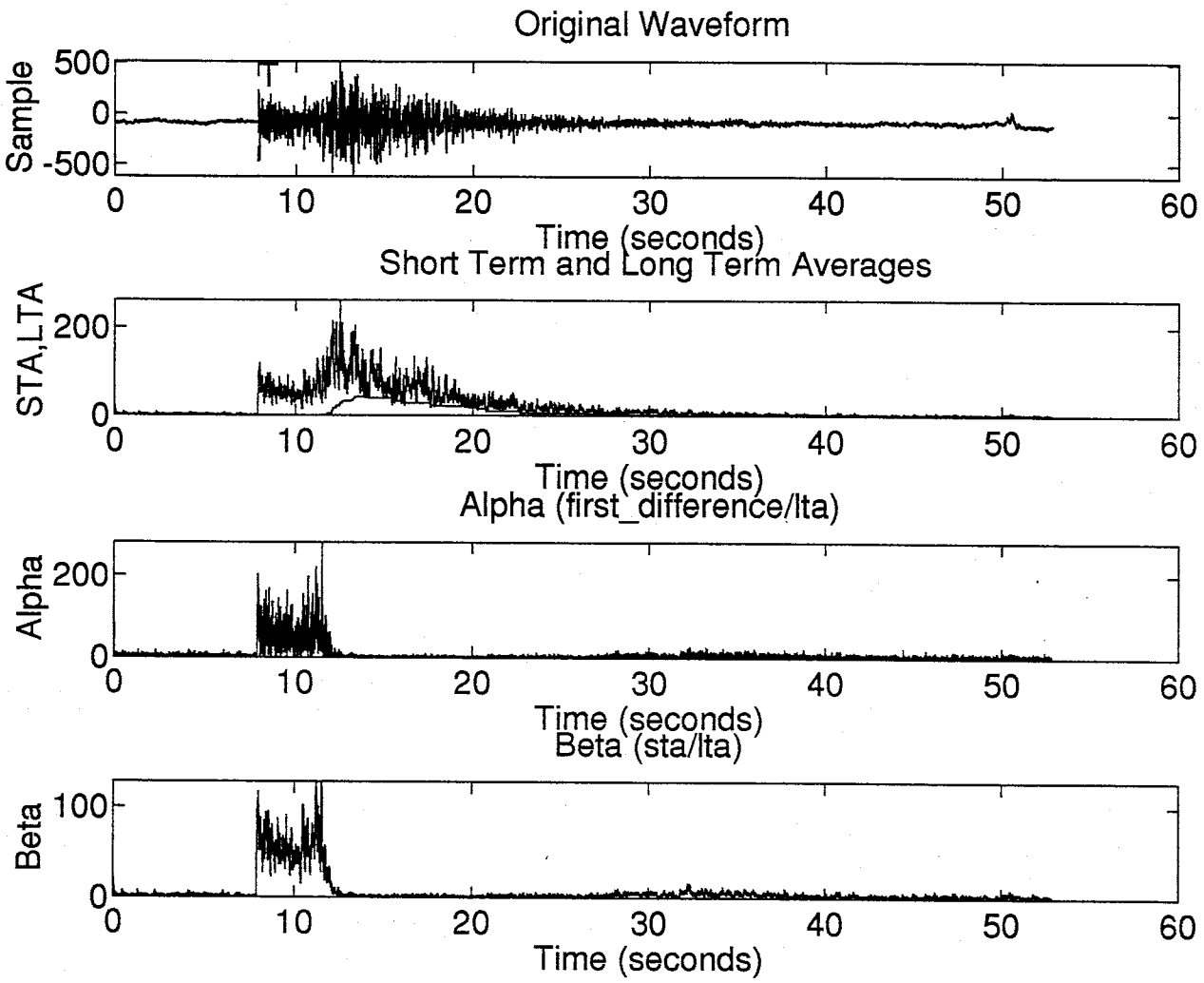

Figure 2 – Trigger parameters for a typical local earthquake recorded by the Socorro Network

STAverageWindow = 4; LTAverageWindow = 128; LTALowerBound=1;
CriticalAlpha = 28; CriticalBeta = 10; TriggerConfirmationCount = 10;

is lost, therefore thoughtful attention should be given to the MinEventTime and MaxEventTime parameters.

Creating a sensitive trigger is relatively simple, however a balance must be accepted between trigger sensitivity and tolerance of false triggers. Unfortunately this acceptable balance is difficult to achieve. At present, it is desirable for the Socorro Network to trigger on all events from the smallest local to the most emergent teleseism. However, to do so is clearly an unrealistic expectation. Thus, prior to installation, realistic goals need to be set for trigger performance, including expectations for the type and size of event desired *and* the false trigger tolerance level.

The IASPEI XDETECT system is optimized for local event detection, and is not suitable for distant regional and teleseism detection. In fact, the system installed in McMurdo has successfully triggered small events from within low frequency microseisms of higher amplitude. If teleseism detection is desired, a system known as TDETECT, also from IASPEI is available. TDETECT can simply replace XDETECT, with no need to change the analog to digital conversion hardware, or device drivers.

XDETECT Trigger Simulation

Simulating the trigger system described above can provide additional insight into the operation of the IASPEI XDETECT system. A C code was written to calculate the trigger parameters used by XDETECT. These parameters are then used by a matlab script which determines triggertime (if a trigger occurred) and generates a plot such as figure 2.

The source code for the program **xtrigger** is shown in source listing 3. **xtrigger** uses the trigger code from the XDETECT program to create a file containing the various trigger parameters calculated for each point in the time

series. The trigger code was changed slightly to accommodate the single channel operation of **xtrigger**.

```
/*    FILE: xtrigger.c
      Simulation of the XDETECT trigger system.
      Michael Skov 1993
      Dept. of Geoscience
      New Mexico Tech
      Socorro, NM 87801
      Portions of this code from modified IASPEI
       XDETECT trigger code.
*/
/*****************************************************
      Includes
*****************************************************/
#include<math.h>
#include<stdio.h>
#include<string.h>
main(argc,argv)       /* xtrigger */
int argc;
char *argv[];
{
  char   *fname[80];
  float  time,intrace;
  int    trace,traceold;
  int    dx,sta,lta,alpha,beta;
  float  deltatime,sample_rate;
  int    sta_window,lta_window,lta_minimum;
  int    sta_shift, lta_shift;
  FILE   *fin;
  FILE   *fout;
  if(argc !=6)
  {
    printf("usage: xtrigger filename  sampling_rate sta_window lta_window lta_minimum\ n");
    exit(0);
  }
  strcpy(fname,argv[1]);
  sample_rate=atof(argv[2]);
  sta_window=atoi(argv[3]);
  lta_window=atoi(argv[4]);
  lta_minimum=atoi(argv[5]);
  sta_shift= (int) (log2((double) (sta_window)));
  lta_shift= (int) (log2((double) (lta_window)));
  sta_window=(int) exp2((double) sta_shift);
  lta_window=(int) exp2((double) lta_shift);
  deltatime=1.0/sample_rate;
```

```
    printf("trace file: %s \n", fname);
    printf("sta_window: %i \n", sta_window);
    printf("lta_window: %i \n", lta_window);
    printf("lta_minimum: %i \n", lta_minimum);
    printf("sta_shift:    %i \n",sta_shift);
    printf("lta_shift:    %i \n",lta_shift);
    printf("sample_interval:    %f \n",deltatime);
  /*
    Initialize variables
  */
    sta=0;
    lta=0;
    trace=0;
    traceold=0;
    if ((fin=fopen(fname,"r"))==NULL)
    {
      printf("cannot open file %s \n",fname);
      exit(0);
    }
    if ((fout=fopen("wave.asc","w"))==NULL)
    {
      printf("cannot open output file wave.asc \ n");
      fclose(fin);
      exit(0);
    }
    while(!feof(fin))
    {
      fscanf(fin,"%g",&intrace);
      trace=(int) intrace;
      time+=deltatime;
      /*
         Trigger code from IASPEI XDETECT
         modified for single channel operation
      */
      dx=abs(trace - traceold);
      traceold=trace;
      sta+=(dx - sta) >> sta_shift;
      lta+=(sta - lta) >> lta_shift;
      if (lta < lta_minimum)
      {
        lta = lta_minimum;
      }
      alpha = dx/lta;
      beta  = sta/lta;
      fprintf(fout,"%10.6f %e %5i %5i %5i %5i %5i \ n", time,intrace,dx,sta.lta,alpha,beta);
    }
    fclose(fin);
    fclose(fout);
}
```

Source Listing 3 – Source code for the **xtrigger** program.

The **xtrigger** program expects the input file name, sampling rate, short term average window length, long term average window length, and the minimum long term average to be given in that order on the command line. **xtrigger** will load the input file and write the file "wave.asc" containing the original time series, plus the first difference, short term average, long term average, alpha and beta values for each point in the time series.

Like the input file, "wave.asc" is an ascii file. The input file needs to be the time series, with one entry per line. "wave.asc" will contain one set of parameters per line, and one line per element of the time series.

Once the wave.asc file is created, matlab scripts are used to evaluate and plot the trigger parameters. Source listing 4 shows the **matlabtrigger.m** script used to determine the trigger time. Source listing 5 shows the **plotitall.m** script used to create figures 2 - 17.

```
[n,m] = size(wave);
alphat=0;
triggertime=0;
betacount=0;
triggercode=0;
sampleint=1/samplerate;
for z = 1:n
  if triggercode==0,
    if alphat==0,
      if wave(z,6)>criticalalpha,
        alphat = 1;
        triggertime=z*sampleint;
      else
        alphat = 0;
        triggertime=0;
      end
    end
```

```
    if alphat==1,
        if wave(z,7)>criticalbeta,
          betacount=betacount+1;
        else
          betacount=0;
          triggertime=0;
          alphat=0;
        end
      if betacount>concount,
        triggertime
        triggercode=1;
      end
    end
  end
end
```

Source Listing 4 – matlabtrigger.m script.

The matlab scripts were created to simplify and automate the process of trigger evaluation. The codes used here are, admittedly, crude, however they do perform the task of trigger evaluation. Before using the **matlabtrigger.m** script, matlab must be started, and the file "wave.asc" must be loaded. In addition, the variables, samplerate, criticalalpha, criticalbeta, and concount must be set. These variables are the same as the variables of similar name described earlier in this section (concount is the the TriggerConfirmationCount).

The **plotitall.m** matlab script is executed after the **matlabtrigger.m** script. The **plotitall.m** script uses the triggertime, as calculated by **matlabtrigger.m** and plots the data from the file "wave.asc".

```
clg
subplot(411)
plot(wave(:,1),wave(:,2),'green')
hold on;
title('Original Waveform')
xlabel('Time (seconds)')
ylabel('Sample')
```

```
if triggertime~=0,
   xpos=triggertime;
   ypos1=max(wave(:,2));
   ypos2=min(wave(:,2));
   ypos=ypos1-.25*ypos1;
   text(xpos,ypos,'T')
   xlin=[xpos xpos];
   ylin=[ypos1 ypos2];
   plot(xlin,ylin,'-blue')
end
subplot(412)
plot(wave(:,1),wave(:,4),'green')
title('Short Term and Long Term Averages')
xlabel('Time (seconds)')
ylabel('STA,LTA')
hold on
plot(wave(:,1),wave(:,5),'blue')
subplot(413)
plot(wave(:,1),wave(:,6),'green')
title('Alpha (first_difference/lta)')
xlabel('Time (seconds)')
ylabel('Alpha')
subplot(414)
plot(wave(:,1),wave(:,7),'green')
title('Beta (sta/lta)')
xlabel('Time (seconds)')
ylabel('Beta')
```

Source Listing 5 – plotitall.m script.

Selection of a trigger configuration is, unfortunately, more difficult than simply running simulated seismic signals through a trigger simulation. The simulations can be helpful, and may quickly eliminate a possible configuration, however, peculiarities in XDETECT, unexpected noise sources, and problems with telemetry are all difficult to simulate. Only a field application of a particular configuration can truly prove its usefulness.

Simulations suggest a specific set of trigger parameters may be particularly advantageous. Using a STAverageWindow of 4, an LTAverageWindow of 128, an LTALowerBound of 1, a CriticalAlpha value of 28, a CriticalBeta value of 10, and a TriggerConfirmationCount of 10 proved useful in simulations,

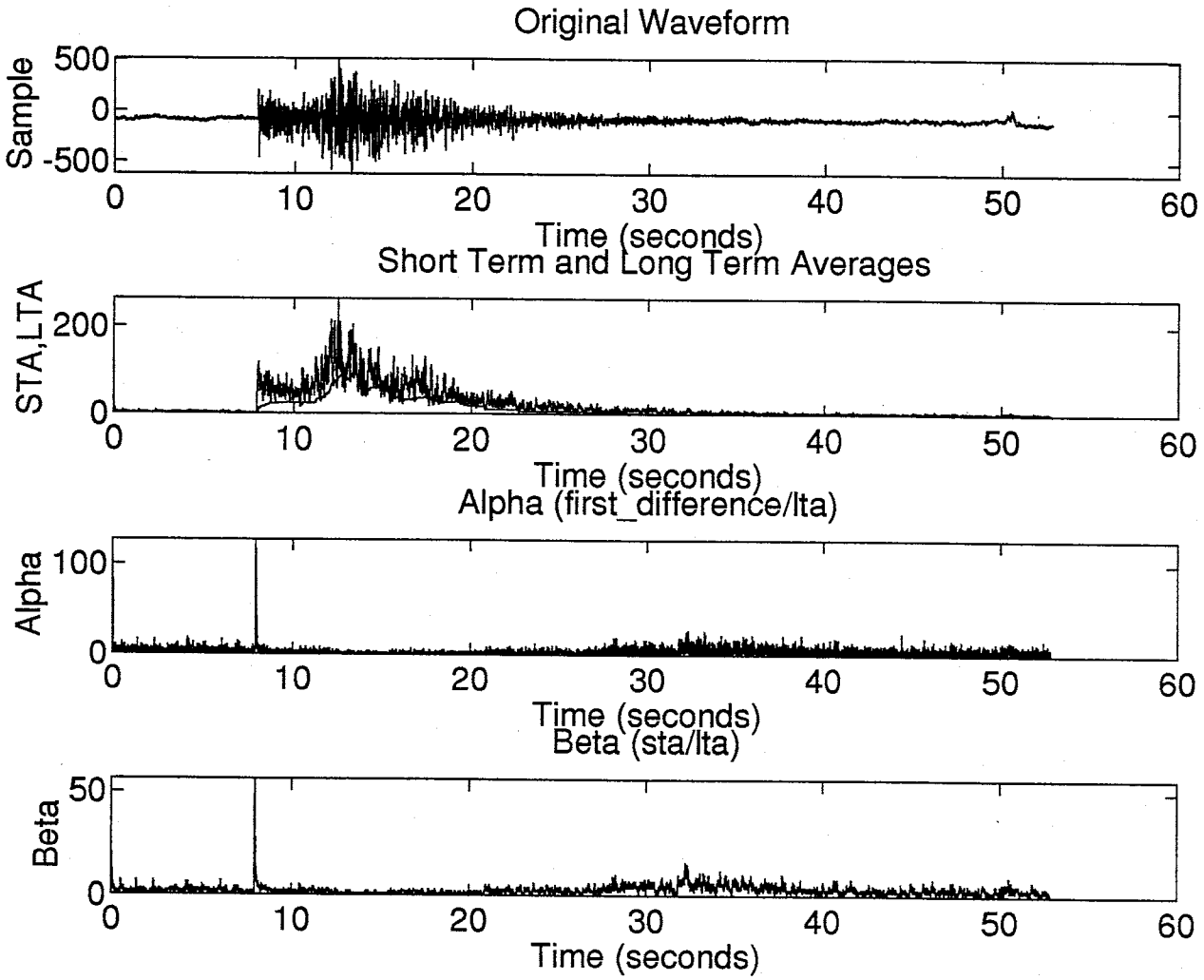

Figure 3 – Trigger parameters for a typical local earthquake recorded by the Socorro Network

STAverageWindow = 4; LTAverageWindow = 64; LTALowerBound=1;
CriticalAlpha = 28; CriticalBeta = 10; TriggerConfirmationCount = 10;

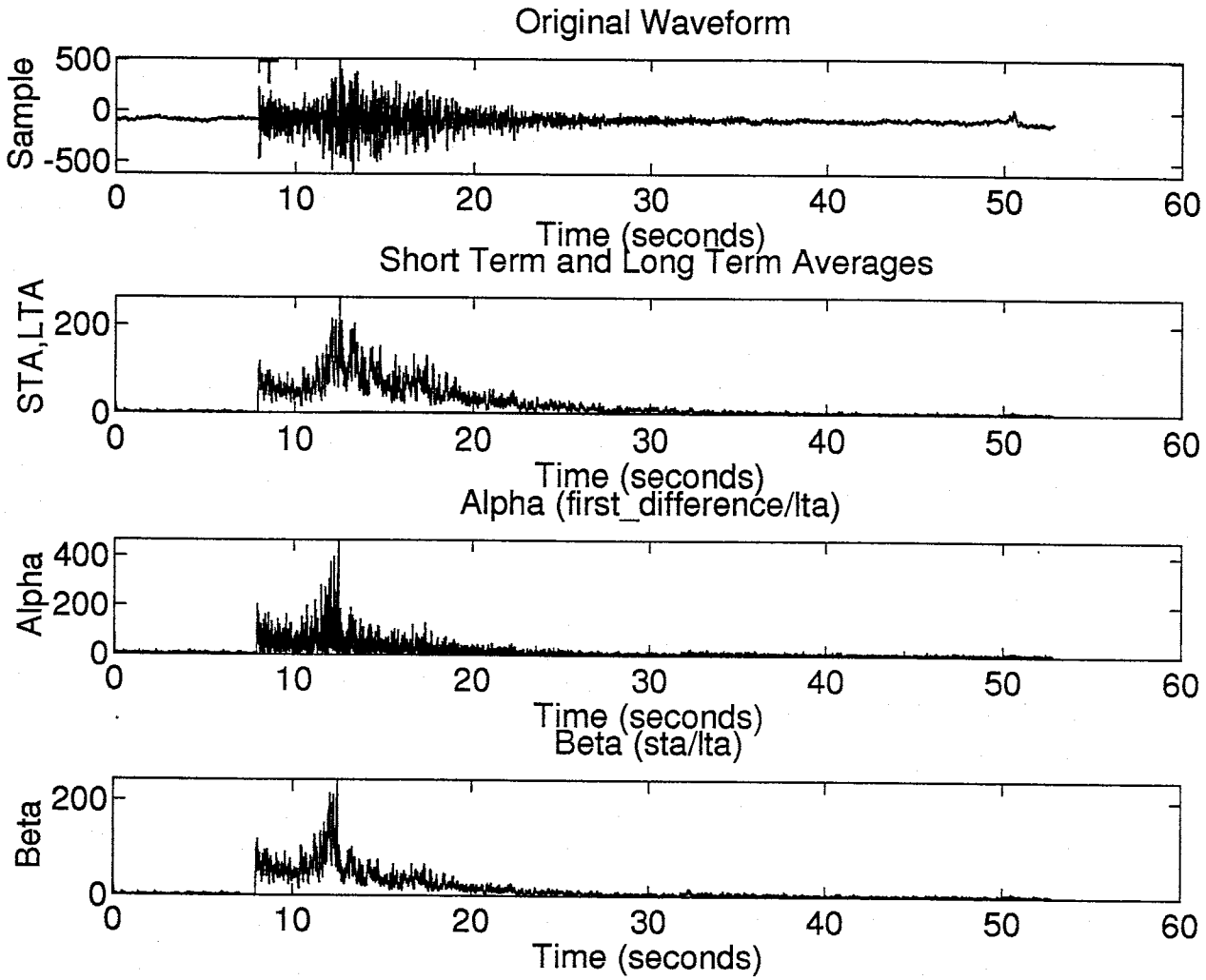

Figure 4 – Trigger parameters for a typical local earthquake recorded by the Socorro Network

STAverageWindow = 4; LTAverageWindow = 256;LTALowerBound=1;
CriticalAlpha = 28; CriticalBeta = 10; TriggerConfirmationCount = 10;

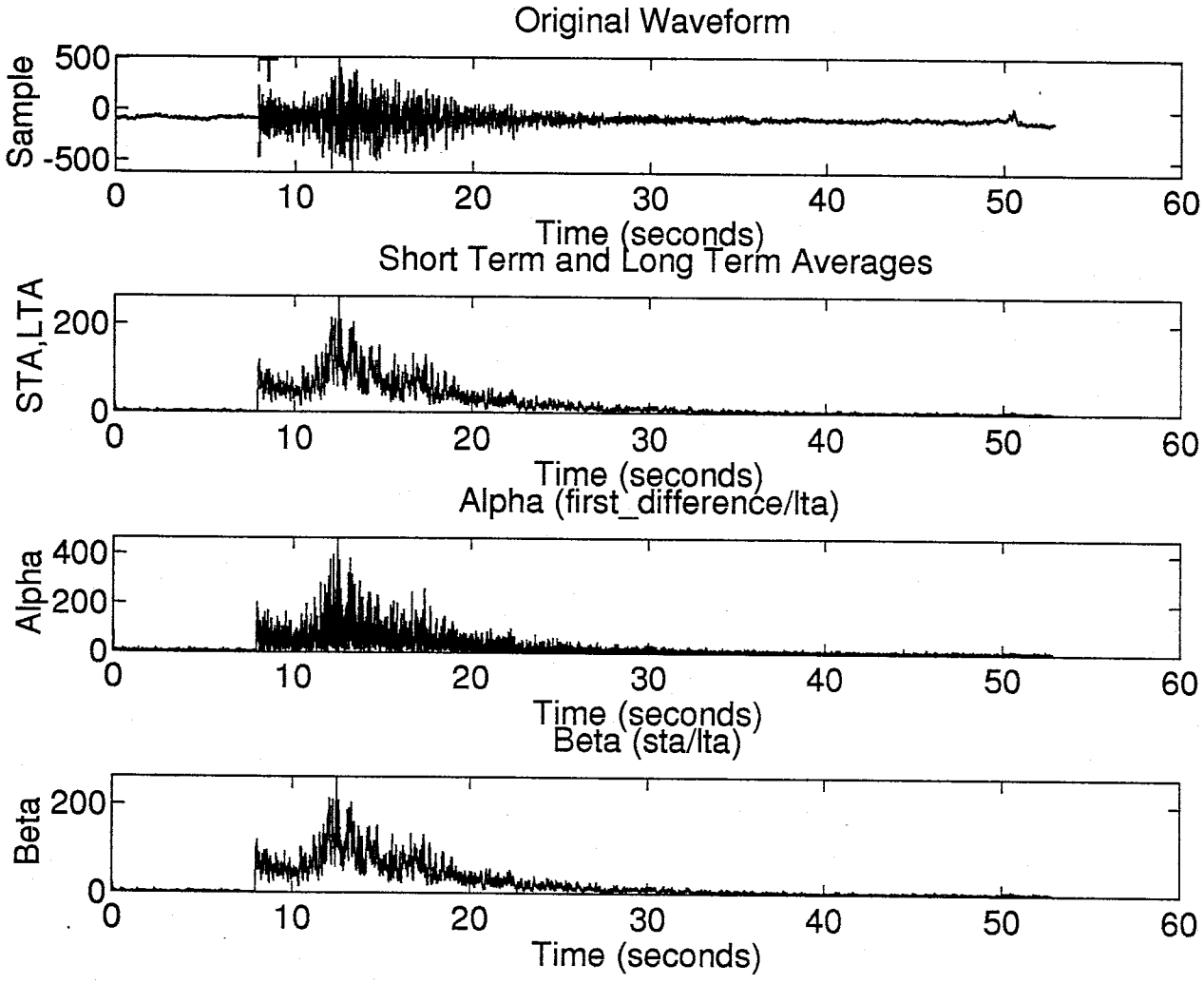

Figure 5 – Trigger parameters for a typical local earthquake recorded by the Socorro Network

STAverageWindow = 4; LTAverageWindow = 512; LTALowerBound=1;
CriticalAlpha = 28; CriticalBeta = 10; TriggerConfirmationCount = 10;

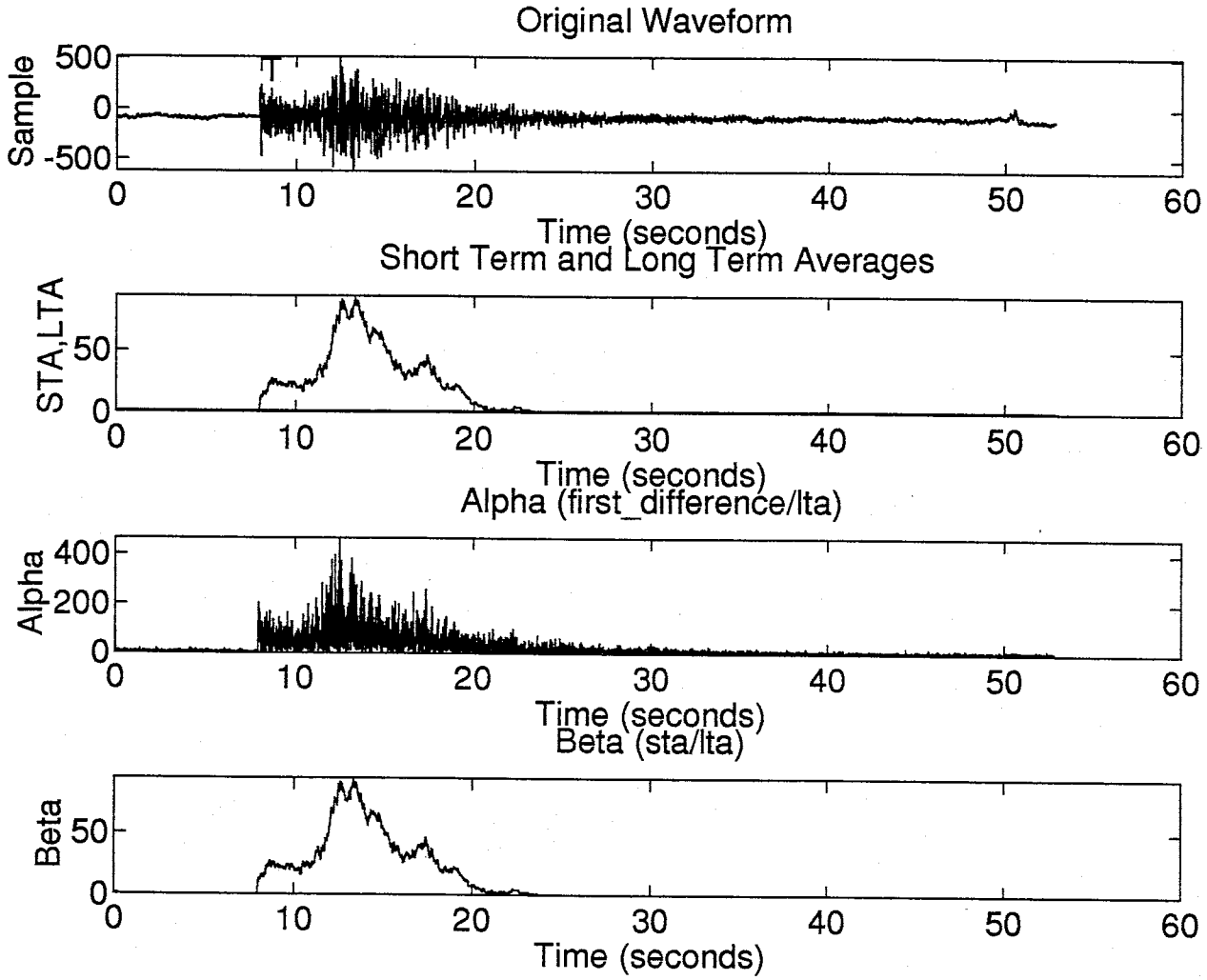

Figure 6 – Trigger parameters for a typical local earthquake recorded by the Socorro Network

STAverageWindow = 64; LTAverageWindow = 8192; LTALowerBound=1;
CriticalAlpha = 28; CriticalBeta = 10; TriggerConfirmationCount = 10;

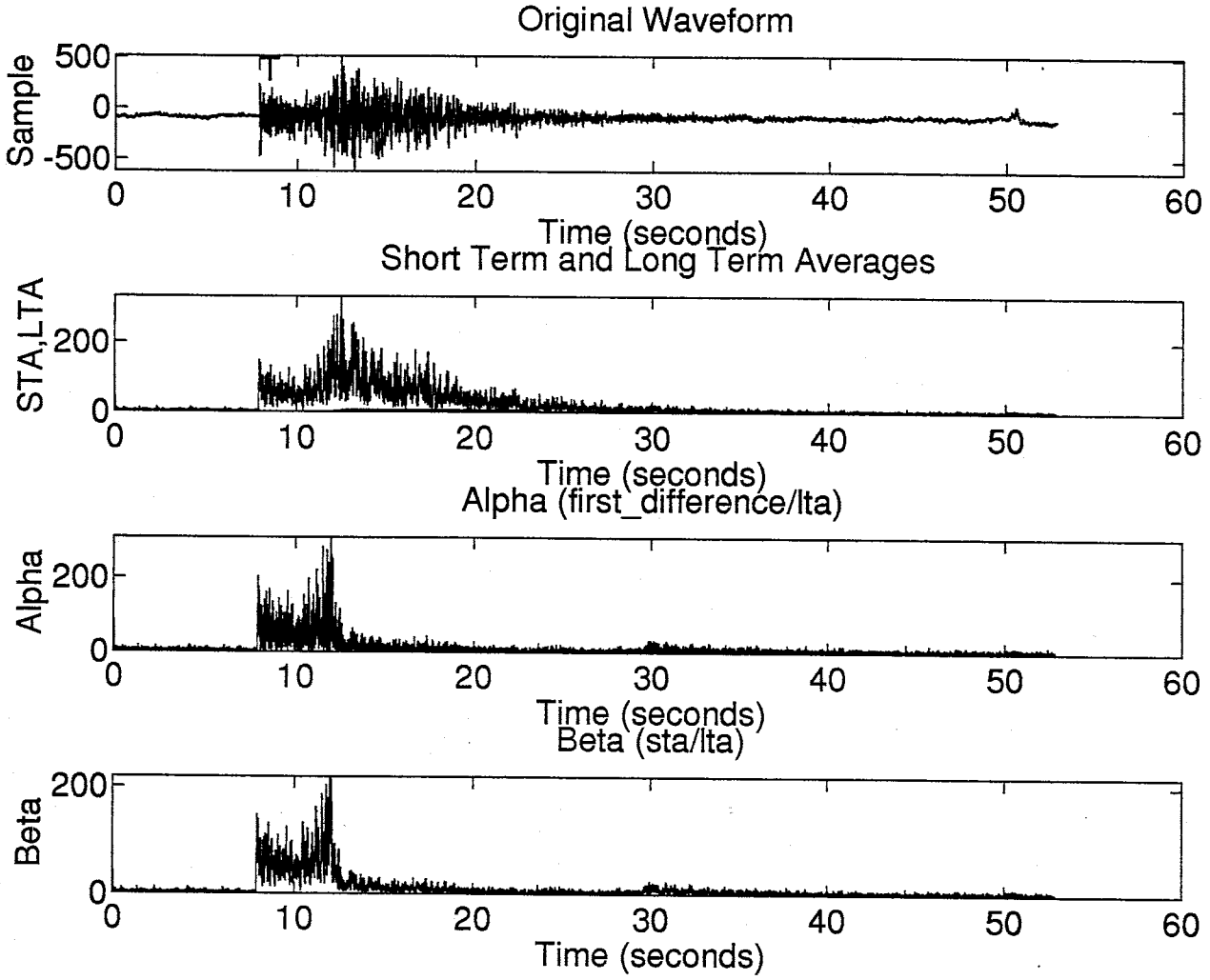

Figure 7 – Trigger parameters for a typical local earthquake recorded by the Socorro Network

STAverageWindow = 2; LTAverageWindow = 256; LTALowerBound=1;
CriticalAlpha = 28; CriticalBeta = 10; TriggerConfirmationCount = 10;

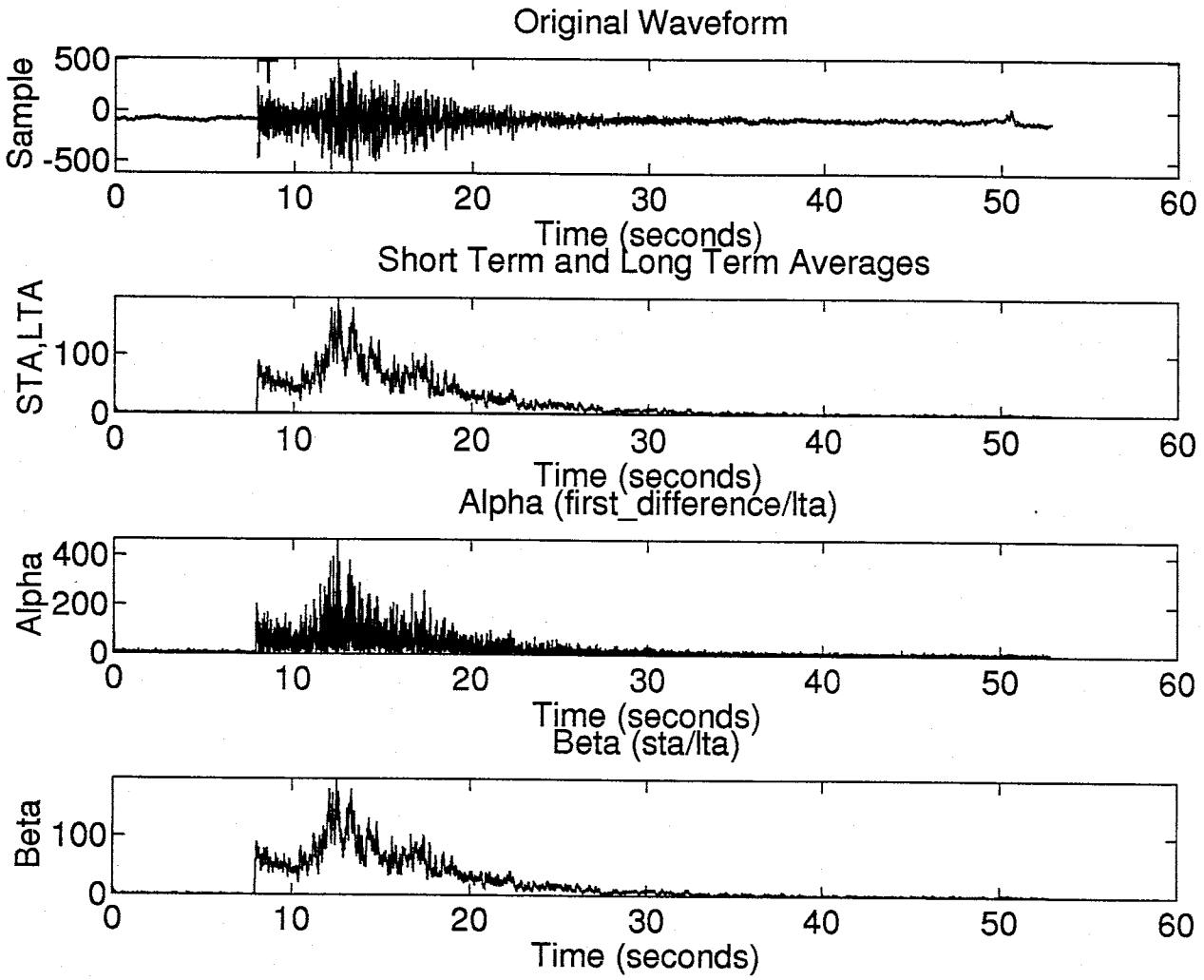

Figure 8 – Trigger parameters for a typical local earthquake recorded by the Socorro Network

STAverageWindow = 8; LTAverageWindow = 256; LTALowerBound=1;
CriticalAlpha = 28; CriticalBeta = 10; TriggerConfirmationCount = 10;

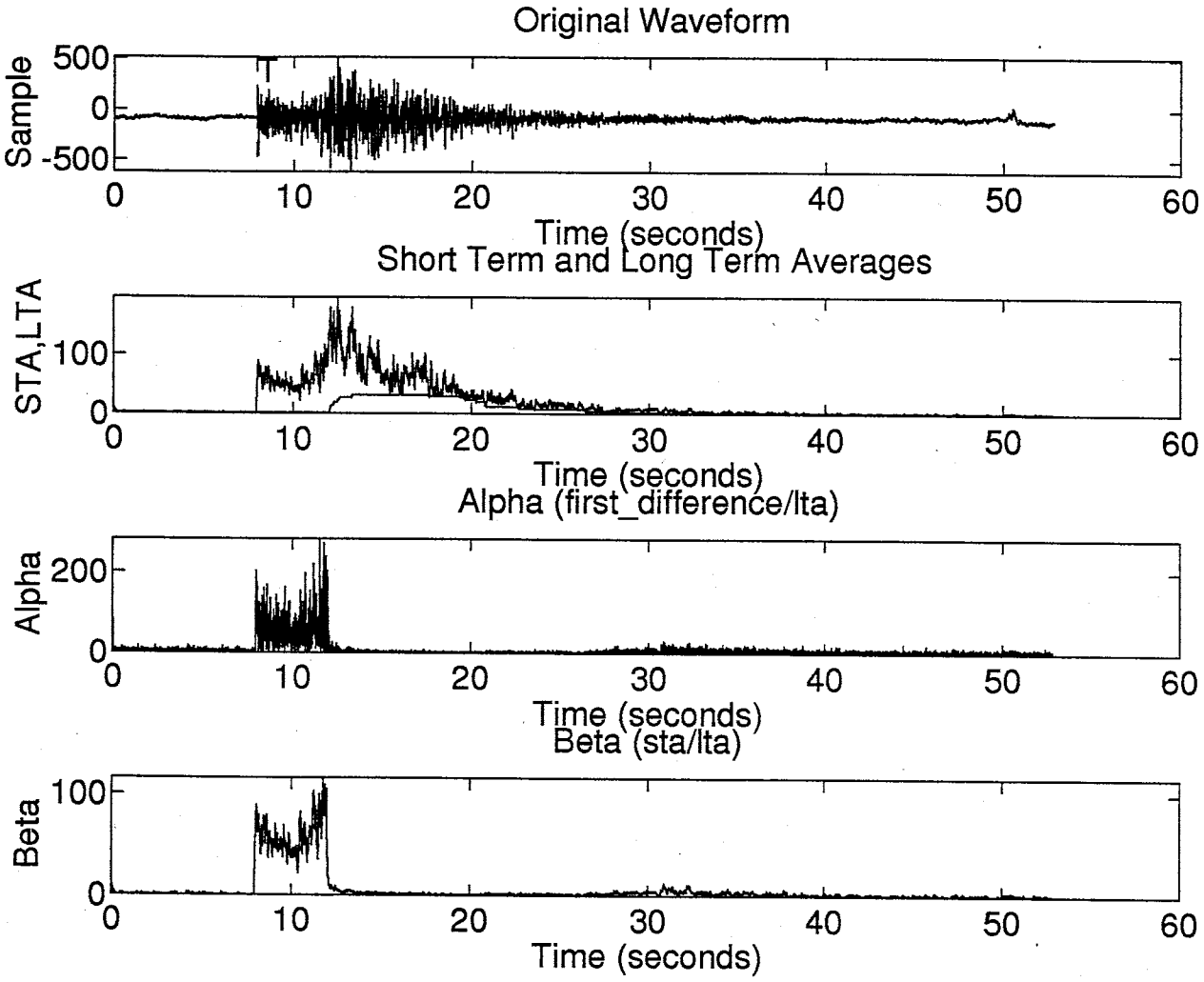

Figure 9 – Trigger parameters for a typical local earthquake recorded by the Socorro Network

STAverageWindow = 8; LTAverageWindow = 128; LTALowerBound=1;
CriticalAlpha = 28; CriticalBeta = 10; TriggerConfirmationCount = 10;

however XDETECT was replaced with TDETECT in the Socorro Observatory before this configuration could be tested. Figure 2 shows trigger performance for this configuration, while figures 3 through 9 show trigger performance for the same earthquake for a wide range of other configurations. A dashed vertical line and a 'T' in the original trace box marks the time of event trigger. Most of the configurations performed well, with the exception of the settings used to produce figure 3, the trigger configuration employed a short **LTAverageWindow** allowing the long-term average to rise quickly. The quickly rising long-term average clamps the Beta value shortly after the first arrival, and prevents a trigger.

Noise rejection must also be evaluated. While not inclusive of all noise, a composite of various noise signals was made to examine the noise rejection capabilities of particular trigger settings. Figures 10 through 17 show the noise rejection characteristics for the same trigger configurations in figures 2 through 9. It is important to note that these figures show only the first trigger– it is obvious that some of these configurations would produce excessive trigger activity.

Examining the two sets of figures together can yield some insight into the operation of the XDETECT system. Adjusting the size of the STAverageWindow changes the response of the system to high frequencies. A longer STAverageWindow has the effect of broadening a signal, this can lengthen a short noise burst in the trigger space domain–see figure 14. The length of the LTAverageWindow controls how quickly the system responds to changing signal levels. Long LTAverageWindows delay system response, generally forcing the long term average to a value equal to the LTALowerBound, while short LTAverageWindows provide quick response, limiting the duration of elevated α and β values.

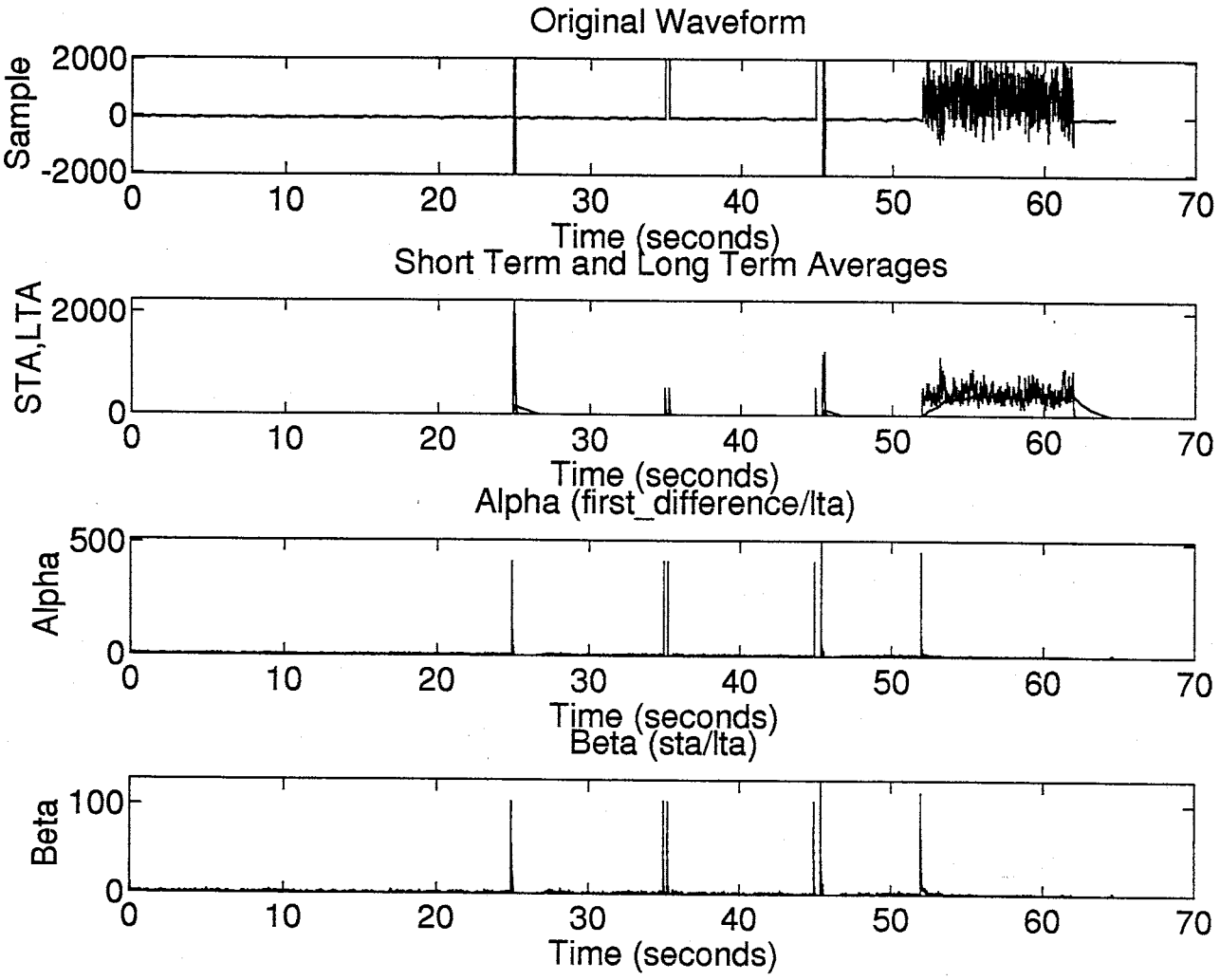

Figure 10 – Trigger parameters for a composite of noise signals
STAverageWindow = 4; LTAverageWindow = 128; LTALowerBound=1;
CriticalAlpha = 28; CriticalBeta = 10; TriggerConfirmationCount = 10;

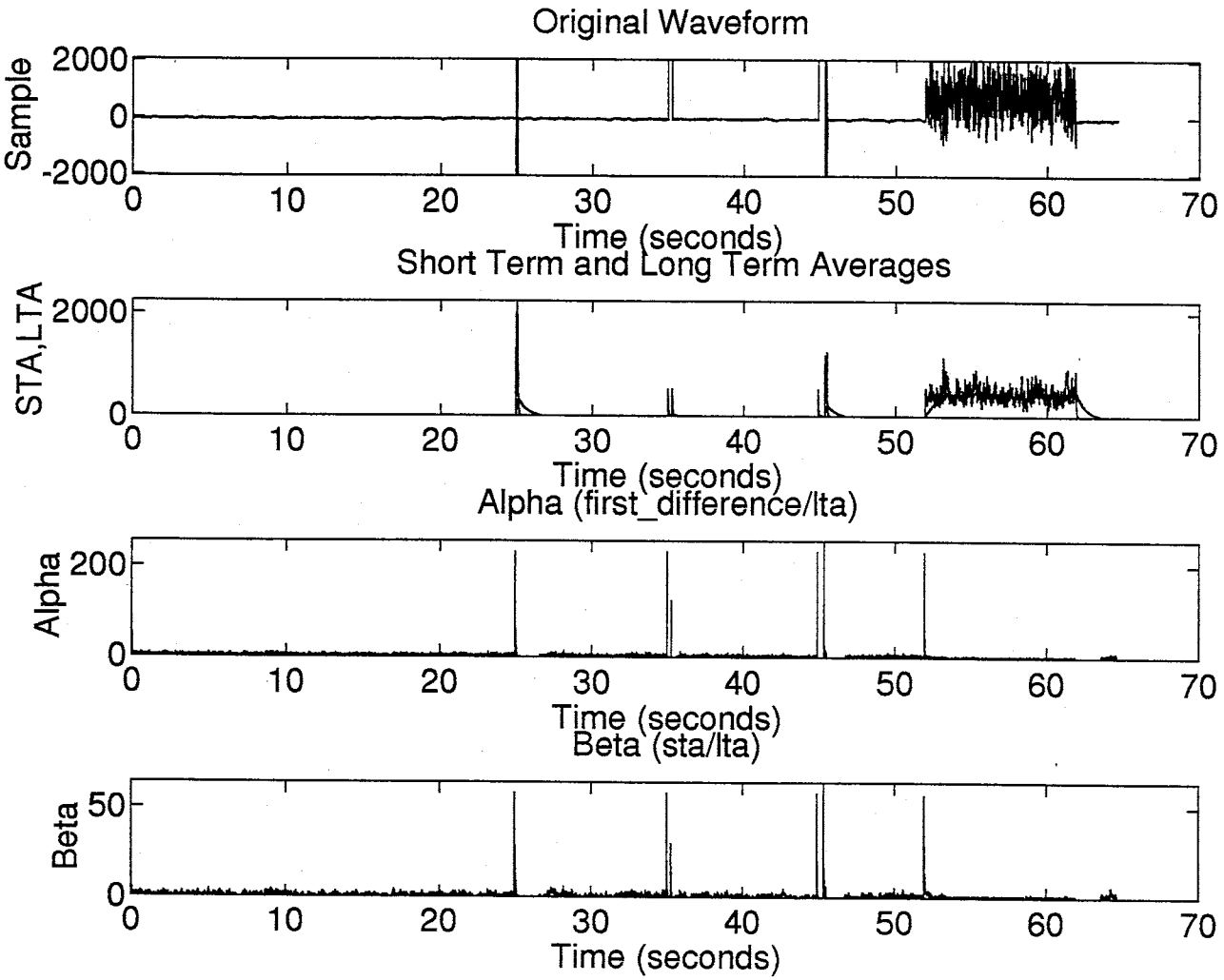

Figure 11 – Trigger parameters for a composite of noise signals
STAverageWindow = 4; LTAverageWindow = 64; LTALowerBound=1;
CriticalAlpha = 28; CriticalBeta = 10; TriggerConfirmationCount = 10;

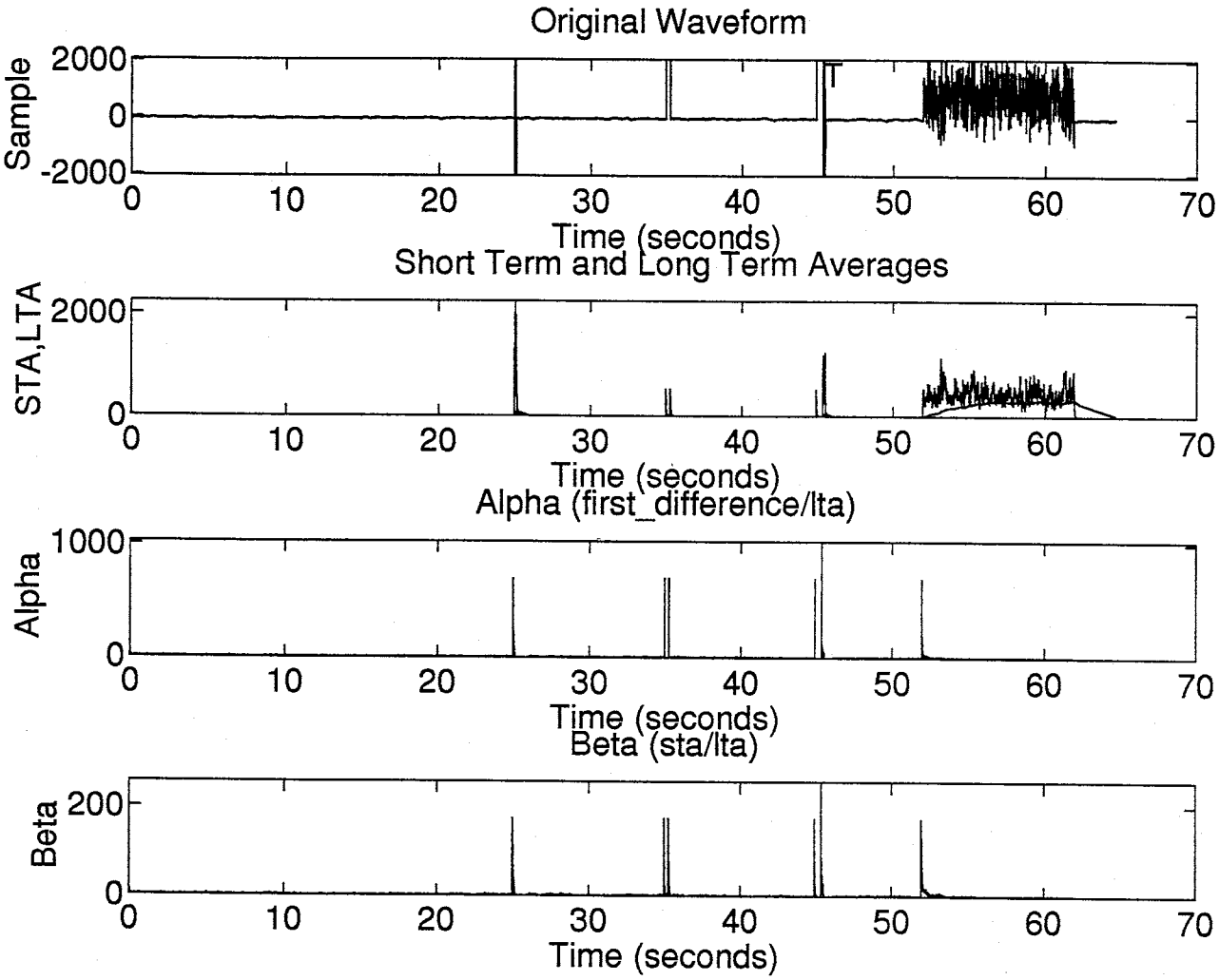

Figure 12 – Trigger parameters for a composite of noise signals
STAverageWindow = 4; LTAverageWindow = 256; LTALowerBound=1;
CriticalAlpha = 28; CriticalBeta = 10; TriggerConfirmationCount = 10;

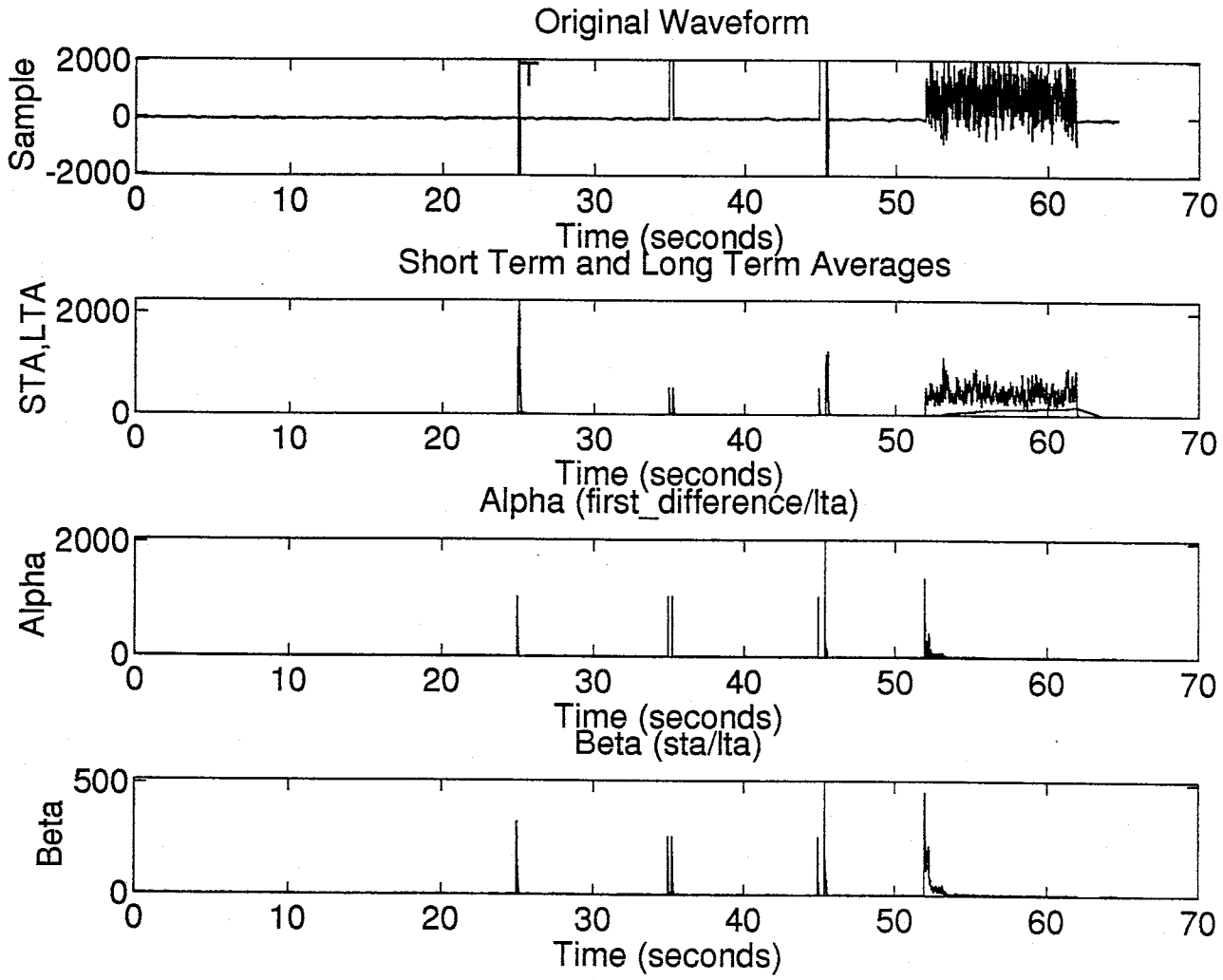

Figure 13 – Trigger parameters for a composite of noise signals
STAverageWindow = 4; LTAverageWindow = 512; LTALowerBound=1;
CriticalAlpha = 28; CriticalBeta = 10; TriggerConfirmationCount = 10;

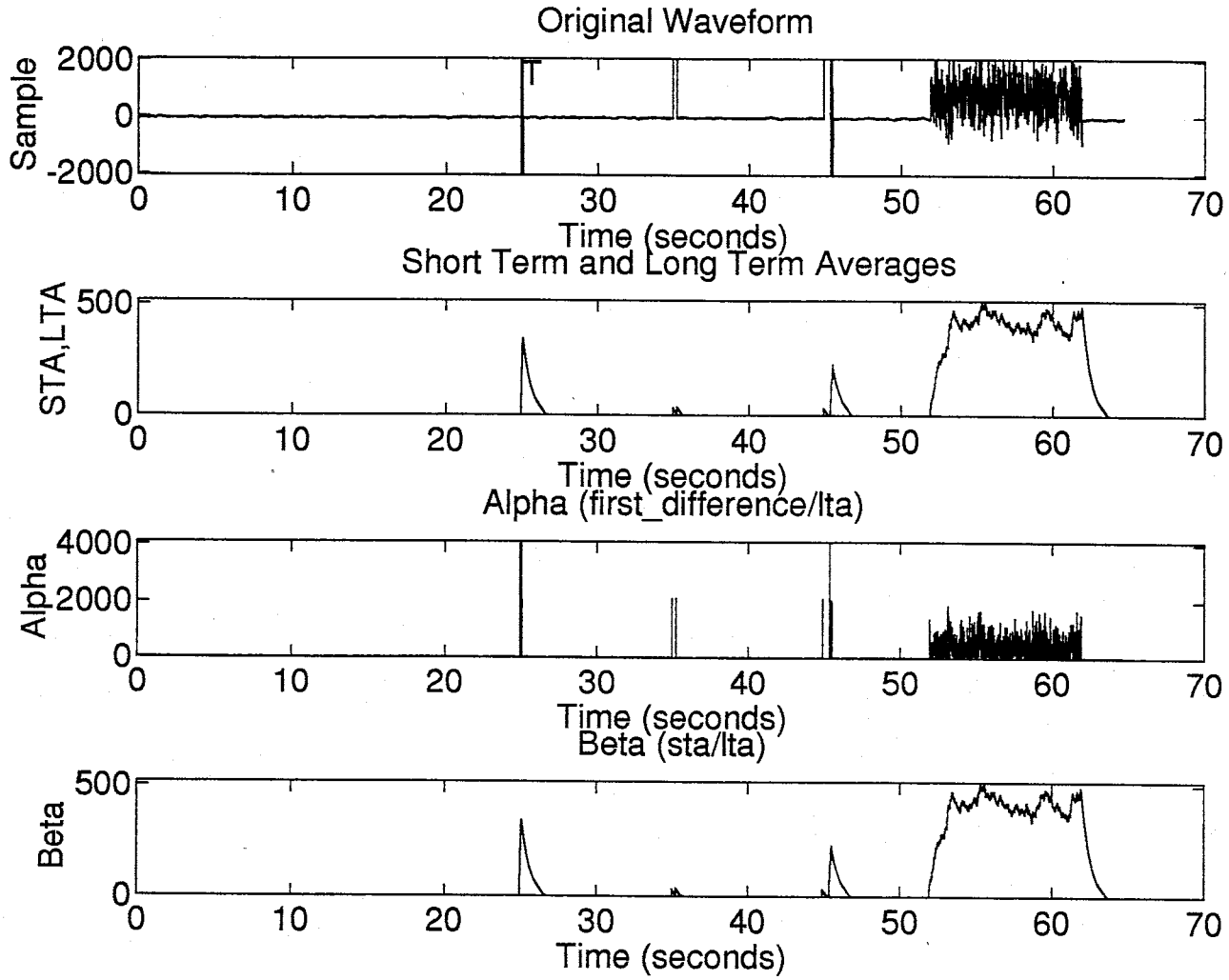

Figure 14 – Trigger parameters for a composite of noise signals
STAverageWindow = 64; LTAverageWindow = 8192; LTALowerBound=1;
CriticalAlpha = 28; CriticalBeta = 10; TriggerConfirmationCount = 10;

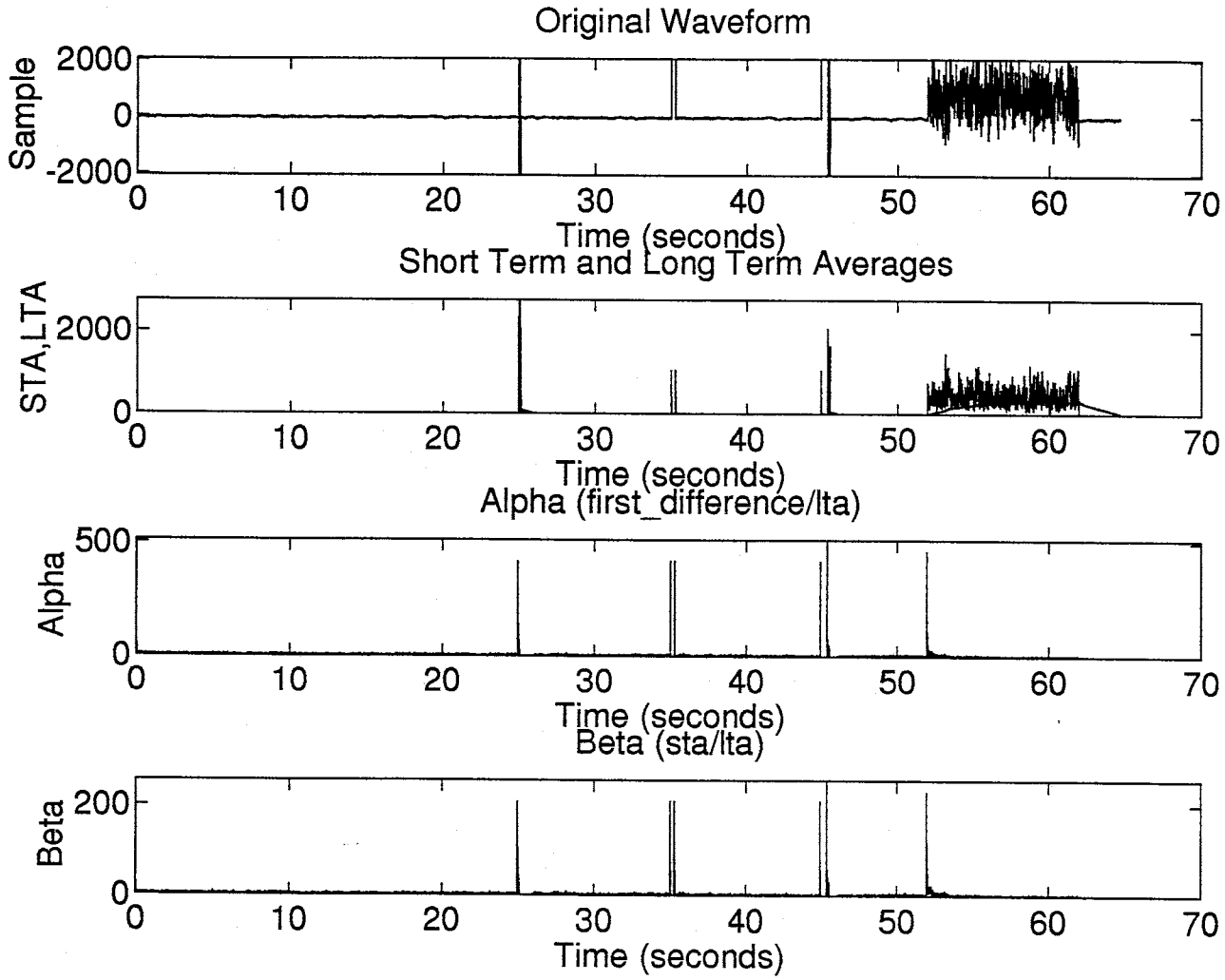

Figure 15 – Trigger parameters for a composite of noise signals
STAverageWindow = 2; LTAverageWindow = 256; LTALowerBound=1;
CriticalAlpha = 28; CriticalBeta = 10; TriggerConfirmationCount = 10;

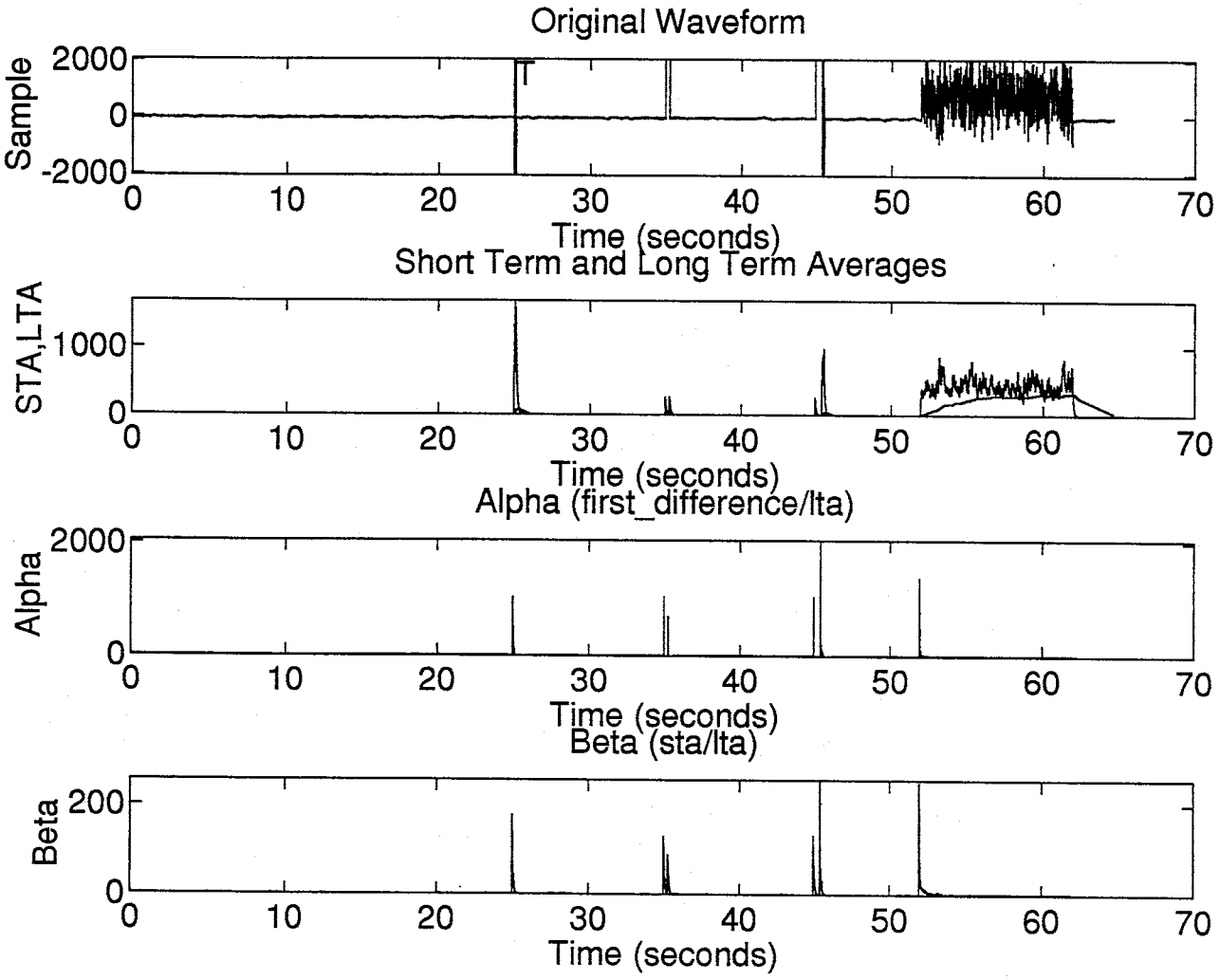

Figure 16 – Trigger parameters for a composite of noise signals
STAverageWindow = 8; LTAverageWindow = 256; LTALowerBound=1;
CriticalAlpha = 28; CriticalBeta = 10; TriggerConfirmationCount = 10;

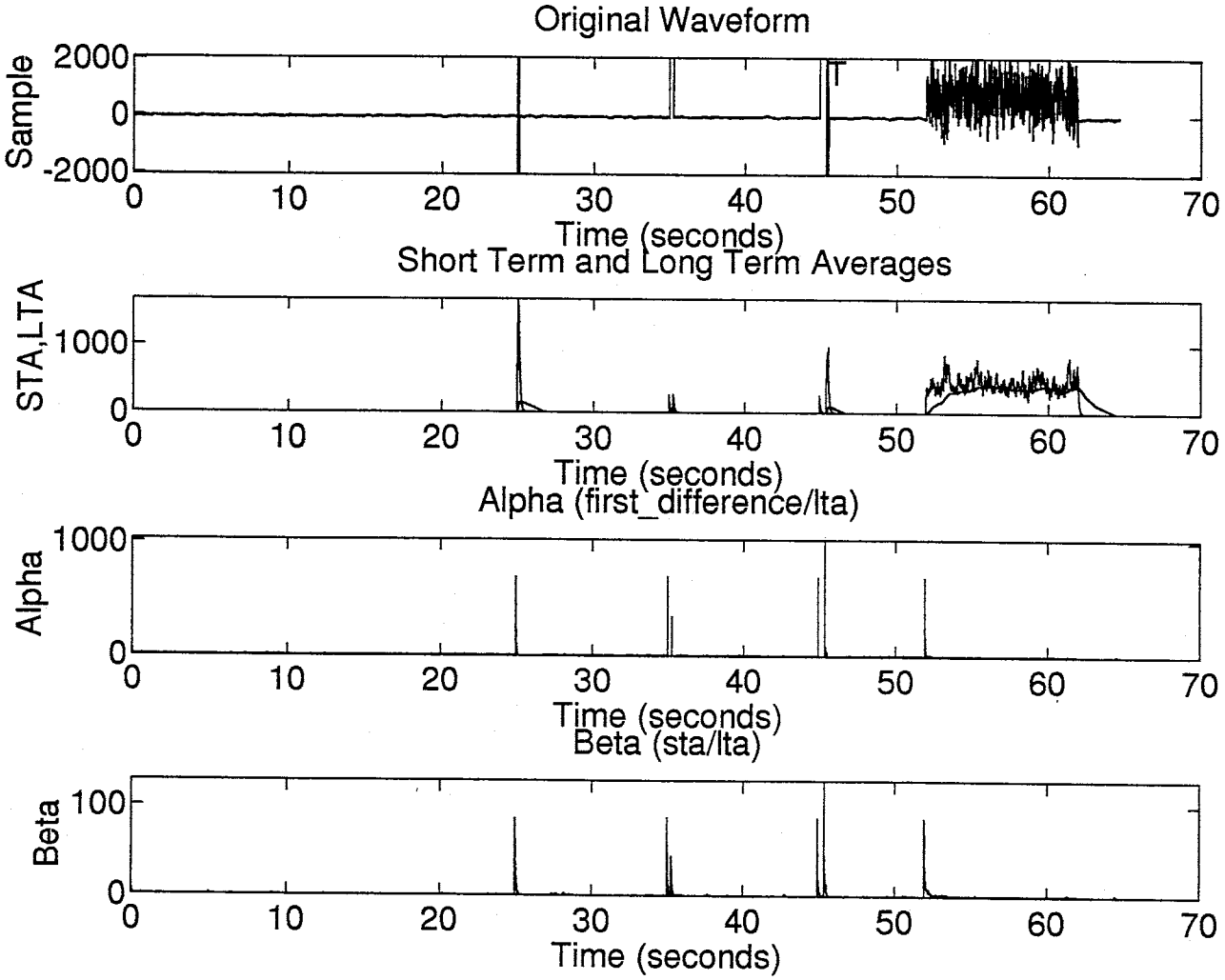

Figure 17 – Trigger parameters for a composite of noise signals
STAverageWindow = 8; LTAverageWindow = 128; LTALowerBound=1;
CriticalAlpha = 28; CriticalBeta = 10; TriggerConfirmationCount = 10;

Summary

While the IASPEI trigger does not provide the desired, broad event detection, the system does fulfill its design requirement of an easily installed and maintained, digital local event recording system. The system has proved to be reasonably stable, and easily installed and maintained. System reliability is high, a majority of operational failures are the result of limited disk space or disruption of electric power. However, the IASPEI system has notable weaknesses. The requirement of a Data Translation, digital data acquisition system restricts the end user's flexibility. Further, the legal licensing of the Data Translation device drivers adds approximately $250 to the price of the system, making the data acquisition hardware the single most expensive component in the system.

The limitations of the trigger algorithm can limit the scope of operation. Ideally a system to detect and record all seismic events, from local microearthquakes to teleseisms is desired. The IASPEI software clearly cannot simultaneously fill this wide requirement. Perhaps a more fundamental observation can be made once recognition is given to the spectacular advancements in computer hardware which have occurred in recent years. The severe computational limitations which plagued designers of previous systems have been lifted. Perhaps this added power is an invitation to reconsider techniques for digital event recording.

Data Analysis: Software Tools

Once digital data is acquired, efforts must be made to sort and reduce the data into a manageable database. This process was made easier by the development and installation of several software tools. These tools range from relatively simple UNIX c-shell scripts to complex assemblages of FORTRAN and C code. A thorough description of each of the tools available would be exhaustive and beyond the scope of this document. However, the more useful tools will be described. General purpose software tools will be described here, applications specific to a network will be presented in the Socorro Seismic Observatory and the Mount Erebus Volcano Observatory sections.

Conversion Tools

The IASPEI system records digital data using the SUDS data format. The analysis software used by the New Mexico Tech Geophysical Computing Center depends on the ah format. The program **suds2ah** (L. House, personal communication, 1991) is used to convert IASPEI data files to the ah format. The **suds2ah** program also performs the necessary byte switching to convert from MS-DOS binary format to UNIX binary format. Notably, **suds2ah** does not convert the fixtime structure, which contains time correction information output by the IASPEI **fixtime** program. The **fixtime** program uses an IRIG-E clock signal digitized simultaneously with the seismic data to recover timing information.

suds2ah expects an input filename to be given on the command line. The ah format data file will be written to a file with the same name as the input file, but with a ".ah" suffix. The ah format file can now be manipulated with any of the ah routines publicly available.

Routinely, data files need to be displayed or printed. Often, however, data files contain more points than can be printed or displayed without spatial aliasing due to limited printer or crt resolution. The **ahresamp** (Lamont distribution) program is used to resample the ah data file to a specified sample interval. **ahresamp** expects the new sample interval to be given on the command line, while the input and output files are handled through stdin and stdout respectively. The program **ahpscale** was created to examine the original ah format data file and calculate the appropriate sample interval given the number of desired data points. **ahpscale** expects the number of data points desired and the input filename to be given on the command line. The calculated sample interval is output to stdout. Ordinarily, **ahresamp** and **ahpscale** are used together. **ahpscale** calculates the correct sample interval, then **ahresamp** resamples the data.

The resampled data file can be converted to postscript with the **ah2ps.house** (L. House, personal communication, 1991) command. This program expects the input ah format data filename to be given on the command line. The postscript file is written to a file with ".ps" appended to the input filename. When using resampled data, the user must determine the number of data points to print. Currently, the Sparc printers used in the Geophysical Computing Center are capable of printing 300 dots per inch. The default postscript file output by **ah2ps.house** will use approximately 9.8 inches for the time series, so 2940 data points can be printed without aliasing.

The **ah2xpick** (L. House, personal communication, 1991) script is the last, commonly used conversion routine. This script calls several of the Lamont ah routines to prepare data files for use with the University of Alaska, Fairbanks' **xpick** software. **ah2xpick** expects the ah filenames to be given on the command line. The ah data file will be separated into individual files for each seismic station. These files will be written to a directory named according to the first sample time in the 'yymmddhhmmss' format.

The **suds2ah**, **ahresamp**, **ahpscale**, **ah2ps.house** and **ah2xpick** routines are generally invoked by script files written specifically for data from the Socorro or Erebus Seismic Networks. These script files are discussed in the Socorro Seismic Observatory and Mount Erebus Volcano Observatory sections.

xpick and seismos

The **xpick** software provides an interactive arrival picking tool. Further, **xpick** was designed to interact with the **hypo71** event location software. Combined, these tools can provide a graceful interface between the user and the event location determination program.

As a first step toward increasing the usefulness of **xpick**, particularly with Socorro area data, an interface to **seismos** (Hartse, 1991) was created. **seismos** is a simultaneous velocity model, hypocenter inversion package designed to include commonly observed mid-crustal magma body reflected phases seen on seismograms written by the Socorro Seismic Observatory. **seismos** depends on a laterally homogeneous velocity model. Luo and Dibble (1993) show that the lateral velocity structure beneath Mount Erebus varies dramatically. This lateral variation prevents the effective use of **seismos** or **hypo71** with Erebus data. As a result, **seismos** is only used with data recorded by the Socorro Seismic Observatory system. A more detailed description of the **xpick–seismos** link is given the Socorro Seismic Observatory section beginning on page 44.

Socorro Seismic Observatory

The Socorro Seismic Observatory provides a unique view into the processes accompanying continental rifting. Located near Socorro, New Mexico, in the Rio Grande Rift, the seismic network yields valuable information about the region's crust. Perhaps the most exciting discovery was the detection of a magma body approximately 19 kilometers beneath Socorro (Sanford et al., 1977; Hartse et al., 1992). Magma body reflected phases from local earthquakes were first seen by Sanford and Holmes (1961), and continue to be an important research topic.

The Seismic Network

The seismic network has experienced several different configurations, however the current network has been in place since 1983 (Sanford, personal communication, 1993). Figure 18 shows the station layout and an outline of the Socorro Magma Body. Station BDO was removed in 1992 (Sanford, personal communication, 1993), and station WTX was damaged during a thunderstorm in 1992. The seven current stations consist of 1Hz vertical-component seismometers and are recorded by both helicorders and by the digital data acquisition system.

Telemetry from the seismic stations uses VHF radio and microwave links. The radio signals are presently received at the Workman Center Tower on the New Mexico Tech Campus. The signals are sent to frequency modulation

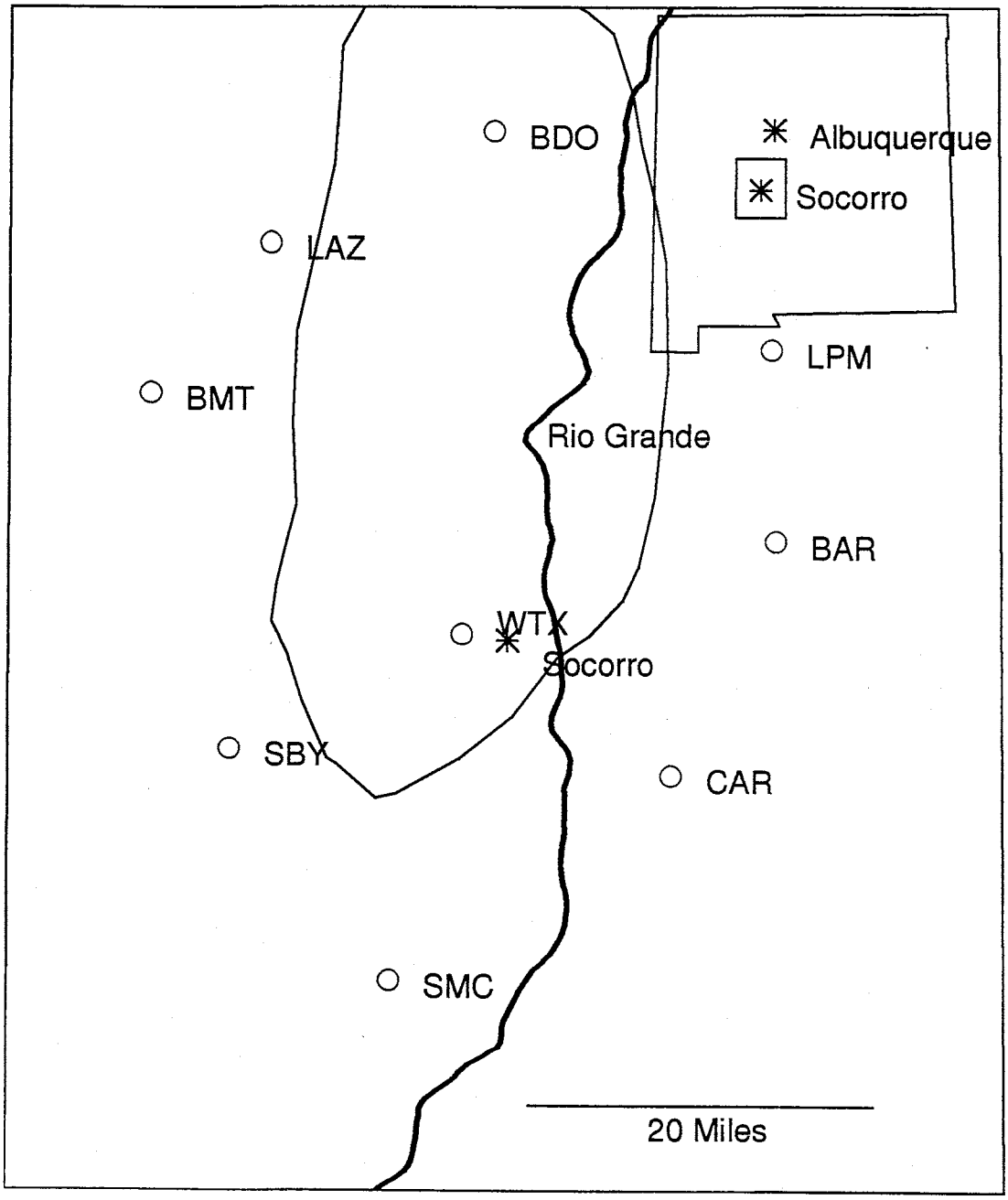

Figure 18 – Station Locations for Socorro Seismic Network

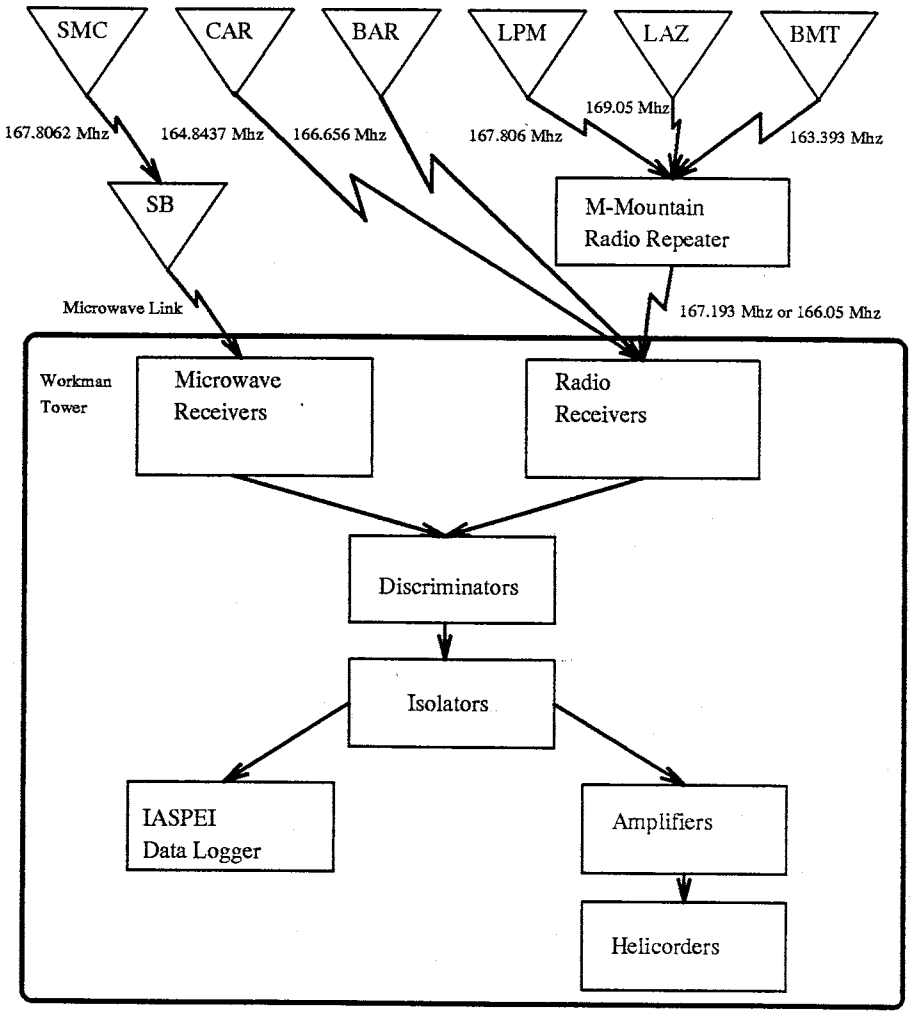

Figure 19 – Data flow diagram

discriminators and prepared for recording. Isolators are used between the digital and analog recording systems to prevent the failure of one system from interfering with the other recording system. Figure 19 provides a broad data flow diagram and the radio frequencies used by the Socorro Network.

Output from the discriminators and isolators is ± 5 volts. The IASPEI Data Acquisition System offers selectable gain settings providing appropriate digitization ranges. A gain setting of unity provides a full scale of ± 10 volts, however, unresolved discrepancies within the IASPEI system prevent the effective use of the gain 2 setting, which should digitize the full scale ± 5 volts as output by the discriminators.

The output from the discriminators/isolators is connected to the Data Translation DT-707 break out board. Control of the Data Translation DT2821 data acquisition and control card is handled by XDETECT as described in the IASPEI Seismic Data Logger section beginning on page 4.

At the time this document was prepared, TDETECT was operating in place of XDETECT. TDETECT is currently used to support a project involving the deployment of 12 portable, 3-component, digital seismographs on loan from the University of Wisconsin-Madison. Long range plans call for the return to XDETECT or the installation of a second data acquisition PC to support simultaneous teleseism and local event recording.

TDETECT is essentially XDETECT with the trigger algorithm replaced by one optimized for teleseism detection (Evans, 1992). The day to day operation of the data logger is thus nearly unchanged, regardless of whether TDETECT or XDETECT is in use.

The data logger PC is configured with several important files in the c:\ directory, plus subdirectories for XDETECT, TDETECT, PC-NFS (network control software), CTS-10 (WWV clock control software) and various software tools. Two essential files are located in the c:\ directory. The **config.sys** file contains information about the various devices, including the data acquisition card. The **autoexec.bat** file includes instructions to be executed at boot-time.

The **config.sys** file is used by MS-DOS to describe the operating environment. Source listing 6 shows the **config.sys** file used by the Socorro Seismic Observatory data acquisition system. Detailed information regarding the **config.sys** file can be found in most MS-DOS manuals, however portions of this file are specific to data logger operation. The "device \xdt204\atldrv.sys /E 768" command is used to install the device driver needed by the Data Translation acquisition card. The /E argument allocates extended memory to be used as buffers for the acquisition card. Several lines in the **config.sys** file are also used to install PC-NFS drivers. Additional information about the operation of PC-NFS can be found in the PC-NFS manuals located with the data logger. Finally, "device = cts10.sys" installs the device driver for the CTS-10 clock card.

```
break on
SHELL C:\COMMAND.COM /E:1000 /P
device = \xdt204\atldrv.sys /E 768
BUFFERS = 20
DEVICE=C:\ANSI.SYS
FILES=20
DEVICE=C:\NFS\PCNFS.SYS
DEVICE=C:\NFS\SOCKDRV.SYS
DEVICE=C:\DRIVERS\VECIE6.SYS /t2
DEVICE=C:\NFS\NFSVEC.SYS
LASTDRIVE=V
device = cts10.sys
```

Source Listing 6 – c:**config.sys** file used for the Socorro Seismic Observatory data logger.

The CTS-10 card provides WWV radio reception and decoding and updates the system clock at user selectable intervals, currently 20 minutes. This action keeps the system clock very close to World Standard Time as given by WWV. Although the system time may be extremely accurate, the IASPEI system maintains time internally according to the Data Translation acquisi-

tion card. If the clock onboard the acquisition card drifts, timing errors will be propagated to event storage. Two processes help reduce the timing errors. First, by rebooting the system once per day, the timing is reset to WWV. Second, 10 second time marks, generated for the analog helicorders, are digitized and recorded as channel CLCK, providing a cross-reference to the analog records.

Sun Microsystem's PC-NFS facilitates the mounting of remote devices on the Geophysical Computing Center's UNIX Domain. The PC-NFS installation currently defines drives D: E: and F:. Drive D: is linked to /wren3, while E: is /wren4 and F: is /mk1/scratch/socorro. Drive D: is the most heavily used network connection, and is currently used for all data transfers. With PC-NFS installed, drives can be accessed across the network as though the drives were physically attached to the PC. Changing the network drive configuration is simple and is well documented in the PC-NFS manuals.

```
echo off
SET TZ=MST7MDT
SET PCTOOLS=C:\PCTOOLS\DATA
echo — Set path
SET PATH=C:\;c:\dos;c:\analysis;c:\xdt204;c:\vi;c:\pctools;c:\mouse;c:\nfs;c:\wp51;c:\house\bin;
mouse
prompt $g
echo — Execute share for hard disk over 32 MB
c:\dos\share
DATAMON /SCREEN+
echo — Turn off NumLock key
c:\xdt204\numoff
echo - Go to xdt204 directory
cd \tdt
SET NFSDRIVE=C
PRT *
NFSRUN
echo — kill interrupt 24 (hack24)
hack24
call tstart.bat
```

Source Listing 7 – c:\autoexec.bat file used for the Socorro Seismic Observatory data logger.

The **autoexec.bat** file is the other control file in the c:\ directory. Source listing 7 shows the **autoexec.bat** file used for the Socorro installation. Like the **config.sys** file, the use of the **autoexec.bat** file is documented in most MS-DOS manuals. The SET commands simply sets environment variables used by different software packages, such as PC-NFS and CTS-10. The hack24 command turns off interrupt 24. This disables the normal dos disk error prompt 'Retry, Abort, Fail' and simply forces a fail condition. By forcing a fail condition, the automatic file transfer script, **tstart.bat** will not hang and disable the data logger if an error occurs. Finally, **autoexec.bat** calls **tstart.bat** which transfers data and restarts TDETECT.

The Auto Transfer Facility – tstart.bat

Once the **autoexec.bat** file has performed its tasks, it passes control to the **tstart.bat** file located in the c:\tdt directory (when XDETECT is in operation, **autoexec.bat** passes control to **xstart.bat** in the c:\xdt204 directory). While the **tstart.bat** control file is shown in source listing 8, the operation of **tstart.bat** and **xstart.bat** is identical except for the last line in the script.

```
if not exist d:data\magma.flg goto start
filecopy *.wvm d:data
if errorlevel 1 goto start
filecopy *.log d:data
if errorlevel 1 goto start
del event3\*.log
del event3\*.wvm
filecopy event2\*.* event3
del event2\*.log
del event2\*.wvm
filecopy event1\*.* event2
del event1\*.log
del event1\*.wvm
filecopy *.wvm event1
```

```
del *.wvm
del *.log
:start
tdetectv tdetect.inp >error.tdt
```

Source Listing 8 – c:\tdt**tstart.bat** file used for the Socorro Seismic Observatory data logger.

---

tstart.bat performs the daily data file transfer to griffy and restarts TDETECT. Several procedures are used to ensure a proper transfer. First, a flag system is used to verify the timing of the transfer. At 23:45 GMT each day a cron command is issued by the UNIX workstation "griffy" which creates a file called magma.flg in the /wren3/data directory, this file is removed by another cron command at 0:15 GMT. The **tstart.bat** script checks for the existence of this file before attempting to transfer data to griffy. This prevents the system from transferring data if **tstart.bat** is executed at any time other than the during the normal 0:00 GMT reboot. If **tstart.bat** does not detect the presence of magma.flg, it simply restarts TDETECT.

The second transfer integrity procedure makes use of the error codes generated by the **filecopy** command. **filecopy** was written by Leigh House of Los Alamos National Labs as a replacement for the normal DOS **copy** command. Unlike the **copy** command, **filecopy** returns an error code of 0 if it operates normally, or a 1 if an error occurred. By checking the DOS errorcode variable "errorlevel", **tstart.bat** can determine if the file transfer was successful. If an errorlevel of 1 is detected, **tstart.bat** assumes that the ethernet is inactive and simply restarts TDETECT.

Finally, **tstart.bat** maintains a revolving backup of the seismic data. If, and only if, the first two procedures return codes indicating a successful file transfer, then **tstart.bat** rotates the backup directories. **tstart.bat** deletes

the data files in the third backup directory, then moves the files from the second directory to the third directory. Next, **tstart.bat** moves the files from the first backup directory into the second directory. Finally, **tstart.bat** moves the current data files into the first backup directory and restarts TDETECT.

If either of the first two procedures indicate a failure, **tstart.bat** will not rotate the backup directories. This prevents untransferred data files from being deleted from the data logger and leaves untransferred files in the c:\tdt directory. The data logger will then attempt to transfer all untransferred files in a single batch during the next scheduled reboot.

The safety procedures described above were implemented on the TDETECT system. The **xstart.bat** file should be modified to reflect these enhancements before XDETECT is used again. Additionally, the crontab file for user digqks on griffy must be modified twice a year to reflect time changes. This is required because the data logger operates on UTC and griffy's clock is set to local time. If the crontab file is not modified, the magma.flg file will be created and deleted at the incorrect time, preventing normal file transfer. Source listing 9 shows the crontab file for user digqks.

```
0 0 * * * /home/griffy/digqks/bin/autoproc >> /wren3/data/autoproc.msgs
45 16 * * * /bin/touch /wren3/data/magma.flg
15 17 * * * /bin/rm /wren3/data/magma.flg
30 * * * * /home/griffy/digqks/bin/pingmagma
```

Source Listing 9 – crontab file for user digqks.

The Auto File Processing Facility–autoproc

The normal operation of the data acquisition and processing system calls for a scheduled reboot of the PC data logger at midnight Universal Time.

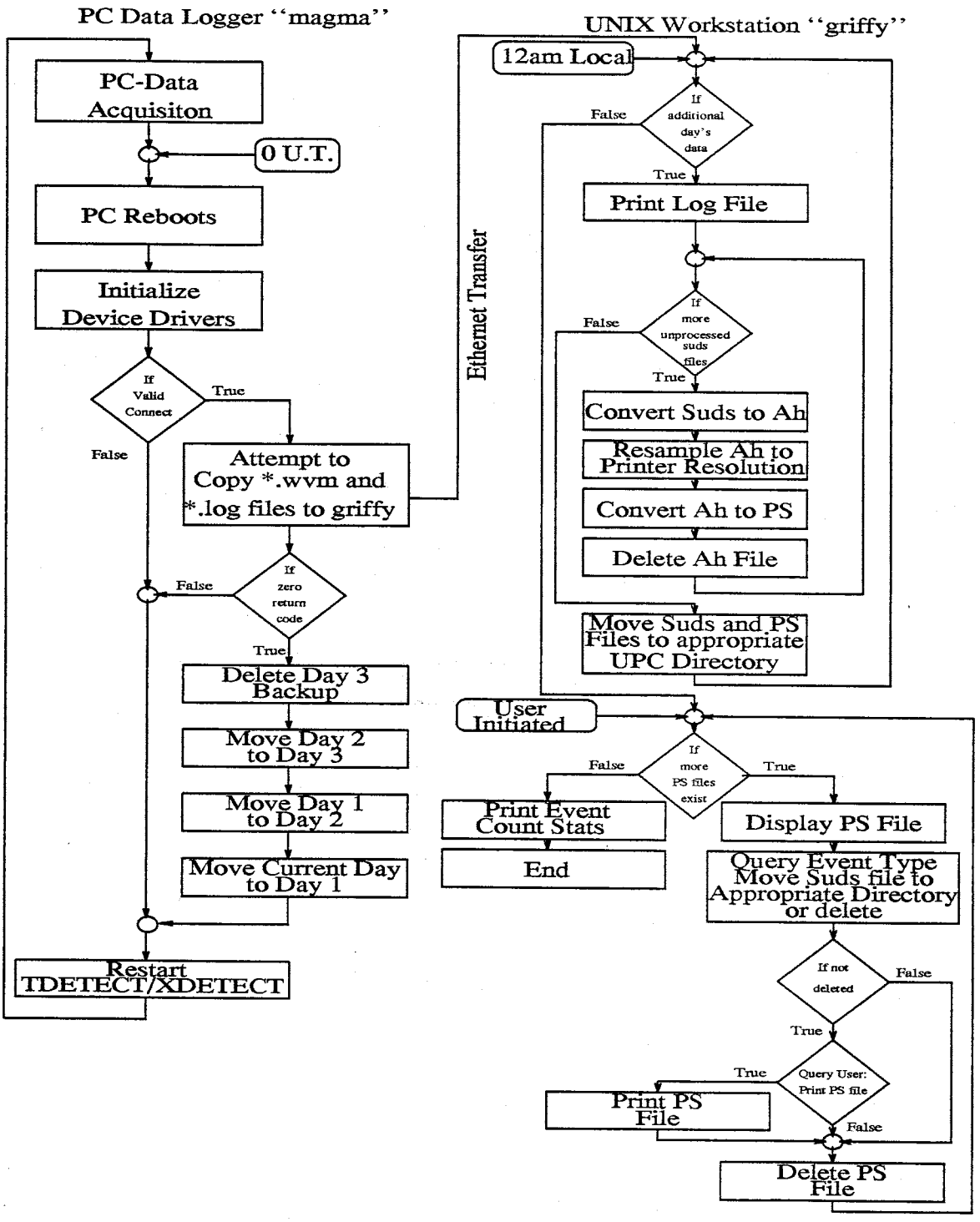

Figure 20 – Global data flow diagram

During this reboot, the procedures discussed above run on the PC. Midnight local time marks the initiation of a series of instructions which preprocess the data on the UNIX workstations. Figure 20 shows a global program/data flow diagram for the data processing cycle. At midnight local time, griffy initiates a command called **autoproc**. This task preprocesses the seismic data, preparing it for analysis.

autoproc is a UNIX c-shell script executed by the UNIX autoscheduling utility, cron. Currently, user digqks owns the cronfile which executes **autoproc** at midnight local time. The **autoproc** script is shown in source listing 10.

```
#!/bin/csh -f
# autoproc
# to be invoked using cron
#
set path=(/home/griffy/nmquakes/netstuff /home/griffy/nmquakes/bin /bin
/wren3/export/newsprint/bin /usr/ucb)
rehash
set noclobber
set nonomatch
echo autoproc running on `date`
#
# set the printer
#
set PRINTER = sparc1
#
# get into the data directory
#
set datadir = /wren3/data
cd $datadir
# find out what files, if any we have to work with
#
set nonomatch
#check for existence of data files
@ numwvm = `ls *.wvm | wc -l` >& /dev/null
if ( $numwvm == 0 ) then
  echo " autoproc: no data to process on" `date`
  echo ----------
  echo " autoproc: no data to process on `date`" | mail digqks@griffy
  exit 0
endif
# identify the number of days worth of unprocessed data in /wren3/data
set days = (`ls *.wvm | cut -c1-6 | sort | uniq`)
echo autoproc: $#days days worth of data to process:
```

```
echo $days
#
#
# print log files and make directory for each day
#
foreach i (`echo $days`)
  set upcdir = $i.upc
  echo autoproc: making $upcdir directory
  if ( -e $datadir/$upcdir ) then
    echo autoproc: warning... $datadir/$upcdir already exists
  else
    mkdir $datadir/$upcdir
  endif
  set logfile = $i.log
  #de-dos the log file
  /bin/dos2unix $i.log tmp$$
  mv tmp$$ $i.log
  if ( -e $logfile ) then
    echo " autoproc: printing log file" $logfile
    /usr/local/bin/enscript -h -G -2r -P$PRINTER $logfile
    #and move it to the logfiles directory
    mv $logfile logfiles/$logfile
  else
    echo " autoproc: cannot find log file" $logfile
  endif
  #process files for this day; generate postscript preview file
  #and pack the wvm data files
  set files= (`ls $i??.wvm`)
  echo " autoproc: processing $#files data files for day" $i
  foreach j ($files)
    suds2ah $j >& /dev/null
   /wren3/usr/users/nmquakes/ah/bin/ahresamp '/wren3/usr/users/nmquakes/ah/bin/ahpscale 2940
$j.ah' <$j.ah >$j.filter.ah
    ah2ps $j.filter.ah > /dev/null
    rm -f $j.ah
    rm -f $j.filter.ah
    echo autoproc: packing $j
    pack $j > /dev/null
  end
  echo autoproc: moving packed wvm files for day $i to $upcdir
  mv $i??.wvm.z $datadir/$upcdir/.
  echo autoproc: moving postscript preview files for day $i to $upcdir
  mv $i??.wvm.filter.ah.ps $datadir/$upcdir/.
end
echo autoproc: done
echo ------------------------------------------------------------
```

Source Listing 10 – /home/griffy/digkqs/bin/**autoproc** script.

The **autoproc** script is designed to correctly process data files transferred from the PC by **tstart.bat**. The script determines the number of days worth of data which need to be processed. This allows the script to correctly handle multiple day's data that may be stacked up on the PC due to failed transfers. A directory will be created for each day of data, named *date*.upc where *date* is the 6 character string containing the date in *year month day* format.

autoproc prints the IASPEI generated logfile and prepares the data files for previewing by **manproc** (see below). The script uses several of the commands described in the Tools for Data Processing and Analysis section beginning on page 41. **suds2ah** is used to create ah format data files. The ah format file is resampled to avoid spatial aliasing when printed. This is accomplished by the **ahresamp** and **ahpscale** programs. Finally, a postscript plot is generated for each data file. The postscript plot is used by **manproc** for data previewing. Once processed, the SUDS and postscript files are moved to the *date*.upc directory while the intermediate ah files are deleted.

The result of the execution of **autoproc** is the creation of a subdirectory for each day of processed data. This subdirectory contains compressed SUDS data files, and postscript plots ready for previewing by **manproc**.

The Interactive Display and Archive Facility – manproc

manproc was developed to provide an interactive environment in which the event data files could be sorted and processed according to event type. Initially, **manproc** provided bins for local, regional, quarry, teleseism, and unknown events. However, the regional and quarry bins were later combined into a single bin. **manproc** also provides the user with the opportunity to print data files, and to delete data files which are not useful.

manproc, like **autoproc**, is a UNIX c-shell script. Source listing 11 shows the **manproc** script. The user digqks was created for the purpose of event file processing, and its operating environment has been tailored for this operation. A special window on digqks's Openwindow display is sized and positioned for the use of **manproc**. Running **manproc** in the window nearest the bottom of the screen enables **manproc** messages to be displayed, and most of this window will remain visible, even when data plots are displayed.

```
#!/bin/csh -f
# man proc
# Preprocessing done by autoproc, a cron executed command.
# Displays event files, query user for event storage information
#
# 3/10/92, R. Aster, based on the Los Alamos script written by Leigh House
# 6/9/93, M. Skov, following:
# 8/11/93 R. Aster revised
# 10/24/93 M. Skov revised
#
set path=(/usr/users/nmquakes/netstuff /wren3/usr/users/nmquakes/bin
/bin /wren3/usr/users/nmquakes/ah/bin /wren3/export/newsprint/bin /usr/ucb)
rehash
set noclobber
set nonomatch
if ($#argv != 1) then
echo "usage: manproc datadir.upc
exit -1
endif
#check output directories
if ! -e wvmfiles mkdir wvmfiles
if ! -e wvmfiles/local mkdir wvmfiles/local
if ! -e wvmfiles/regional mkdir wvmfiles/regional
if ! -e wvmfiles/teleseism mkdir wvmfiles/teleseism
if ! -e wvmfiles/other mkdir wvmfiles/other
#
# set the printer
#
set PRINTER = sparc1
#
# get into the data directory
#
set DATADIR = /wren3/data/$1
cd DATADIR >& /dev/null
# find out what files, if any we have to work with
#
```

```
set numwvm = `ls *.wvm.filter.ah.ps | wc -l` >& /dev/null
#
#
# Preview the event files
#
set n=0
set nlocal=0
set nregional=0
set nteleseism=0
set nother=0
set nnoise=0
set nprint=0
if ( $numwvm > 0 ) then
  set files=`ls *.wvm.z | sed 's/\.z//'`
  foreach i ($files)
    clear
    @ n = $n + 1
    echo "pageviewing data plot for event "$i" ("$n" of "$numwvm"), please be patient..."
    /usr/openwin/bin/xview/pageview -Wp 10 10 -Ws 935 730 -right $i.filter.ah.ps &
    echo ""
    QUERY:
      echo "(1) Local event"
      echo "(2) Regional Earthquake/Explosion"
      echo "(3) Teleseism"
      echo "(4) Other"
      echo "(5) Noise - delete"
      echo "(6) Quit manproc"
      echo -n "Category:"
      set ans = $<
    if($ans != 1 && $ans != 2 && $ans != 3 && $ans != 4 && $ans != 5 && $ans != 6 )goto QUERY
     if ($ans == 1) then
       @ nlocal = $nlocal + 1
       mv $i.z ../wvmfiles/local/.
       goto PRINTYN
     endif
     if ($ans == 2) then
       @ nregional = $nregional + 1
       mv $i.z ../wvmfiles/regional/.
       goto PRINTYN
     endif
     if ($ans == 3) then
       @ nteleseism = $nteleseism + 1
       mv $i.z ../wvmfiles/teleseism/.
       goto PRINTYN
     endif
     if ($ans == 4) then
       @ nother = $nother + 1
       mv $i.z ../wvmfiles/other/.
       goto PRINTYN
     endif
```

```
    if ($ans == 5) then
      @ nnoise = $nnoise + 1
      /bin/rm -f $i.z
      /bin/rm -f $i.filter.ah.ps
      goto NEXTEV
    endif
    if ($ans == 6) goto QUIT
  PRINTYN:
    echo "Print event file (y)"
    set ans = $<
    if ($ans != "n") then
      @ nprint = $nprint + 1
      mv $i.filter.ah.ps /wren3/tmp/.
      lpr -h -s -r -P$PRINTER /wren3/tmp/$i.filter.ah.ps
    else
      /bin/rm $i.filter.ah.ps
    endif
  NEXTEV:
    set procnum = `ps -x | grep pageview | grep Wp | awk '{print $1}'`
    ( kill -9 $procnum ) >& /dev/null
  end
#
endif
QUIT:
clear
echo "Event Statistics for "$1" processed on "`date`":" | tee -a /wren3/data/manproc.msgs
echo "Total number of triggers: "$numwvm | tee -a /wren3/data/manproc.msgs
echo "....." | tee -a /wren3/data/manproc.msgs
echo "Local events:          "$nlocal"/"$numwvm | tee -a /wren3/data/manproc.msgs
echo "Regionals/Explosions:  "$nregional"/"$numwvm | tee -a /wren3/data/manproc.msgs
echo "Teleseisms:            "$nteleseism"/"$numwvm | tee -a /wren3/data/manproc.msgs
echo "Other:                 "$nother"/"$numwvm | tee -a /wren3/data/manproc.msgs
echo "Deleted:               "$nnoise"/"$numwvm | tee -a /wren3/data/manproc.msgs
echo "....." | tee -a /wren3/data/manproc.msgs
echo "Events printed:        "$nprint"/"$numwvm | tee -a /wren3/data/manproc.msgs
cd ..
# don't remove data directory if user selected quit.
if ($ans != 6) then
  rmdir $1
endif
```

Source Listing 11 – /home/griffy/digkqs/bin/**manproc** script.

---

manproc expects an argument providing the directory containing the data files to be processed. The script then individually displays each postscript file in the directory with a prompt allowing the user to select the appropriate event bin for the SUDS data file. When XDETECT is operating, additional

processing is performed depending on the event type selected. Event files tagged as local events are conditioned for use with **xpick**, currently, however, teleseisms are the events of interest, and local events receive no additional processing.

xpick and seismos

While **xpick** could be used to obtain body-wave phase picks from teleseisms recorded by TDETECT, the principal benefits of **xpick** become apparent when studying local events. **xpick** provides an interactive environment from which the user can make P and S picks as well as measure coda length, amplitude and phase frequency. The p and s arrival times, and the coda length can be output to **hypo71** or **seismos** for further processing.

seismos was written by Hans Hartse to provide a simultaneous hypocenter location and velocity model inversion. **seismos** can also be used with a fixed velocity model to determine event hypocenter. **seismos** is also more versatile than **hypo71**; the code can make use of information contained in P and S arrivals, plus information contained in the head waves P_g, S_g, P^*, S^*, P_n, S_n, moho reflections S_mP, S_mS, P_mP, P_mS, and top side magma body reflections S_zP, S_zS, P_zP, and P_zS (Hartse, 1991). The importance of mid-crustal reflections cannot be overstated, as reflected phases significantly enhance the ability to determine hypocenters, particularly hypocentral depth (Hartse et al. 1992).

The connection between **xpick** and **seismos** does not, however, presently allow the use of reflected phases. Difficulties with the **xpick** code have delayed local attempts to update the software for additional phase picking. Reflected phases can, however, be picked and entered manually into **seismos** with the present software.

The communication system between **xpick** and **seismos** is based on a script originally designed for the **xpick** to **hypo71** interface. The script is called **XHYPOE**, and it contains the necessary program calls to pass information to and from **seismos**. Source listing 12 shows the **XHYPOE** script.

```
#! /bin/csh
# c shell script to run SEISMOS
echo The base name is $2
echo The path to phase file is $1
rm picfil.dat
echo " "
echo " "
echo " "
xpick2seismos <$1
cp picfil.dat /home/griffy/digqks/model_param
cd /home/griffy/digqks/model_param
echo " "
echo " "
echo " "
/home/griffy/nmquakes/bin/seismos
echo " "
echo " "
echo " "
echo " "
echo " "
echo " "
echo " "
echo " "
echo "SEISMOS OUTPUT..."
echo " "
echo " "
more -l refloc.dat
echo " "
echo "press <return> to continue"
/usr/local/bin/pause
echo " "
headplt
echo " "
cp $1 seismos2xpick.tmp
seismos2xpick <seismos2xpick.tmp > $1
rm seismos2xpick.tmp
echo " "
echo " "
echo end of script
```

Source Listing 12 – The **XHYPOE** UNIX shell script called by **xpick** to pass pick file information to **seismos**.

Because **xpick** was designed to interact with **hypo71**, the necessary code is already in place to provide a user initiated location program. The user can simply press the hypoe button in **xpick** to locate an event. This will call the **XHYPOE** script which performs the task of calling the event location software. While **hypo71** can provide hypocenter locations, **seismos** is better suited to operate on Socorro area data. This will become even more true when the **xpick** modifications are completed allowing the interactive picking of reflected phases.

The pick file data formats for **hypo71** and **seismos** are different, however, all that is needed is a routine to convert pick files between **xpick** and **seismos** formats. To facilitate the pick file conversion, the program **xpick2seismos** was created. This program reads a **xpick** pick file through stdin, and writes a **seismos** compatible *picfil.dat* file. Similarly, a program is required to parse the **seismos** output file for hypocenter location. **seismos2xpick** reloads the original **xpick** format pick file through stdin and enters the hypocenter location generated by **seismos**. **seismos2xpick** then rewrites the **xpick** file to stdout. **xpick** will save the event location information with the ah data files, providing a compact, portable archive.

Permanent Tape Archive

The final task in the data processing cycle is the creation and maintenance of a permanent, tape archive. Presently, the SUDS data files, along with logfiles, are grouped together and stored on exabyte tape using the UNIX *tar* archive utility. The exabyte drive is physically attached to the Sparcstation "zerbina", while the data is stored on drive "/wren3" which is physically attached to "griffy". To reduce the network load, it is suggested that the archive process make use of a remote shell between griffy and zerbina. From a

griffy window, execute the command: "tar cvfb - 20 logfiles/*yearmonth**.log wvmfiles/local/*yearmonth**.wvm.Z wvmfiles/regional/*yearmonth**.wvm.Z wvmfiles/teleseism/*yearmonth**.wvm.Z wvmfiles/other/*yearmonth* | rsh zerbina dd obs=20b of=/dev/rst0", where *yearmonth* is the 4 character string containing the year and month to be archived. Ordinarily, a new archive is created for each month of data, and two tape copies are made. When XDETECT returns to operation, and **xpick** is used to pick and locate events, the ah format data files need to be included in the archive. If archive scheduling, or naming conventions change, the filenames and wildcards in the above tar command will need to be changed. The SunOS Reference Manual (1990) contains more information about tar and rsh.

IASPEI Operation Notes for the Socorro Seismic Observatory

The Socorro network data processing cycle is a accomplished using a well-defined collection of software tools. The optimal operation of XDETECT, however, remains more difficult due to the nonstationarity of the noise field. Further evaluation of the trade-offs between numerous false triggers and sensitivity to small local events would be helpful. Frequent attention to climatic and other network influences is currently required to provid the added selectivity necessary to maintain system sensitivity and reduce the volume of noise triggers.

The IASPEI Seismic Data Logger section of this paper describes the operation of the trigger, however, a few comments can be made with regard to the specific installation for the Socorro Seismic Observatory. The Socorro Seismic Network is aging, as a result, station operation is sometimes intermittent. Careful attention should be given to the selection of triggering stations.

Selection criteria should include telemetry considerations. Figure 19 shows the telemetry for the Socorro Network. As many as three stations share the same radio link, therefore electronic noise on a single channel can affect up to three stations. XDETECT is prone to trigger on telemetry drop outs (Figures 12, 13, 14, 16 and 17), therefore trigger status from stations sharing telemetry should be chosen carefully.

The telemetry trigger problems can be reduced by selecting a critical μ (minimum number of stations required to trigger) greater than 3, or by limiting the number of stations which with shared telemetry are enabled for triggering. By increasing critical μ above the number of stations sharing a radio link, the IASPEI system cannot trigger on a telemetry glitch alone. Similarly, changing the trigger status of stations sharing a radio link will reduce the number of triggered channels affected by a telemetry dropout. Frequently, however, local microearthquakes will not trigger across the network. Selection of a large critical μ value, or the removal of a station from the trigger list will thus reduce the sensitivity of the system to small events.

Adjustments to trigger parameters are also required as the seasons change. Winter storms off the Pacific coast induce large microseisms with periods greater than a few seconds which can cause trigger problems, particularly for TDETECT. Spring winds, and summer thunderstorms produce high frequency noise which causes XDETECT to false trigger. Attention to climatic changes is crucial for the successful operation of the seismic data logger.

Despite these caveats, the IASPEI system can still yield impressive results. Figure 21 shows an event recorded in June of 1993 during a period of particularly intense network problems. Although several stations were either down completely, or were producing unusually high noise levels, the IASPEI system triggered this $M_d \approx 0.5$ local event.

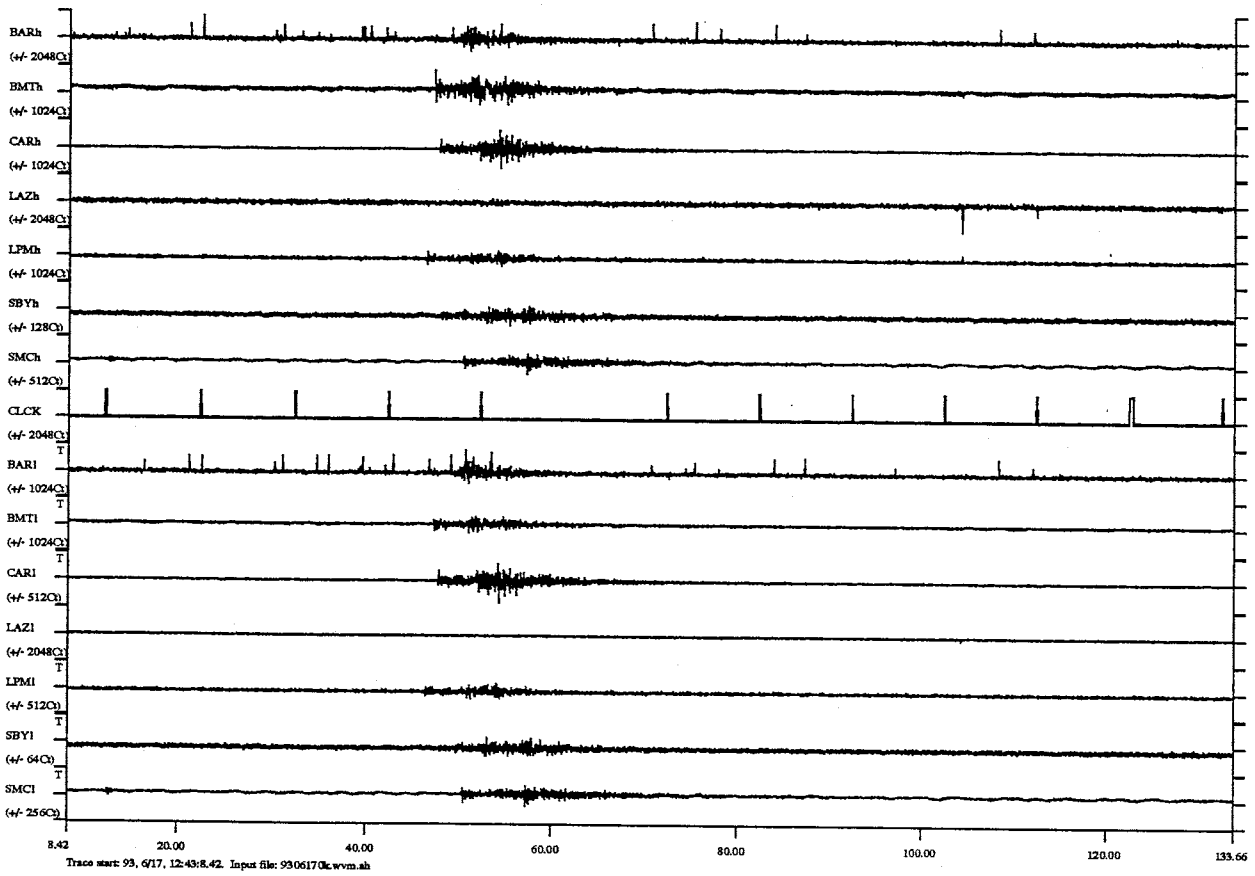

Figure 21 – Typical local event near Socorro, New Mexico as recorded by the IASPEI system.

Mt. Erebus Volcano Observatory

Mount Erebus is a 3794 m high active volcano on Ross Island, Antarctica. The volcano has a long history of continuous or near continuous activity. In 1841, Sir James Ross observed volcanic activity on the mountain he named for his ship *Erebus*. Other observations made throughout the 20th century confirm the activity of Mount Erebus (Giggenbach et al., 1973). Since 1972, Mount Erebus has been subject to near yearly geochemical and seismic observation.

The continuous activity of Mount Erebus makes it an excellent candidate for seismic observations. Seismometers were first deployed in 1973. The first successful observations were made in 1974 (Kyle et al., 1982). The current network was deployed during the 1980-81 field season as part of the International Mount Erebus Seismic Study (IMESS) (Rowe and Kienle, 1986). Instrumentation has also included infrasonic detectors and an electromagnetic induction loop (Dibble et al., 1984). The induction loop was an attempt to measure gas emissions and ion flux, while the infrasonic detectors yielded air wave data from explosions in the exposed magma chamber.

The Observatory

The Mount Erebus Volcano Observatory (MEVO) was created in 1992 as a continuation of the long term study of Mount Erebus. The project is designated as S-081 under the direction of Dr. Philip Kyle of The New Mexico Institute of Mining and Technology. Research efforts include geochemical and

geophysical measurements of volcanic activity. The primary focus here is the operation of the digital seismic data acquisition system installed during the 1992-93 field season.

The MEVO data logger installation makes use of new resources in McMurdo Station, Antarctica. The data logger is physically located in phase two of the new Crary Science Lab. This lab was still under construction during the 1992-1993 field season, however phases one and two of the the three phase project are complete. A new communication system called STARS went on-line during the 1992-93 field season, which provides voice and high-speed data communication capabilities. The STARS system allows, for the first time ever, the daily transfer of seismic data from the Mount Erebus Seismic Network to research facilities in the United States.

The availability of the new resources inspired the development of a nearly automated data acquisition and handling system. While the promise of STARS was known during the design and purchasing phase of the project, the exact implementation was not known until after the S-081 deployment in November, 1992. As a result of the uncertainty, many of the procedures had to be developed while on the ice. While these procedures are effective, hindsight suggests several improvements, which could be implemented during subsequent field seasons.

The current MEVO system is similar, in many ways, to the Socorro Seismic Observatory implementation. The system employs XDETECT to provide data acquisition and control. A set of script files provides control over data transfer, and a Sun Sparcstation provides data reduction and archiving. There are also significant differences between the two systems, specifically, the MEVO system requires additional file handling to make use of the STARS system as well as the Crary Lab local area network.

The Mount Erebus Seismic Network

The Mount Erebus Seismic Network consists of six permanent stations on Mount Erebus and one temporary station located at McMurdo Station. One Hz vertical-component seismometers are used, and the six permanent stations employ Very High Frequency radio for telemetry. Voltage Controlled Oscillators (VCO) are used used by the six permanent stations to modulate the signal around an audible center frequency, providing signal multiplexing.

The radio receivers are located in the old water plant on Observation Hill. This sight was selected for its line of sight attributes – other sites in McMurdo can not provide line of sight to Mount Erebus. Antarctic Support Associates generously installed 25 pair phone cable between the radio receivers and the data acquisition hardware in Crary 205.

Signals from the seven seismometers converge in Crary Lab 205 where they are prepared for digitization by the IASPEI system. Signals from the six permanent stations are discriminated and sent to the IASPEI data acquisition hardware. The signal from the temporary McMurdo station, MCMz, is amplified before digitization. Table 1 shows the radio frequencies and VCO center frequencies for the six permanent stations and figure 22 shows the station locations.

MEVO Station Information				
Station name	Receiver	VCO Center	Transmitter	Destination
Abbott Peak	- - - - - - -	1700 Hz	169.825 MHz	Hooper's Shoulder
Hooper's Shoulder	169.825 MHz	1360 Hz/1700 Hz	164.846 MHz	Observation Hill
Truncated Cones	- - - - - - -	680 Hz	163.809 MHz	Observation Hill
E1	- - - - - - -	2720 Hz	161.809 MHz	Observation Hill
Bomb	- - - - - - -	2720 Hz	165.809 MHz	Macz
Macz	165.809 MHz	1020 Hz/2720 Hz	167.809 MHz	Observation Hill

Table 1 – Station telemetry information

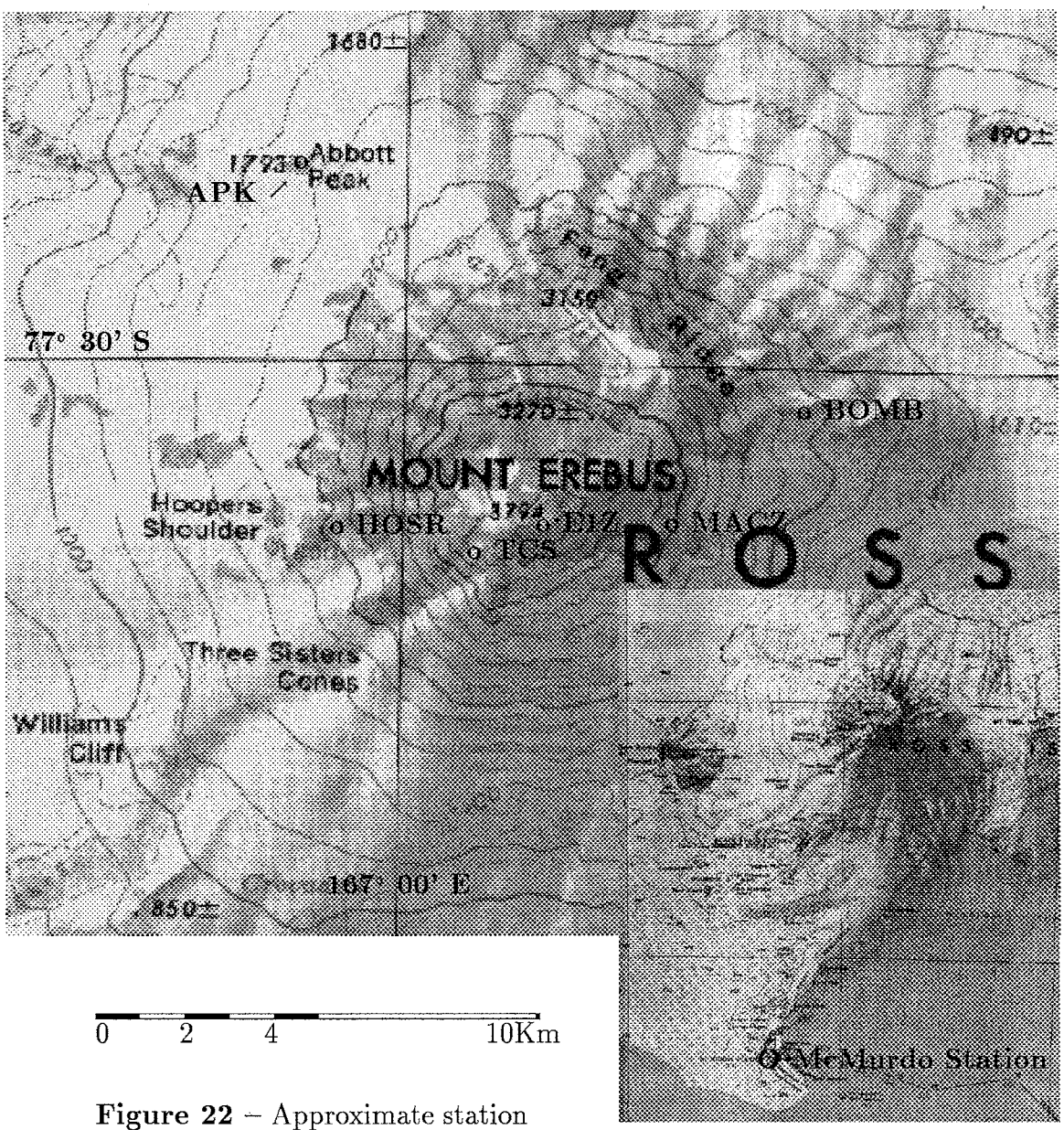

Figure 22 – Approximate station locations for the Mount Erebus Seismic Network. Station locations and elevations are given in Table 2. McMurdo Station is approximately 37km from Erebus Summit. Background map: USGS, Washington, D.C. 20242 Ross Island, Antarctica ST 57-60/6*(162°E-170°E.)

During the 1993-94 field season, the USGS conducted a Differential Global Positioning System survey of 5 sites on Mount Erebus. The results of the survey are consistant with prior station location efforts, and the results are shown in Table 2.

MEVO Station Locations			
Station name	Station ID	Original Location	1993-94 GPS Survey*
Abbott Peak	APK	77.45700°S 166.90908°E 1789m	77.45702°S 166.90931°E 1794.0m
Hooper's Shoulder	HOSR	77.53158°S 166.93236°E 2121m	77.53159°S 166.93247°E 2126.6m
Truncated Cones	TCS	77.53464°S 167.08514°E 3476m	77.53461°S 167.08544°E 3458.2m
E1	E1Z	77.53058°S 167.14047°E 3708m	----- ----- -----
Bomb	BOMB	77.50894°S 167.44017°E 2012m	77.50890°S 167.43991°E 2018.1m
MacZ	MACZ	----- ----- -----	77.53247°S 167.24639°E 3336.8m

*1993-94 USGS Differential Global Positioning Survey at a point near the station location, but not necessarily at the seismometer location.

Table 2 – Station locations (Kyle, personal communication, 1994).

IASPEI Operation Notes for the Mount Erebus Seismic Network

Operation of the IASPEI system for MEVO is nearly identical to the operation in Socorro. Like the Socorro implementation, trigger parameters need to be changed throughout the year. Power limitations result in station failure during the dark austral winter. During the summer months, waves in the open water around Ross Island create long period noise which can cause trigger difficulties. Attention to changing conditions is vital, particularly when one considers the communication time required to update the trigger configuration.

Communication between Socorro and McMurdo depends on email via the STARS communication system. Configuration updates require assistance from the winter over technician. Email can currently be sent to COS-RAY@mcmvax.mcmurdo.gov to request a system modification. The winter over technician regularly reads email and will make the requested changes as

time permits. It is important to remember that the technician is responsible for several projects from other science groups. As a result, requested changes may not be made for several days.

The control files are configured as described in the IASPEI section beginning on page 4. Currently, the acquisition system is configured with a restrictive trigger because of limited station operation. A more robust trigger configuration will be installed once the seismic stations are serviced during the 1993-94 field season.

Operational Overview

The data transfer system for the MEVO installation is considerably more complex than the Socorro system because of the difficulties associated with the utilization of the Crary Lab local area network and the STARS internet connection. Figure 23 shows the global data flow diagram for the MEVO seismic monitoring system.

The daily data transfer begins at midnight McMurdo time when XDETECT forces the PC to reboot. During the reboot process, the PC attempts to establish a network connection and, if successful, copies the data to the Sparcstation "mcmsun5" in the Crary Lab Computer Center. At 1:00 am McMurdo time, (5:00 am MST, one day earlier) mcmsun5 initiates a script which copies the seismic data to the Sparcstation "griffy" at New Mexico Tech via the STARS communication system.

The reboot process begins by booting the PC from the $3\frac{1}{2}$ inch floppy disc (booting from floppy is required because the network interface card in the PC attempts to boot the PC from the network unless the computer is started from floppy, which has a higher boot priority). The floppy contains only the necessary files to make it a bootable disc. The **config.sys** and **autoexec.bat**

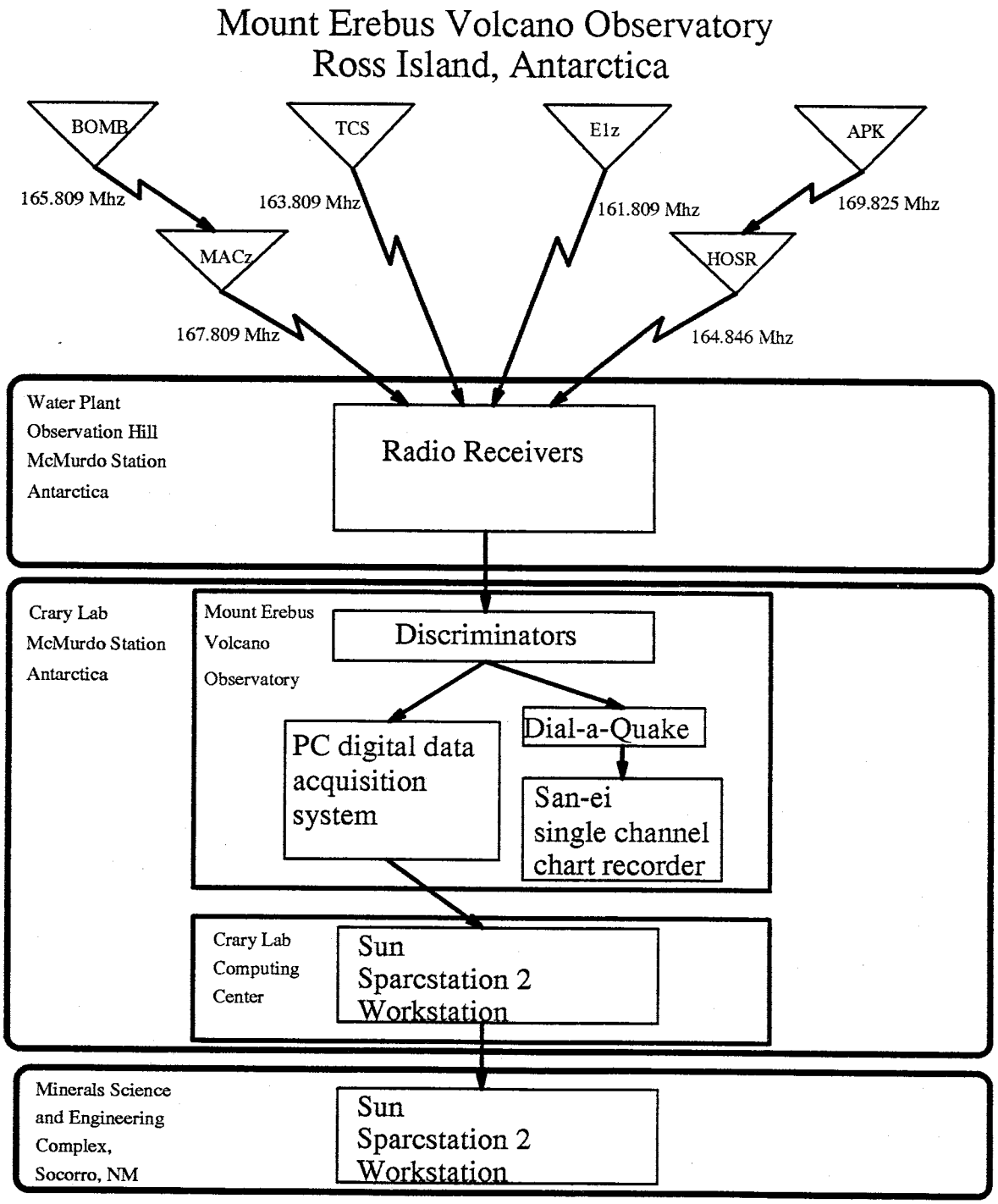

Figure 23 – Data Flow diagram for the Mount Erebus Volcano Observatory Seismic Network

files, shown in source listings 13 and 14, provide minimum support to start the PC before passing control to script files located on the 210 megabyte hard disc, c:.

```
rem Do NOT use HIMEM or attempt to load DOS HIGH
rem Interferes with XDETECT
rem DEVICE=C:\DOS\HIMEM.exe
rem DOS=HIGH,UMB
rem DEVICE=C:\DOS\CEMM.EXE /NOEMS
SHELL=C:\DOS\COMMAND.COM /E:1024 /P
BUFFERS=40
FILES=35
DEVICE=C:\DOS\CACHE.EXE 1856
DEVICE=C:\xdt204\atldrv.sys /E 2048
rem old clock card driver below
rem DEVICE=C:\cts10.sys
```

Source Listing 13 – a:**config.sys**

c:**autoexec.bat**

Source Listing 14 – a:\autoexec.bat

The **config.sys** file contains information about devices on the PC. The atlab.sys driver controls the Data Translation data acquisition hardware, allocating 2048 buffers. Although placing DOS in highmem can improve system performance, this action apparently interferes with the operation of the acquisition hardware. Because of this incompatibility, the first three lines were commented to prevent implementation. Finally, the cts10.sys driver is used by the CTS-10 WWV radio receiver. This card would synchronize the PC clock to WWV, however, radio reception is poor and this device could not be implemented during the 1992/93 field season.

The **a:\autoexec.bat** file simply passes control to the **c:\autoexec.bat** shown in source listing 15. The **c:\autoexec.bat** file calls other script files which establish the network connection, backup and transfer the data files, and restart XDETECT.

```
@ECHO OFF>NUL
cd c:\
c:
rem Set non-network path
SET PATH=C:\; C:\DOS; C:\KEDIT; C:\HOUSE\BIN; C:\xln\bin40
SET PROMPT=$P$G
sort <c:\xdt204\startup\sortfile.2 >nul
SET EXCELAN=C:\XLN
VER
sort <c:\xdt204\startup\sortfile.2 >nul
rem Call the network script
call c:\net\net.bat
C:
rem Set network path
SET PATH=C:\; C:\DOS; C:\KEDIT; C:\HOUSE\BIN; C:\xln\bin40; C:\XDT204; Z:.; Y:.; X:.; W:.;
cd C:\xdt204
rem Call transfer and xdetect startup script
xstart.bat
```

Source Listing 15 – c:\autoexec.bat

Embedded in the **autoexec.bat** file are several unusual instructions. One of these instructions is the sort command which is used to create a short delay. The SET command is used to set environment variables. The PATH environment variable is set twice. Initially, PATH is set to include only directories required by **autoexec.bat** or by a user who interrupts **autoexec.bat** before completion. Later, PATH is set to include the network drives obtained by the **net.bat** script.

The Auto Transfer Facility

The **net.bat** script is called by **c:\autoexec.bat**, but may be recalled by **xstart.bat**. The **net.bat** script is used to establish a connection to the Crary Lab local area network. Source listing 16 shows the **net.bat** script.

The implementation of this particular type of network connection is common throughout the Crary Science Lab. The Antarctic Support Associates computer personnel understand and can provide documentation for the operation of the network hardware and software.

```
REM  Network startup script
REM  This script executes the commands necessary to establish
REM    a connection to the CSEC Local Area Network
REM  No network documentation was available when this script
REM    was created - but it works
REM Repeated commands to "ensure" connection
@ECHO OFF >NUL
sort <c:\xdt204\startup\sortfile.2 >nul
LH C:\NET\LSL >NUL
LH C:\NET\LSL >NUL
sort <c:\xdt204\startup\sortfile.2 >nul
LH C:\NET\NE2000 >NUL
LH C:\NET\NE2000 >NUL
LH C:\NET\NE2000 >NUL
sort <c:\xdt204\startup\sortfile.2 >nul
LH C:\NET\IPXODI >NUL
LH C:\NET\IPXODI >NUL
sort <c:\xdt204\startup\sortfile.2 >nul
LH C:\XLN\BIN40\TCPIP >NUL
LH C:\XLN\BIN40\TCPIP >NUL
LH C:\XLN\BIN40\TELAPI >NUL
LH C:\XLN\BIN40\TELAPI >NUL
LH C:\NET\NETX PS=SEC >nul
LH C:\NET\NETX PS=SEC >nul
sort <c:\xdt204\startup\sortfile.2 >nul
C:\NET\LSL >NUL
C:\NET\NE2000 >NUL
C:\NET\IPXODI >NUL
sort <c:\xdt204\startup\sortfile.2 >nul
LH C:\XLN\BIN40\TCPIP >NUL
LH C:\XLN\BIN40\TELAPI >NUL
LH C:\NET\NETX PS=SEC >nul
cd c:\
```

Source Listing 16 – c:\net**net.bat**

When **net.bat** finishes, it passes control back to the calling script, usually **autoexec.bat**. **autoexec.bat** then calls **xstart.bat** which backs up and copies data, and restarts XDETECT. The **xstart.bat** script is shown in source listing 17.

```
@ECHO OFF >nul
REM Xdetect startup script
REM Michael Skov Jan 1993
REM sort commands used for delay purposes
REM
REM
```

```
REM IF the network connection does not exist, attempt to
REM   establish the connection by calling net.bat up to 4 times
REM
REM The login.exe command is the command normally executed when
REM   logging onto the PC network. We just check for the
REM   existence of login.exe as a test of our network connection.
REM
if not exist f:login.exe call c:\net\net.bat
if not exist f:login.exe call c:\net\net.bat
if not exist f:login.exe call c:\net\net.bat
if not exist f:login.exe call c:\net\net.bat
REM
REM Allow the user to exit the script with a <ctrl>-c
break on
rem *** xdetect startup ***
cd c:\xdt204
c:
cls
REM
REM Alert the user about importance of using this script
REM   Only at midnight
tone
echo ********** WARNING    WARNING    WARNING    ****************
echo **********          WARNING    WARNING          ****************
echo ********** WARNING    WARNING    WARNING    ****************
sort <c:\xdt204\startup\sortfile.2 >nul
echo.
echo.
echo The end of day backup procedure is about to begin...
echo.
sort <c:\xdt204\startup\sortfile.2 >nul
REM
REM Do not want data to transfer unless this is midnight reboot
echo This procedure should be performed only once per day during the
echo    auto-reboot (midnight local.)
sort <c:\xdt204\startup\sortfile.2 >nul
sort <c:\xdt204\startup\sortfile.2 >nul
echo Press ctrl-break to abort this procedure
sort <c:\xdt204\startup\sortfile.2 >nul
sort <c:\xdt204\startup\sortfile.2 >nul
sort <c:\xdt204\startup\sortfile.2 >nul
sort <c:\xdt204\startup\sortfile.2 >nul
sort <c:\xdt204\startup\sortfile.2 >nul
REM
REM Turn break off. Do not allow user to exit script with
REM   a <ctrl>-c. Avoid partial data transfer.
break off
echo.
echo.
echo Auto backup procedure in progress ...
echo do NOT halt
echo.
rem *** fixtime using IRIG-E code on channel o ***
```

```
for %%f in (event1\*.wvm) do fixtime 0 %%f
echo Times recovered from IRIG-E
echo Moving files to backup directories ...
rem copy files to backup directories ***
cd event7
REM
REM Delete unnecessary log files (those more than 1 week old)
REM   from the xdt204 directory
for %%f in (*.log) do del ..\%%f
REM
REM Shuffle data through backup directories
REM Note, current day's data will only be moved if
REM we have a valid network connection.
cd ..
del event7\*.wvm
del event7\*.log
cd ..\event6
mv *.wvm ..\event7
mv *.log ..\event7
cd ..\event5
mv *.wvm ..\event6
mv *.log ..\event6
cd ..\event4
mv *.wvm ..\event5
mv *.log ..\event5
cd ..\event3
mv *.wvm ..\event4
mv *.log ..\event4
cd ..\event2
mv *.wvm ..\event3
mv *.log ..\event3
cd ..\event1
REM
REM If valid network connection, move current data files to
REM   day old directory (event2). Otherwise leave data
REM   until tomorrow's transfer
REM Should change the file check to a file on mcmsun5 rather
REM than the PC-server – However, we don't actually mount
REM discs on mcmsun5, so we check the PC-fileserver
if exist f:login.exe mv *.wvm ..\event2
cd ..
REM
REM Copy config file to a logfile, so it will be transferred
REM to Socorro
copy xdetect.inp xdtinp.log
REM
REM If valid network connection, move current log files to
REM   day old directory (event2). Otherwise leave logs
REM   until tomorrow's transfer
if exist f:login.exe copy *.log event2\*.log
echo Files copied to local backup directories
REM
REM If valid network connection,
```

```
rem *** copy files to mcmsun5 ***
if exist f:login.exe ftp -i <ftplink.bat
rem
echo Files copied to mcmsun5
echo.
if not exist f:login.exe echo WARNING... NO NETWORK CONNECTION !!!
cd c:\xdt204
echo BACKUP COMPLETE
echo starting xdetectv
rem *** start xdetectv with normal settings (xdetect.inp and station.@@@)
rem
rem But first wait 10 minutes to a avoid a second reboot - see below
sort <c:\xdt204\startup\sortfile.2 >nul
echo MUST DELAY START OF XDETECT BY ABOUT 10 MINUTES:
ECHO ...10
sort <c:\xdt204\startup\sortfile.3 >nul
ECHO ...9
sort <c:\xdt204\startup\sortfile.3 >nul
ECHO ...8
sort <c:\xdt204\startup\sortfile.3 >nul
ECHO ...7
sort <c:\xdt204\startup\sortfile.3 >nul
ECHO ...6
sort <c:\xdt204\startup\sortfile.3 >nul
ECHO ...5
sort <c:\xdt204\startup\sortfile.3 >nul
ECHO ...4
sort <c:\xdt204\startup\sortfile.3 >nul
ECHO ...3
sort <c:\xdt204\startup\sortfile.3 >nul
ECHO ...2
sort <c:\xdt204\startup\sortfile.3 >nul
ECHO ...1
sort <c:\xdt204\startup\sortfile.3 >nul
ECHO ...0
rem
rem Start XDETECT
xdetectv xdetect.inp
rem *** Misc. Operation Notes:
rem *** approx. script running time 11 - 14 minutes
rem *** possible autoreboot problem as a result of timing errors
rem ***   on A/D card. If xdetectv starts within approx 10 minutes of
rem ***   reboot, it may force a second reboot.
rem ***   This is a result of the time drift over 24 hours being
rem ***   roughly 10 minutes. At reboot time (timing from the A?D card)
rem ***   the system will restart and reset the A/D clock to the PC
rem ***   clock. The A/D will thus be turned BACK approx. 10 minutes,
rem ***   thus allowing the pc to reboot a second time. The boot process
rem ***   must therefore require more than 10 minutes to complete.
rem ***   Further study is required at this time.
rem ***   26-DEC-92 M. Skov
```

Source Listing 17 – c:\xdt204\xstart.bat

xstart.bat is similar to the **tstart.bat** file described in the Socorro Seismic Observatory section beginning on page 44. This script first verifies the network connection. If the network is not detected, by the existence of the **login.exe** file on the PC-network file server, then **xstart.bat** recalls **net.bat** up to four times. **xstart.bat** then displays a warning message reminding the user of the importance of the timely execution of the remainder of the script. If this script is run at any time other than midnight local time, the user should exit the script with a control-c while the warning message is displayed. Exiting the script will prevent the untimely transfer of data to mcmsun5. If **xstart.bat** is interrupted, XDETECT can be restarted by entering the command: *xdetectv xdetect.inp* while in the c:\xdt204 directory.

Once **xstart.bat** has waited a few seconds to allow the user to exit, it turns off the break, preventing a user from interrupting the script with control-c. Now the script begins the process of preparing the data for transfer. First, the **fixtime** command is used to correct the trace time to the time encoded on channel 0. The time code on channel 0 is an IRIG-E, TTL level signal output from the time code generator. The time code generator is governed by a 1 Mhz stable oscillator. This time code is stable, however it is not slaved to any worldwide time standard. Future enhancements of the data acquisition system should include the installation of a world standard time code receiver.

After decoding the IRIG-E time code, **xstart.bat** initiates the seven day backup procedure. This procedure is similar to the three day backup used by the Socorro Seismic Observatory system. Data files are shuffled through seven directories named event1 through event7. Each day, files are moved to the next directory until they are deleted out of the directory, event7. The seven day storage system works well, but it taxes the 210 megabyte harddisc.

Reducing the number of backup days to four would probably maintain data storage safety and reduce the demand for disc storage space.

Once the data files are moved to the correct backup directory, the File Transfer Protocol (ftp) is used to transfer the current day's data to mcmsun5. The transfer is controlled by a list of instructions in the **ftplink.bat** file shown in source listing 18.

```
open mcmsun5


user s081
password
lcd event2
cd wvmfiles
binary
mput *.wvm
cd ../logfiles
ascii
mput *.log
bye
```

Source Listing 18 – c:\xdt204**ftplink.bat**. Portions of this file were edited for system security.

The format of the **ftplink.bat** file is critical. In particular, the two blank lines after the open mcmsun5 command provide carriage returns to respond to the user: and password: prompts issued by ftp. Unlike the other data logger script files, this file is used verbose in place of manual command entry. The commands in this file are piped to the input of the ftp command as if a user entered the commands manually. This system simplifies the handling of the ftp data transfer, however, even the smallest error in the **ftplink.bat** file could cause the transfer to fail.

The operation of the transfer system makes use of simple ftp commands. The open mcmsun5 command requests a connection to the Sparc workstation, mcmsun5, in the Crary Lab Computer Center. As stated above, the two blank

lines provide carriage returns to answer the normal ftp prompts. User s081 requests a login, and *password* is the password for the s081 account.

Once logged onto mcmsun5, the lcd event2 command sets the local current directory to c:\xdt204\event2. Cd wvmfiles sets the remote current directory to ~s081\wvmfiles. The file type is set to binary and the suds data files are transferred with the mput *.wvm command. Mput normally requests permission to send each individual file, however the -i option forces ftp to transfer files without interaction. The -i flag is set in the **xstart.bat** file when ftp is initiated. After transferring the suds data files, the remote directory is set to ~s081\logfiles and an ascii transfer of the logfiles is performed. Finally, the ftp command bye, terminates the transfer session and logs out of mcmsun5. The ftp command terminates and control is passed back to **xstart.bat**.

The next process in the **xstart.bat** file ordinarily would not be needed. A delay of approximately 10 minutes is introduced to compensate for the time drift associated with the operation of the Data Translation acquisition card. The delay is necessitated as a result of the way the IASPEI system maintains internal timing. Rather than using the system clock, the IASPEI system counts samples from the acquisition card. If the acquisition card samples at the incorrect rate, timing errors are propagated to the IASPEI timing system. In this case, the IASPEI clock gains approximately 10 minutes per day. Each time XDETECT is restarted, the IASPEI clock is set to the computer's clock, however, in the course of one day, the IASPEI clock gains 10 minutes relative to the computer's clock. If the 10 minute delay was not implemented, XDETECT would reboot the computer at approximately 23:50 (0:00 IASPEI drifted time) then again at 0:00. The 10 minute delay simply forces the computer to wait until midnight to restart XDETECT, preventing a double reboot.

MS-DOS does not directly support a delay command, however one was created by making use of the sort command. The Compaq 486 computer currently used by MEVO requires approximately one minute to sort the file sortfile.3 using the standard DOS sort command. The sort command is repeated ten times producing roughly 10 minutes of delay. The delay process is a crude but necessary step. Once completed, XDETECT is restarted.

The data handling procedures on the PC data logger are only a portion of the complete system. Three more control files are subsequently executed by mcmsun5, the Sun Sparcstation 2 in the Crary Lab computer center.

The first of the control files is a crontab file. This file is part of a standard UNIX facility called cron. Cron executes commands at regularly scheduled times. More information about the crontab utility can be found in the Desktop Sparc – Sun System & Network Manager's Guide (1991).

The MEVO account, s081, executes one command each day using the crontab utility. This command calls a script file called **s081** at 1:00 am each day. The crontab listing is shown in source listing 19.

```
0 1 * * * /u2/csec/grants/s081/scripts/s081
```

Source Listing 19 – Crontab file for user s081 on mcmsun5.

At 1:00 am each day, cron initiates the **s081** script shown in source listing 20. This script handles data compression, backup, transfer and mail notifier processes. The **s081** script also writes several log files which can be used to diagnose problems.

```
#!/bin/csh
#
# S081 - MOUNT EREBUS VOLCANO OBSERVATORY
# SEISMIC DATA LOGGER
# CRARY LAB 205
#
```

```
# MIKE SKOV
# DEPARTMENT OF GEOSCIENCE
# NEW MEXICO TECH
# SOCORRO, NM 87801
# (505)835-5691
#
# SKOV@GRIFFY.NMT.EDU (129.138.1.69)
#
# This script runs once daily on mcmsun5 at 1:00 AM Local Time, as
# specified by the following crontab entry:
#
# 0 1 * * * /u1/s081/scripts/s081
#
# This script does the following:
#
# 1. Compresses the wvm data files located in the wvmfiles directory.
#
# 2. Creates a tar file containing the compressed files.
#
# 3. Transfers several files to erebus@griffy.nmt.edu via ftp.
#
# 4. Saves old files for 3 days as follows:
#
# 1) remove 3 day old wvm files from directory wvmfiles/backup3
# 2) move 2 day old wvm files from wvmfiles/backup2 to wvmfiles/backup3
# 3) move 1 day old wvm files from wvmfiles/backup1 to wvmfiles/backup2
# 4) move new wvm files from directory wvmfiles to wvmfiles/backup1
#
# 5) remove 3 day old log files from directory logfiles/backup3
# 6) move 2 day old log files from logfiles/backup2 to logfiles/backup3
# 7) move 1 day old log files to directory logfiles/backup2
# 8) move new log files to directory logfiles/backup1
#
# 5. Sends a mail message to erebus@griffy containing statistics about the
# compressed wvm files.
#
# 6. Sends a mail message to erebus@griffy containing a transcript of ftp
# activity.
#
# Compressed and tar'd wvm files are saved for 3 days, in case the file
# transfer fails.

#
# MAKE SURE WE'RE IN THE CORRECT DIRECTORY
#
cd  s081

#
# PACK THE DATA FILES
#
compress -fv wvmfiles/*.wvm > logfiles/compress.log
```

```
#
# CREATE A TAR FILE CONTAINING PACKED DATA FILES
#
tar cf wvmfiles/wvmtar wvmfiles/*.wvm.Z

#
# FTP FILES TO EREBUS@GRIFFY.NMT.EDU
#
ftp -iv 129.138.1.69 > logfiles/ftplog.log

#
# MAKE SURE WE'RE IN THE CORRECT DIRECTORY
#
cd  s081

#
# SAVE 3 DAYS WORTH OF WVM FILES
#
rm wvmfiles/backup3/*.wvm.Z
rm wvmfiles/backup3/wvmtar

mv wvmfiles/backup2/*.wvm.Z wvmfiles/backup3
mv wvmfiles/backup2/wvmtar wvmfiles/backup3

mv wvmfiles/backup1/*.wvm.Z wvmfiles/backup2
mv wvmfiles/backup1/wvmtar wvmfiles/backup2

mv wvmfiles/*.wvm.Z wvmfiles/backup1
mv wvmfiles/wvmtar wvmfiles/backup1

#
# SAVE 3 DAYS WORTH OF LOG FILES
#
rm logfiles/backup3/*.log
mv logfiles/backup2/*.log logfiles/backup3
mv logfiles/backup1/*.log logfiles/backup2

mv logfiles/*.log logfiles/backup1

#
# SEND THE LIST OF PACKED FILES
#
mail erebus@griffy < logfiles/backup1/compress.log
#
# SEND THE FTP ACTIVITY LOG
#
mail erebus@griffy < logfiles/backup1/ftplog.log
#
# EXIT WITH STATUS 0
#
exit 0
```

Source Listing 20 – ~s081/scripts/**s081** file for user s081 on mcmsun5.

The operation of the **s081** script is nearly self explanatory. The SUDS data files are compressed using the compress command. A logfile called compress.log is created which contains information about the effectiveness of the compression routine. The compressed files are packaged together into the wvmtar file using the standard UNIX tar command. The files are packed together to ease file handling.

Once the files are compressed and packaged, the File Transfer Protocol (ftp) is used to transfer the data to Socorro via the STARS communication system. Two ftp options, i and v, are used to provide automation and improved transfer logging. These options turn off the interactive prompts and turn on the verbose messages. ftp on UNIX systems can also make use of an external control file called **.netrc**. The **.netrc** file contains commands which ftp executes once a connection is made. While the **.netrc** file can be an extremely valuable tool, it is a potential security risk. Because the **.netrc** file contains sensitive information, it is vital that only user s081 have access to this file. Group and other users should have no permissions. The owner, s081, should have read, write and execute privileges. Source listing 21 shows the **.netrc** file. Portions of source listing 21 were edited to maintain system security.

```
machine 129.138.1.69 login erebus password password macdef init
binary
cd /mk1/usr/erebus/data
status
put wvmtar
ascii
lcd ../logfiles
mput *.log
bye
```

Source Listing 21 – ~s081/**.netrc** file used by the MEVO system. Portions of this listing were edited for security.

The **.netrc** file instructs ftp to issue a certain set of instructions if a connection to griffy is made. The transfer type is set to binary, and the remote directory is set to the erebus data directory on drive /mk1. The wvmtar tar file is transferred, followed by the daily logfiles. Finally the bye command breaks the connection with griffy and the **s081** script continues execution.

Once the data is transferred to Socorro, the **s081** script protects the data for three days. This backup procedure is similar to the backup routine executed by the data logger. The data is simply moved through three directories, one each day, and finally deleted from mcmsun5.

Logfiles created by the compression and ftp routines are electronically mailed directly to user erebus on griffy. The mail command is issued after completion of the transfer, so the erebus user in Socorro can simply check this mail to determine the status of the daily transfer.

The Auto File Processing Facility

The script files required to transfer the data from the PC data logger to Socorro, New Mexico represent the most complex portion of the data handling system. In Socorro, the data is handled by two small script files. The first file, **movetar**, is initiated by cron. The second file, **printcomp**. is a routine used to print graphical representations of the seismic data.

movetar renames the wvmtar file and moves it into the tarfiles directory. The **movetar** script is started at 3:00 pm on griffy and is shown in source listing 22.

The data files transferred from mcmsun5 to griffy are always named wvmtar. The wvmtar file must be renamed daily to prevent the transfer from overwriting the previous file. **movetar** renames the wvmtar file according to the current date and moves it to the tarfiles directory. Conveniently, the

time difference between McMurdo and Socorro is nearly one full day. Files renamed in Socorro according to Socorro's current date will be given a name corresponding to the date they were actually recorded in McMurdo.

```
#!/bin/csh -f
# script file to move wvmtar to datetar
# invoked by cron at 1500 daily
cd /mk1/usr/erebus/data
mv wvmtar 'date '+tarfiles/%y%m%dtar''
```

Source Listing 22 – ~erebus/bin/**movetar** script to move wvmtar to tarfiles directory

The final script file, **printcomp** is executed manually. It executes an automated data file conversion and print routine which will temporarily convert a group of SUDS data files to postscript plots which are printed. The **printcomp** script expects individual SUDS data files located in the ~erebus/data/wvmfiles directory. The tar command is used to extract a copy of the data files from the wvmtar file. tar will automatically place the SUDS files in the wvmfiles directory if the wvmtar file is still located in the ~erebus/data directory.

```
#!/bin/csh -f
# printproc
# auto printing of log files and plotting of suds
# data files (*.wvm) generated by xdetect2.02.
# Reformats suds data into ah format (program 'suds2ah')
# Converts ah data to a postscript plot (program 'ah2ps')
# and plots the postscript file on the designated printer
#
# 6/18/92, M. Skov, modified from script by:
# 3/10/92, R. Aster, based on the Los Alamos script written by Leigh House
#
set path=(/usr/users/nmquakes/netstuff /home/griffy/nmquakes/bin /bin /wren3/export/newsprint/bin
/usr/ucb)
rehash
set noclobber
set nonomatch
#
# set the printer
#
```

```
set PRINTER = sparc1
#
# get into the data directory
#
# cd /wren3/data
cd /mk1/usr/erebus/data/wvmfiles

# find out what files, if any we have to work with
#

#print out all log files
#set numlog = `ls *.log | wc -l` >& /dev/null

#print out only the last log file
set numlog = 1

set numwvm = `ls *.wvm.Z | wc -l` >& /dev/null

#
#
# print log files, if any
#
if ( $numlog > 0 ) then
  #print out the latest log file
  set files=`ls -l *.log | awk 'print $8' | tail -1`
  #print out all log files
  #set files=`ls *.log`
  echo " autoproc: plotting $#files log file(s)."
  foreach i ($files)
    enscript -h -P$PRINTER $i
  end
#
#
# convert suds files, if any to ah format, postscript format and plot
# the traces
#
if ( $numwvm > 0 ) then
  set files=`ls *.wvm.Z | colrm 13`
  echo " autoproc: converting and plotting $#files wvm file(s)."
  foreach i ($files)
    echo " `date` - plotting file: $i"
    uncompress -v $i.Z
    /usr/local/bin/suds2ah $i
    /usr/local/bin/ahresamp '/usr/local/bin/ahpscale 2940 $i.ah' <$i.ah >$i.filter.ah
    /home/griffy/digqks/bin/ah2ps.house $i.filter.ah
    lpr -h -P$PRINTER $i.filter.ah.ps
    rm -f $i.ah $i.ah.ps $i.filter.ah.ps $i.filter.ah
    compress -v $i
  end
#
```

Source Listing 23 – ~erebus/bin/**printcomp** script to move wvmtar to tarfiles directory

The **printcomp** script is based on the **autoproc** script discussed in the Socorro Seismic Observatory beginning on page 44. The script prints the latest logfile then uncompresses the SUDS data files. The SUDS files are converted to ah format, resampled to avoid spatial aliasing, converted to postscript and printed. The SUDS files are compressed and left in the wvmfiles directory. Normally, this copy of the SUDS data files will not be needed and can be deleted, however, they are not presently deleted automatically.

printcomp assumes all SUDS files should be printed. If only a select few files are to be printed, either convert the files individually, or modify a copy of the **printcomp** script. By changing the "set files = 'ls *.wvm.Z | colrm 13' " line in the **printcomp** script to select only the files desired, the automatic script can be updated to meet changing requirements.

Permanent Tape Archive

The final standard procedure is the monthly data backup. Once a month, tarfiles and logfiles should be copied to exabyte tape. During periods of intense seismic activity, the timely backup and removal of data from drive /mk1 could be critical. The backup procedure is not automated, however, only a simple UNIX tar command is required to copy the data to exabyte tape. While in a griffy window, execute the command "tar cvfb - 20 logfiles/*yearmonth**.log.Z tarfiles/*yearmonth**.tar | rsh zerbina dd obs=20b of=/dev/rst0", where *yearmonth* is the four digit year and month code corresponding to the data to be archived. This assumes the drive /mk1 is physically attached to griffy, the tape drive is physically attached to zerbina and the current directory is ~erebus/data. Like the Socorro data, two tape copies should be created before removing data from /mk1. If archive scheduling, or naming conventions change, the filenames and

wildcards in the tar command will need to be changed. The SunOS Reference Manual (1990) contains more information about the use of tar and rsh.

Currently, no additional processing is performed on seismic data from the Mount Erebus Volcano Observatory. Systems similar to those used by the Socorro Seismic Observatory could be readily implemented to support an expanded processing system. Even the current, limited system provides a nearly automated collection of routines to transfer and print data files. The **movetar** command could be easily expanded to include the operation of **printcomp**, providing automatic data file printing. Presently, **printcomp** is operated as a user initiated script to prevent voluminous amounts of data from consuming the current printer resources. If automatic printing is desired, **printcomp** should be modified to print all SUDS files only if less than a specified number of data files exist. If a large number of data files were transferred, **printcomp** could simply print every 12th file. This is accomplished by adjusting the wildcards employed by the script file in the "set files = 'ls *.wvm.Z | colrm 13' " command.

Possible Improvements for the MEVO System

The Mount Erebus Volcano Observatory digital seismic data acquisition and processing system is clearly in its infancy. The S-081 team is currently improving the system. Like any new data handling system, needed improvements become apparent during normal operation. The data integrity checks installed for the Socorro data system could be modified and applied to the MEVO system. Improving the data transfer integrity would decrease the pressure on disc space intensive data backups at each data transfer stage. The current requirement that all PC trigger modifications must be made by the on-site technician is time consuming, both for the technician and the update process itself. The

data logger's transfer system could be modified to automatically retrieve new **config.sys** and **xdetect.inp** files from mcmsun5. Operators in Socorro could update the control files and copy them to mcmsun5, automatically updating the control files during the next scheduled PC reboot.

One particularly important concern is the issue of timing. Currently, internal timing is assured by simulataneous digitization. However, future research will almost certainly require data which contains a world standard time code. Perhaps the most robust sollution would be the installation of a Global Positioning System (GPS) clock. Companies such as *True Time* produce families of products which would satisfy the requirement for improved timing. While the cost of a high quality timing system may approach $10k, the time signal could be used by other science groups throughout McMurdo.

The system, if properly maintained, will continue to evolve. This evolutionary process will eventually yield a system which both serves the purpose of data acquisition and transfer, but also provides a versatile system which can be readily updated to meet new requirements. The installation created during the 1992-93 field season represents a major advance in the usefulness of the MEVO seismic network. Improvements made during future field seasons will continue to expand the capabilities of the Mount Erebus Volcano Observatory seismic network.

Future Developments

Experience gained while working with the IASPEI data logger has pointed to several shortcomings of the current system. Current systems provide useful data, however a more thorough system could be developed. While the IASPEI system provided for data analysis, these tools were developed for MS-DOS systems and do not meet today's requirements. An integrated system consisting of programmable data acquisition and exhaustive analysis tools is needed. No system can meet the needs of all users, however a system designed for and around smaller seismic networks could be a valuable tool for research seismologists.

The rapid increases in computer hardware technology have clearly outclassed the improvements in software. The IASPEI system was designed around personal computer technology that is only a decade old, yet today personal computers can provide computing power and storage capacity which was almost unimaginable in the early 1980's. This increase in computer power demands a reevaluation of the data acquisition strategy.

The recent advances in storage technology question the need for real time triggered systems. Perhaps data should be recorded continuously, with a post processing trigger. Certainly the performance of a trigger algorithm could be greatly enhanced if concerns about real time acquisition and evaluation did not exist. Yet, some situations may require a triggered system. The IASPEI

system was designed to record and locate events continuously, a delay in hypocenter determination would occur if the real time system was replaced with a post processing trigger.

If a real time triggered system is needed, an improved triggering algorithm should be developed to exploit the capabilities of current computer hardware. Digital signal processing hardware is available which would make possible a frequency domain trigger. A frequency domain trigger might provide the capability to record local and teleseismic events as well as provide better noise rejection. Perhaps a neural net system would provide even better performance, with the capability to recognize seismic events from within noise.

By the end of the 1980's, computer scientists had recognized a severe problem. The problem was termed the "Software Crisis" and it was largely an expression of the difficulties of producing well planned systems. The primary concern was toward business applications, still the driving force in computer science, yet it is a problem which should not be overlooked by research scientists. An overall strategy should be constructed before creating an acquisition system. For the small seismic networks operated by New Mexico Tech, several very specific problems must be addressed.

First, the scope of the acquisition system must be defined. Previously, the term acquisition system referred specifically to the process of digitizing and recording seismic data. The term should refer to the overall system. Creating one system to record, preprocess, and archive the seismic data will yield better results than simply combining several different tools.

Difficulties with telemetry represent one of the largest problems facing the Socorro Seismic Observatory. With three of the current seven stations telemetered together, a single noise glitch can affect nearly one half of the network. This problem is even more acute for the WIPP network operated

by New Mexico Tech in Southeastern New Mexico. Each of the seven WIPP Network channels is telemetered to Socorro by a single microwave link. An acquisition system must be designed to properly reject this type of coupled telemetry noise.

Due to the small number of stations and relatively small number of seismic events, it becomes very important to produce a system which records virtually all events of interest. Current research efforts using local seismic data require consistent recording of extremely small seismic events. Events with duration magnitudes as low as M_d -1.0 are used to explore the mid-crustal magma body under Socorro, New Mexico. Other research interests mandate teleseism and regional event recording. Additionally, trigger performance should be maintained even during the stormy fall monsoon season, when lightning glitches are especially severe.

The Erebus Network demonstrates other requirements. The conditions are obviously difficult and remote, making field repairs a seasonal effort. Seismic stations shut down due to a variety of operational difficulties, and the recording system should easily adjust to the changing network. Ideally, control over the recording system should be remote, something which the current IASPEI system under MS-DOS cannot handle. Trigger parameters should be easily changed without physical access to the data acquisition system.

Inclusion of non-seismic monitoring equipment should be considered regardless of network location. Individual channels within the data acquisition system should have programmable digitization rates. Anemometer data, for example, may only need to be sampled once per second, significantly reducing the data storage requirements. Other, non-traditional equipment should be considered. Gas emission detectors, including induction loops have been deployed on Mount Erebus. As technology increases, absorption spectrometers

may become available which would provide accurate emission information. A well designed system should easily expand to include such diverse equipment.

Video may become a significant tool, particularly for volcanic seismology. The ability to record video, or at least still frames, with seismic data could greatly assist interpretation. The availability of JPEG and MPEG video compression hardware at "prosumer" prices is greatly enhancing the ability to deploy video systems as a supplement to seismic data.

Finally, considerations should be made for future, unimaginable expansions. If the IASPEI system would "report" triggers to the digital output of the Data Translation hardware, then users could control other recording equipment with the XDETECT triggering system. Further, if the IASPEI system supported external triggers, then multiple IASPEI data loggers could be assembled into efficient "subnets." While no one can anticipate every conceivable enhancement, the design should be flexible enough to incorporate new technology.

Acknowledgments

I would like to thank Drs. Richard Aster, Philip Kyle, and Allan Sanford for their assistance during the development of the Socorro and Mount Erebus data acquisition systems. The Socorro system was partially funded by the Geophysical Research Center, Socorro, New Mexico. The efforts of Larry Jaksha are greatly appreciated. His knowledge of the Socorro Seismic Observatory's instrumentation systems was invaluable. I also thank Leigh House for his assistance during the development of the file handling and control software necessary for this project.

The Mount Erebus installation was supported by National Science Foundation grant DPP-9118056. I thank the United States Navy's VXE-6 squadron for the air support provided. Special thanks to Sarah Doherty for her assistance during the Antarctic Winter of 1993. Her efforts to maintain the MEVO data logger are greatly appreciated. I thank the many other people who assisted with this work and I extend my thanks to Antarctic Support Associates, Paul Rose, Bill McIntosh, Bill Schmitt, Ray Dibble and Katsutada Kaminuma.

I also thank Willie Lee for his assistance during the development of the Socorro and Erebus installations. Thank you John Evans for locating very elusive documentation which provided a more thorough understanding of the IASPEI system.

Thank you to my fellow New Mexico Tech Geophysics Graduate students (Robert Balch, Roderick Flores, Joseph Henton, Mitch Withers, and George Slad) who assisted me throughout this project.

Finally, I wish to thank my parents for the encouragement to continue when progress seemed impossible.

References

Balch, R. S. (1992). New Constraints on the Socorro Magma Body Based on Improved Hypocenters. M.S. Independant Study, New Mexico Institute of Mining and Technology, 118pp.

Dibble, R. R., Kienle, J., Kyle, P. R., Shibuya, K. (1984). Geophysical Studies of Erebus Volcano, Antarctica, from 1974 December to 1982 January, New Zealand Journal of Geology and Geophysics **27** 425-455.

Evans, J. R. (1992). The Tdetect Program, *A Course on: PC-Based Seismic Networks*, U.S. Department of the Interior, U.S. Geological Survey Open-File Report 92-441, (Lee, W. H. K. and Dodge, D. A. editors) 152-164.

Giggenbach, W. F., Kyle, P. R. Graeme, L. L. (1973). Present Volcanic Activity on Mount Erebus, Ross Island, Antarctica, Geology **1**, 135-136.

Hartse, H. E. (1991). Simultaneous Velocity Model and Hypocenter Estimation Using Direct and Reflected Phases from Microearthquakes Recorded Within the Central Rio Grande Rift. Ph.D. Dissertation, New Mexico Institute of Mining and Technology, 251pp.

Hartse, H. E., Sanford, A. R., Knapp, J. S. (1992). Incorporating Socorro Magma Body Reflections into the Earthquake Location Process, Bulletin of the Seismological Society of America, **82**, 2511-2532.

Kyle, P. R., Dibble, R. R., Giggenbach, W. F., Keys, J. (1982). Volcanic Activity Associated with the Anorthoclase Phonolite Lava Lake, Mount Erebus, Antarctica, Antarctic Geoscience (Craddock, C. editor), University of Wisconsin Press, Madison, 735-745.

Lee, W. H. K. (1992). RealTime Seismic Data Acquisition, *A Course on: PC-Based Seismic Networks*, U.S. Department of the Interior, U.S. Geological Survey Open-File Report 92-441, (Lee, W. H. K. and Dodge, D. A. editors) 115-137.

Lee, W. H. K. (1992b). The Xdetect Program, *A Course on: PC-Based Seismic Networks*, U.S. Department of the Interior, U.S. Geological Survey Open-File Report 92-441, (Lee, W. H. K. and Dodge, D. A. editors) 138-151.

Luo, X and Dibble, R. R. (1993). A 3-Dimensional Topographic Inversion of the Velocity Structure of Erebus Volcano, Antarctica, *pre-print.*

Rowe, C. A. and Kienle, J. (1986). Seismicity in the Vicinity of Ross Island, Antarctica, Journal of Geodynamics, **6**, 375-385.

Sanford, A. R. and Holmes, C. R. (1961). Note on the July 1960 Earthquakes in Central New Mexico, Bulletin of the Seismological Society of America, **51**, 311-314.

Sanford, A. R., Mott, R. P., Shuleski, P. J., Rinehart, E. J., Caravella, F. J. Ward, R. M., Wallace, T. C. (1977). Geophysical Evidence for a Magma Body in the Vicinity of Socorro, New Mexico, *The Earth's Crust: Its Nature and Physical Properties*, AGU, Washington D. C. (Heacock, J. G. editor) 385-404.

Skov, M. J. and Kyle, R. R. (1993). Mt. Erebus Volcano Observatory: Seismic Observations, Antarctic Journal of the United States, *in press.*

Sun Microsystems (1991). Desktop Sparc: Sun System & Network Manager's Guide, pp 192.

Sun Microsystems (1990). SunOS Reference Manual, pp 2224.

Appendix A

Content :

2 geologic maps

Appendix B

Content :

3 sonic logs
1 density log

SCHLUMBERGER

LOG SONIC BHC
GAMMA RAY

PAYS FRANCE
CHAMP LA MOSQUE
SONDAGE MAC EH 26
COMPAGNIE GEOSEL

COMPAGNIE GEOSEL
SONDAGE MAC EH 26
CHAMP MANOSQUE
DEPARTEMENT PROVENCE PAYS FRANCE
COORDONNÉES

Autres opérations:

Origine permanente des profondeurs T.R. Elév.: 3
Zéro log. 0 m. au-dessus origine permanente
Zéro Sondeur 0 m. au-dessus origine permanente

Elévation : Sol
T.R.

Date	1972		
Opération N°	ENG-GR 1	1/100	
Profondeur Sond.			
Profondeur Log.			
Première lecture			
Dernière lecture			
Sabot Sondeur			
Sabot Log			
Diamètre trépan	15		
Boue : Nature	BENTONITIQUE		
Densité | Viscosité	1.22 | 40		
pH | Eau libre	| ml	| ml	| ml
Origine échant.	CIRCULATION		
Rm Temp. Mesure	1.59 à	à	à
Rmf Temp. Mesure	0.75 à	à	à
Rmc Temp. Mesure	3.3 à	à	à
Origine Rmf Rmc		à	à
Rm à Temp. Fond	à	à	à
Temps après circ.			
Temp. Maximum			
Camion N°	4530 | POYFS		
Opérateur	VANDEVERELE		
Observateur Cie	KANDEL		

PLIER ICI

REMARQUES

Changements de Boue - Echantillons supplémentaires

Date | Echant. N°			
Profond. Sondeur			
Boue | Nature			
Densité | Viscosité			
pH | Eau libre	ml	ml	
Origine échantil.			
Rm Temp. Mesure	à	à	
Rmf Temp. Mesure	à	à	
Rmc Temp. Mesure	à	à	
Origine : Rmf | Rmc			
Rm à Temp. Fond	à	à	
Rmf à Temp. Fond	à	à	
Rmc à Temp. Fond	à	à	

Changements d'échelle

Log	Profondeur	Echelle Montée	Echelle Descente

Références équipement

Opérat. N°	Outil	Patin	Central.	Divers

Centreur : X S.O. :
Equipement : CARTOUCHE N° SLC-DB 100
Panel N° SLP-GA 100
Sonde N° SLS-A 200

ETALONNAGE :	Bruit de fond	Source	Div. add.	Sens. Panel	Sens. Panel	Const. de	Vitesse
	IPS	IPS	GALVA.	(étalon.)	(enreg.)	Temps	Enregistrement
GAMMA RAY			32.5	200	150	2	9M

Vitesse (pieds par seconde) = $\frac{1{,}000{,}000}{\text{Temps de parcours (microsecondes par pied)}}$

GAMMA RAY
UNITES API

0 7

Profondeurs

1/200

INTERVALLE DE TEMPS DE PARCOURS
Microsecondes par pied

T R1 2 R2

140 90 40

240 190 140

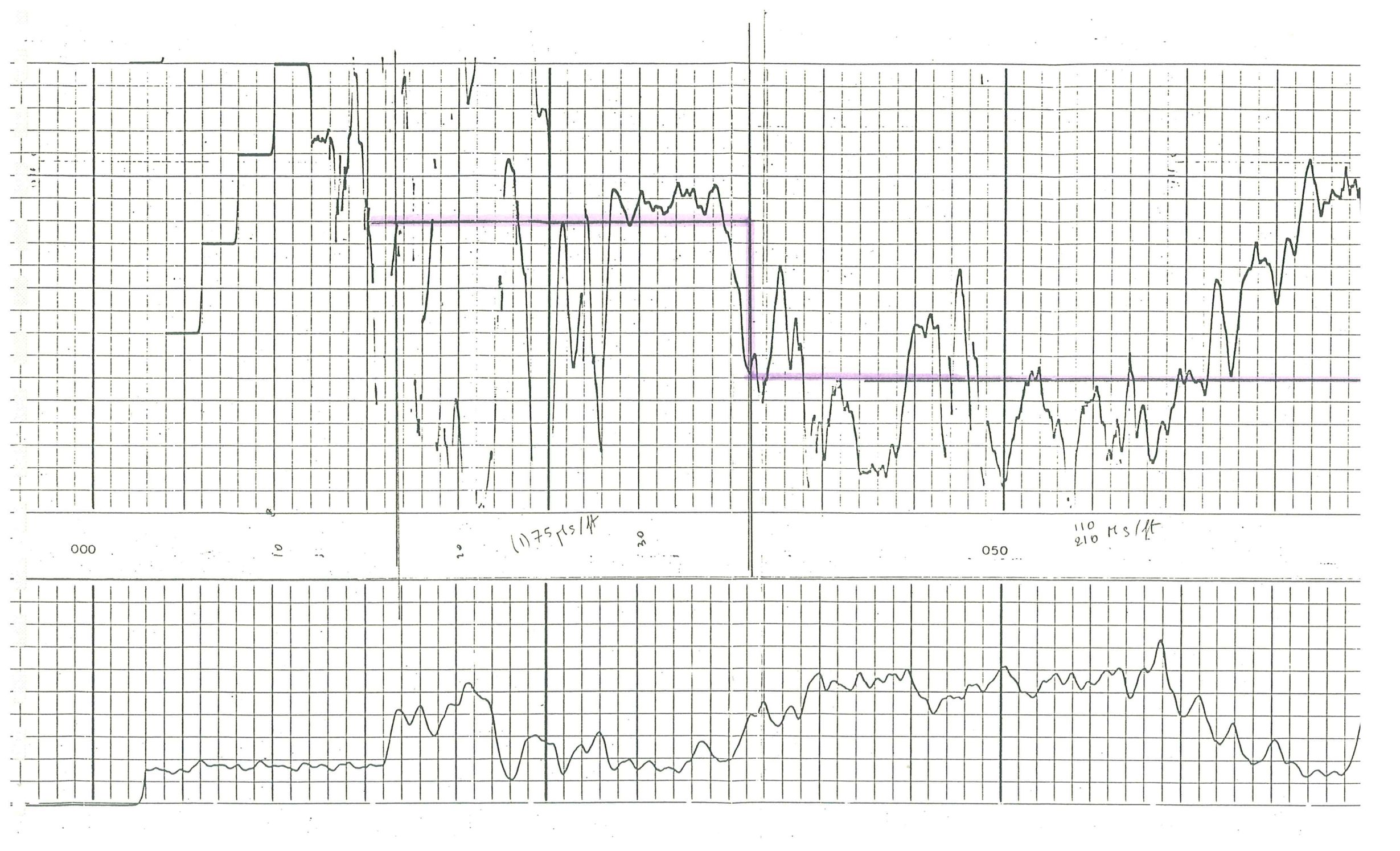
000
050
1175 μs/μ
110
210 μs/μ

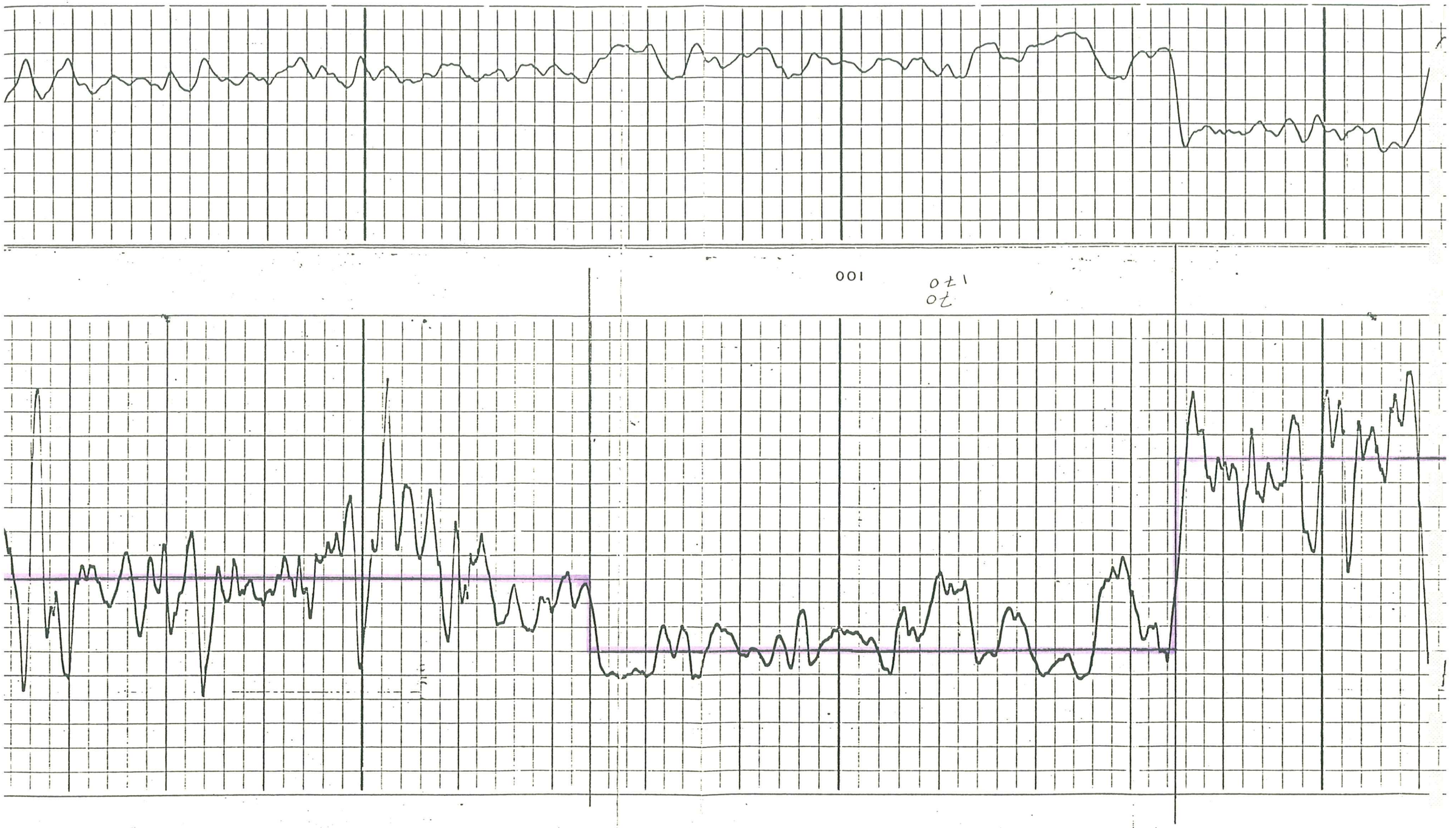
100
120
70

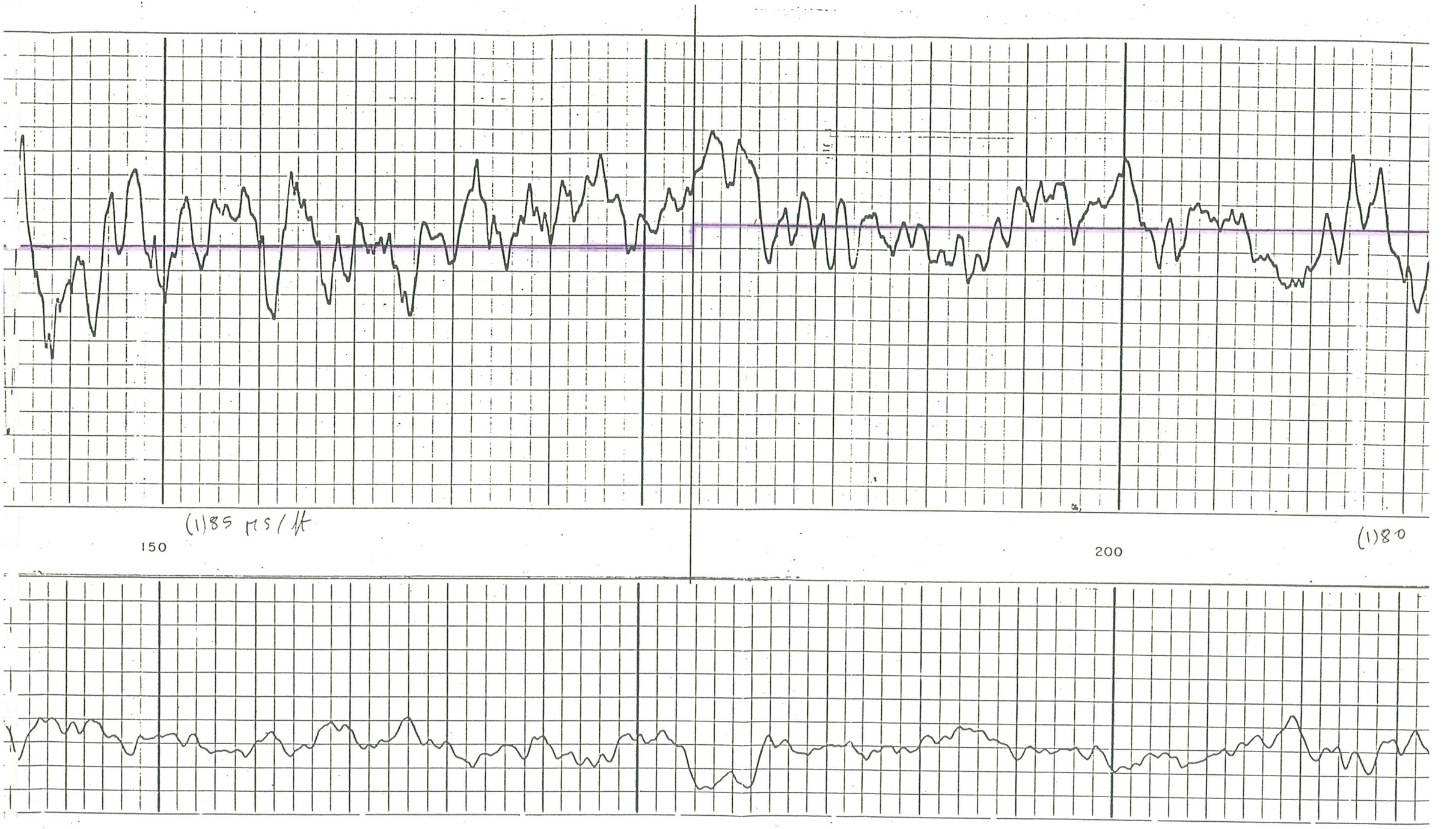
(1)85 MS/H
150
200
(1)80

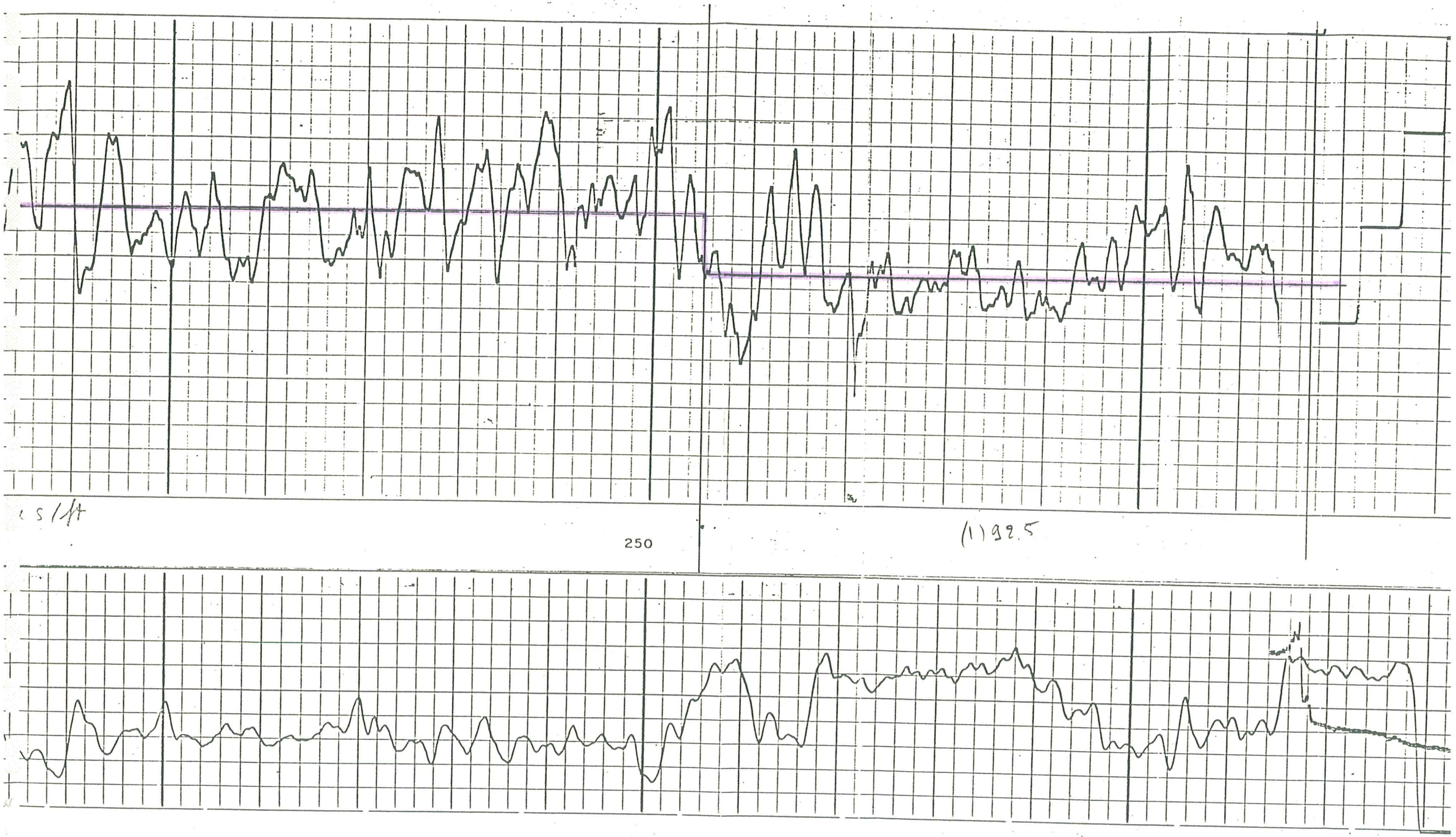
250

SCHLUMBERGER

PAYS FRANCE

CHAMP MANOSQUE

SONDAGE MAC EH 26

COMPAGNIE GEOSEL

COMPAGNIE

SONDAGE MAC EH 26

CHAMP MANOSQUE

DEPARTEMENT PROVENCE PAYS FRANCE

COORDONNÉES

Autres opérations:

Origine permanente des profondeurs T.R. Elév. :

Zéro log 0 m. au-dessus origine permanente

Zéro Sondeur 0 m. au-dessus origine permanente

Elév.: K.B.
SOL
T.R.

Date			
Opération N°	1	2	3
Sabot Sondeur			
Sabot Log	231.6m		
Diamètre trépan	17" 1/2 jusqu'à 926.0m puis 15"		
Boue : Nature			
Densité Viscosité	1.33 | 44		
pH | Eau libre	– | 3.5 ml	| ml	| ml
Origine échant.	CIRCULATION		
Rm Temp. Mesure	0.063à 21°C	à	à
Rmf Temp. Mesure	0.046à 21°C	à	à
Rmc Temp. Mesure	0.140à 21°C	à	à
Origine Rmf Rmc			
Rm à Temp. Fond	0.036 à 56°C	à	à
Temp. après circ.			
Temp. Maximum	56°C		
Camion N°	4330		
Opérateur	VANDENABEELE		
Observateur Cie	KANDEL		

PLIER ICI

REMARQUES 2 ENREGISTREMENTS : 231.6m à 900.0m puis 350.0m à 1000.0m

Changements de Boue - Echantillons supplémentaires

Date | Echant. N°		
Profond. Sondeur		
Boue | Nature		
Densité | Viscosité		
pH | Eau libre	| ml	ml
Origine échantil.		
Rm Temp. Mesure	à	à
Rmf Temp. Mesure	à	à
Rmc Temp. Mesure	à	à
Origine : Rmf Rmc	|	|
Rm à Temp. Fond	à	à
Rmf à Temp. Fond	à	à
Rmc à Temp. Fond	à	à

Changements d'échelle

Log	Profondeur	Echelle Montée	Echelle Descente

Références équipement

Opérat. N°	Outil	Central.	Divers

Centreur : S.O. : X

Equipement CARTOUCHE N° SLC-DB 257

PANEL N° SLP-JB 257 SLO-A 161

SONDE N° SLS-D 234

Vitesse (pieds par seconde) = 1,000,000 / Temps de parcours (microsecondes par pied)

POLARISATION SPONTANÉE

MILLIVOLTS

– ↔ +

DIAMETREUR

Diamètre du trou en pouces

Profondeurs

1 500

INTERVALLE DE TEMPS DE PARCOURS

Microsecondes par pied

T 3 R1 2 R2

140 90 40

240 190 140

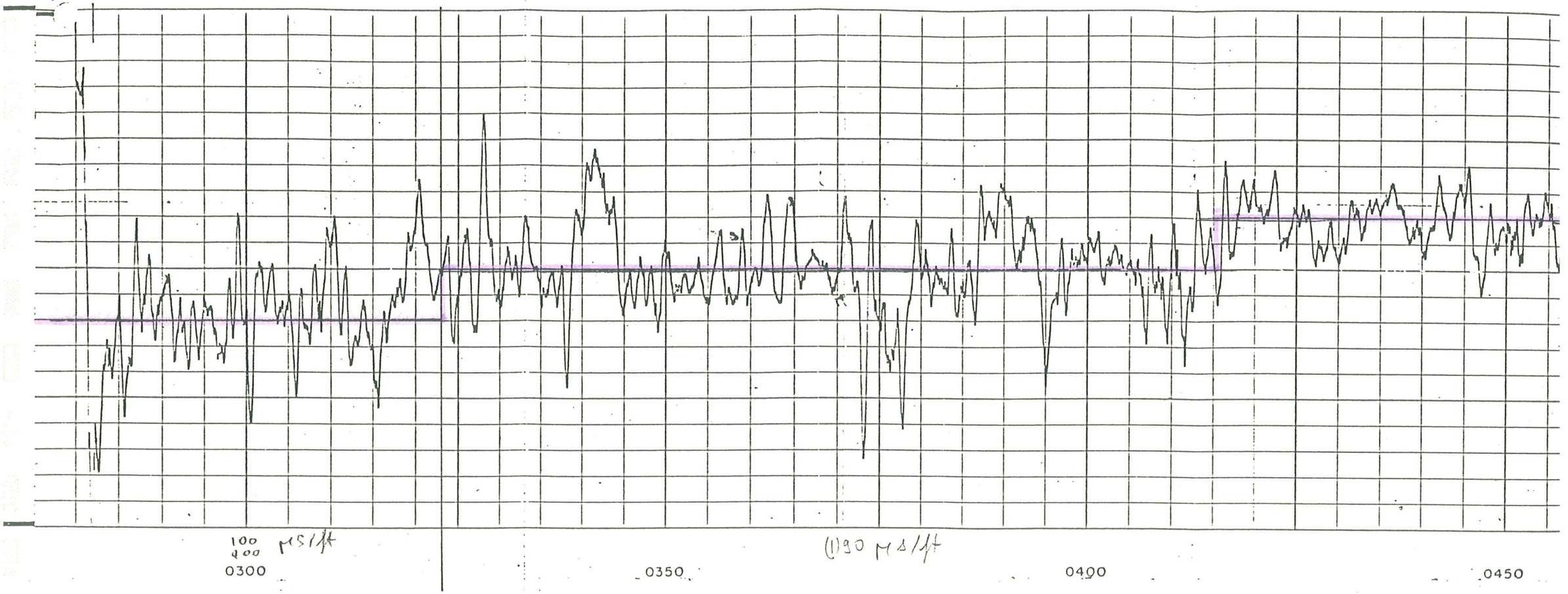
100 µs/ft
1190 µs/ft
0300
0350
0400
0450

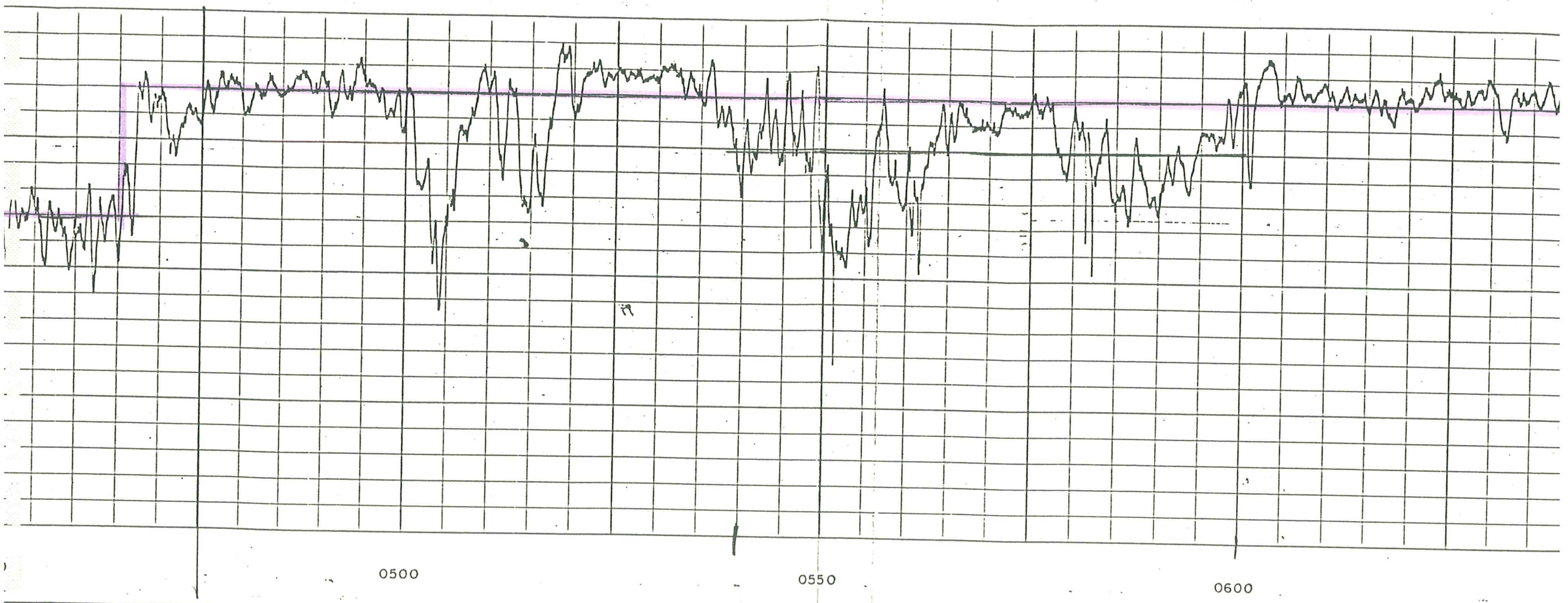
0500
0550
0600

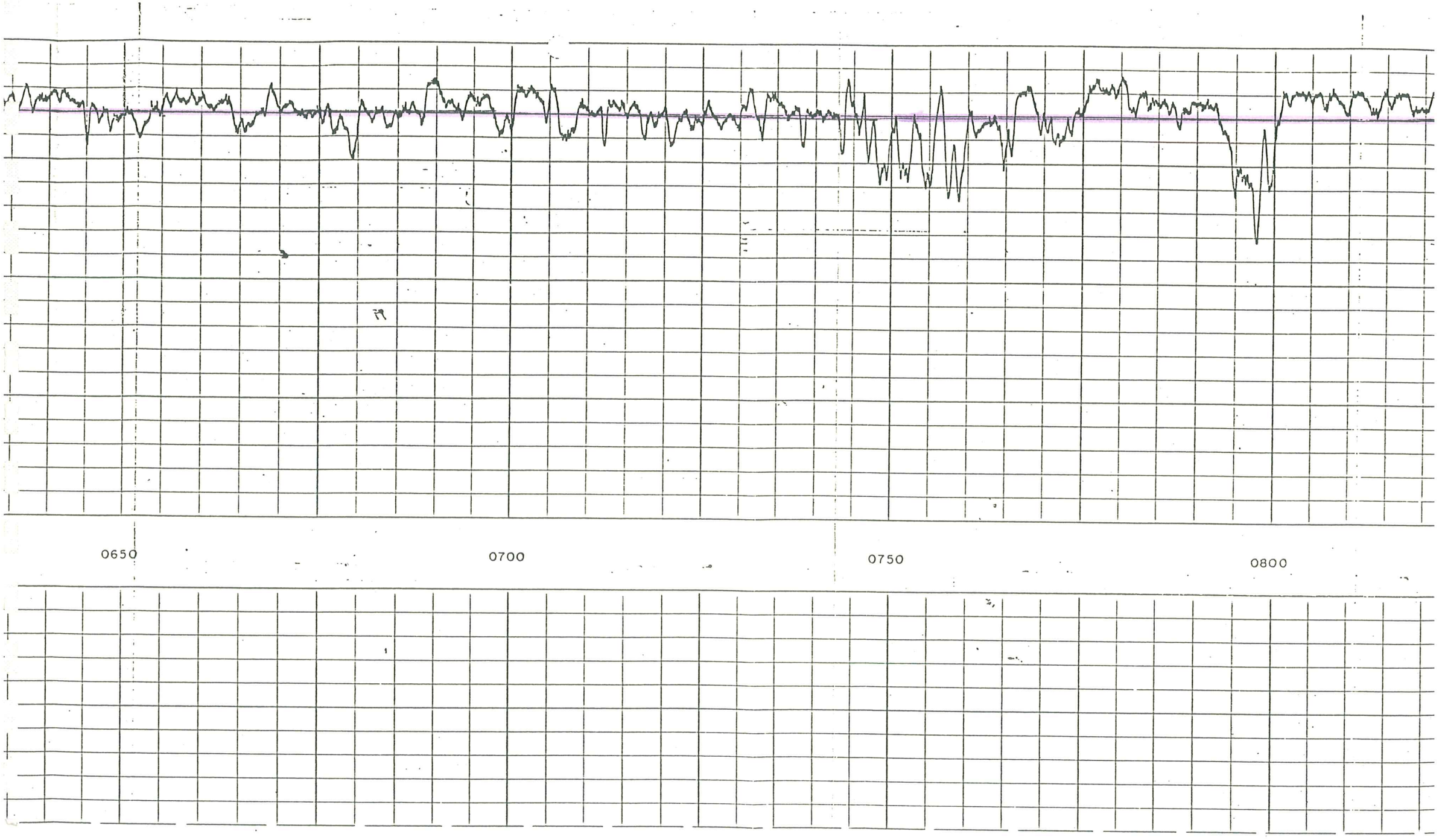
0650
0700
0750
0800

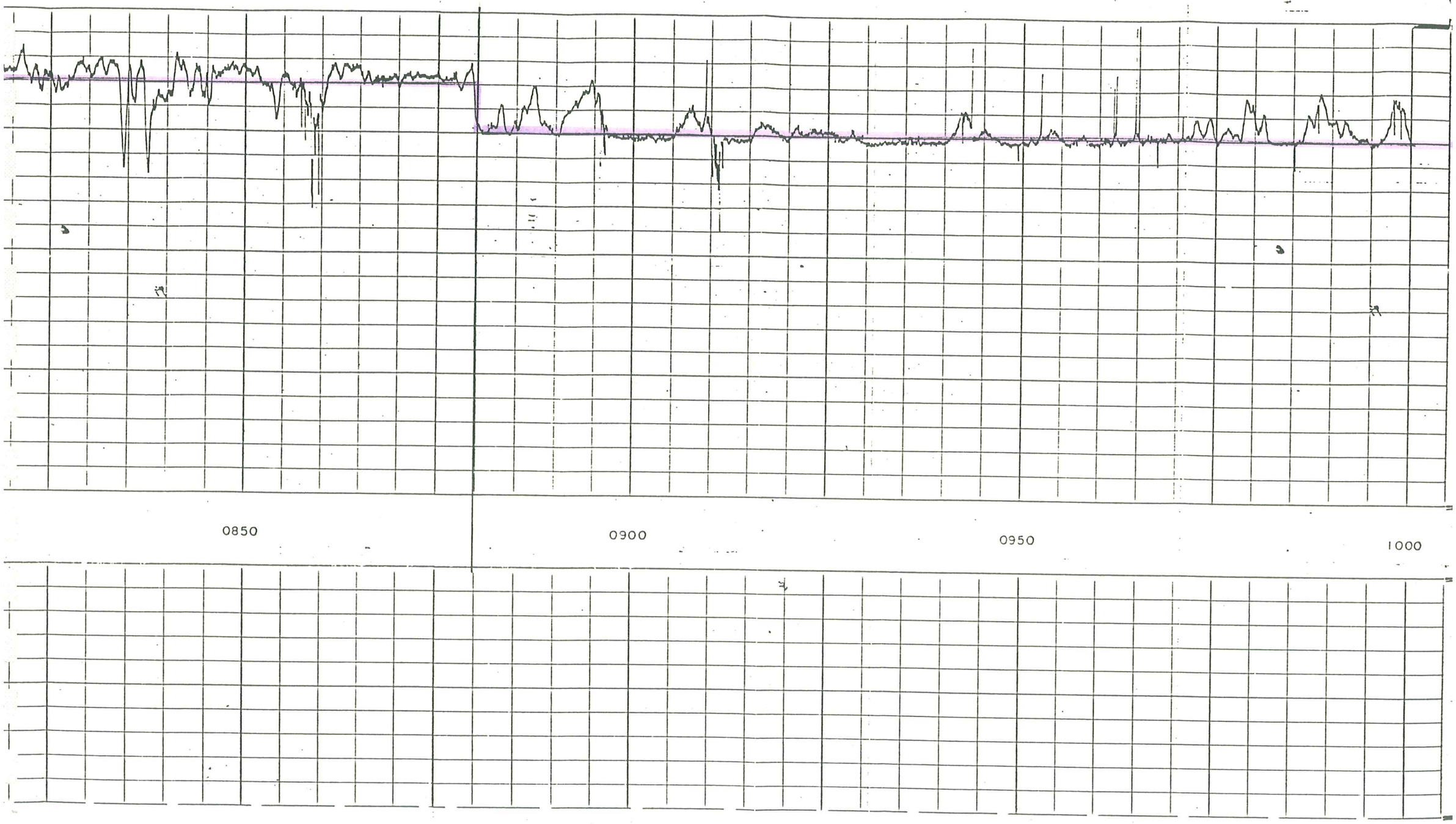
0850
0900
0950
1000

SCHLUMBERGER

LOG SIMPLE BOB

(avec diamétreur)

PAYS FRANCE

CHAMP MANOSQUE

SONDAGE MAC EH 26

COMPAGNIE GEOSEL

COMPAGNIE GEOSEL

SONDAGE MAC EH 26

CHAMP MANOSQUE

DEPARTEMENT PROVENCE PAYS FRANCE

COORDONNÉES

Autres opérations: GRN IO FDC

Elév.: K.B. ____ SOL ____ T.R. ____

Origine permanente des profondeurs T.R. Elév.: ____

Zéro log 0 m. au-dessus origine permanente

Zéro Sondeur 0 m. au-dessus origine permanente

Date	16 [illegible] 72					
Opération N°	DHC-3 1/3					
Profondeur Sond.	1394.0					
Profondeur Log.	1394.0					
Première lecture	1892.2					
Dernière lecture	1772.0					
Sabot Sondeur	932.1 m					
Sabot Log	[illegible]					
Diamètre trépan	12 1/4 [illegible] 1835.0 m [illegible] 8 1/2					
Boue : Nature	SALEE SATUREE					
Densité | Viscosité	1.39 | 42					
pH | Eau libre	10.5 | 7 ml	ml	ml	ml	ml	ml
Origine échant.	CIRCULATION					
Rm Temp. Mesure	0.074 à 18°C	à	à	à	à	à
Rmf Temp. Mesure	0.063 à 18°C	à	à	à	à	à
Rmc Temp. Mesure	0.070 à 18°C	à	à	à	à	à
Origine Rmf Rmc	[illegible]					
Rm à Temp. Fond	0.023 à 39°C	à	à	à	à	à
Temp. après circ.	39°C					
Temp. Maximum	39°C					
Camion N°	4530					
Opérateur	[illegible]					
Observateur Cie	GEOSEL					

PLIER ICI

REMARQUES

Changements de Boue - Echantillons supplémentaires

Date | Echant. N°	|	|
Profond. Sondeur		
Boue | Nature		
Densité | Viscosité	|	|
pH | Eau libre	| ml	| ml
Origine échantil.		
Rm Temp. Mesure	à	à
Rmf Temp. Mesure	à	à
Rmc Temp. Mesure	à	à
Origine : Rmf Rmc	|	|
Rm à Temp. Fond	à	à
Rmf à Temp. Fond	à	à
Rmc à Temp. Fond	à	à

Changements d'échelle

Log	Profondeur	Echelle Montée	Echelle Descente

Références équipement

Opérat. N°	Outil	Central.	Divers

Centreur : X S.O. :

Equipement CARTOUCHE N° SLC-DD 257

PANEL N° SLP-JB 257 SLO-A 161

SONDE N° SLS-D 234

Vitesse (pieds par seconde) = 1,000,000 / Temps de parcours (microsecondes par pied)

POLARISATION SPONTANÉE

MILLIVOLTS

— |↔| +

DIAMETREUR

Diamètre du trou en pouces

Profondeurs

1 500

INTERVALLE DE TEMPS DE PARCOURS

Microsecondes par pied

T 3 R1 2 R2

140 90 40

210 190 140

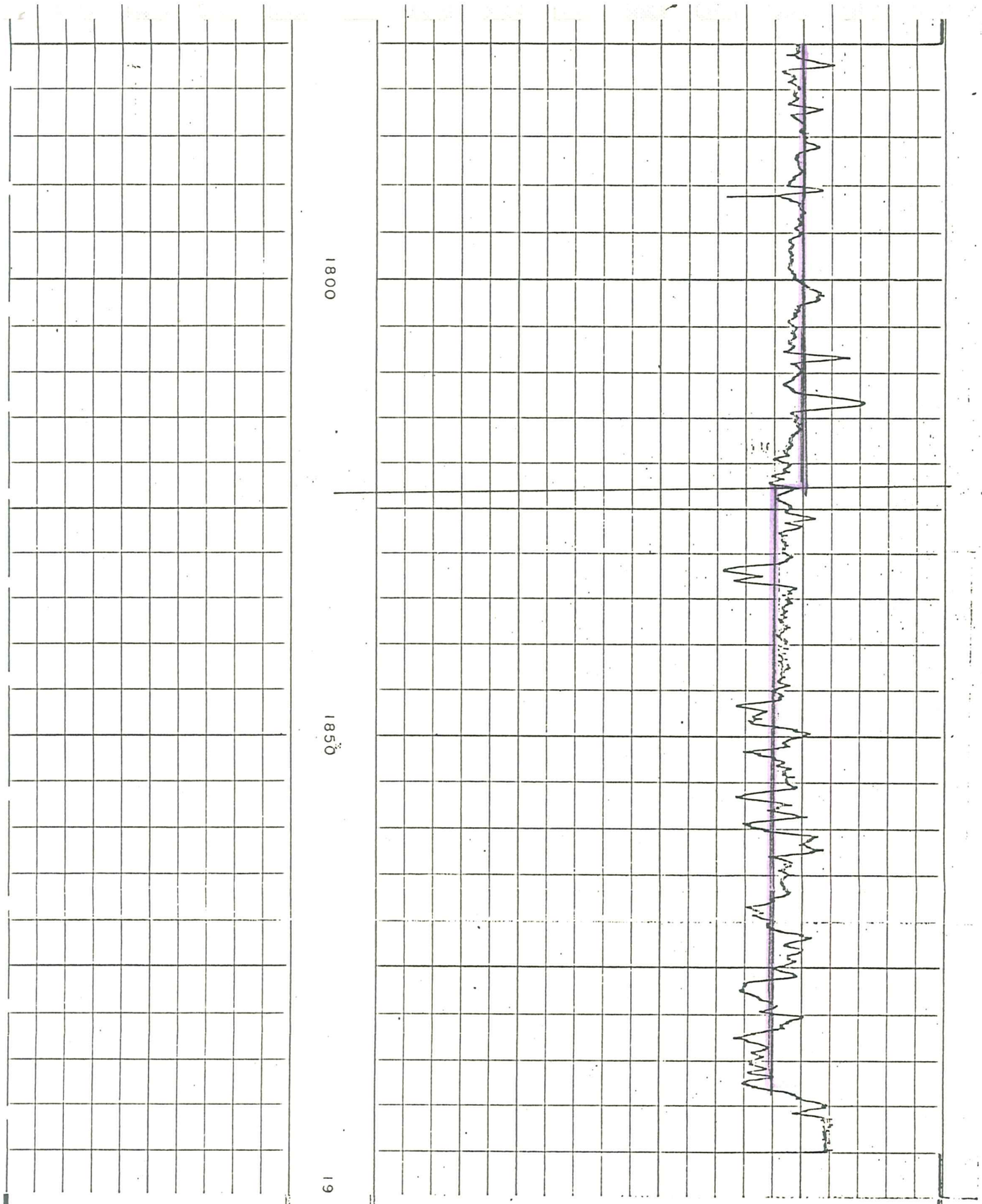

DIAMETREUR

Diamètre du trou en pouces

— |↔| +

POLARISATION SPONTANÉE

MILLIVOLTS

Profondeurs

T 3 R1 2 R2

140 90 40

240 190 140

INTERVALLE DE TEMPS DE PARCOURS

Microsecondes par pied

COMPAGNIE GEOSEL

SONDAGE MAC EH 26

CHAMP MANOSQUE

DEPARTEMENT PROVENCE [illegible] FRANCE

Prem. lecture 1892.2M

Prof. tot. log. 1894.0M

Prof. tot. sondeur 1894.0M

Elév. : K.B. _____

SOL _____

STRUCTURE SALIFERE DE MANOSQUE

ETUDE GEOLOGIQUE DE SYNTHESE

LOG LITHOSTRATIGRAPHIQUE SYNTHETIQUE DES FORMATIONS TRAVERSEES EN FORAGE DANS L'ANTICLINAL DE MANOSQUE

Echelle : 1/500

Département RECHERCHES

Date : MAI - JUIN 1970

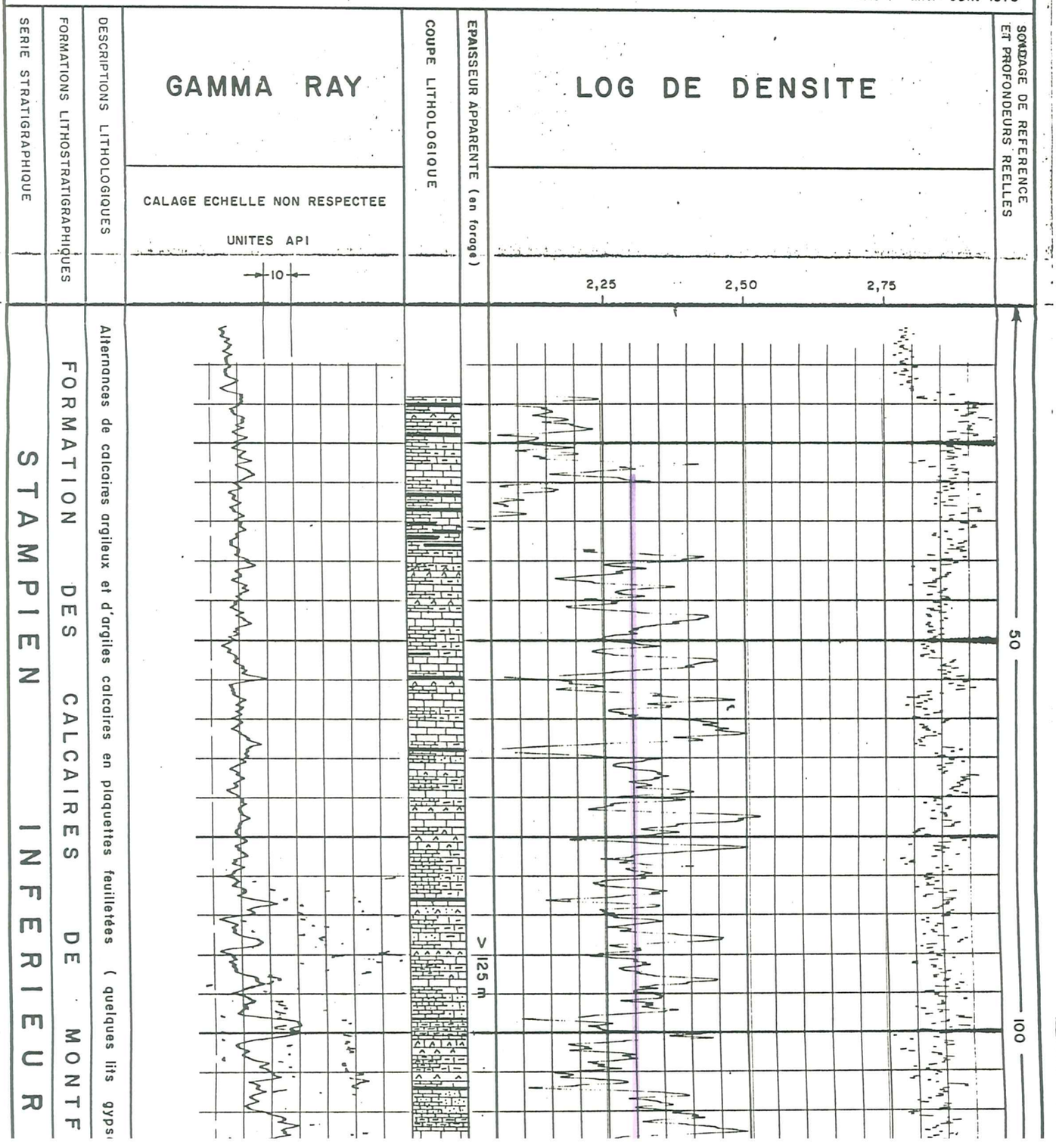

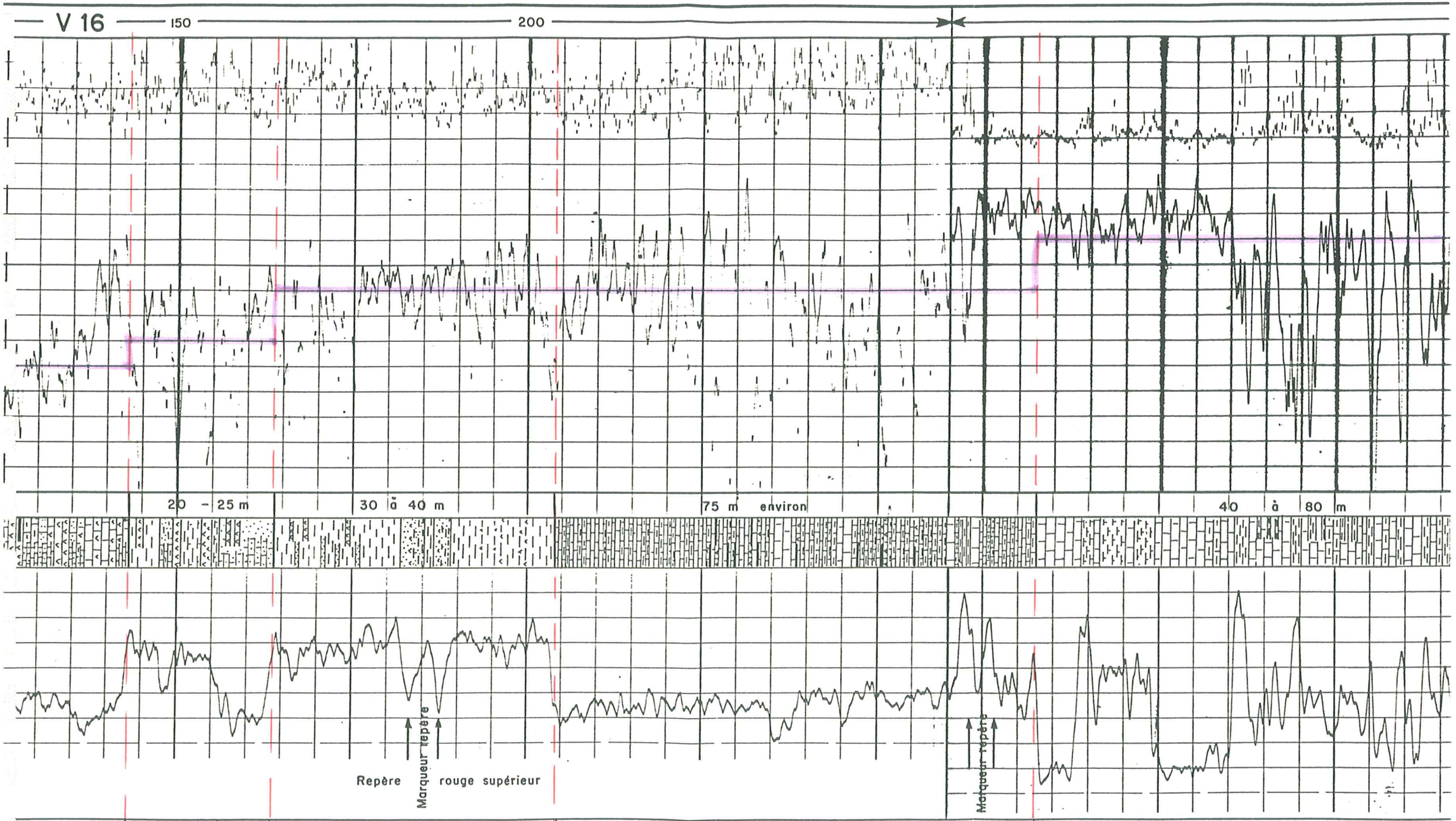

eux)	Marnes argileuses grises (gypse)	Niveau gréso-gypseux repère	Marnes et argiles grises et rouges niveaux de gypse.	Zone marno-calcaire, constituée de niveaux et bancs très minces de calcaires argileux (en plaquettes) et de lits argileux	Alternances de bancs calcaires ou calcaires argileux massifs et de lits et intercalations plus argileuses (indices de bitum
	FORMATION MARNEUSE SUPERIEURE				FORMATION des CALCAIRES à INDICES de BIT
	FORMATIONS DE LA MORT D'I				

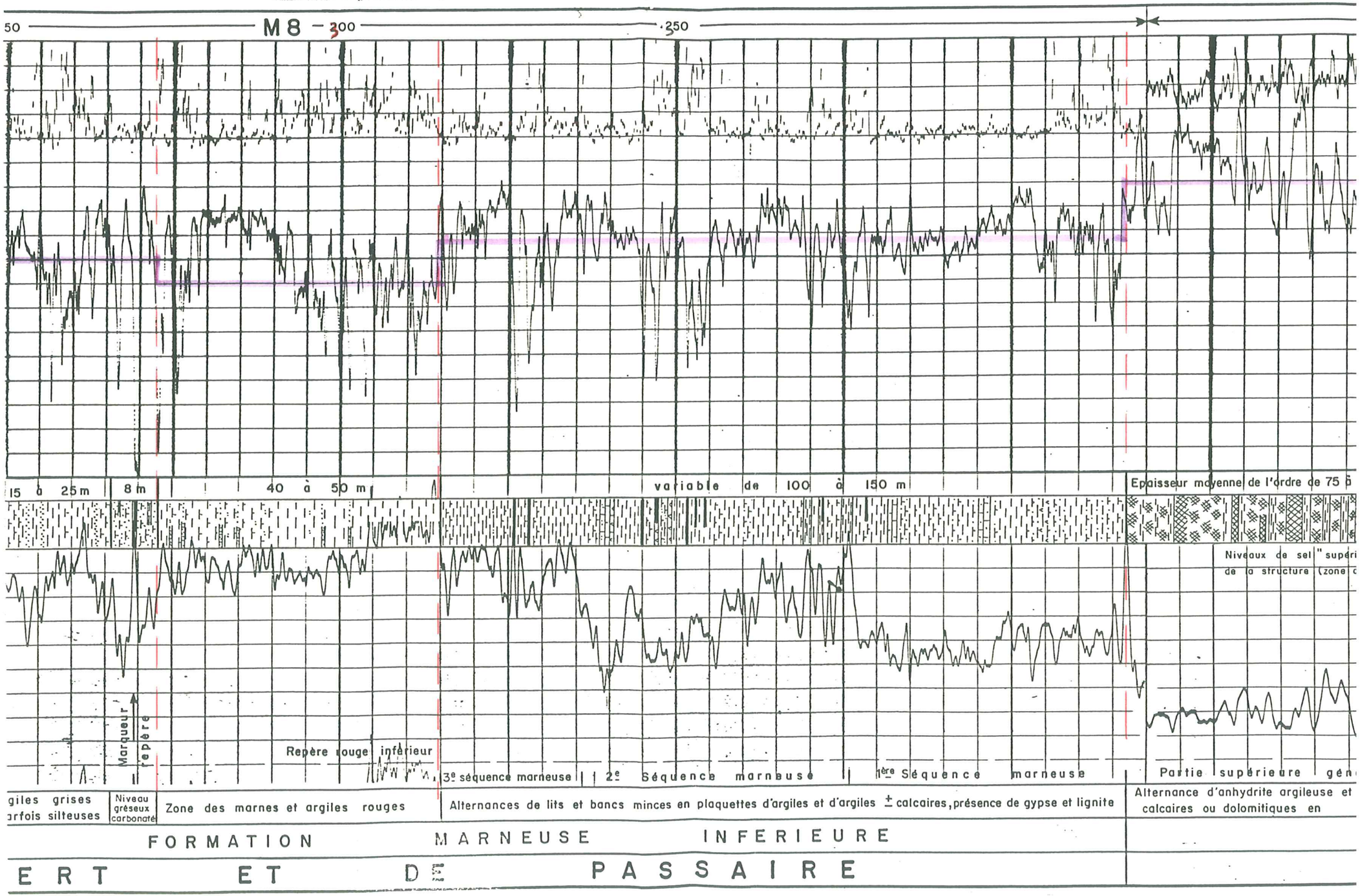
50
M 8 – 300
250
15 à 25 m
8 m
40 à 50 m
variable de 100 à 150 m
Epaisseur moyenne de l'ordre de 75 à
Niveaux de sel "supéri
de la structure (zone c
Marqueur
repère
Repère rouge inférieur
3e séquence marneuse
2e Séquence marneuse
1ère Séquence marneuse
Partie supérieure gén
giles grises
arfois silteuses
Niveau gréseux carbonaté
Zone des marnes et argiles rouges
Alternances de lits et bancs minces en plaquettes d'argiles et d'argiles ± calcaires, présence de gypse et lignite
Alternance d'anhydrite argileuse et
calcaires ou dolomitiques en
FORMATION MARNEUSE INFERIEURE
E R T ET DE PASSAIRE

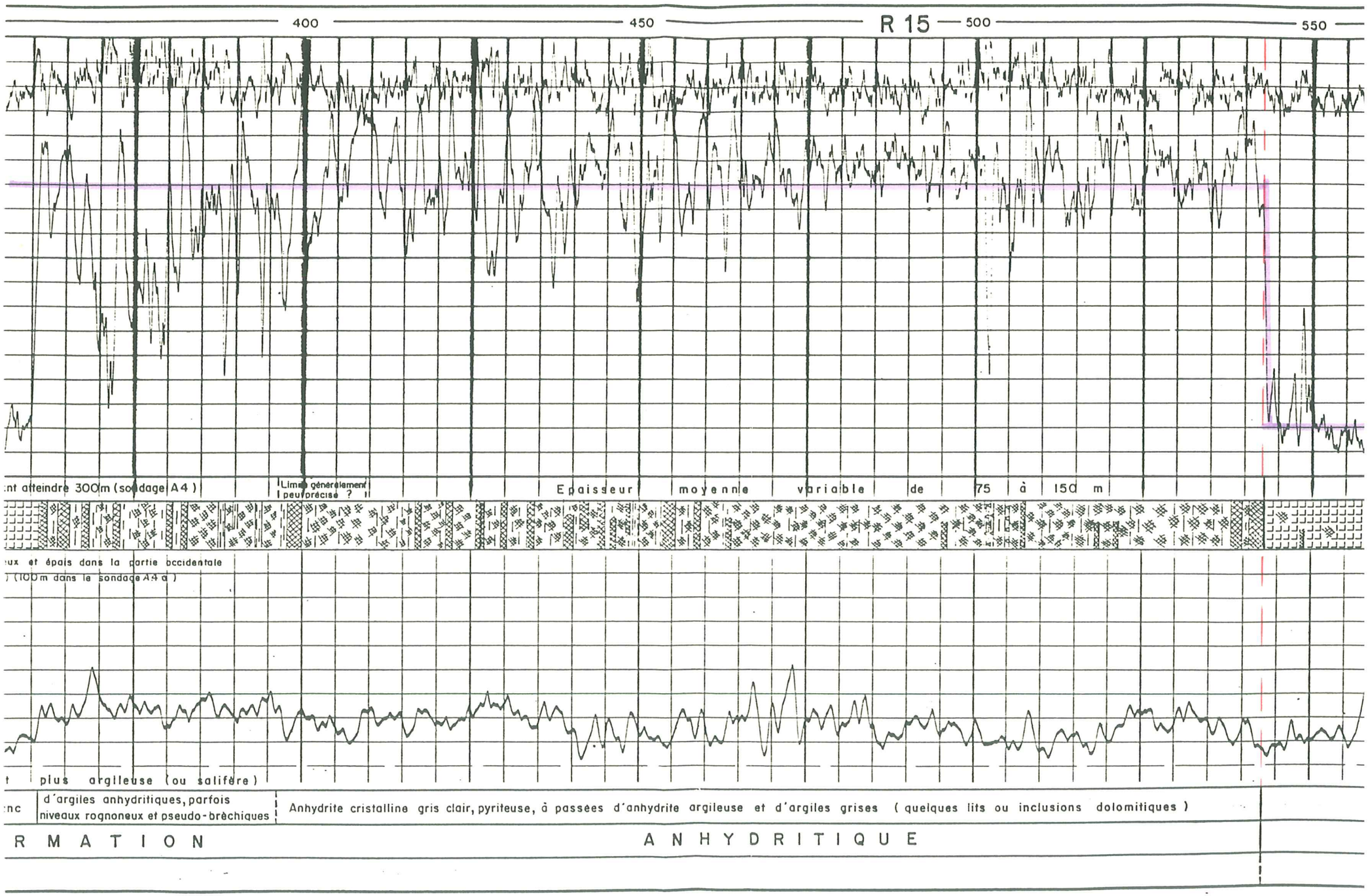
400
450
R 15
500
550
nt atteindre 300m (sondage A4)
Limite généralement peu précise ?
Epaisseur moyenne variable de 75 à 150 m
ux et épais dans la partie occidentale
) (100m dans le sondage A4 a)
t plus argileuse (ou salifère)
nc
d'argiles anhydritiques, parfois niveaux rognoneux et pseudo-brèchiques
Anhydrite cristalline gris clair, pyriteuse, à passées d'anhydrite argileuse et d'argiles grises (quelques lits ou inclusions dolomitiques)
R M A T I O N
A N H Y D R I T I Q U E

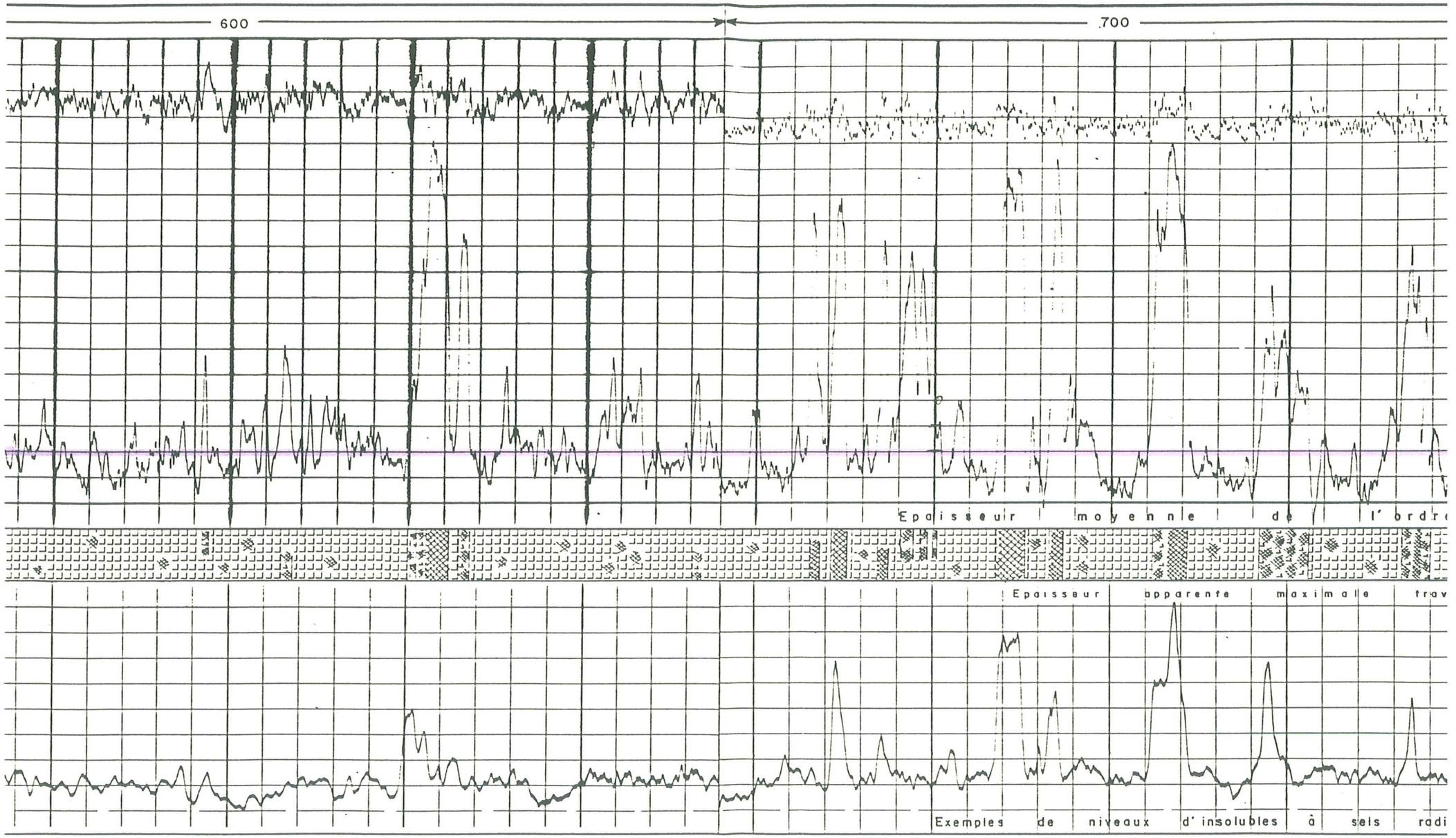

jemme rose à rose - orangé , rarement blanc ou blanc - gris , renfermant de nombreuses inclusions millimétriques à décimétriques d'anhydrite cristalline , gris - clair , par

F O R M A T I O N S A L I F E R E

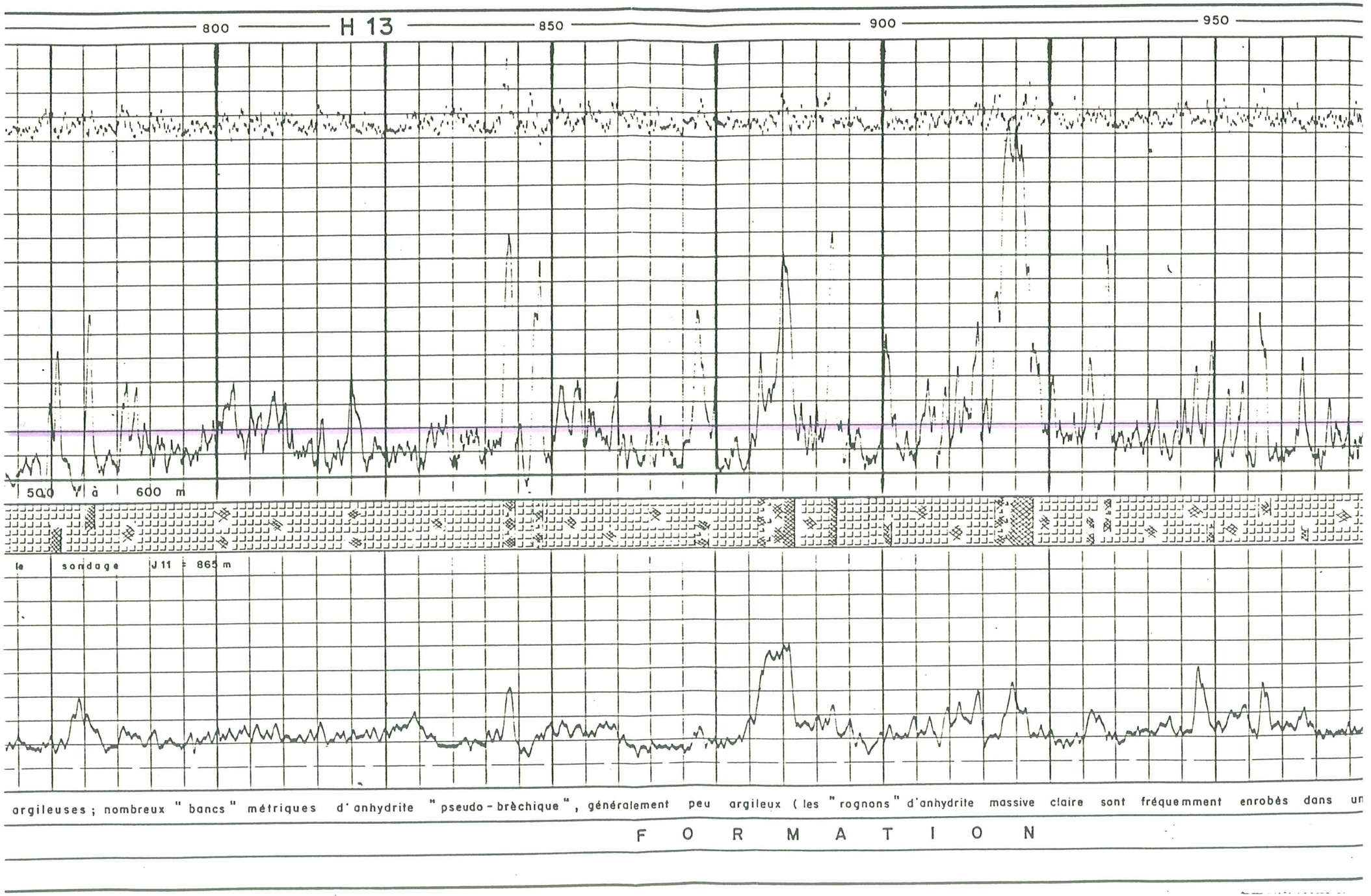
800
H 13
850
900
950
500 m à 600 m
le sondage J 11 = 865 m
argileuses ; nombreux " bancs " métriques d'anhydrite " pseudo-brèchique ", généralement peu argileux (les " rognons " d'anhydrite massive claire sont fréquemment enrobés dans un
F O R M A T I O N

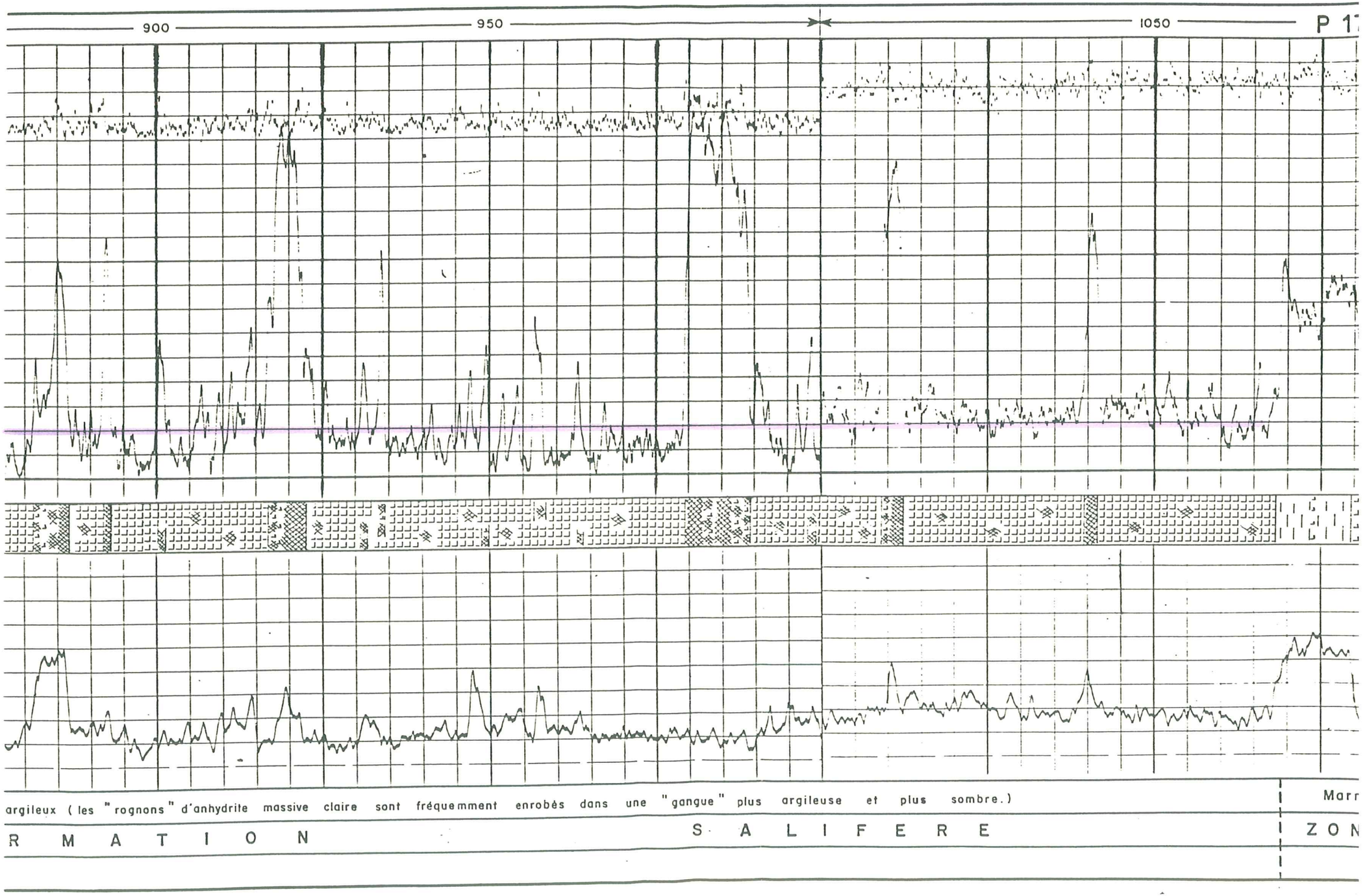
900
950
1050
P 1
argileux (les " rognons " d'anhydrite massive claire sont fréquemment enrobés dans une " gangue " plus argileuse et plus sombre.)
Marr
R M A T I O N
S A L I F E R E
ZON

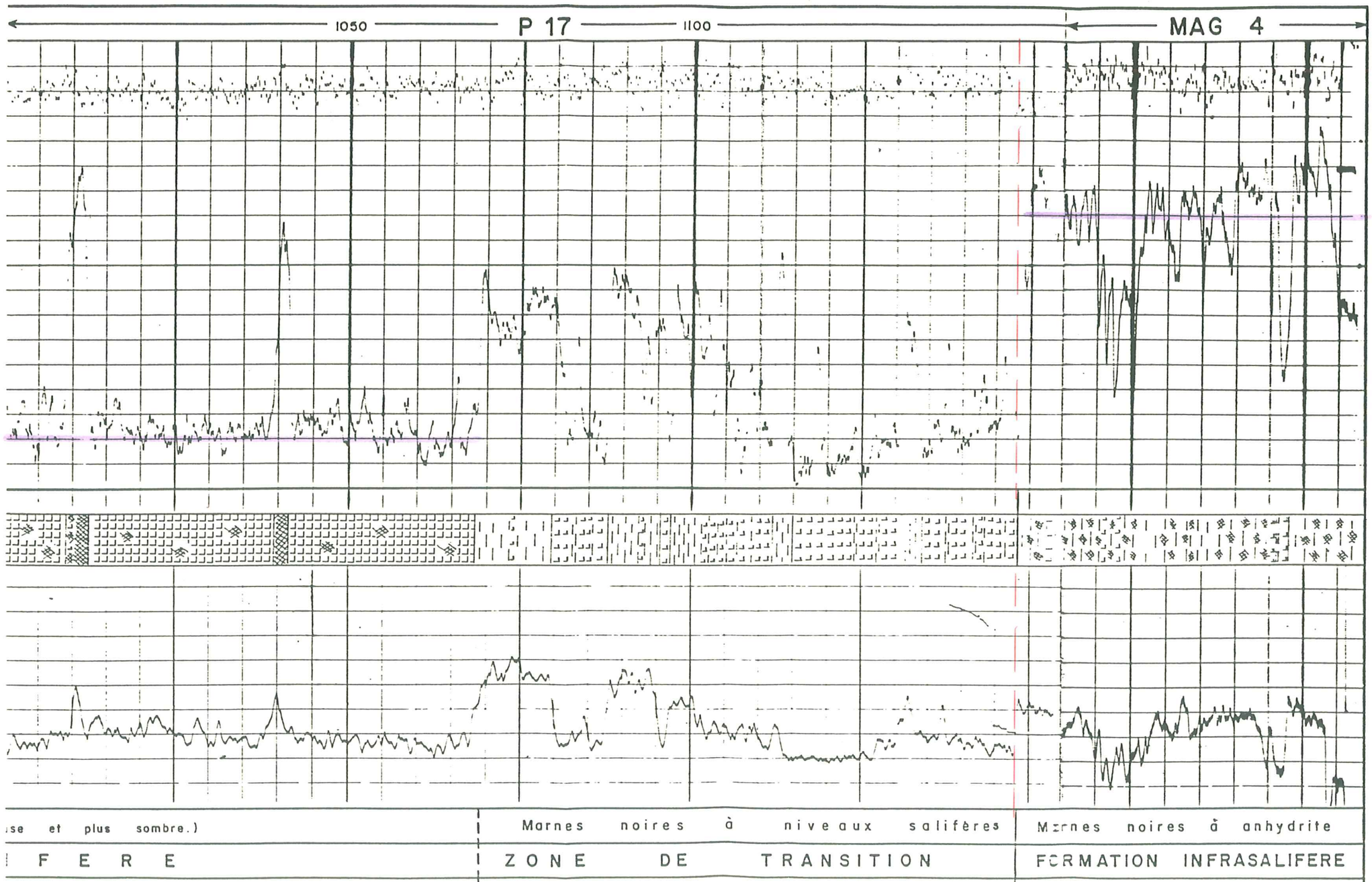
1050
P 17
1100
MAG 4
se et plus sombre.)
Marnes noires à niveaux salifères
Marnes noires à anhydrite
F E R E
ZONE DE TRANSITION
FORMATION INFRASALIFERE

Appendix C

Content :

40 seismogram profiles with frequency content 0 to 10 Hz

Ux

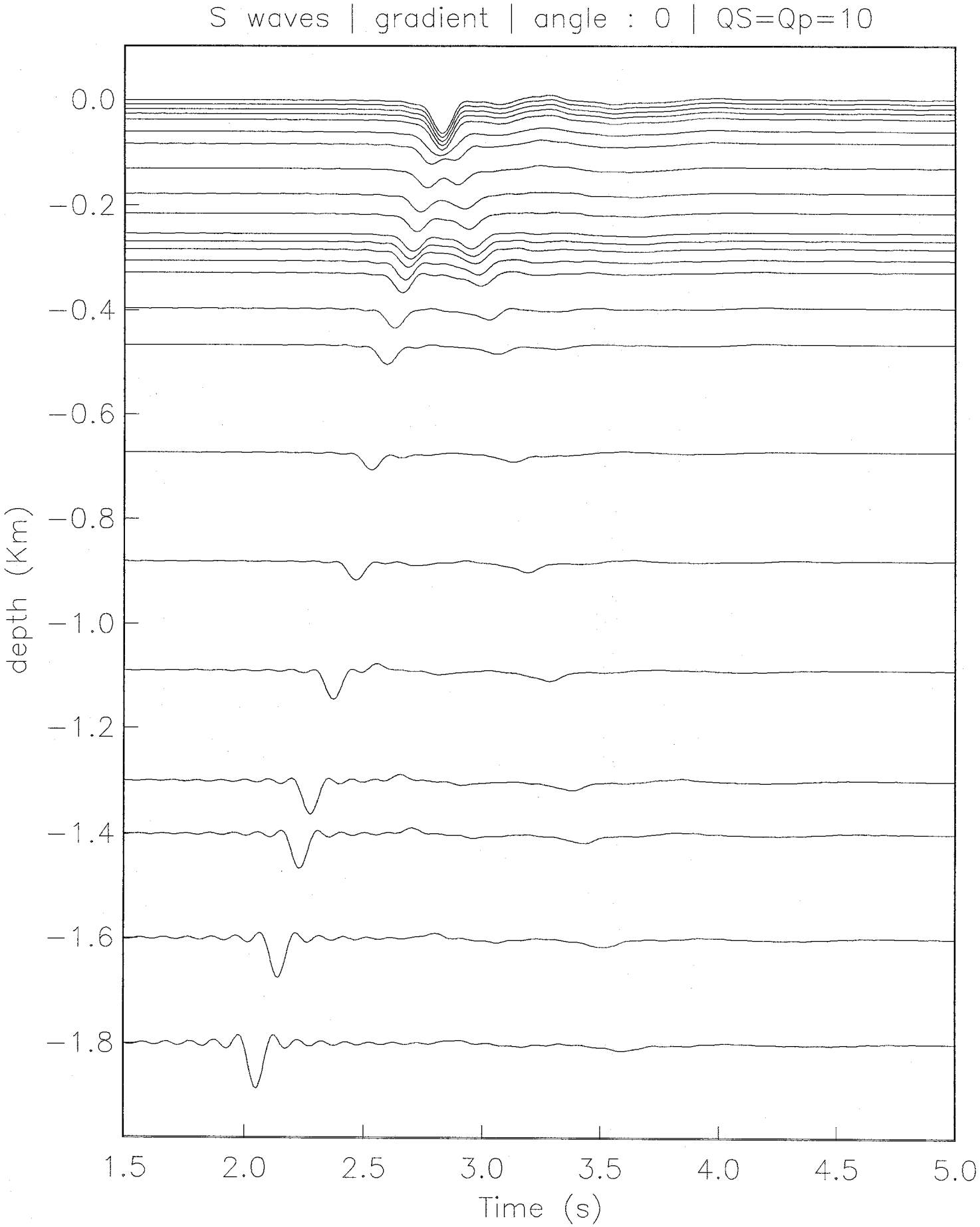
S waves | gradient | angle : 0 | QS=Qp=10
0.0
−0.2
−0.4
−0.6
−0.8
−1.0
−1.2
−1.4
−1.6
−1.8
depth (Km)
1.5
2.0
2.5
3.0
3.5
4.0
4.5
5.0
Time (s)

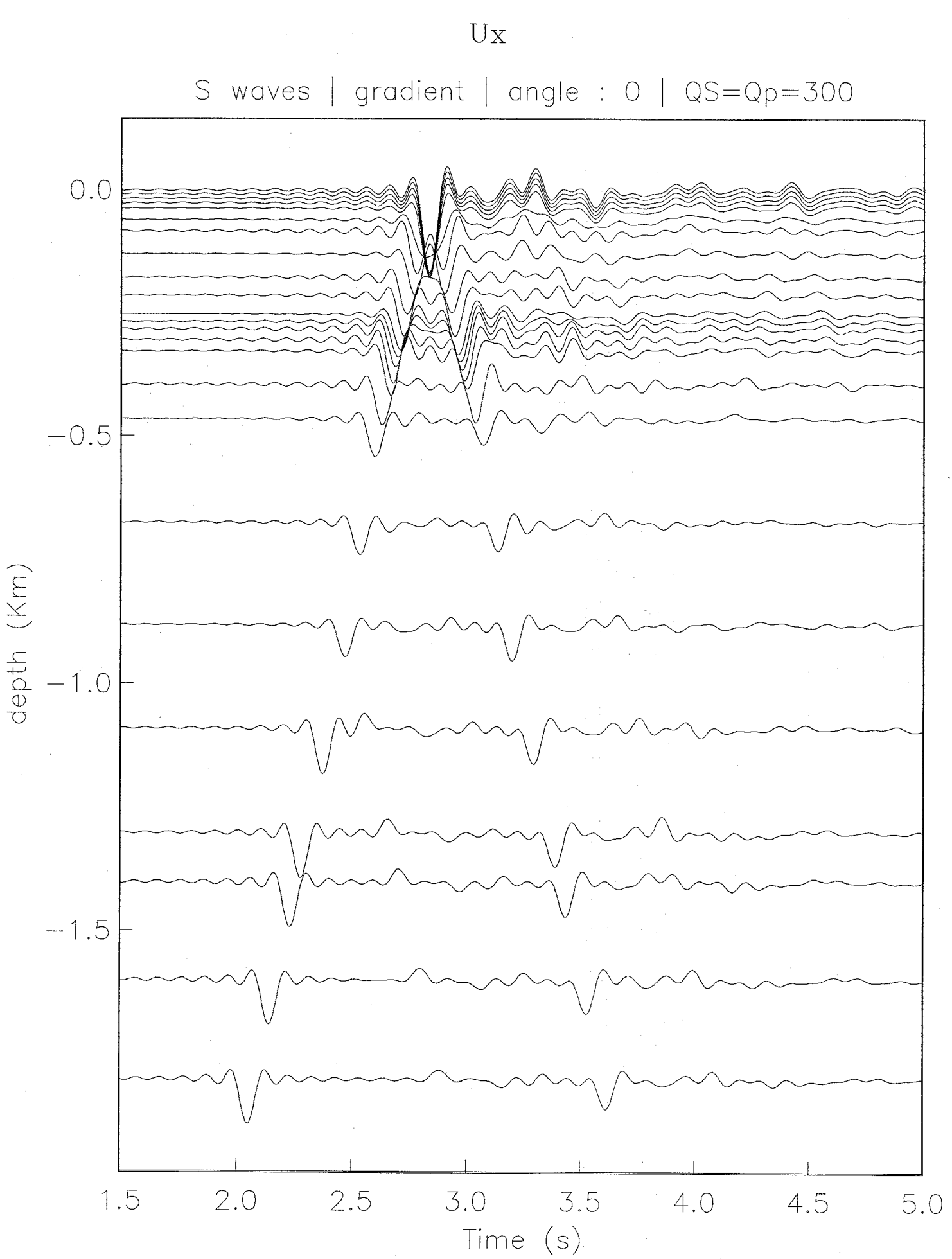
Ux
S waves | gradient | angle : 0 | QS=Qp=300
0.0
−0.5
−1.0
−1.5
depth (Km)
1.5
2.0
2.5
3.0
3.5
4.0
4.5
5.0
Time (s)

Ux

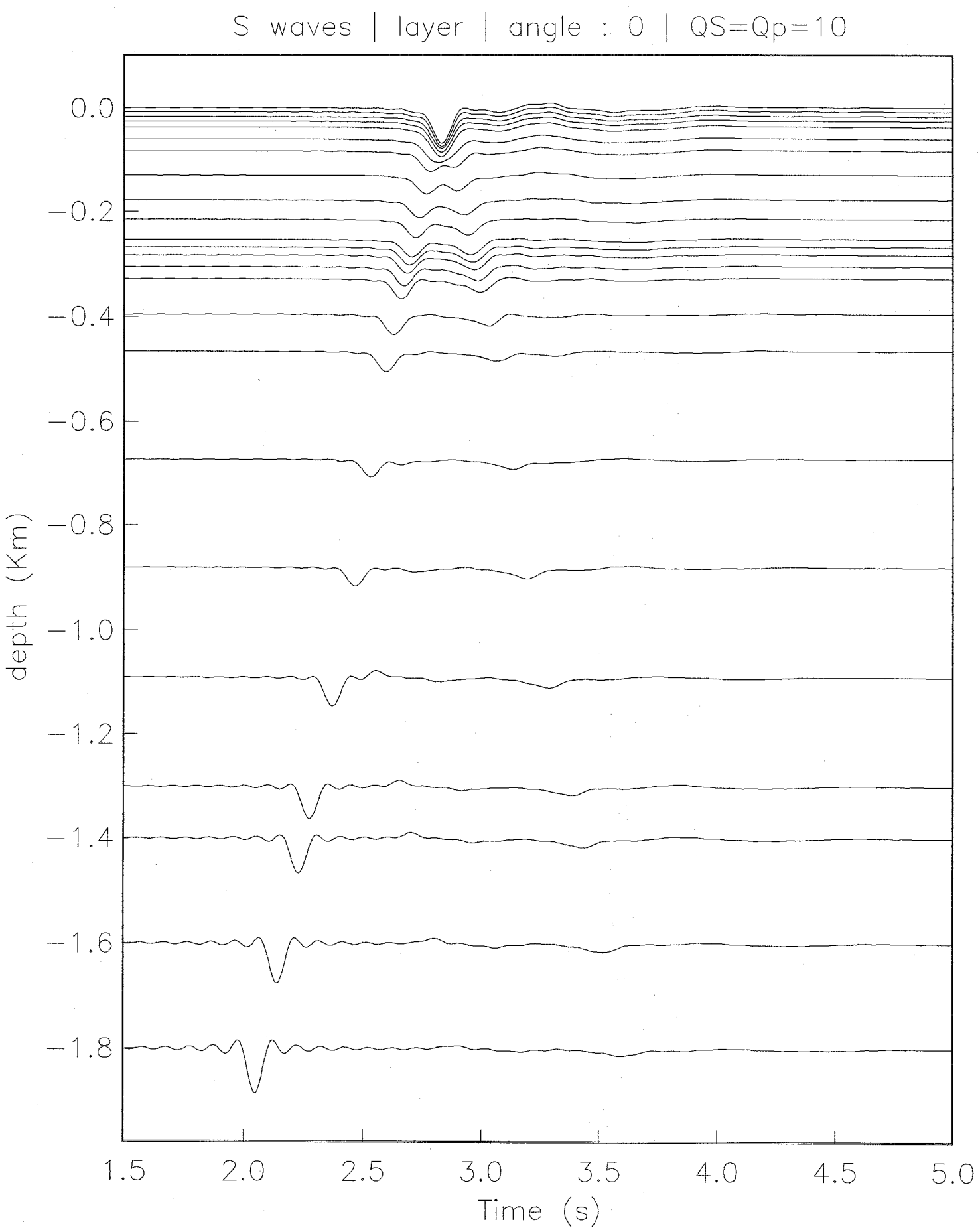
S waves | layer | angle : 0 | QS=Qp=10
0.0
−0.2
−0.4
−0.6
−0.8
−1.0
−1.2
−1.4
−1.6
−1.8
depth (Km)
1.5
2.0
2.5
3.0
3.5
4.0
4.5
5.0
Time (s)

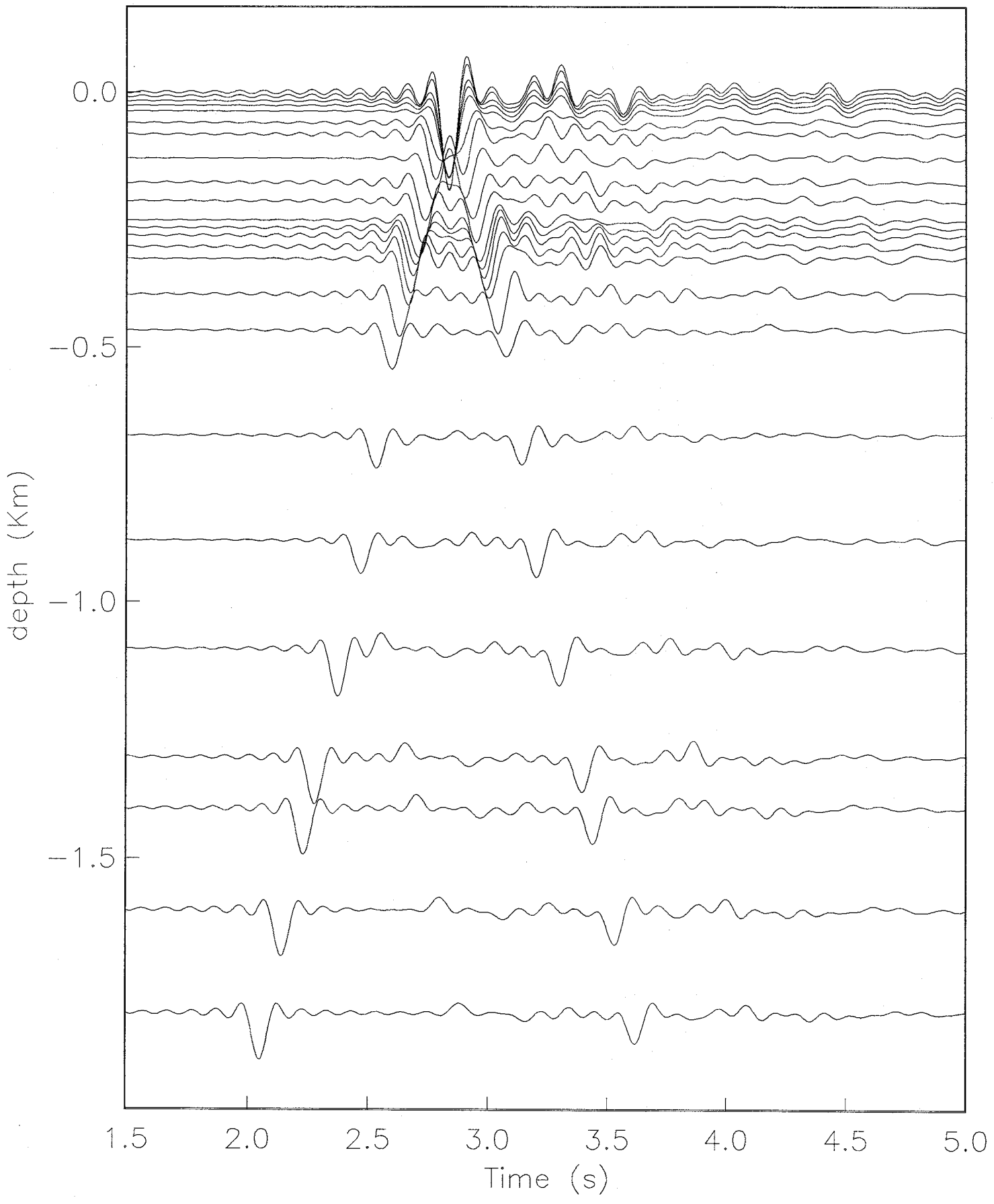
Ux
S waves | layer | angle : 0 | QS=Qp=300
0.0
−0.5
−1.0
−1.5
depth (Km)
1.5
2.0
2.5
3.0
3.5
4.0
4.5
5.0
Time (s)

Uz

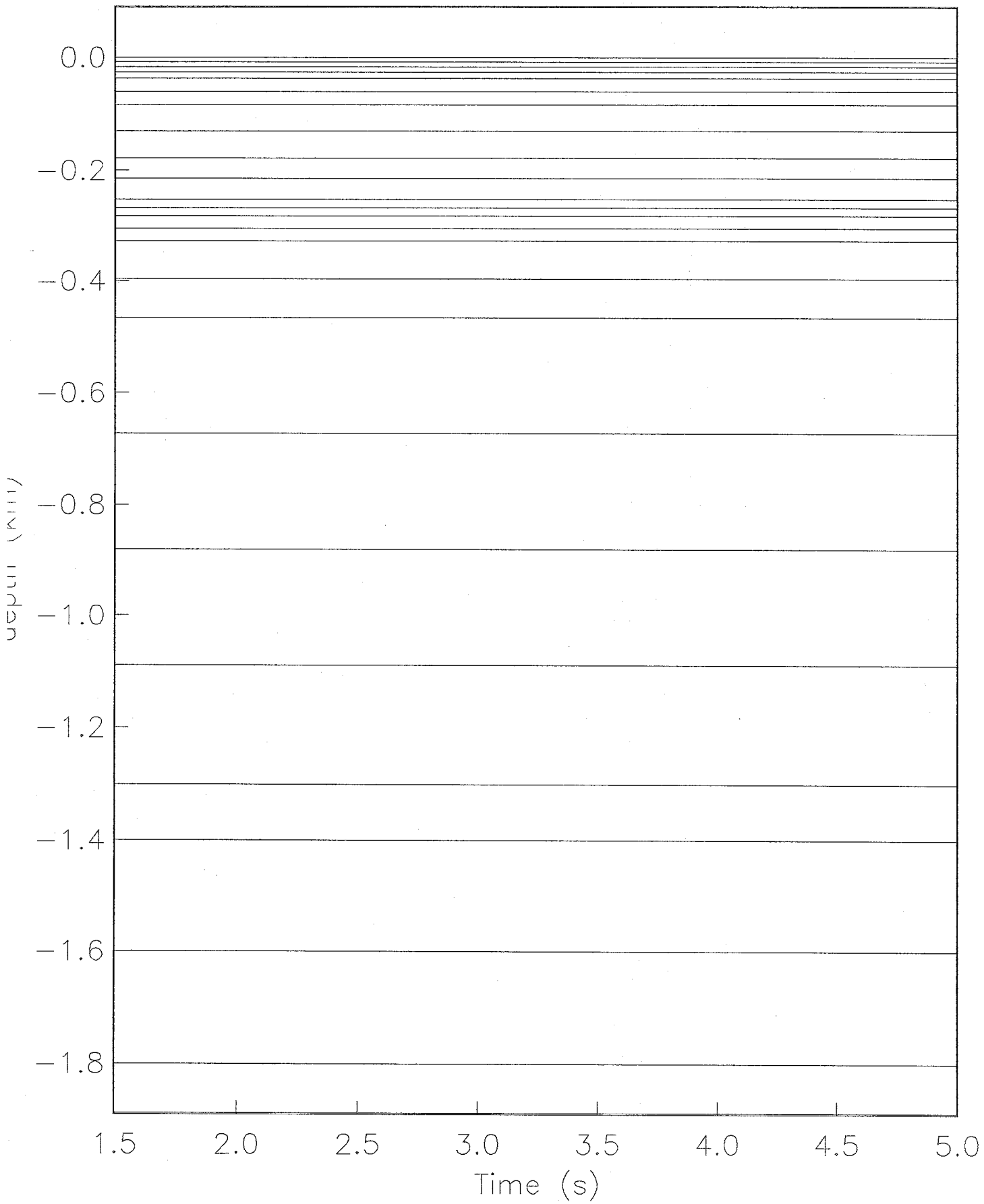
S waves | gradient | angle : 0 | Qs=Qp=10
0.0
−0.2
−0.4
−0.6
−0.8
−1.0
−1.2
−1.4
−1.6
−1.8
1.5
2.0
2.5
3.0
3.5
4.0
4.5
5.0
Time (s)

Uz

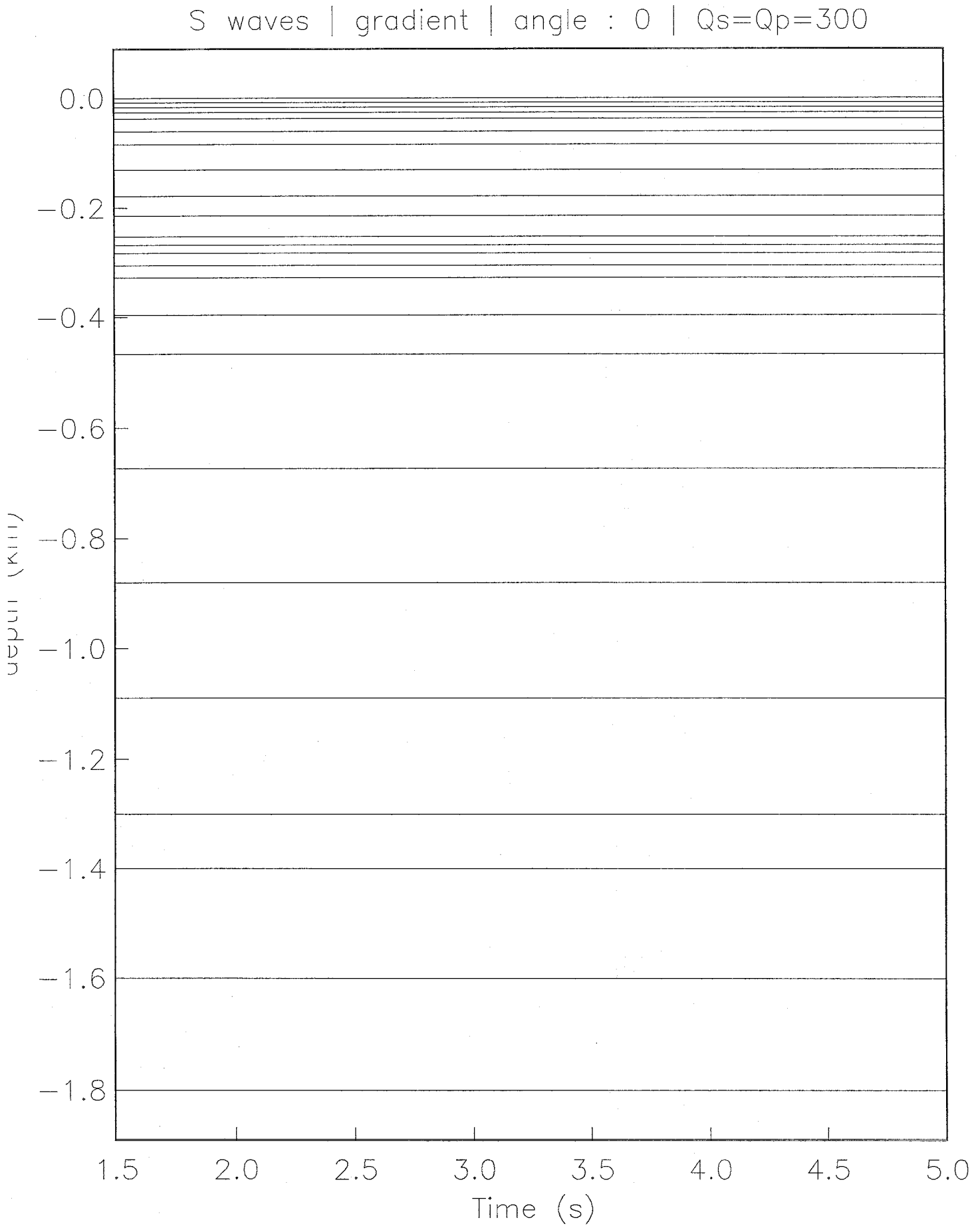
S waves | gradient | angle : 0 | Qs=Qp=300
0.0
−0.2
−0.4
−0.6
−0.8
−1.0
−1.2
−1.4
−1.6
−1.8
depth (km)
1.5
2.0
2.5
3.0
3.5
4.0
4.5
5.0
Time (s)

Uz

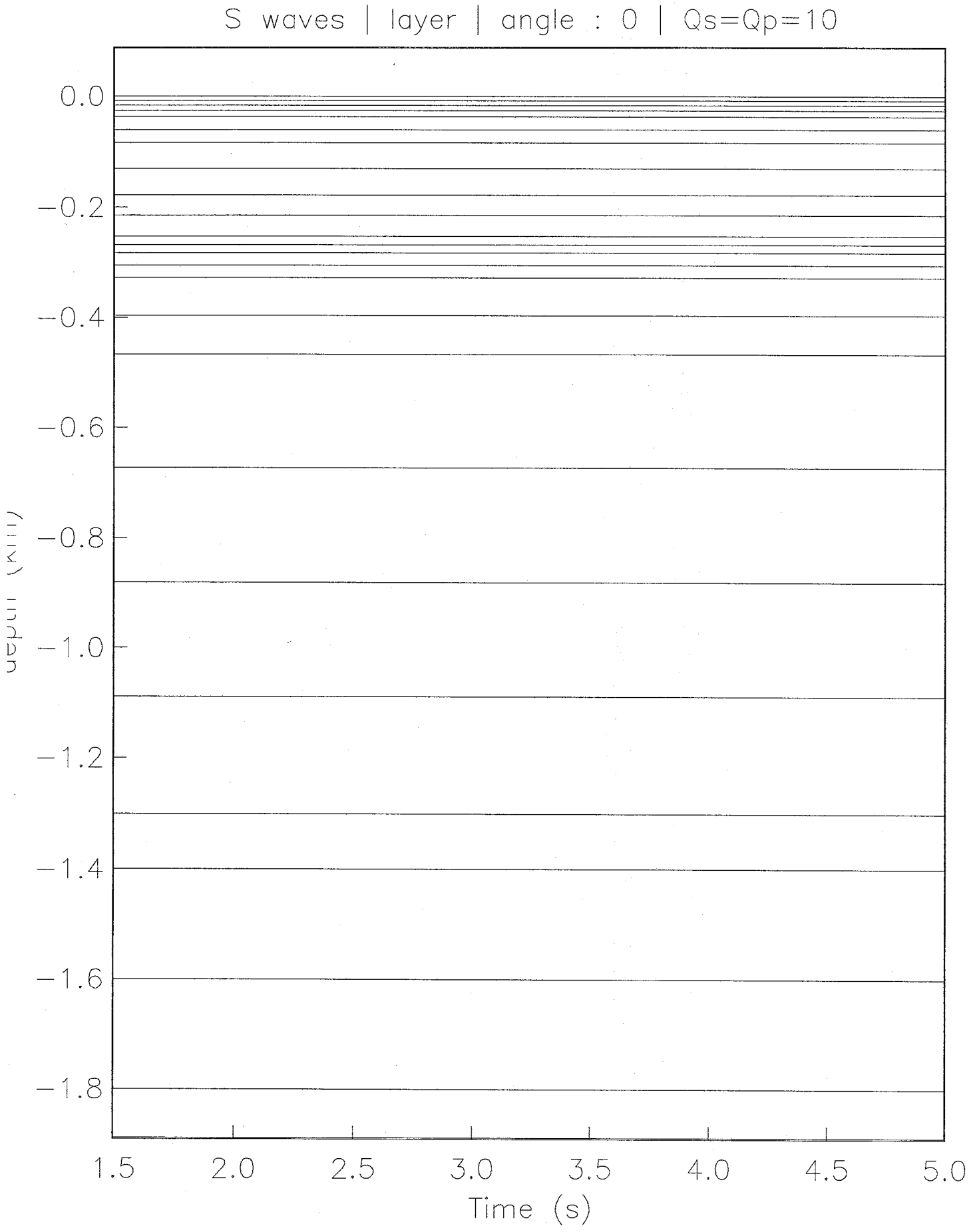
S waves | layer | angle : 0 | Qs=Qp=10
0.0
−0.2
−0.4
−0.6
−0.8
−1.0
−1.2
−1.4
−1.6
−1.8
Depth (km)
1.5
2.0
2.5
3.0
3.5
4.0
4.5
5.0
Time (s)

Uz

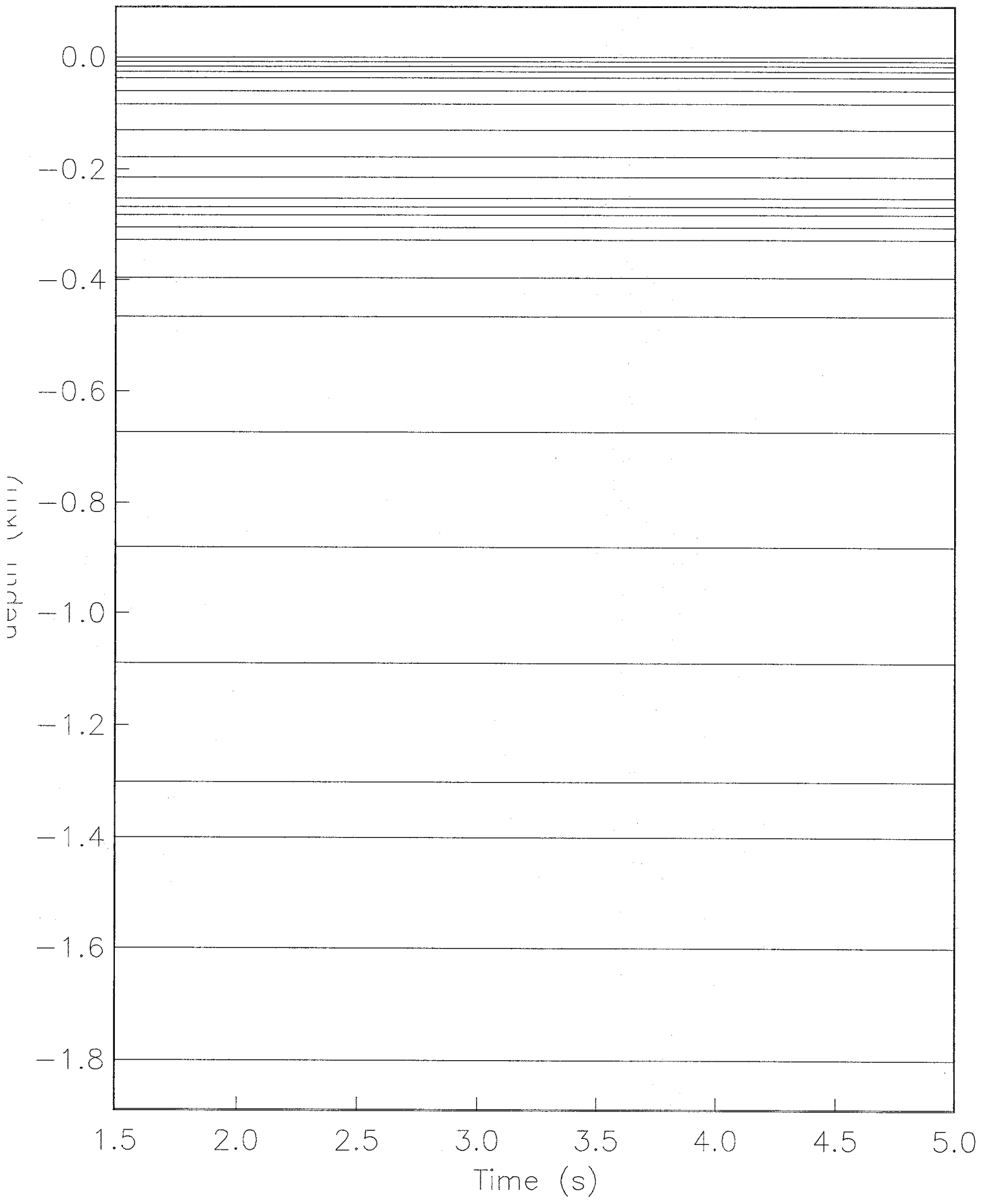
S waves | layer | angle : 0 | Qs=Qp=300
0.0
−0.2
−0.4
−0.6
−0.8
−1.0
−1.2
−1.4
−1.6
−1.8
depth (km)
1.5
2.0
2.5
3.0
3.5
4.0
4.5
5.0
Time (s)

Ux

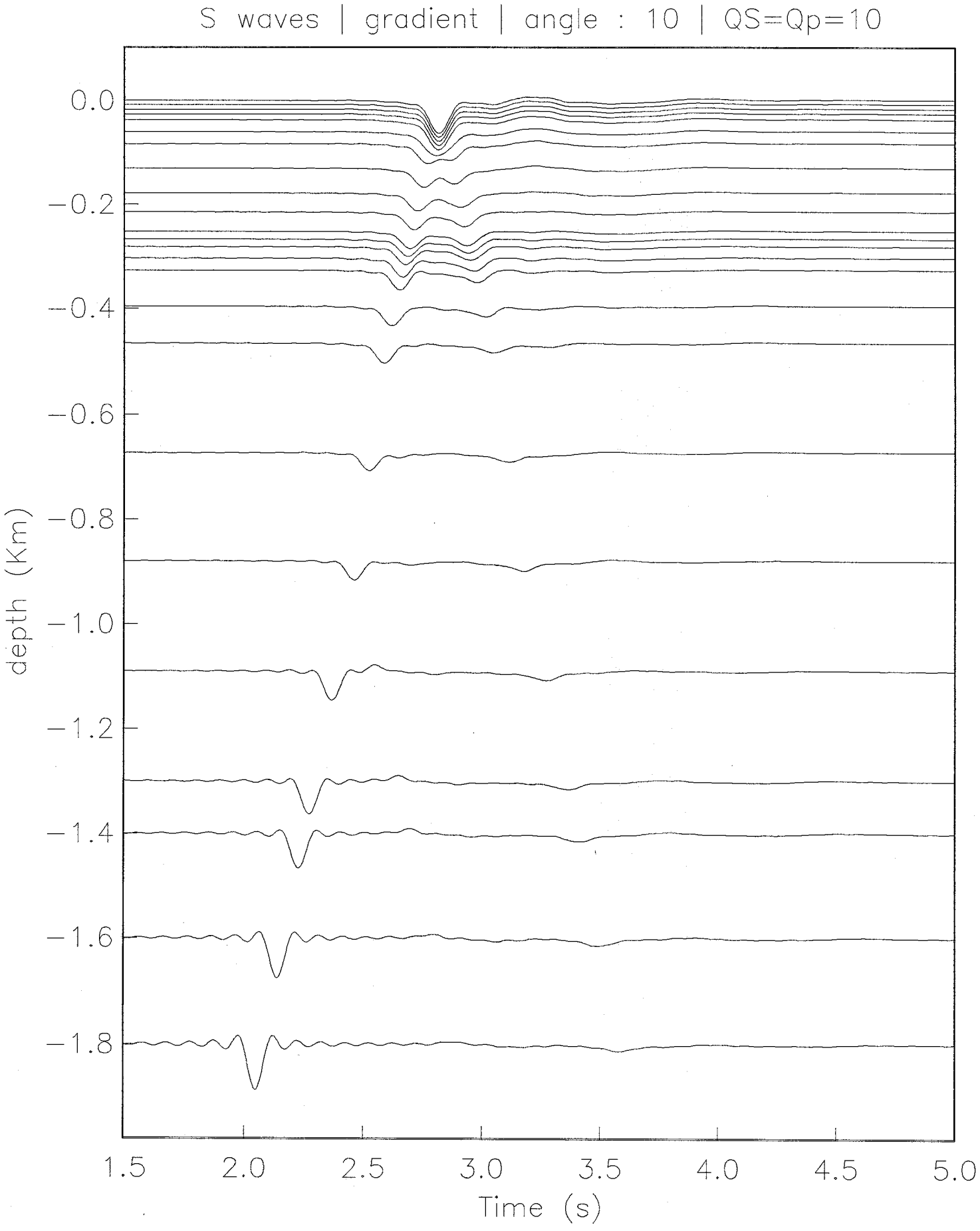
S waves | gradient | angle : 10 | QS=Qp=10
0.0
-0.2
-0.4
-0.6
-0.8
-1.0
-1.2
-1.4
-1.6
-1.8
depth (Km)
1.5
2.0
2.5
3.0
3.5
4.0
4.5
5.0
Time (s)

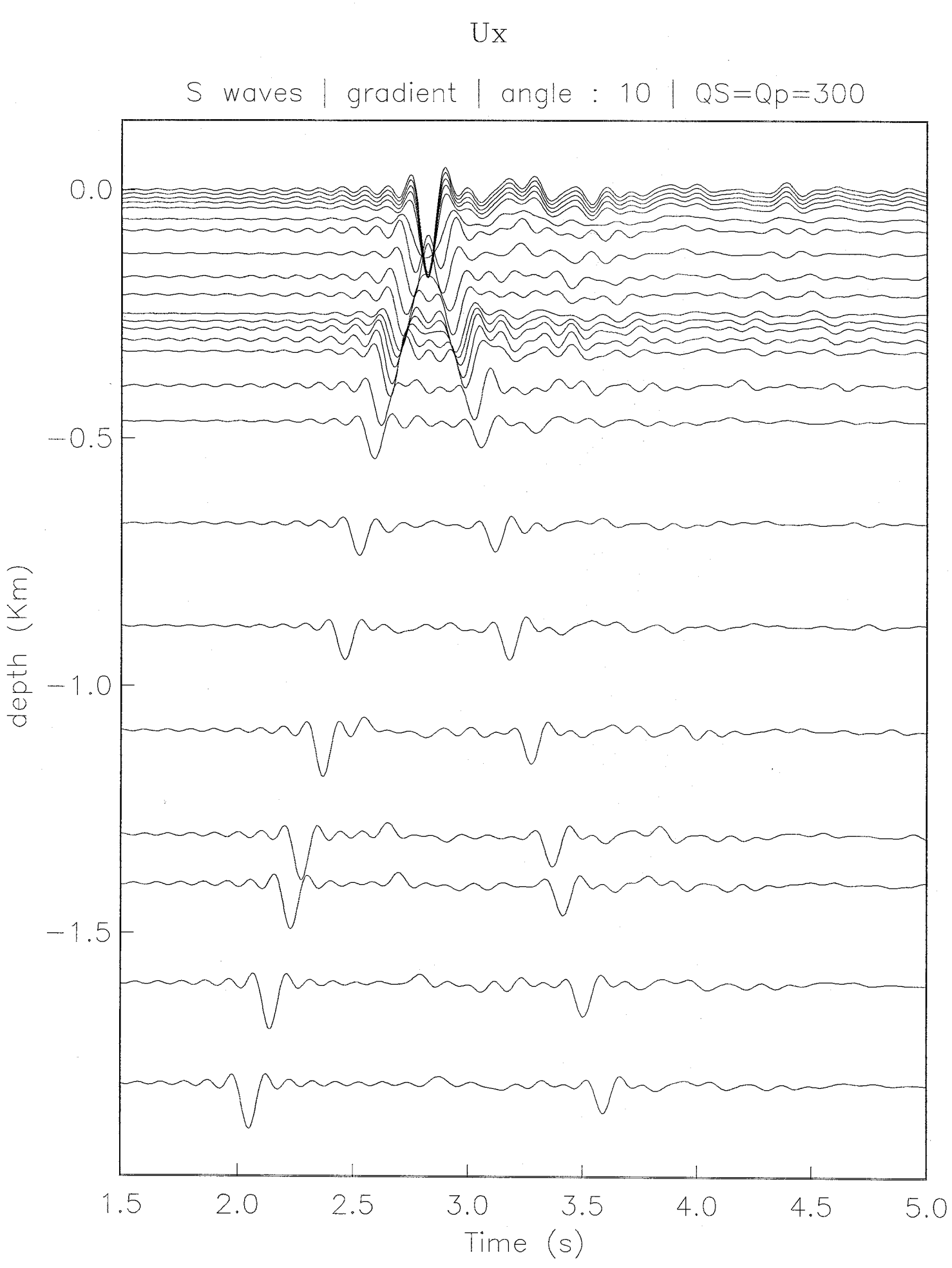
Ux
S waves | gradient | angle : 10 | QS=Qp=300
0.0
-0.5
-1.0
-1.5
depth (Km)
1.5
2.0
2.5
3.0
3.5
4.0
4.5
5.0
Time (s)

Ux

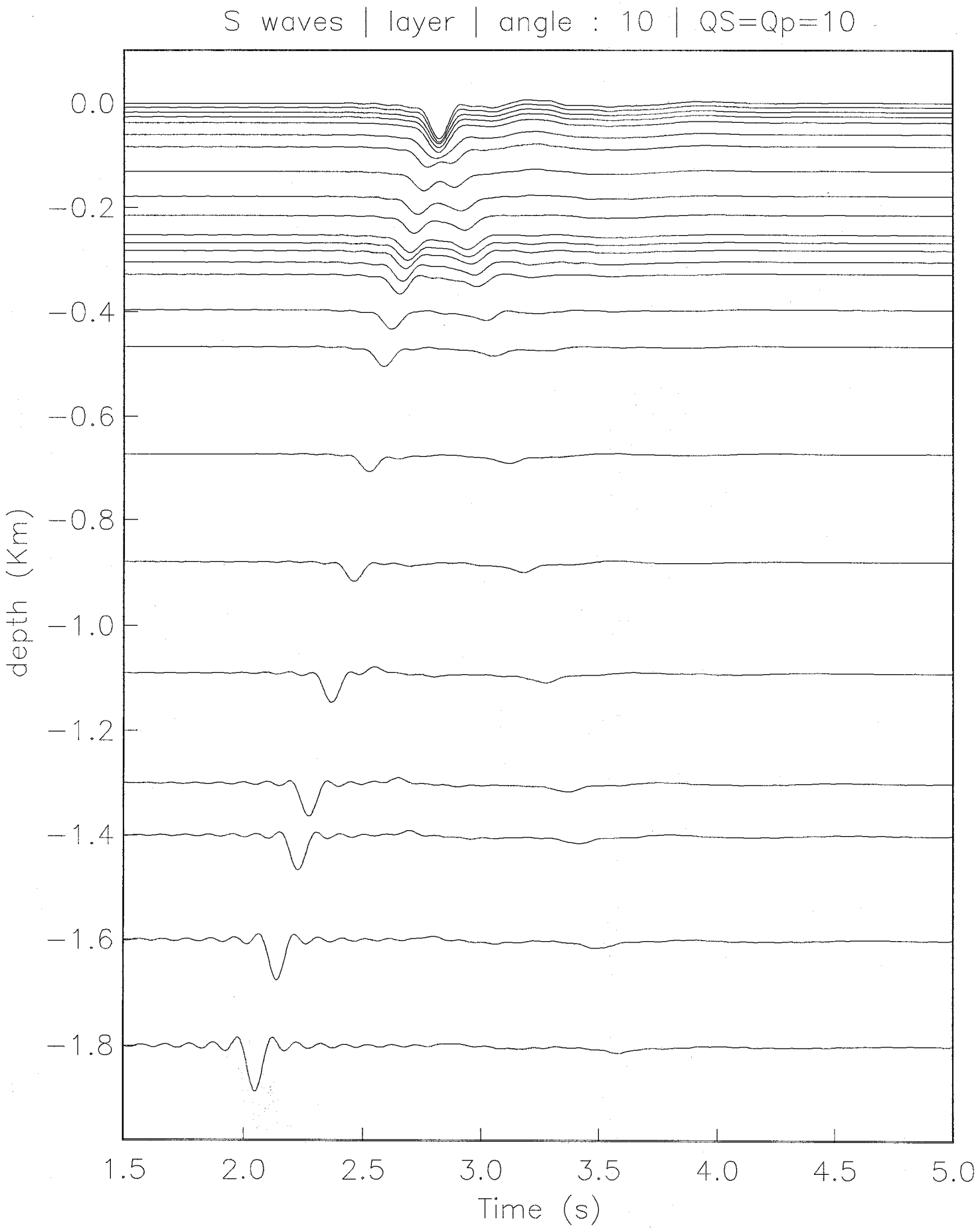
S waves | layer | angle : 10 | QS=Qp=10
0.0
-0.2
-0.4
-0.6
-0.8
-1.0
-1.2
-1.4
-1.6
-1.8
depth (Km)
1.5
2.0
2.5
3.0
3.5
4.0
4.5
5.0
Time (s)

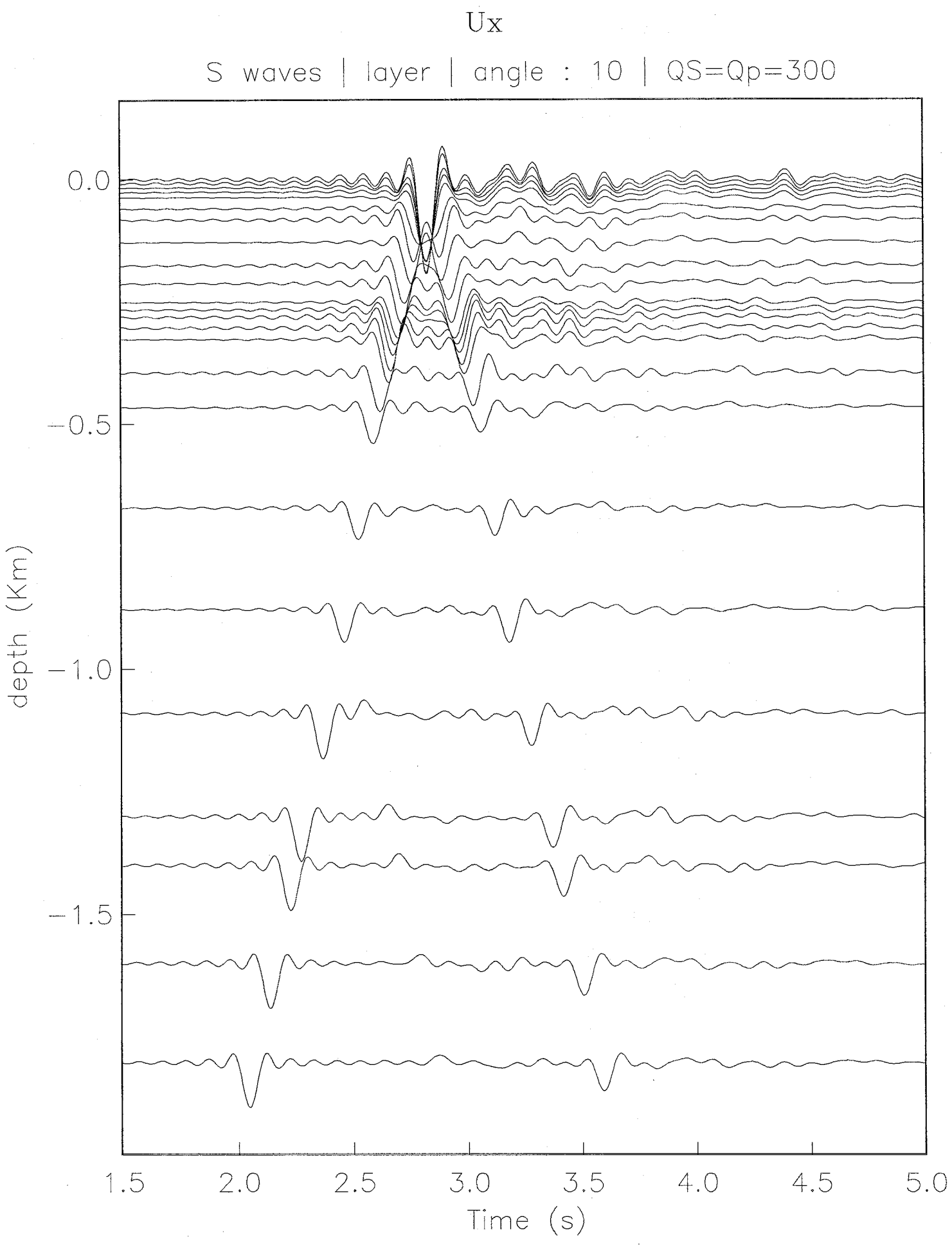
Ux
S waves | layer | angle : 10 | QS=Qp=300
0.0
-0.5
-1.0
-1.5
depth (Km)
1.5
2.0
2.5
3.0
3.5
4.0
4.5
5.0
Time (s)

Uz

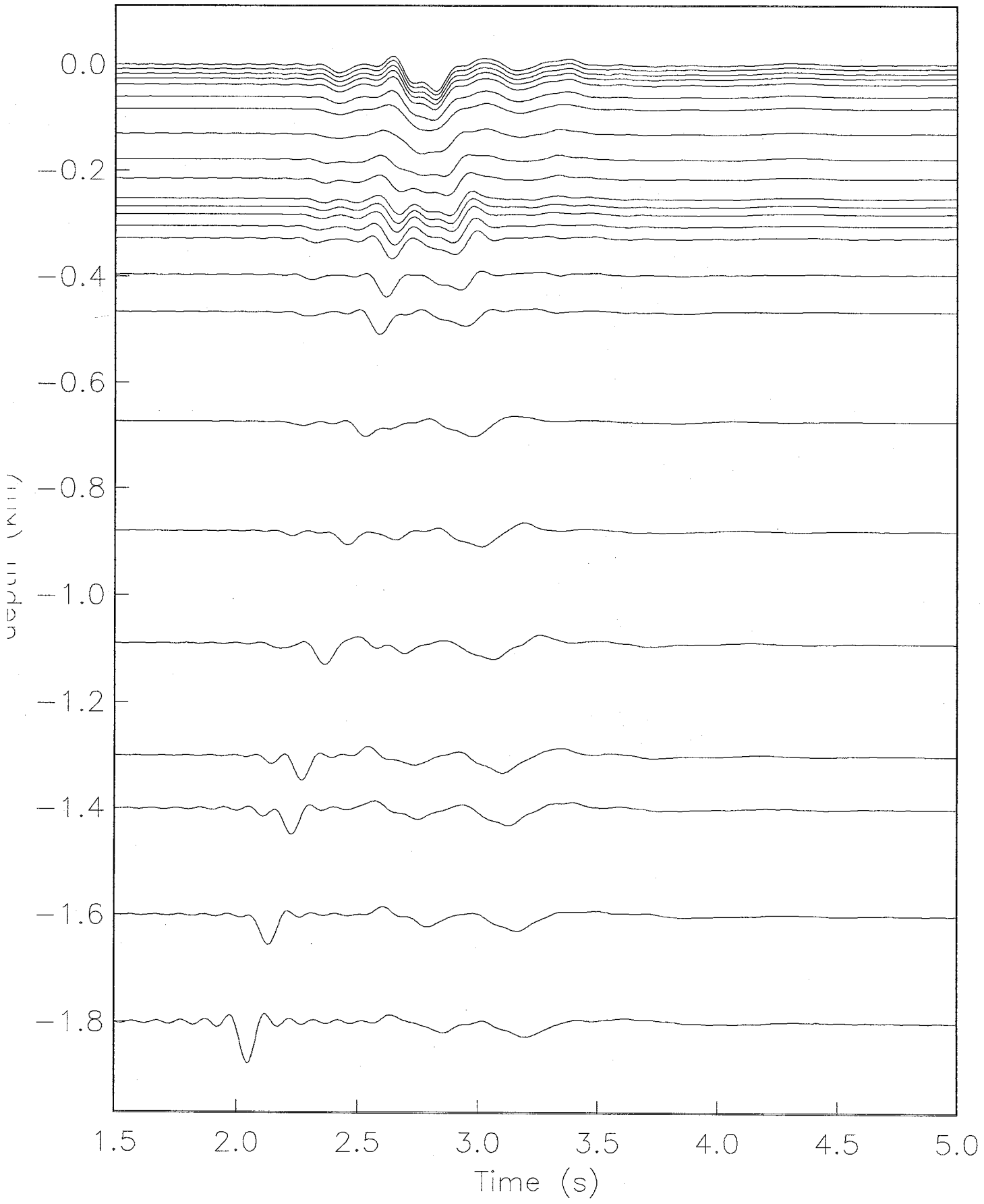
S waves | gradient | angle : 10 | Qs=Qp=10
0.0
-0.2
-0.4
-0.6
-0.8
-1.0
-1.2
-1.4
-1.6
-1.8
1.5
2.0
2.5
3.0
3.5
4.0
4.5
5.0
Time (s)

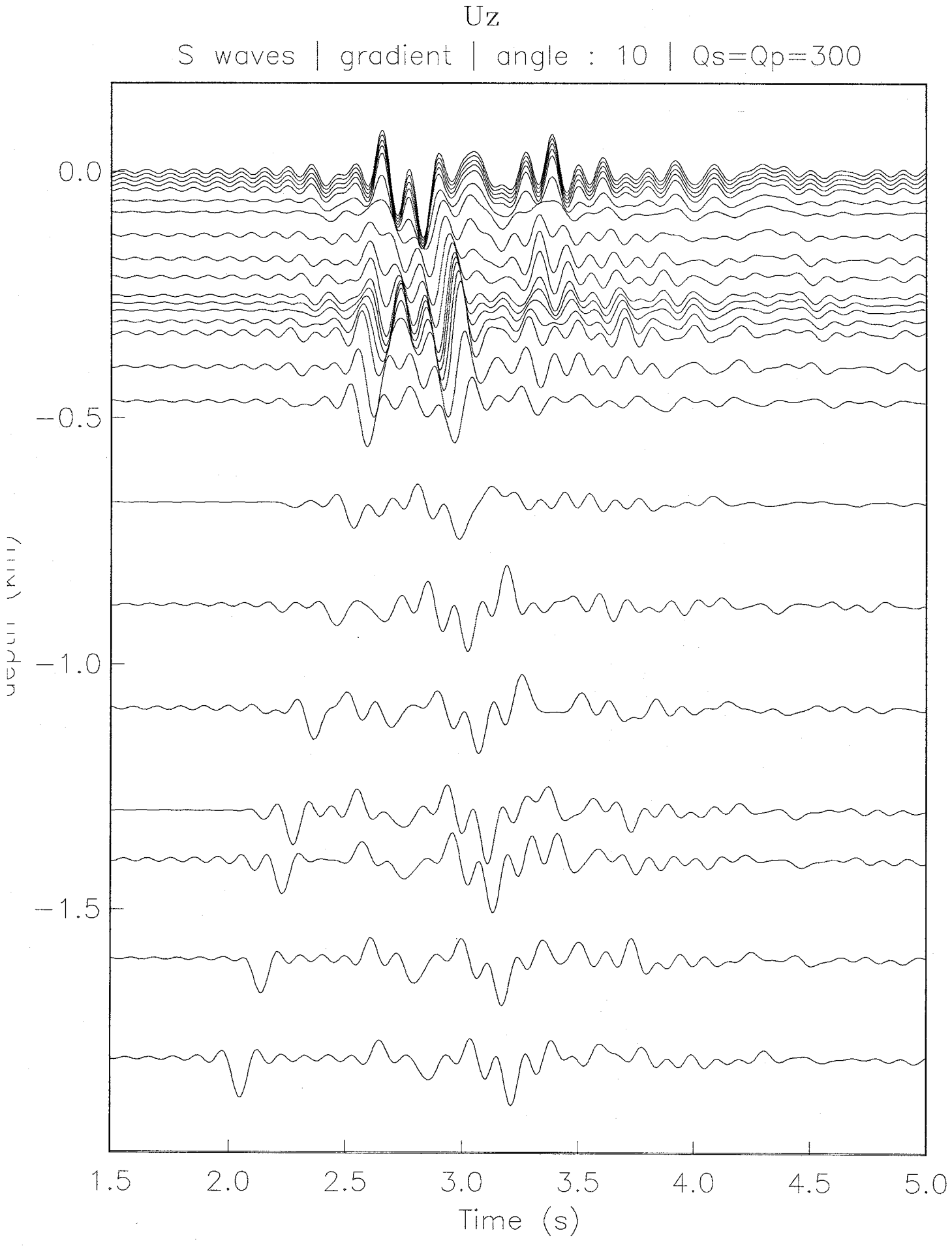
Uz
S waves | gradient | angle : 10 | Qs=Qp=300
0.0
−0.5
−1.0
−1.5
depth (km)
1.5
2.0
2.5
3.0
3.5
4.0
4.5
5.0
Time (s)

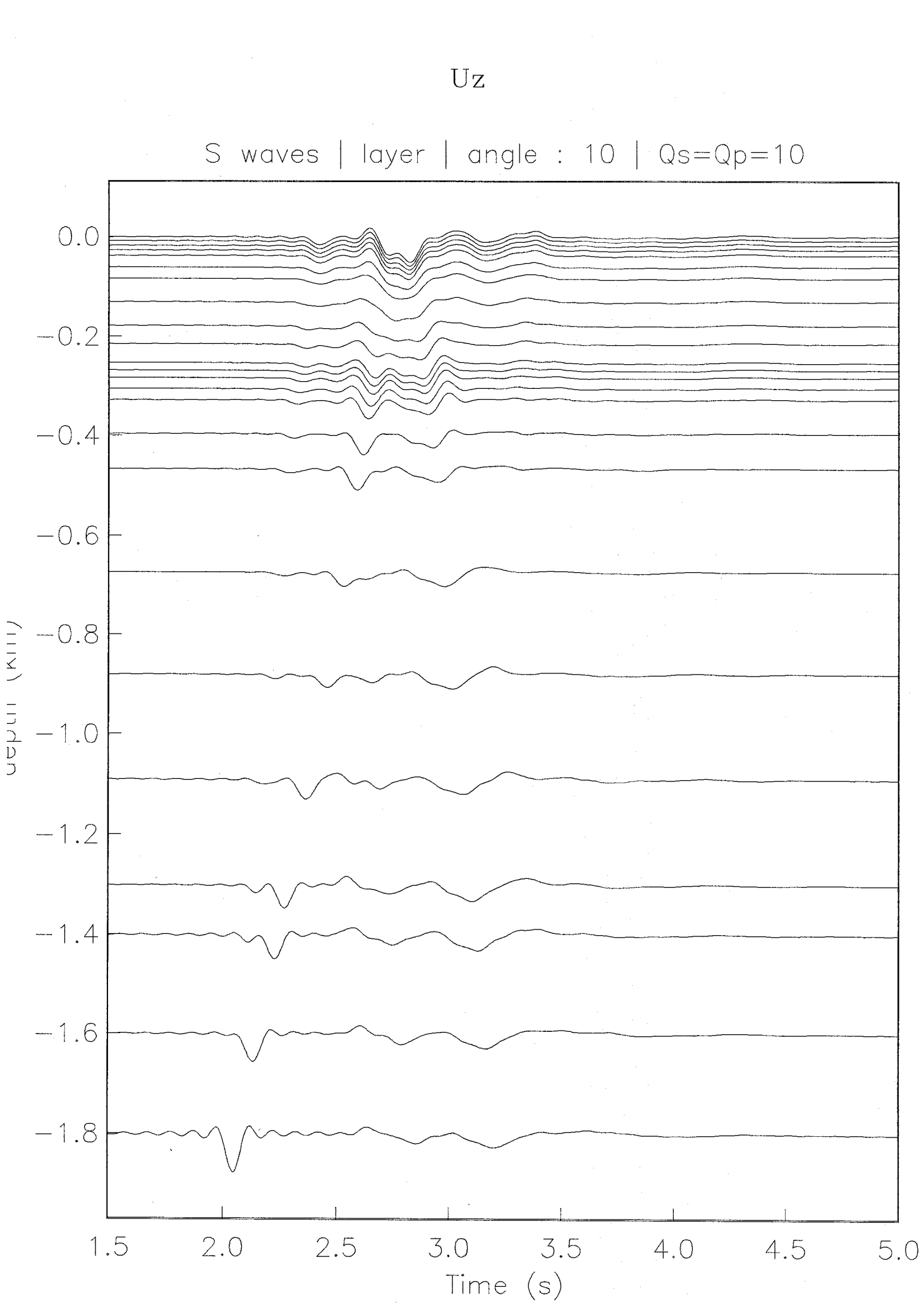
Uz
S waves | layer | angle : 10 | Qs=Qp=10
0.0
-0.2
-0.4
-0.6
-0.8
-1.0
-1.2
-1.4
-1.6
-1.8
Depth (km)
1.5
2.0
2.5
3.0
3.5
4.0
4.5
5.0
Time (s)

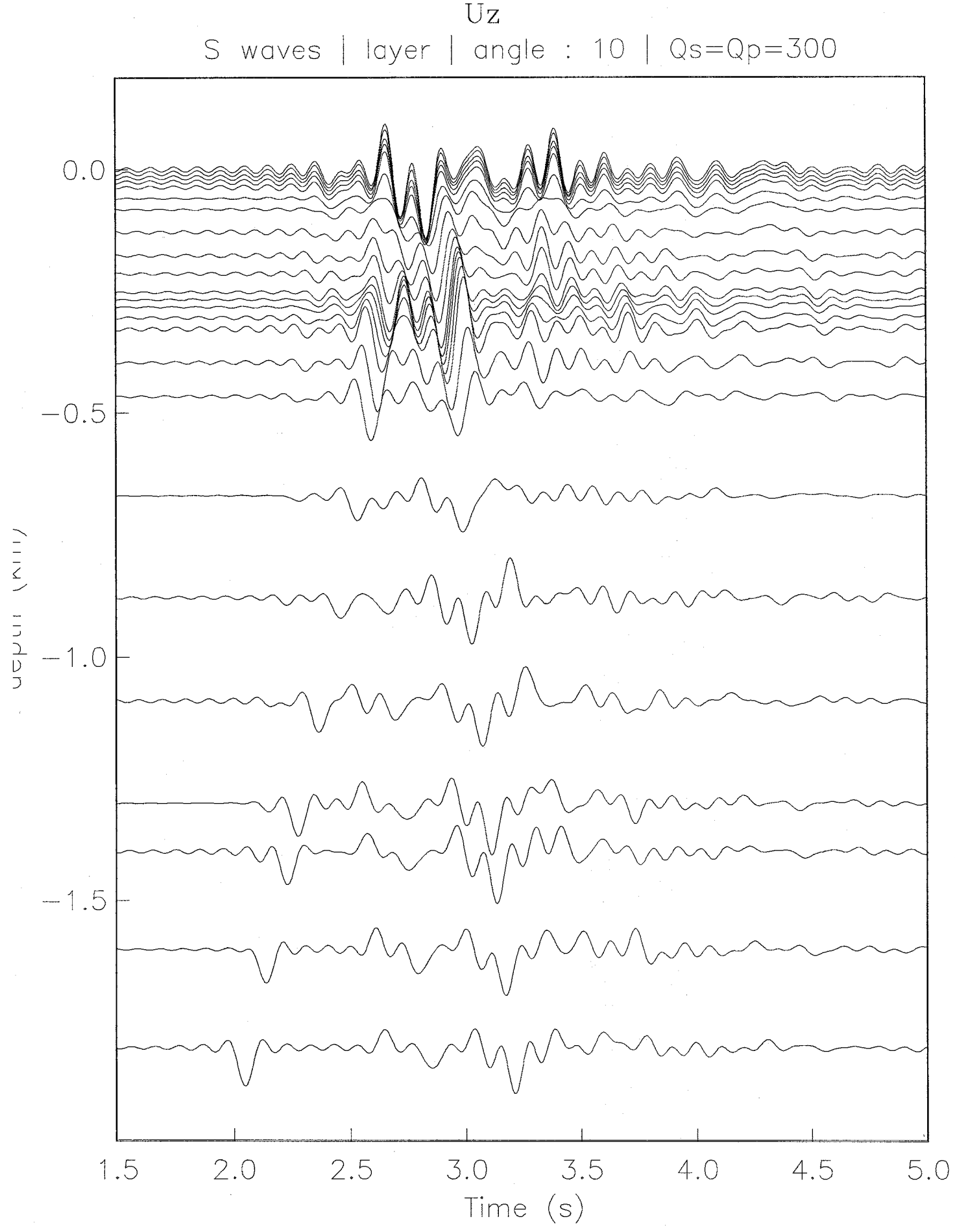
Uz
S waves | layer | angle : 10 | Qs=Qp=300
0.0
−0.5
−1.0
−1.5
depth (km)
1.5
2.0
2.5
3.0
3.5
4.0
4.5
5.0
Time (s)

Ux

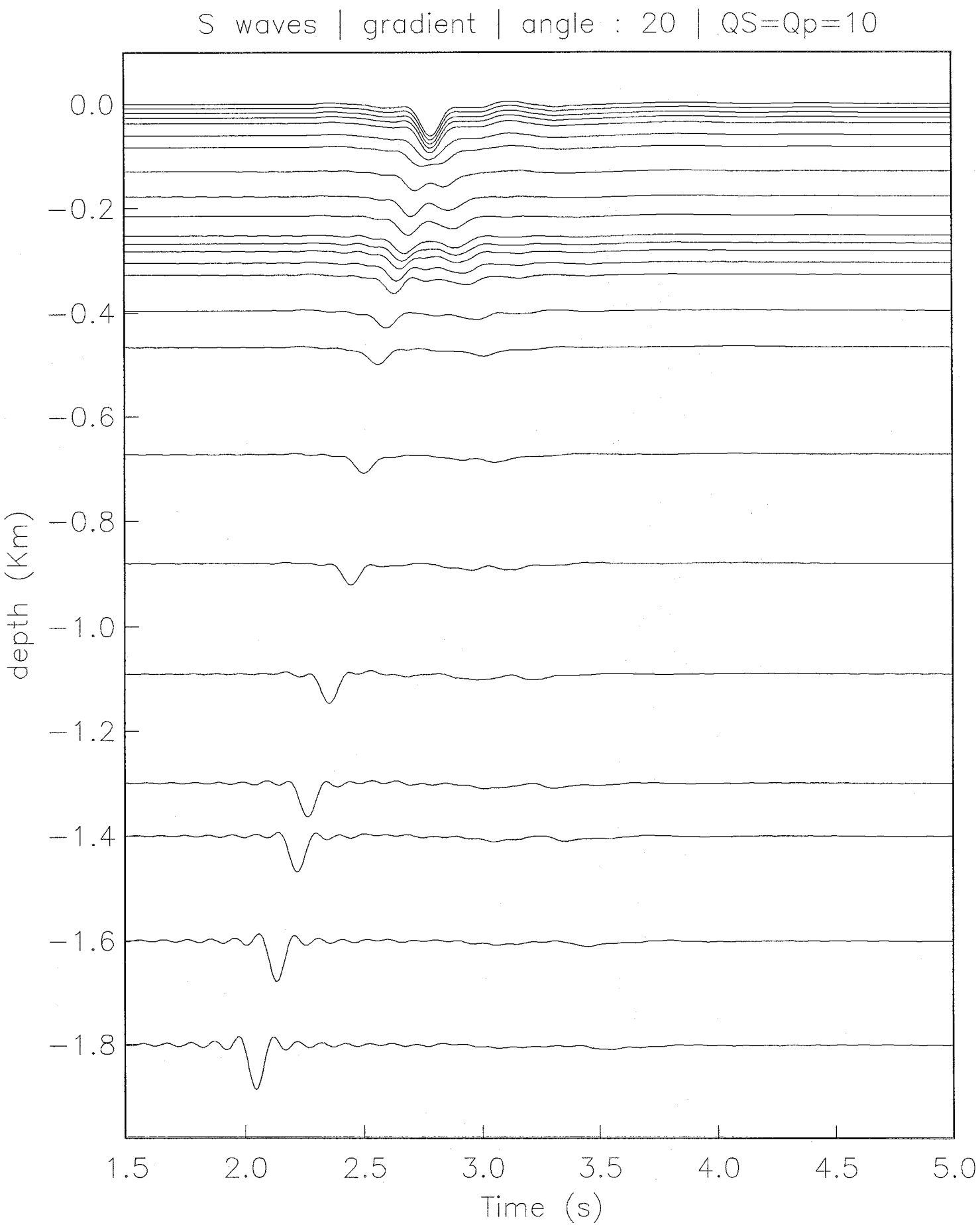
S waves | gradient | angle : 20 | QS=Qp=10
0.0
−0.2
−0.4
−0.6
−0.8
−1.0
−1.2
−1.4
−1.6
−1.8
depth (Km)
1.5
2.0
2.5
3.0
3.5
4.0
4.5
5.0
Time (s)

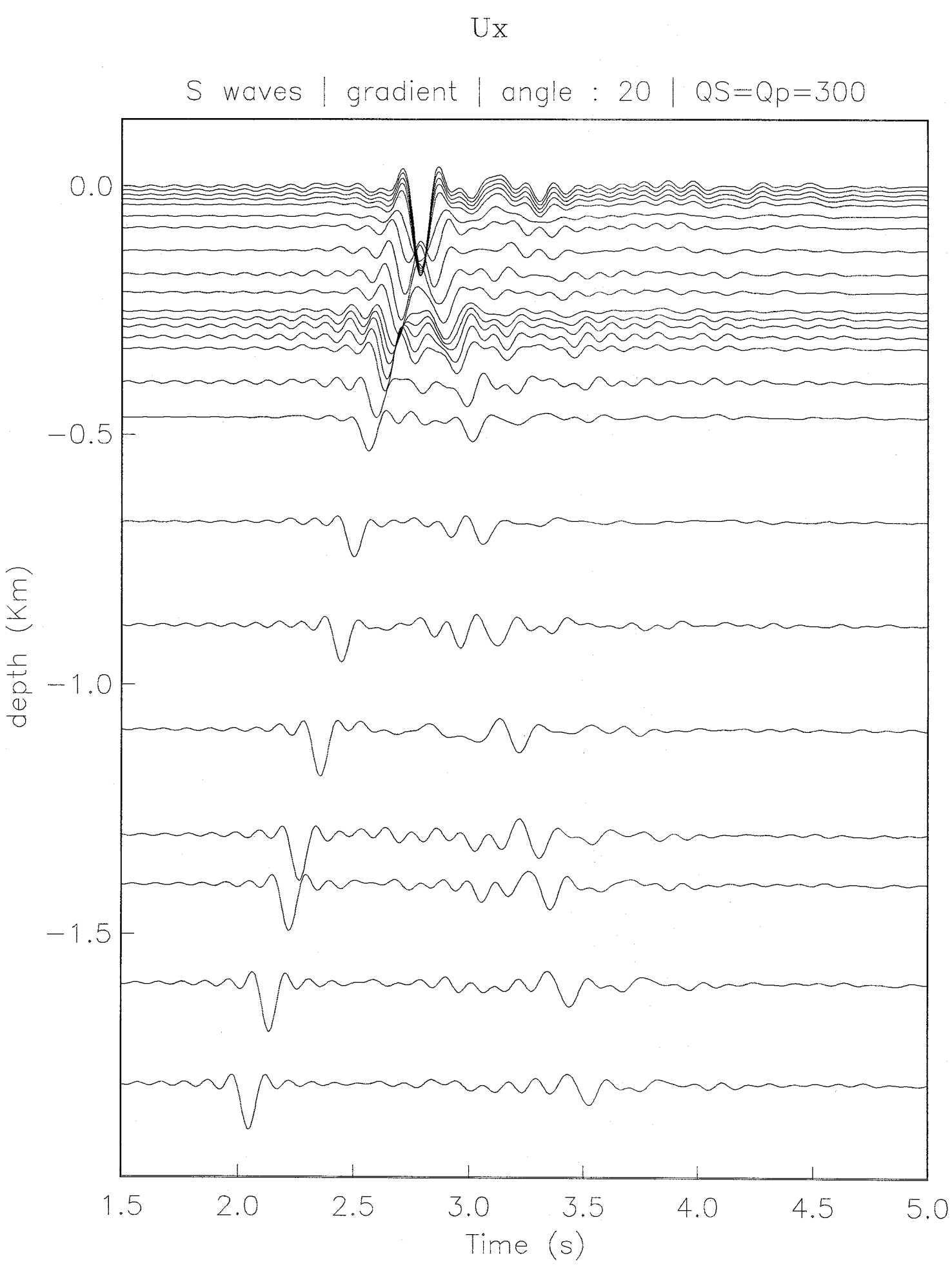
Ux
S waves | gradient | angle : 20 | QS=Qp=300
0.0
−0.5
−1.0
−1.5
depth (Km)
1.5
2.0
2.5
3.0
3.5
4.0
4.5
5.0
Time (s)

Ux

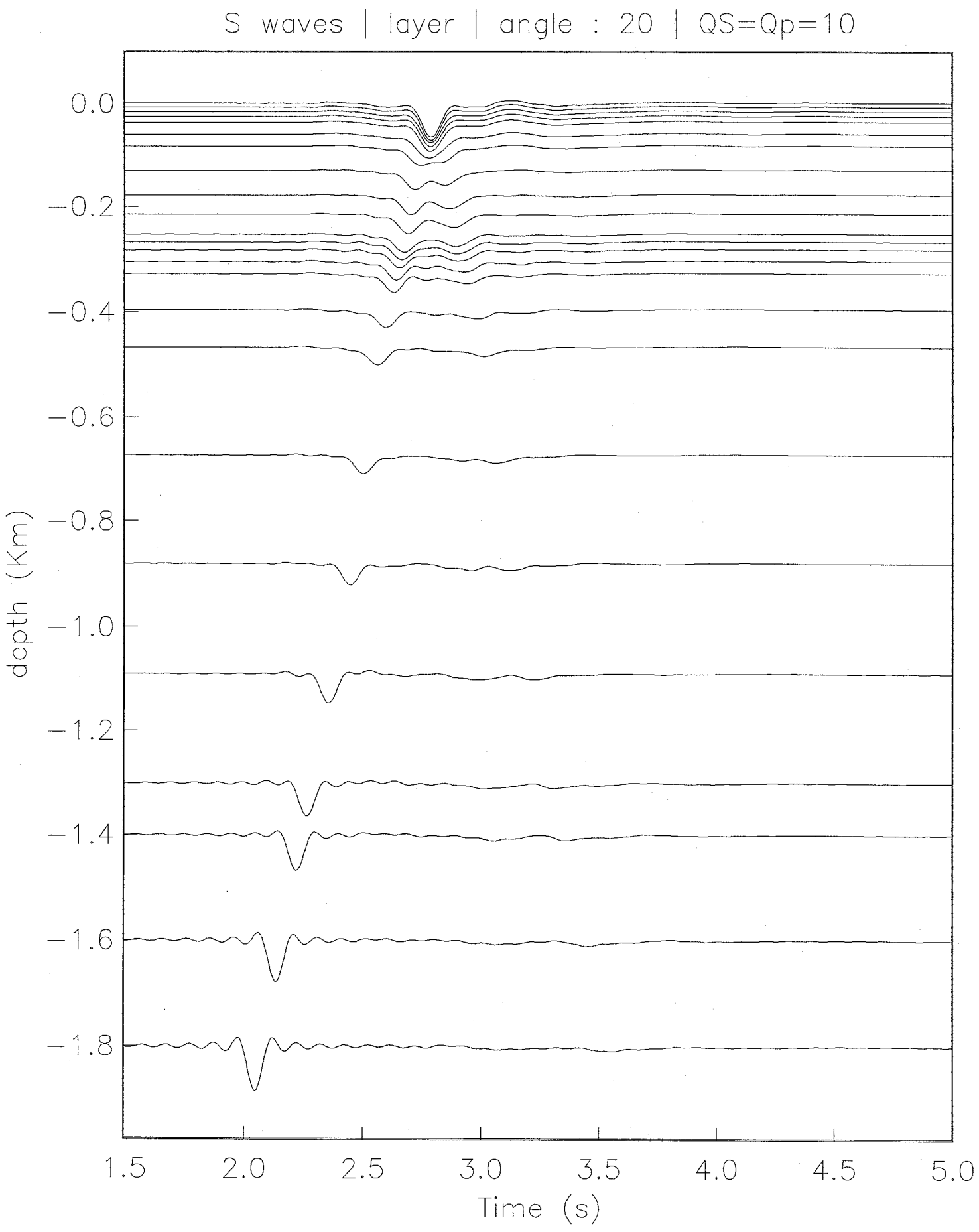
S waves | layer | angle : 20 | QS=Qp=10
0.0
−0.2
−0.4
−0.6
−0.8
−1.0
−1.2
−1.4
−1.6
−1.8
depth (Km)
1.5
2.0
2.5
3.0
3.5
4.0
4.5
5.0
Time (s)

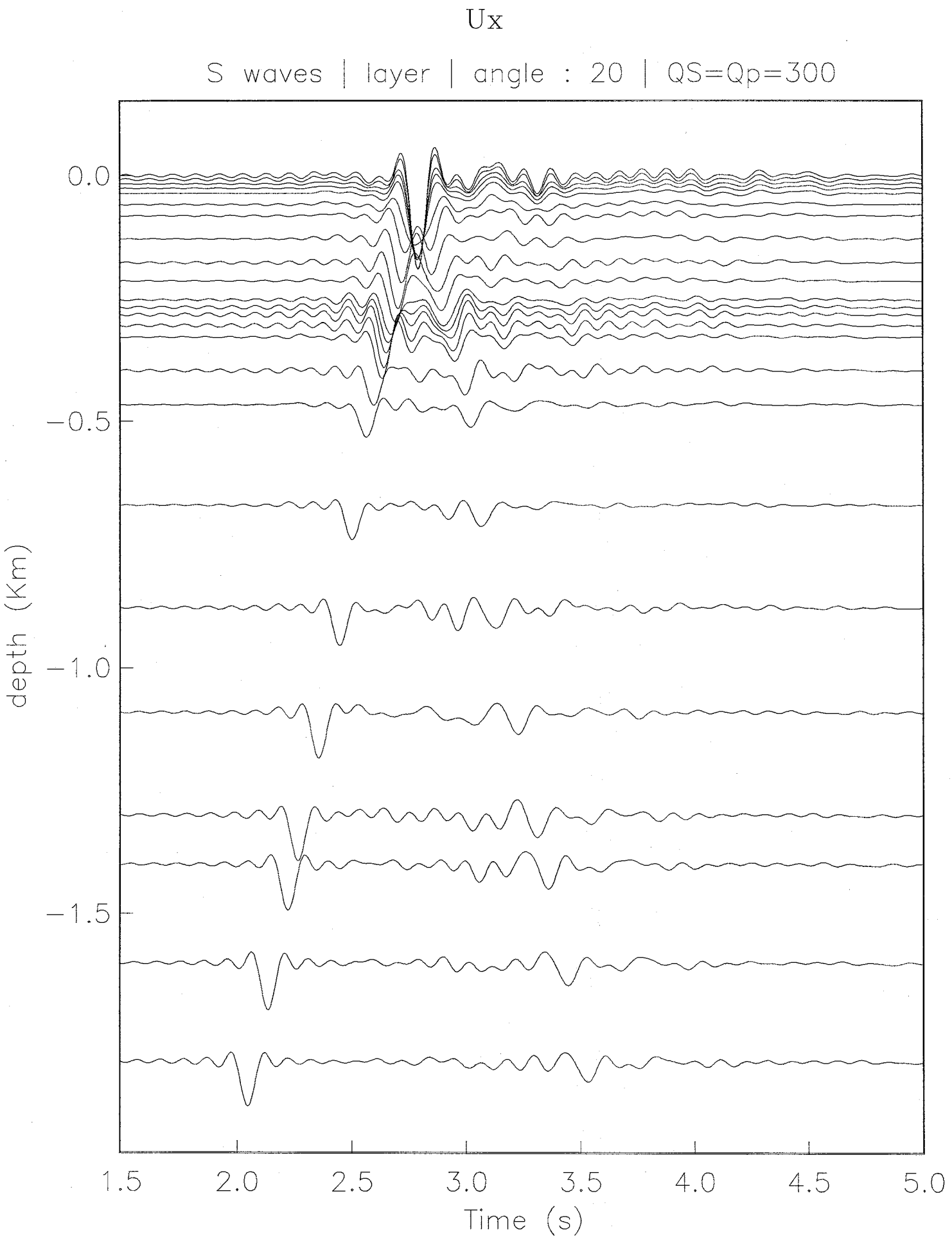
Ux
S waves | layer | angle : 20 | QS=Qp=300
0.0
−0.5
−1.0
−1.5
depth (Km)
1.5
2.0
2.5
3.0
3.5
4.0
4.5
5.0
Time (s)

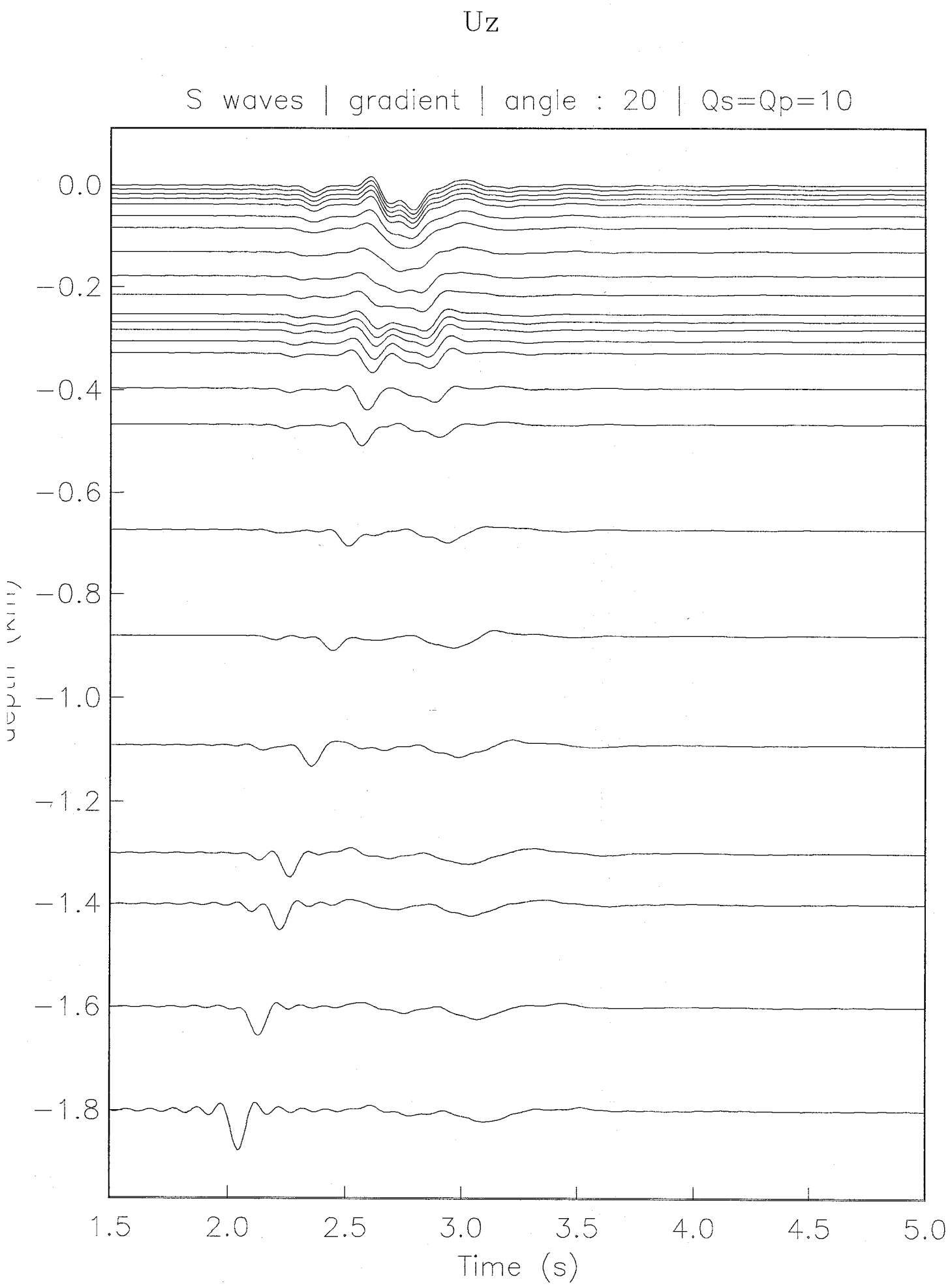
Uz
S waves | gradient | angle : 20 | Qs=Qp=10
0.0
−0.2
−0.4
−0.6
−0.8
−1.0
−1.2
−1.4
−1.6
−1.8
1.5
2.0
2.5
3.0
3.5
4.0
4.5
5.0
Time (s)

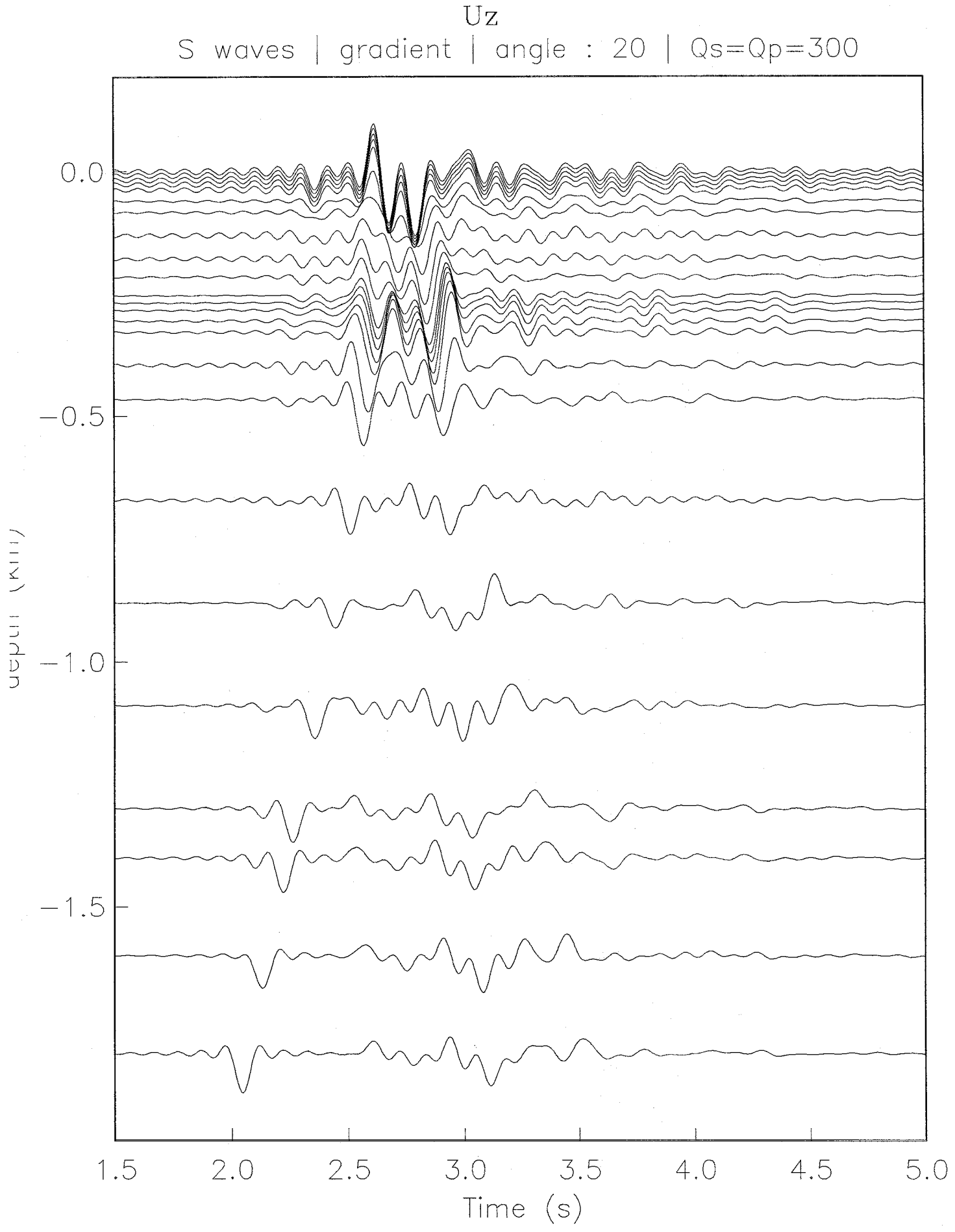
Uz
S waves | gradient | angle : 20 | Qs=Qp=300
0.0
−0.5
−1.0
−1.5
depth (km)
1.5
2.0
2.5
3.0
3.5
4.0
4.5
5.0
Time (s)

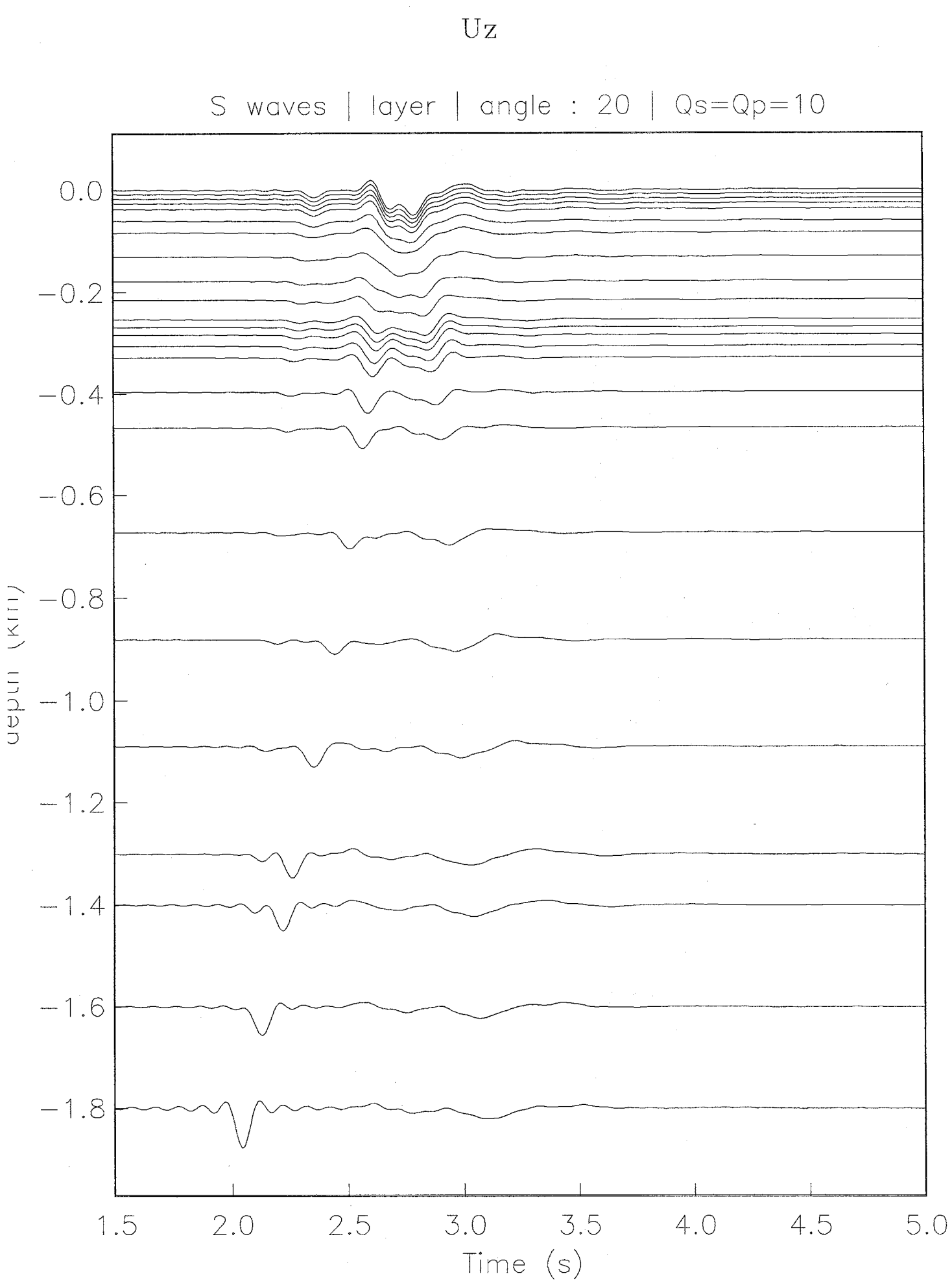
Uz
S waves | layer | angle : 20 | Qs=Qp=10
0.0
−0.2
−0.4
−0.6
−0.8
−1.0
−1.2
−1.4
−1.6
−1.8
depth (km)
1.5
2.0
2.5
3.0
3.5
4.0
4.5
5.0
Time (s)

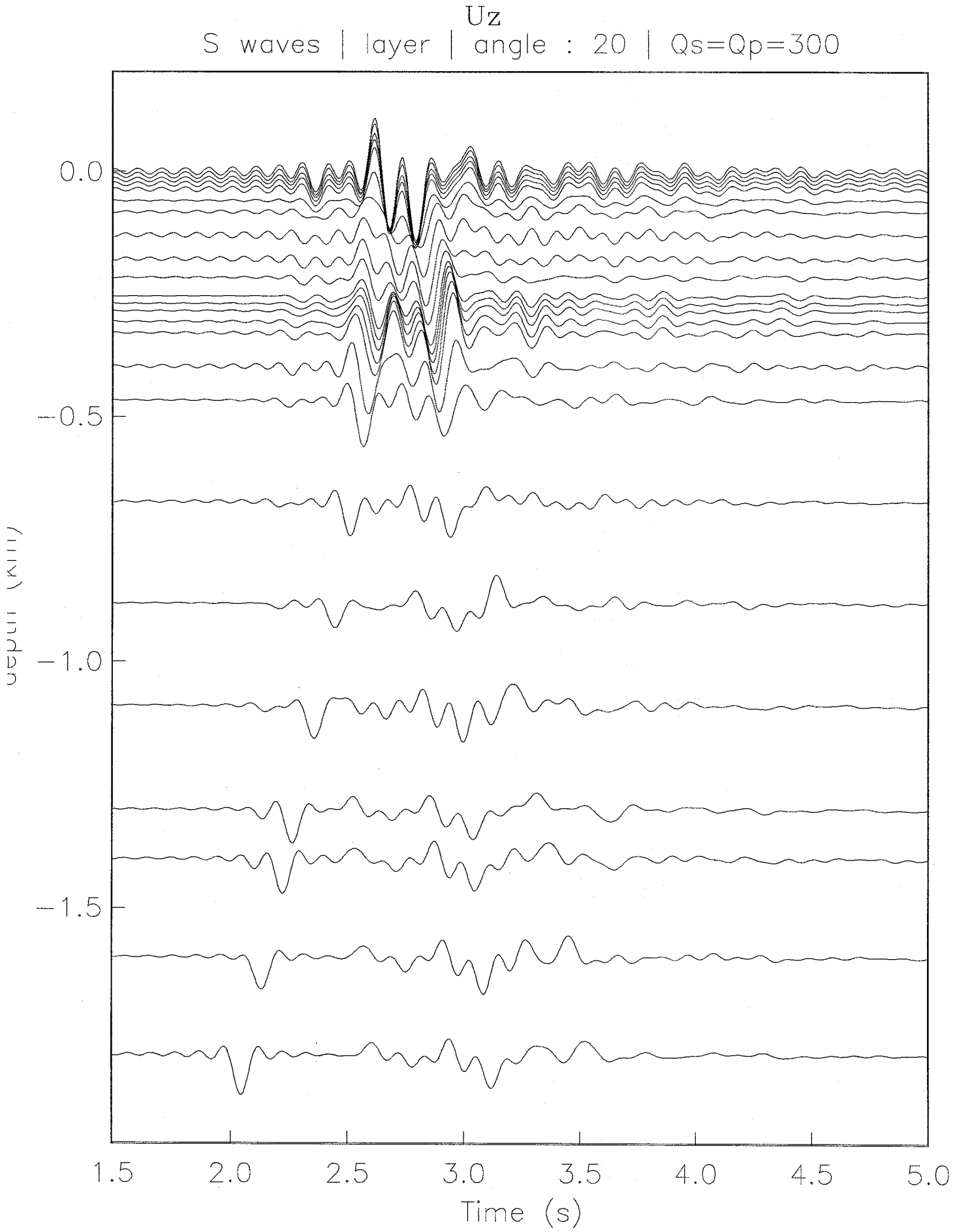
Uz
S waves | layer | angle : 20 | Qs=Qp=300
0.0
-0.5
-1.0
-1.5
depth (km)
1.5
2.0
2.5
3.0
3.5
4.0
4.5
5.0
Time (s)

Ux

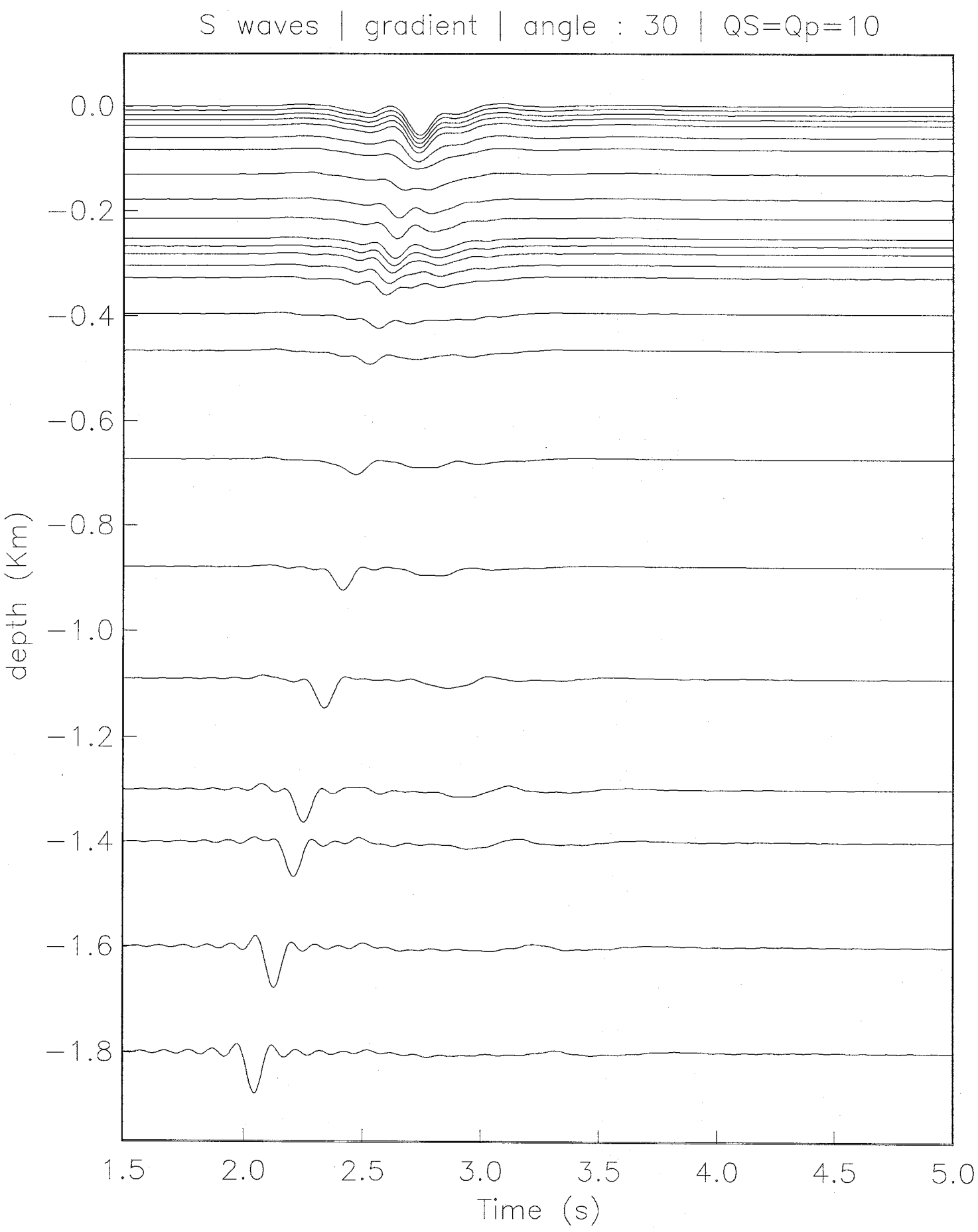
S waves | gradient | angle : 30 | QS=Qp=10
0.0
−0.2
−0.4
−0.6
−0.8
−1.0
−1.2
−1.4
−1.6
−1.8
depth (Km)
1.5
2.0
2.5
3.0
3.5
4.0
4.5
5.0
Time (s)

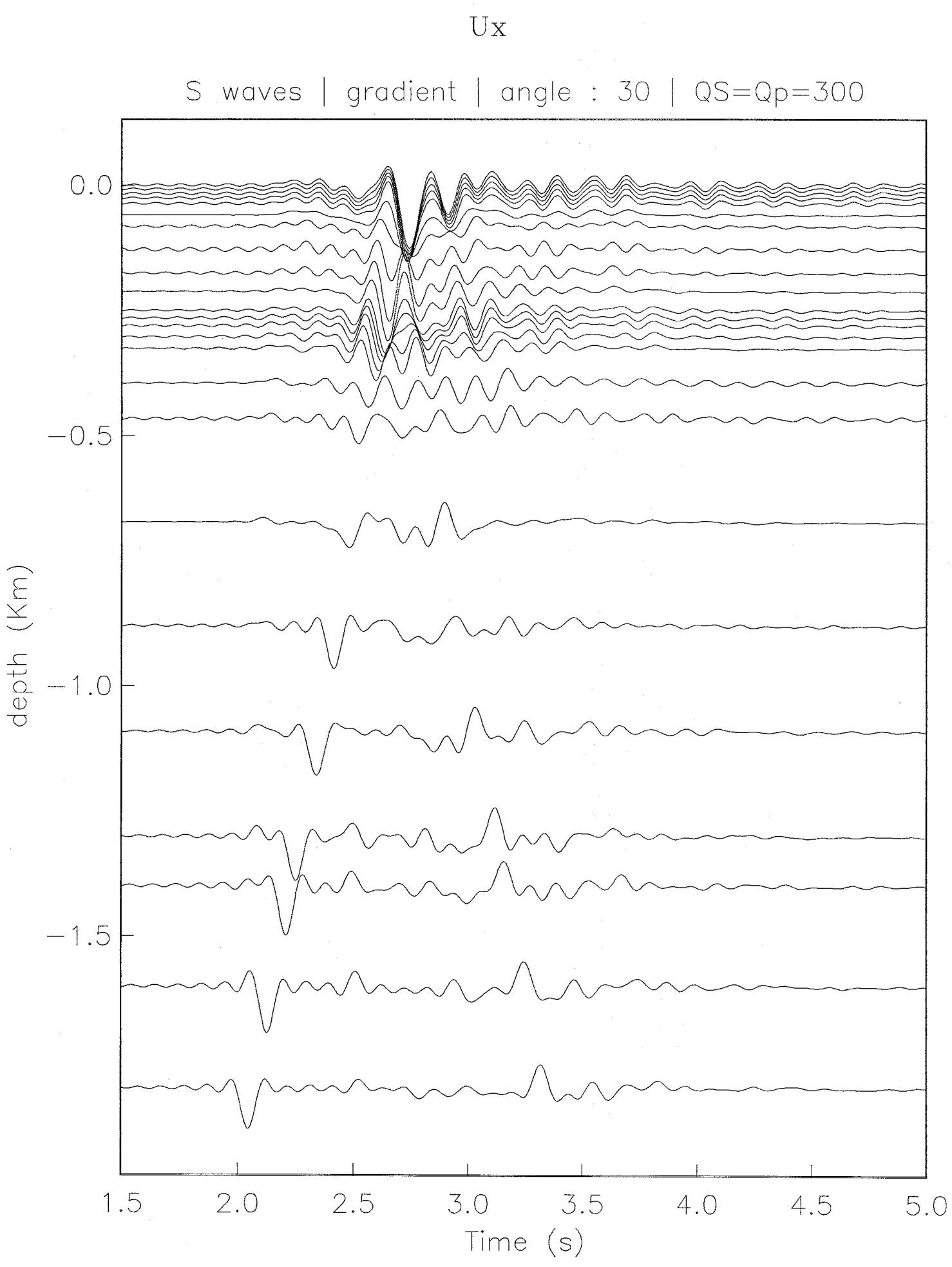
Ux
S waves | gradient | angle : 30 | QS=Qp=300
0.0
−0.5
−1.0
−1.5
depth (Km)
1.5
2.0
2.5
3.0
3.5
4.0
4.5
5.0
Time (s)

Ux

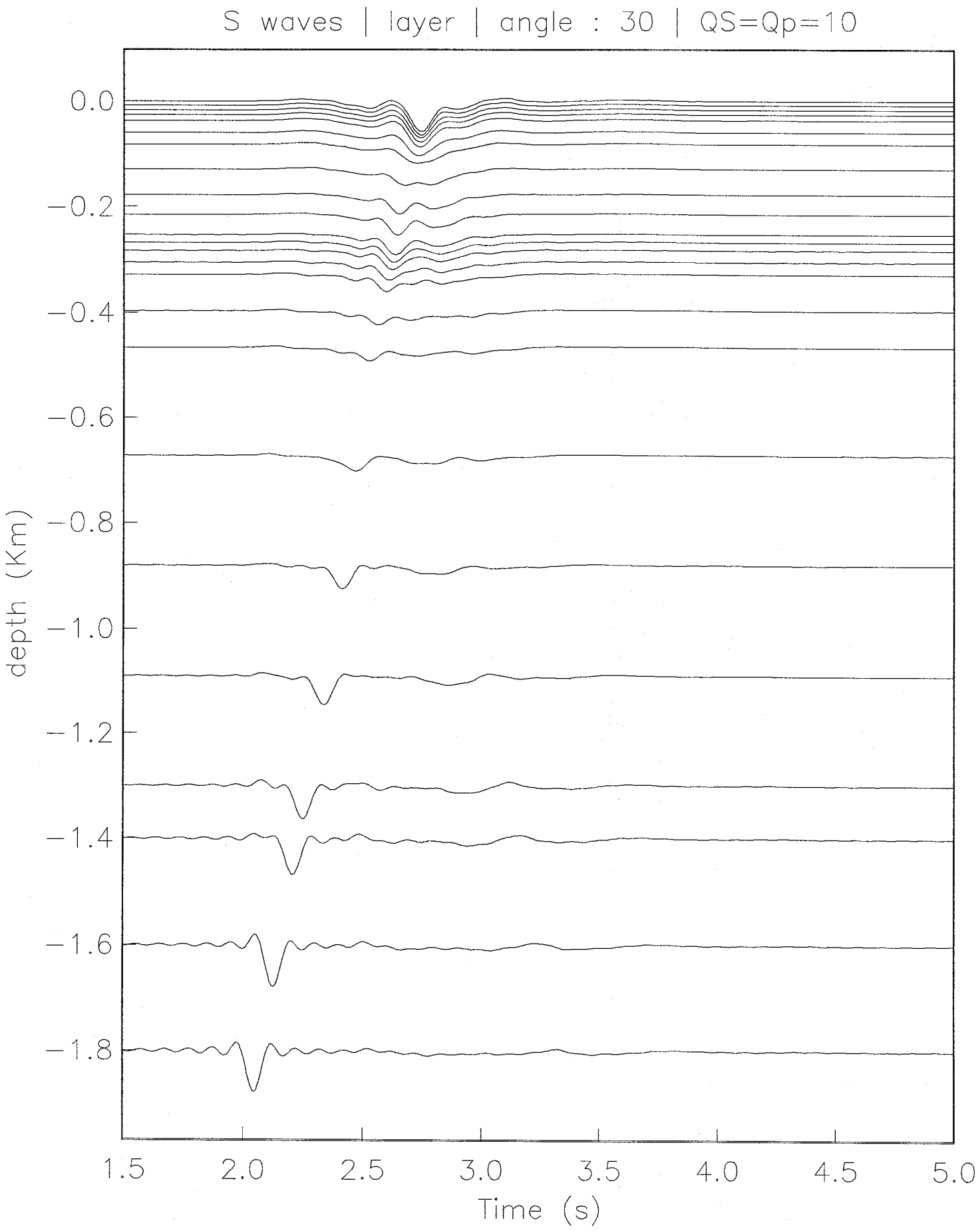
S waves | layer | angle : 30 | QS=Qp=10
0.0
−0.2
−0.4
−0.6
−0.8
−1.0
−1.2
−1.4
−1.6
−1.8
depth (Km)
1.5
2.0
2.5
3.0
3.5
4.0
4.5
5.0
Time (s)

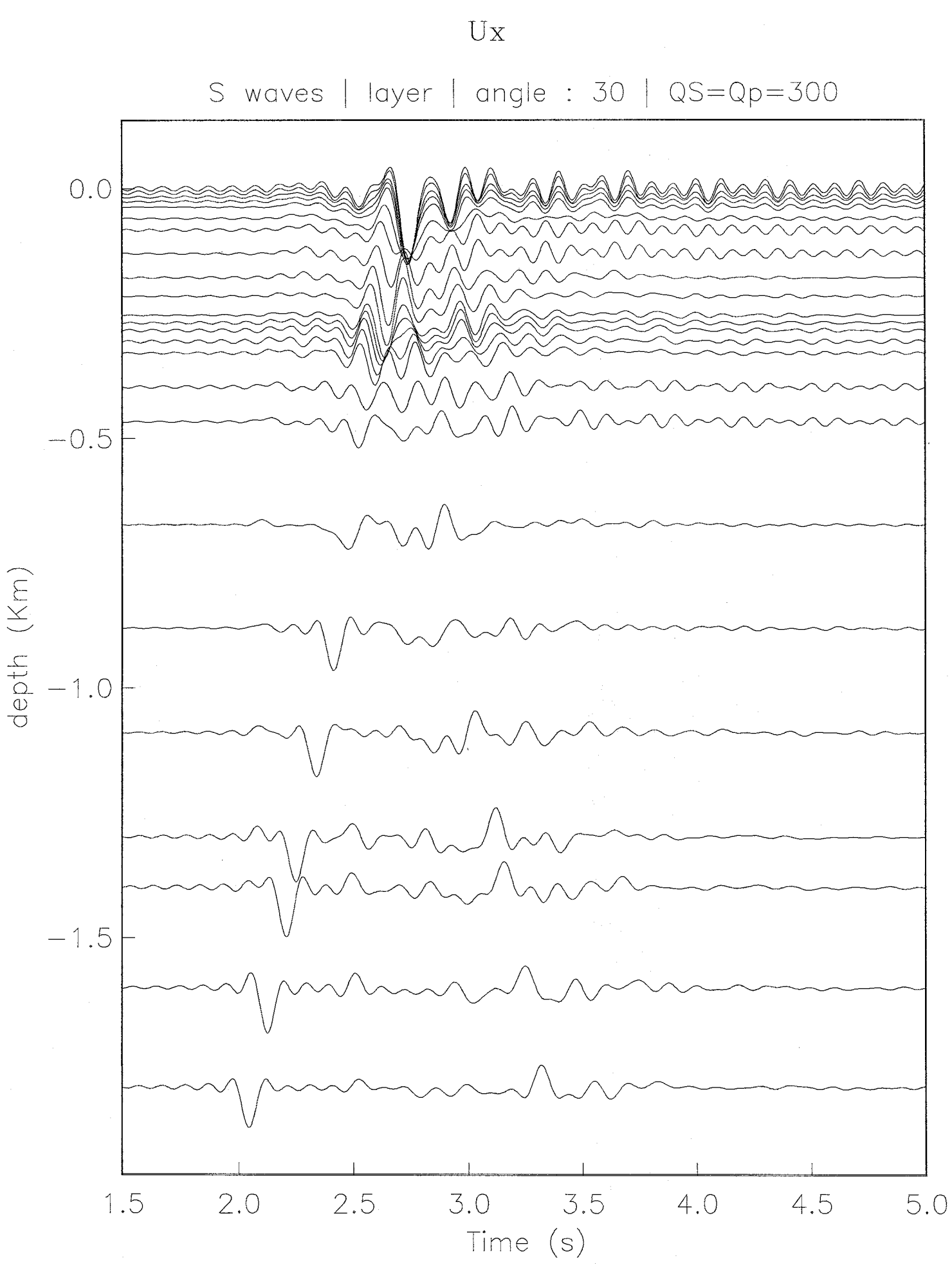
Ux
S waves | layer | angle : 30 | QS=Qp=300
0.0
-0.5
-1.0
-1.5
depth (Km)
1.5
2.0
2.5
3.0
3.5
4.0
4.5
5.0
Time (s)

Uz

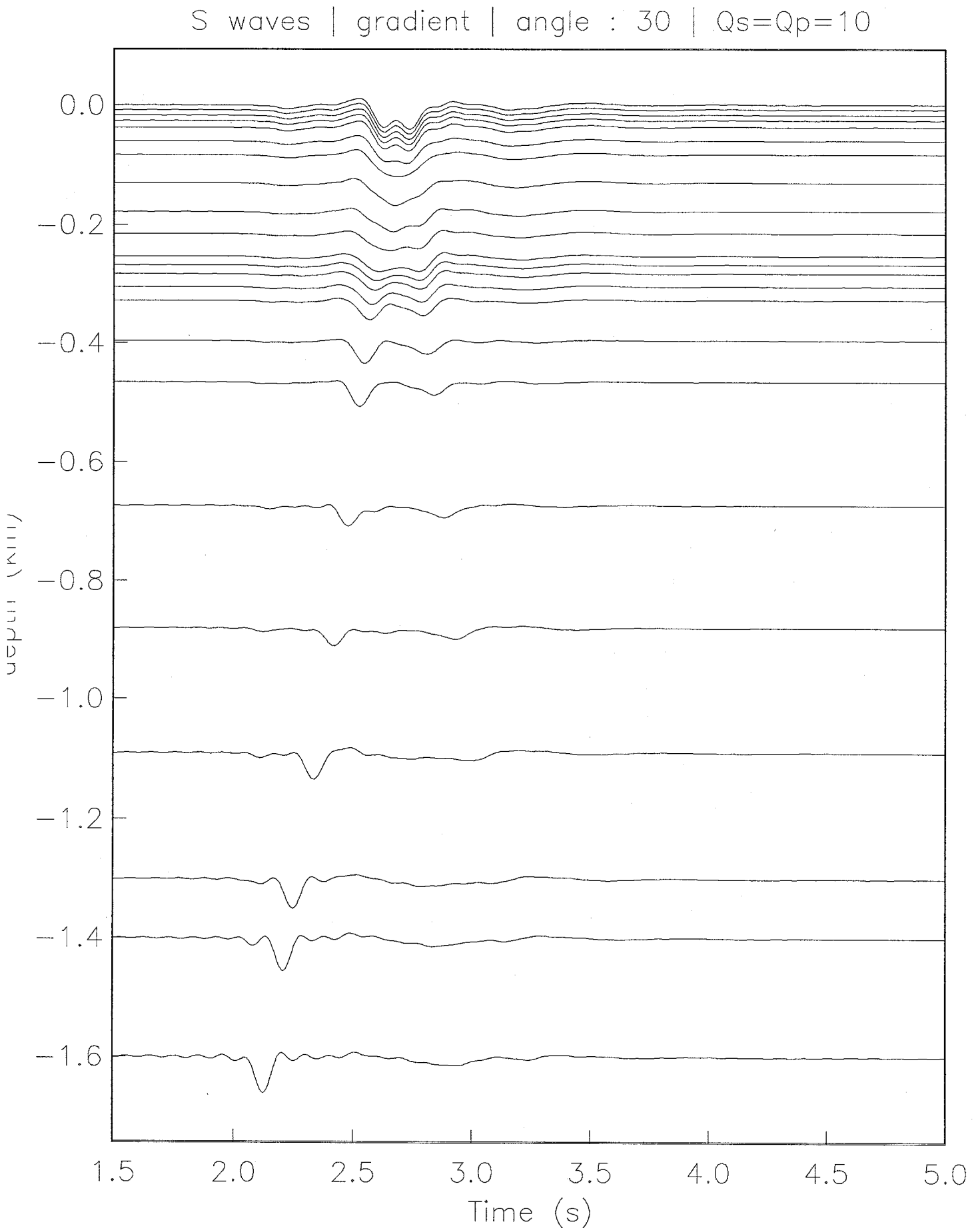
S waves | gradient | angle : 30 | Qs=Qp=10
0.0
−0.2
−0.4
−0.6
−0.8
−1.0
−1.2
−1.4
−1.6
depth (km)
1.5
2.0
2.5
3.0
3.5
4.0
4.5
5.0
Time (s)

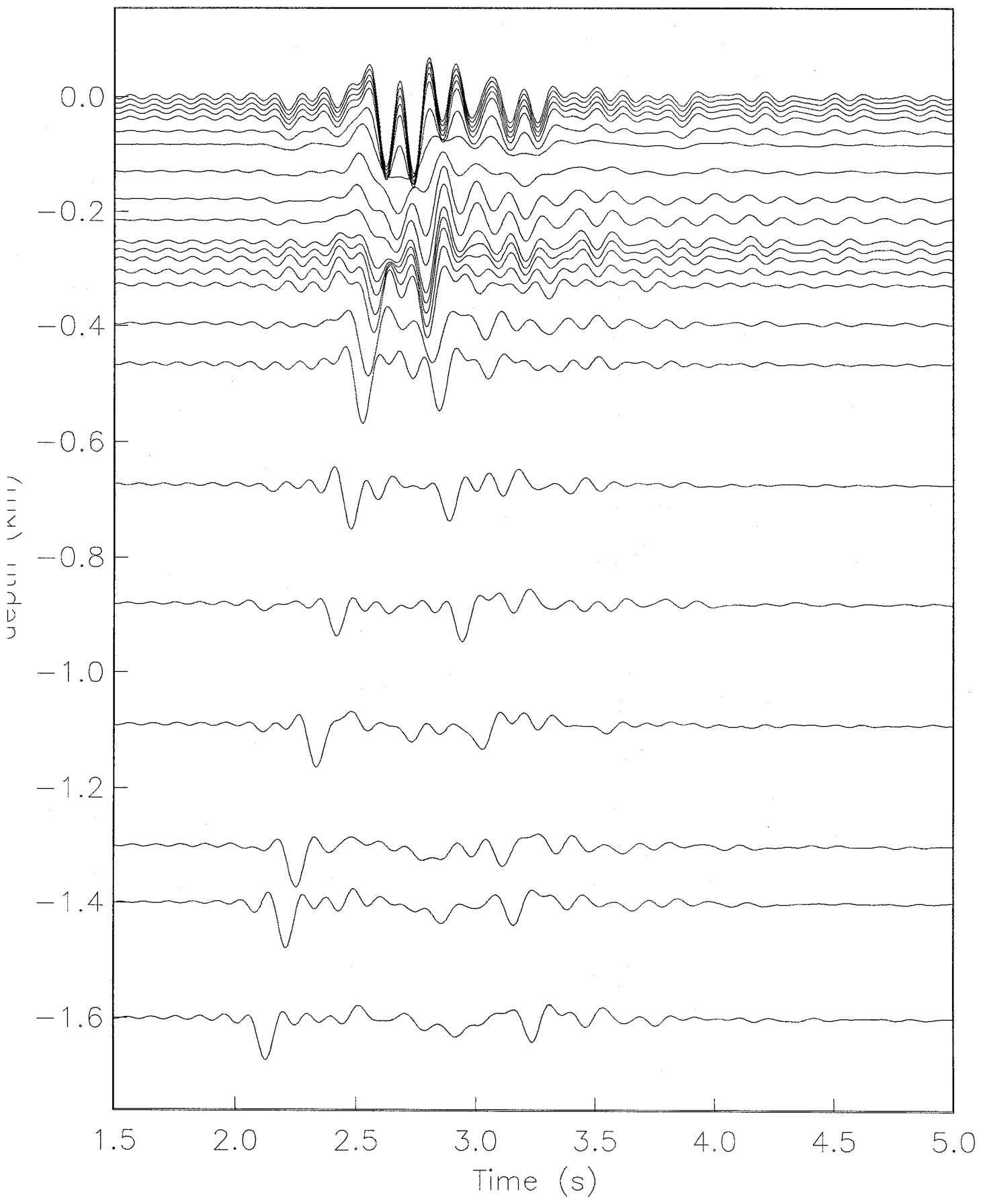
Uz
S waves | gradient | angle : 30 | Qs=Qp=300
0.0
−0.2
−0.4
−0.6
−0.8
−1.0
−1.2
−1.4
−1.6
Depth (km)
1.5
2.0
2.5
3.0
3.5
4.0
4.5
5.0
Time (s)

Uz

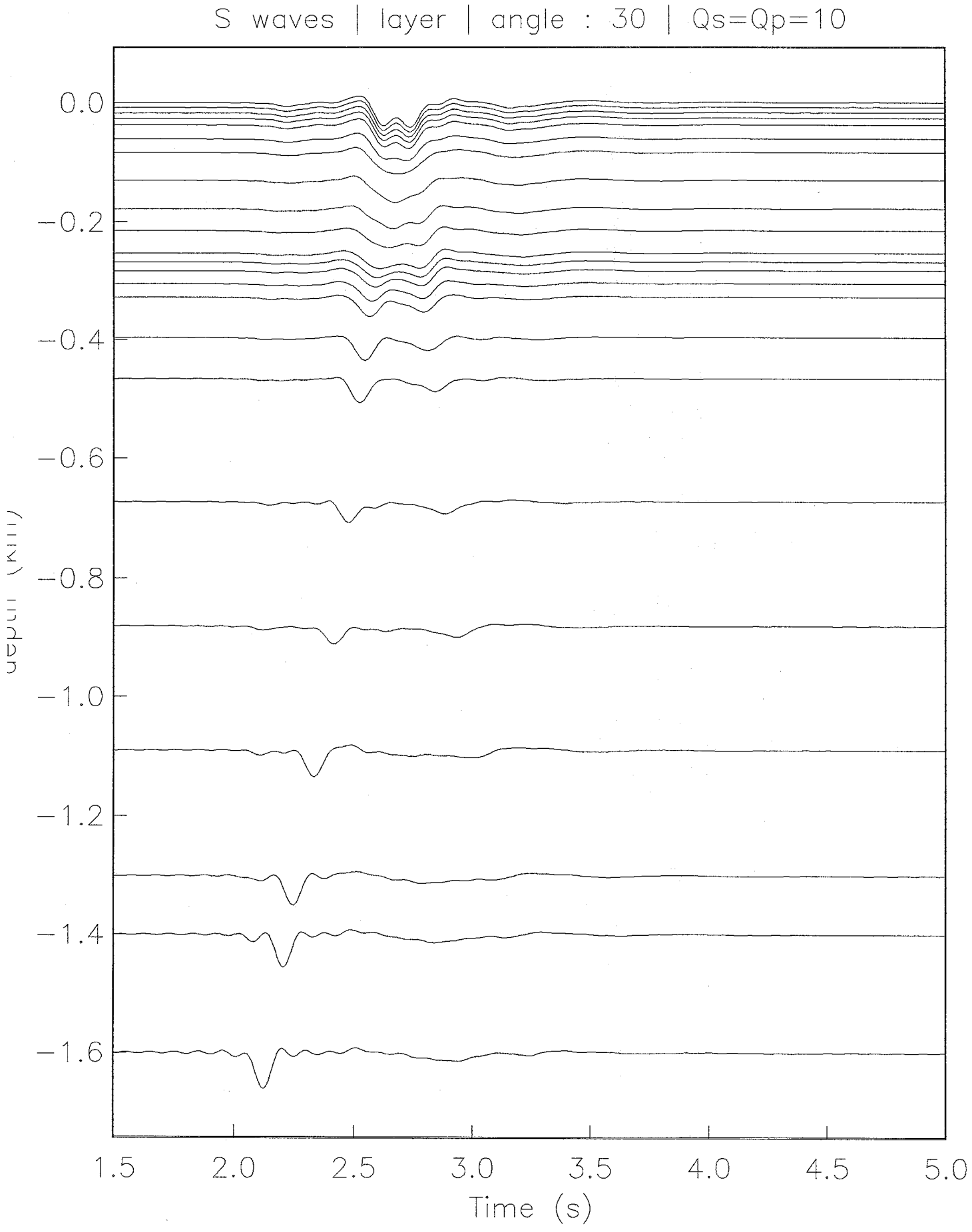
S waves | layer | angle : 30 | Qs=Qp=10
0.0
−0.2
−0.4
−0.6
−0.8
−1.0
−1.2
−1.4
−1.6
1.5
2.0
2.5
3.0
3.5
4.0
4.5
5.0
Time (s)

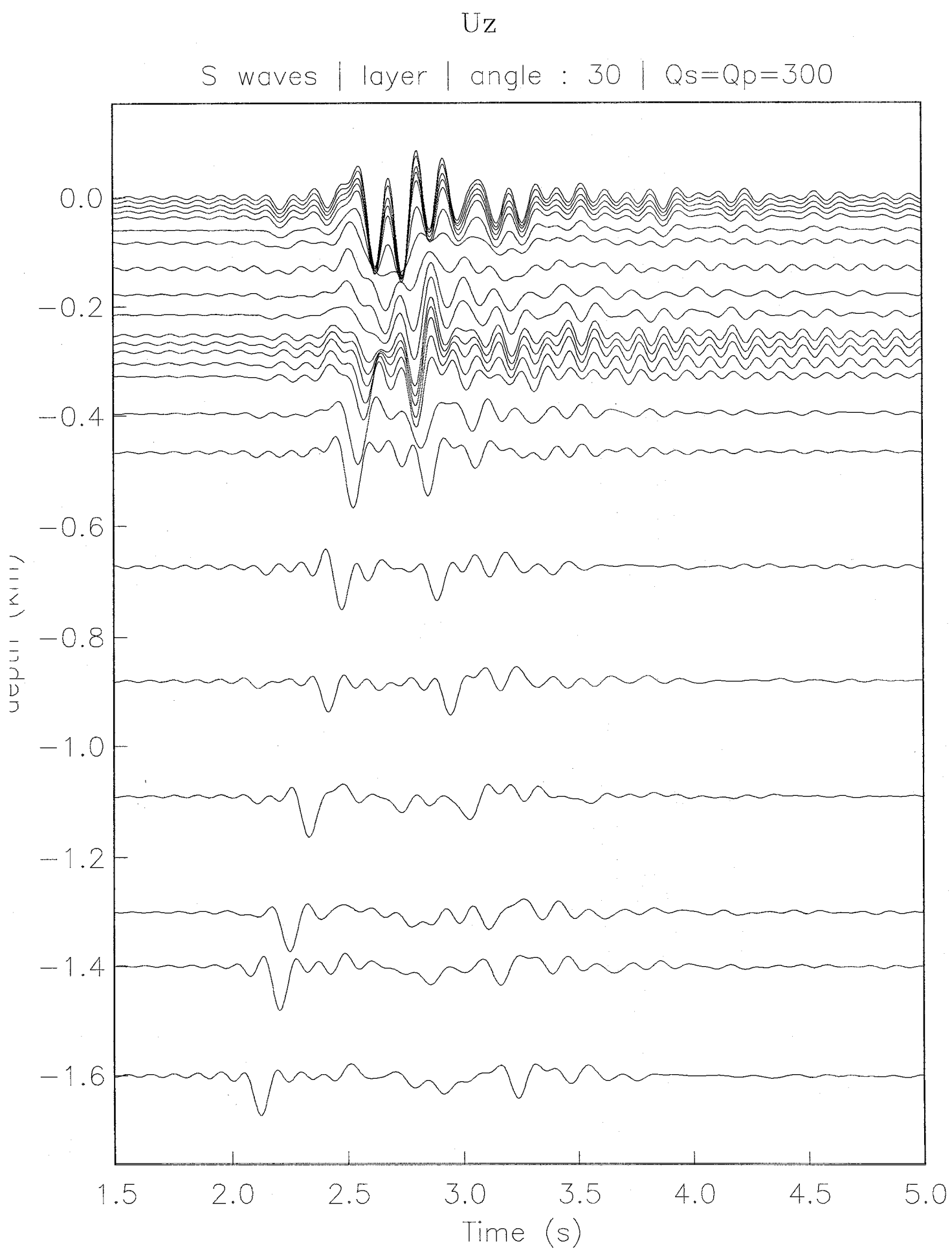
Uz
S waves | layer | angle : 30 | Qs=Qp=300
0.0
−0.2
−0.4
−0.6
−0.8
−1.0
−1.2
−1.4
−1.6
(km) nidaA
1.5
2.0
2.5
3.0
3.5
4.0
4.5
5.0
Time (s)

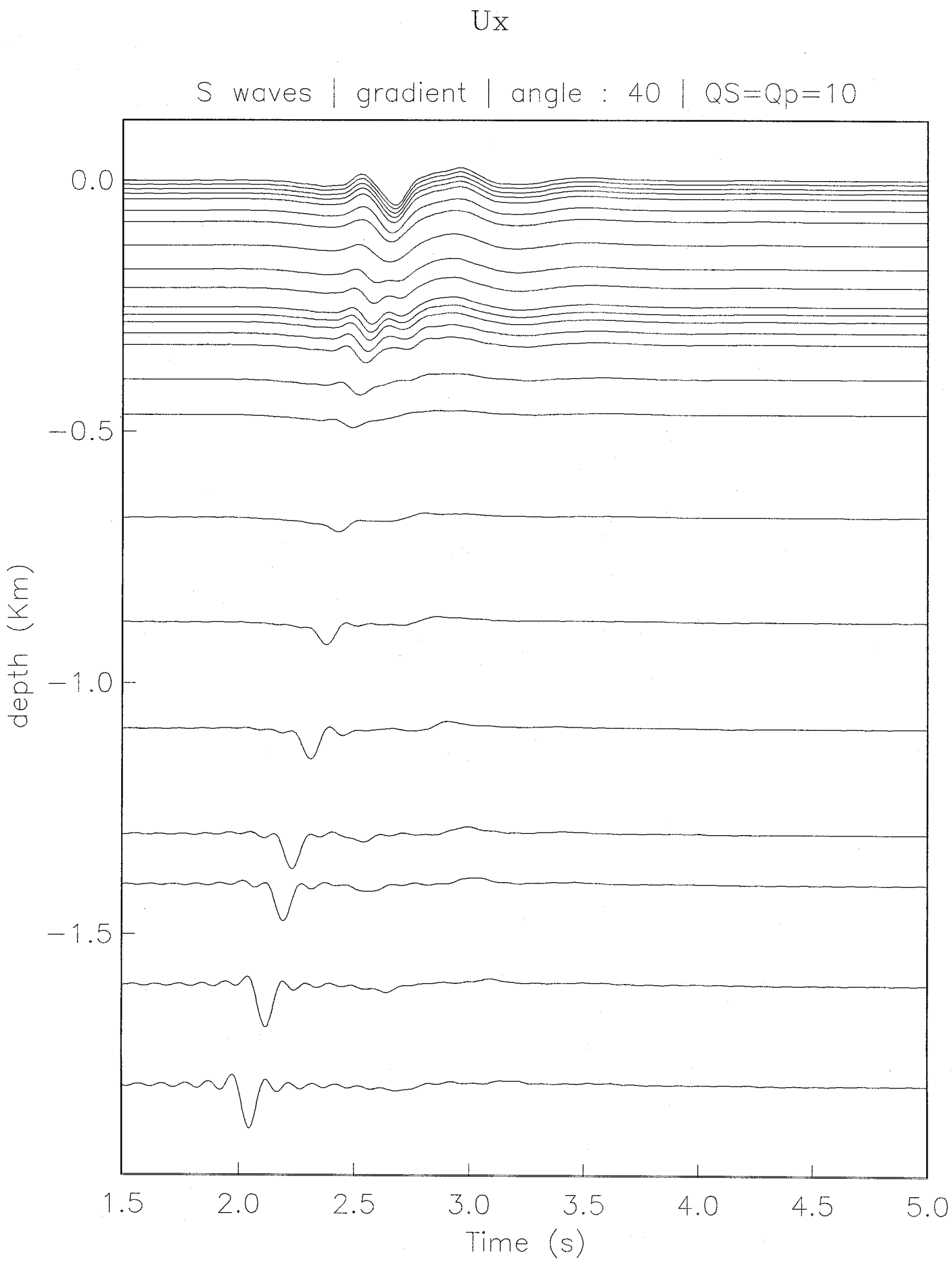
Ux
S waves | gradient | angle : 40 | QS=Qp=10
0.0
−0.5
−1.0
−1.5
depth (Km)
1.5
2.0
2.5
3.0
3.5
4.0
4.5
5.0
Time (s)

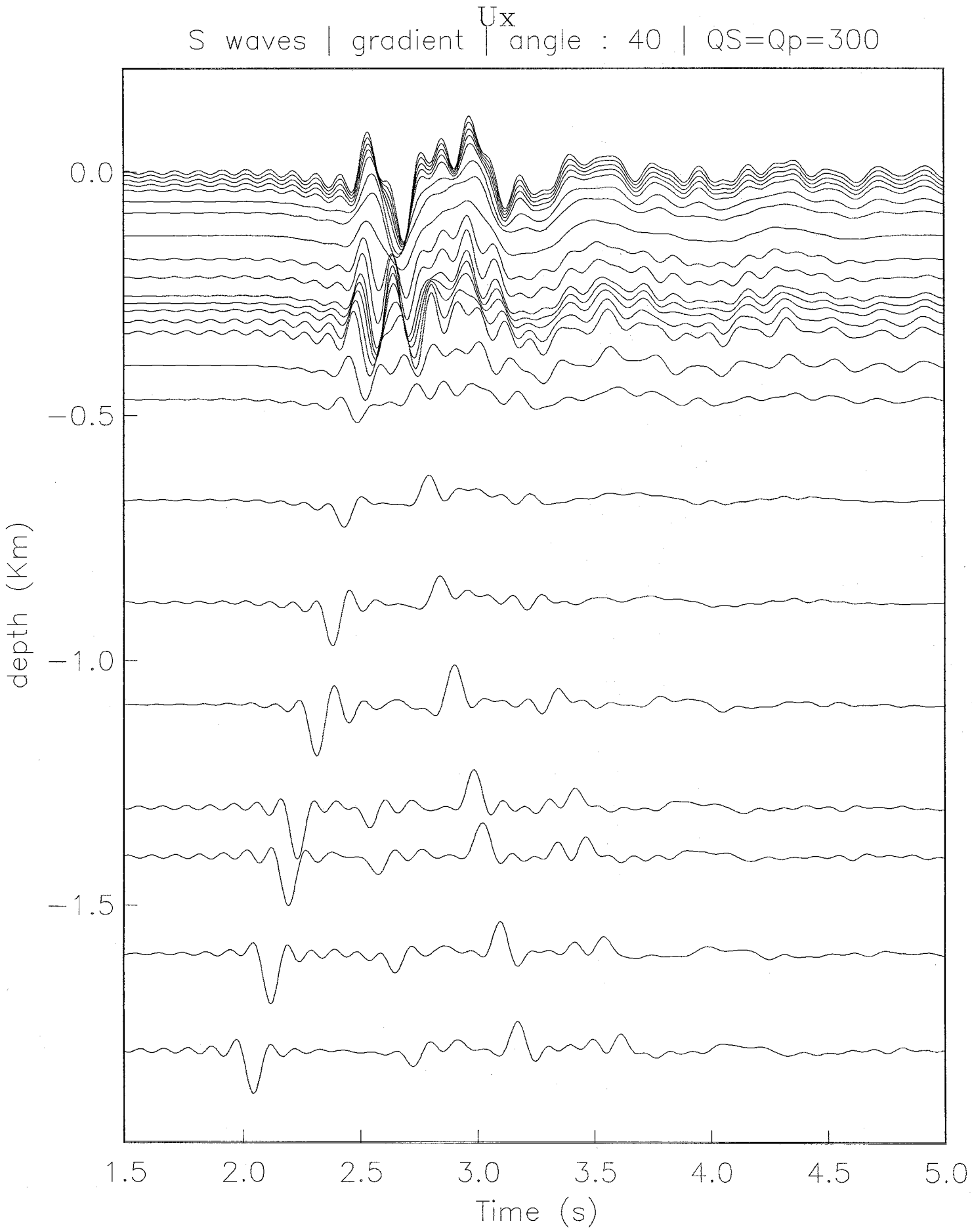
Ux
S waves | gradient | angle : 40 | QS=Qp=300
0.0
−0.5
−1.0
−1.5
depth (Km)
1.5
2.0
2.5
3.0
3.5
4.0
4.5
5.0
Time (s)

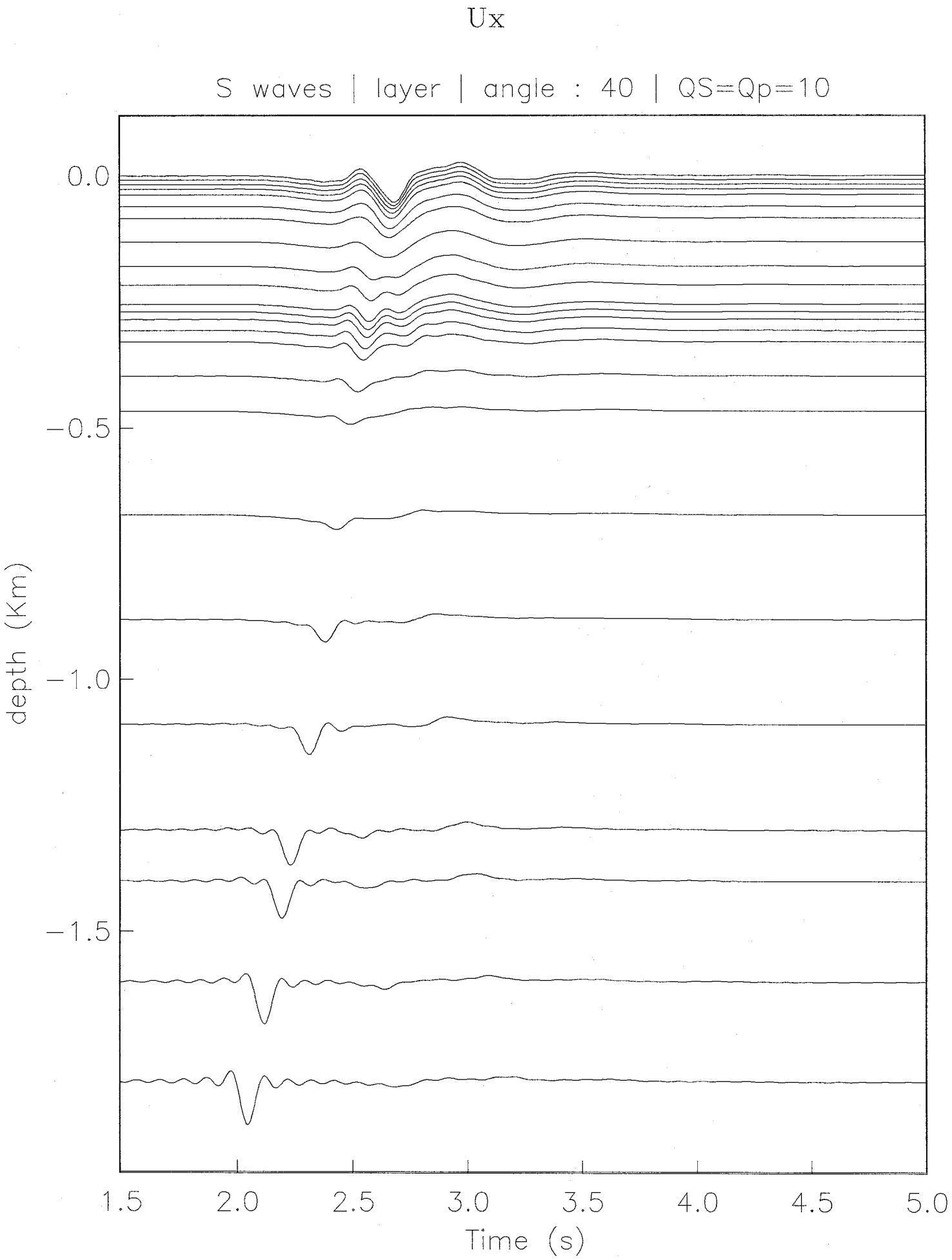
Ux
S waves | layer | angle : 40 | QS=Qp=10
0.0
−0.5
−1.0
−1.5
depth (Km)
1.5
2.0
2.5
3.0
3.5
4.0
4.5
5.0
Time (s)

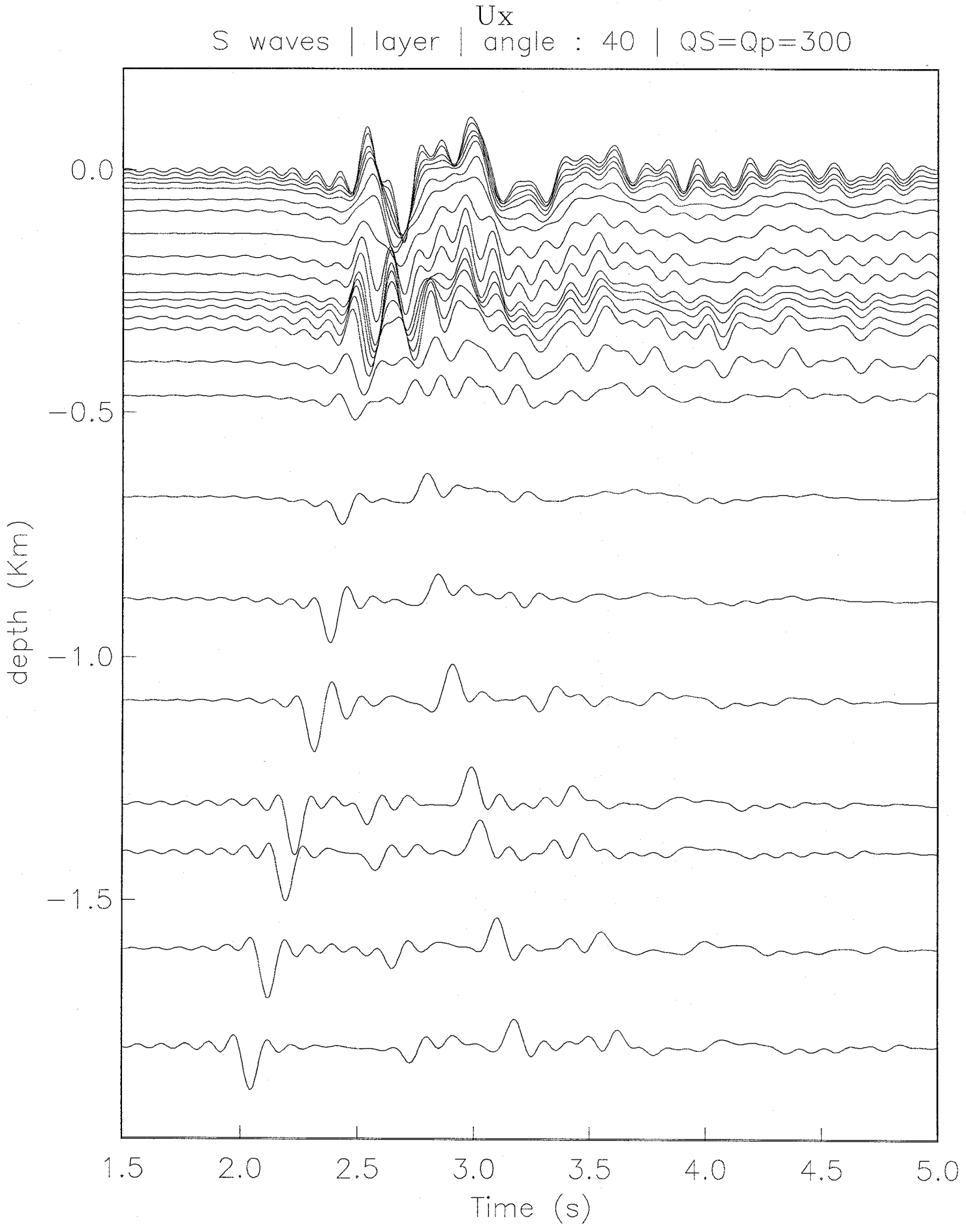
Ux
S waves | layer | angle : 40 | QS=Qp=300
0.0
−0.5
−1.0
−1.5
depth (Km)
1.5
2.0
2.5
3.0
3.5
4.0
4.5
5.0
Time (s)

Uz

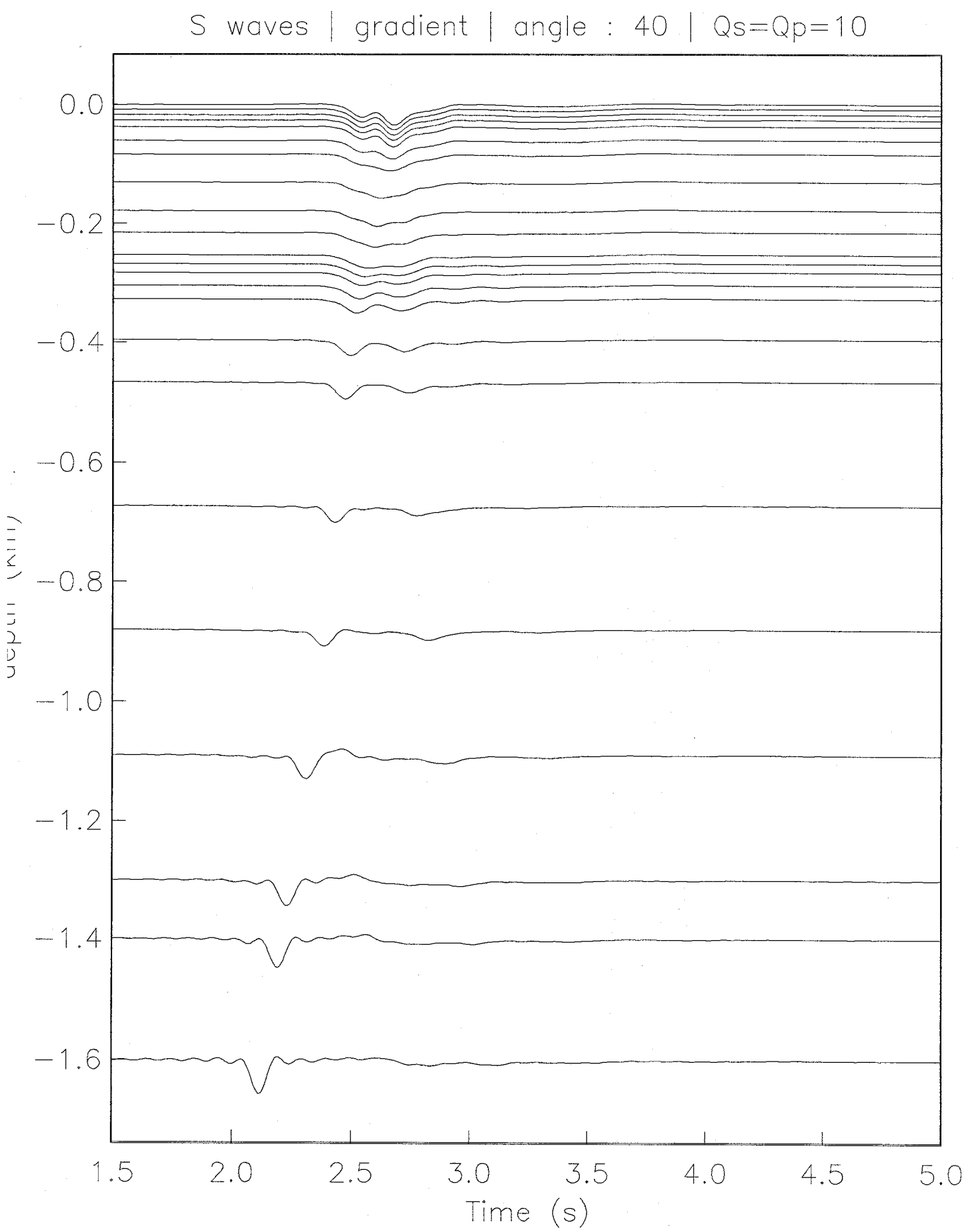
S waves | gradient | angle : 40 | Qs=Qp=10
0.0
−0.2
−0.4
−0.6
−0.8
−1.0
−1.2
−1.4
−1.6
1.5
2.0
2.5
3.0
3.5
4.0
4.5
5.0
Time (s)

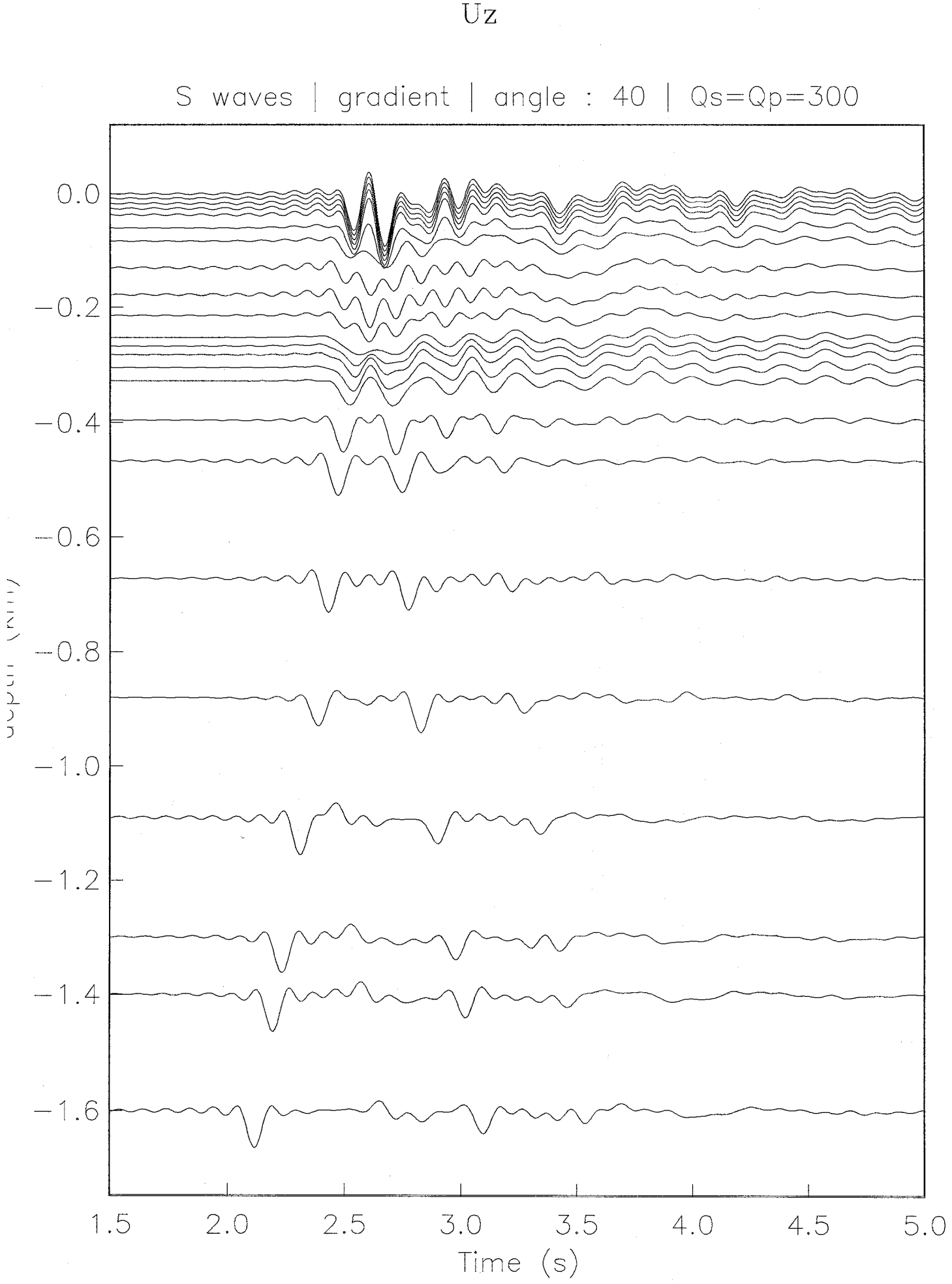
Uz
S waves | gradient | angle : 40 | Qs=Qp=300
0.0
−0.2
−0.4
−0.6
−0.8
−1.0
−1.2
−1.4
−1.6
1.5
2.0
2.5
3.0
3.5
4.0
4.5
5.0
Time (s)

Uz

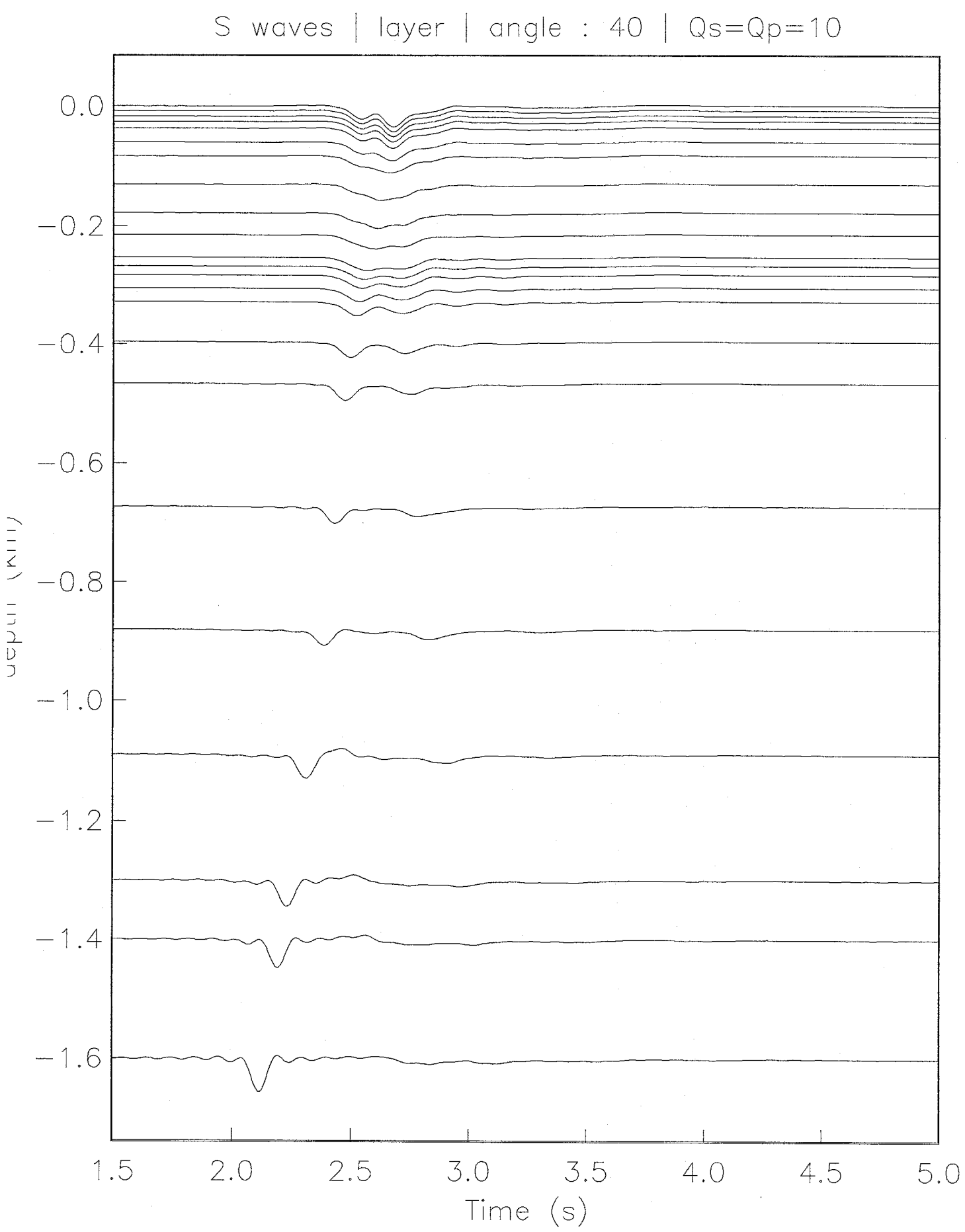
S waves | layer | angle : 40 | Qs=Qp=10
0.0
−0.2
−0.4
−0.6
−0.8
−1.0
−1.2
−1.4
−1.6
Depth (km)
1.5
2.0
2.5
3.0
3.5
4.0
4.5
5.0
Time (s)

Uz

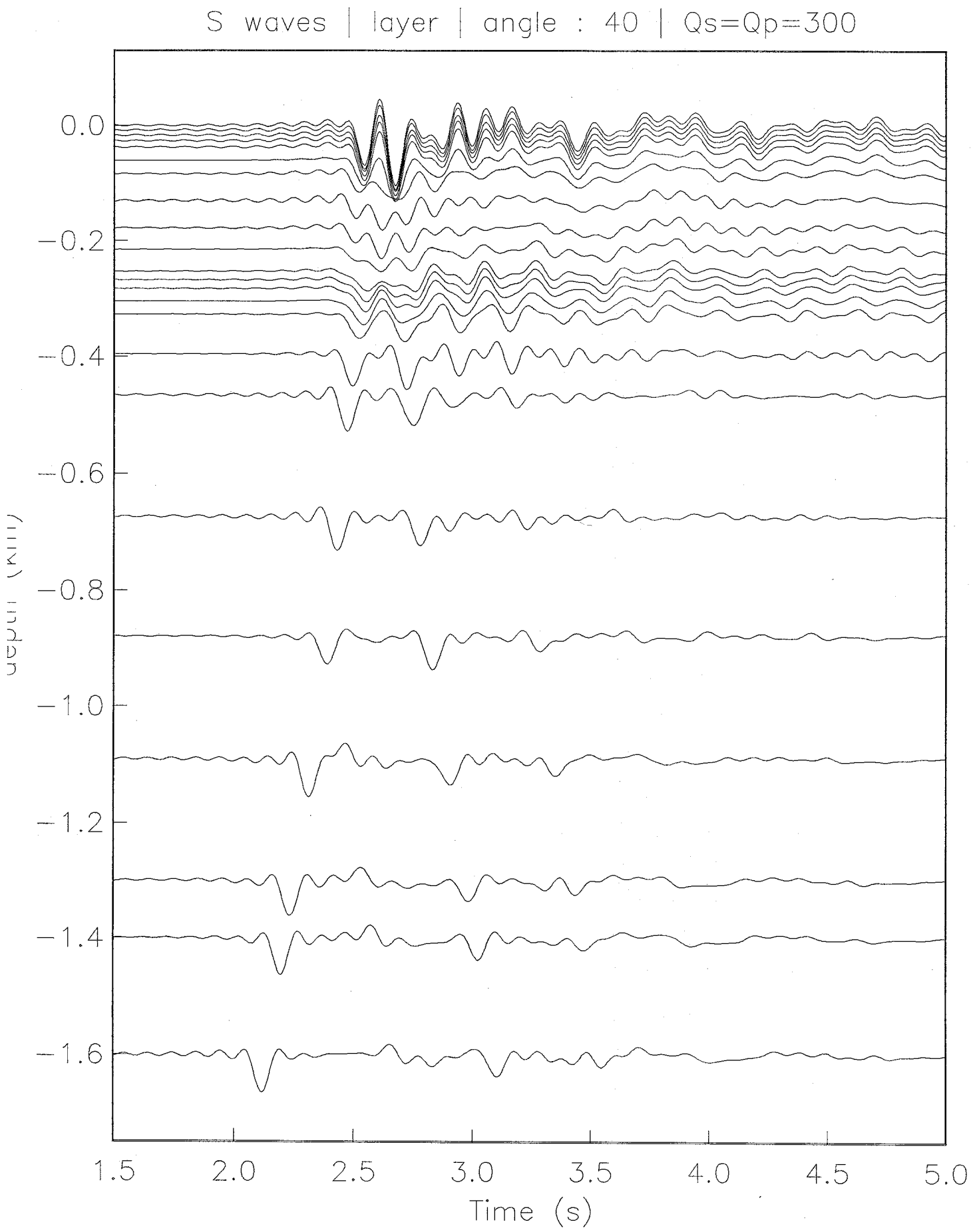
S waves | layer | angle : 40 | Qs=Qp=300
0.0
−0.2
−0.4
−0.6
−0.8
−1.0
−1.2
−1.4
−1.6
Depth (km)
1.5
2.0
2.5
3.0
3.5
4.0
4.5
5.0
Time (s)

Appendix D

Content :

9 maximum displacement profiles for frequency content 0 to 10 Hz.
9 maximum velocity profiles for frequency content 0 to 10 Hz.
9 maximum acceleration profiles for frequency content 0 to 10 Hz.

Maximum Displacement
incident angle : 0

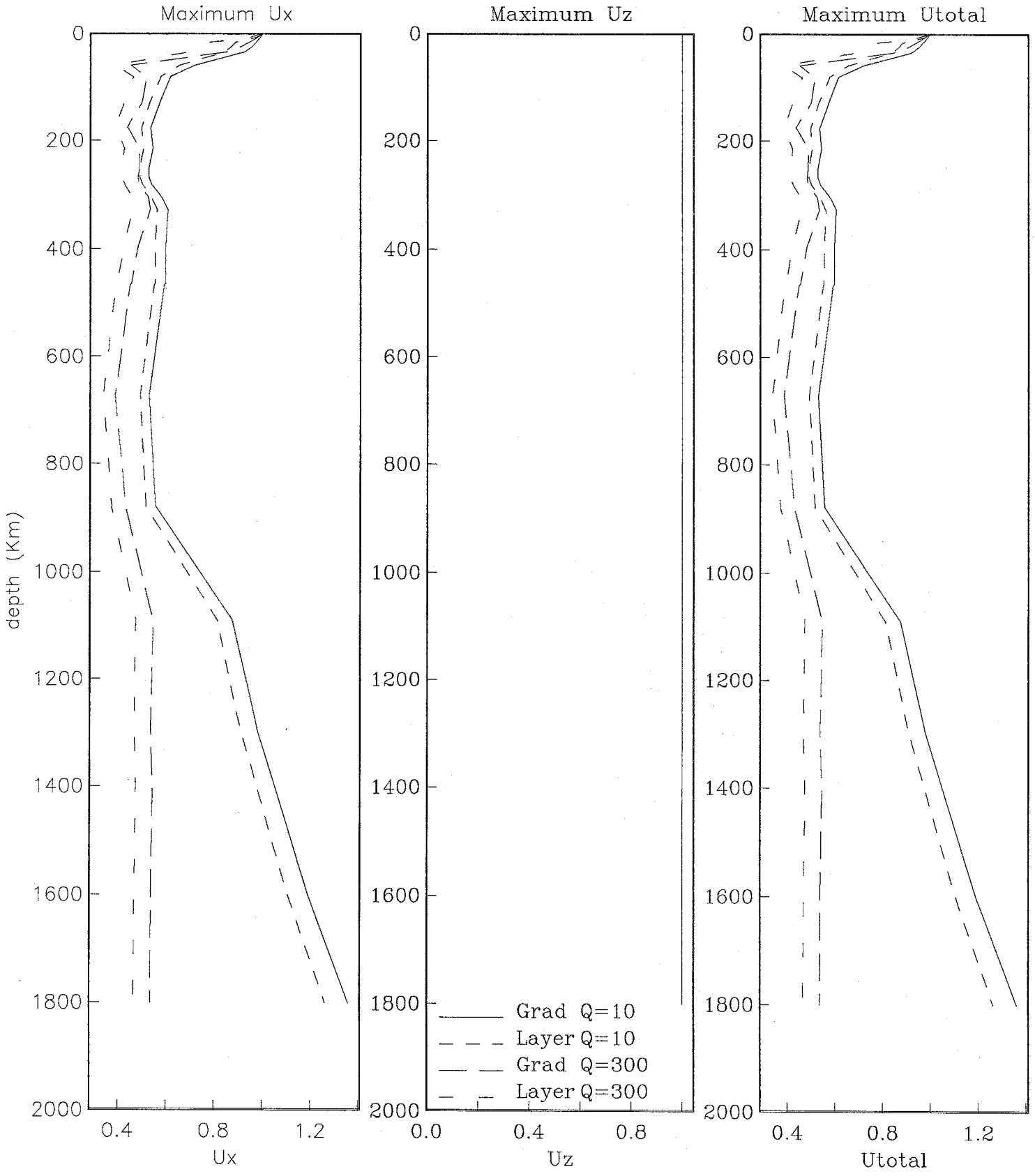

Maximum Displacement
incident angle : 10

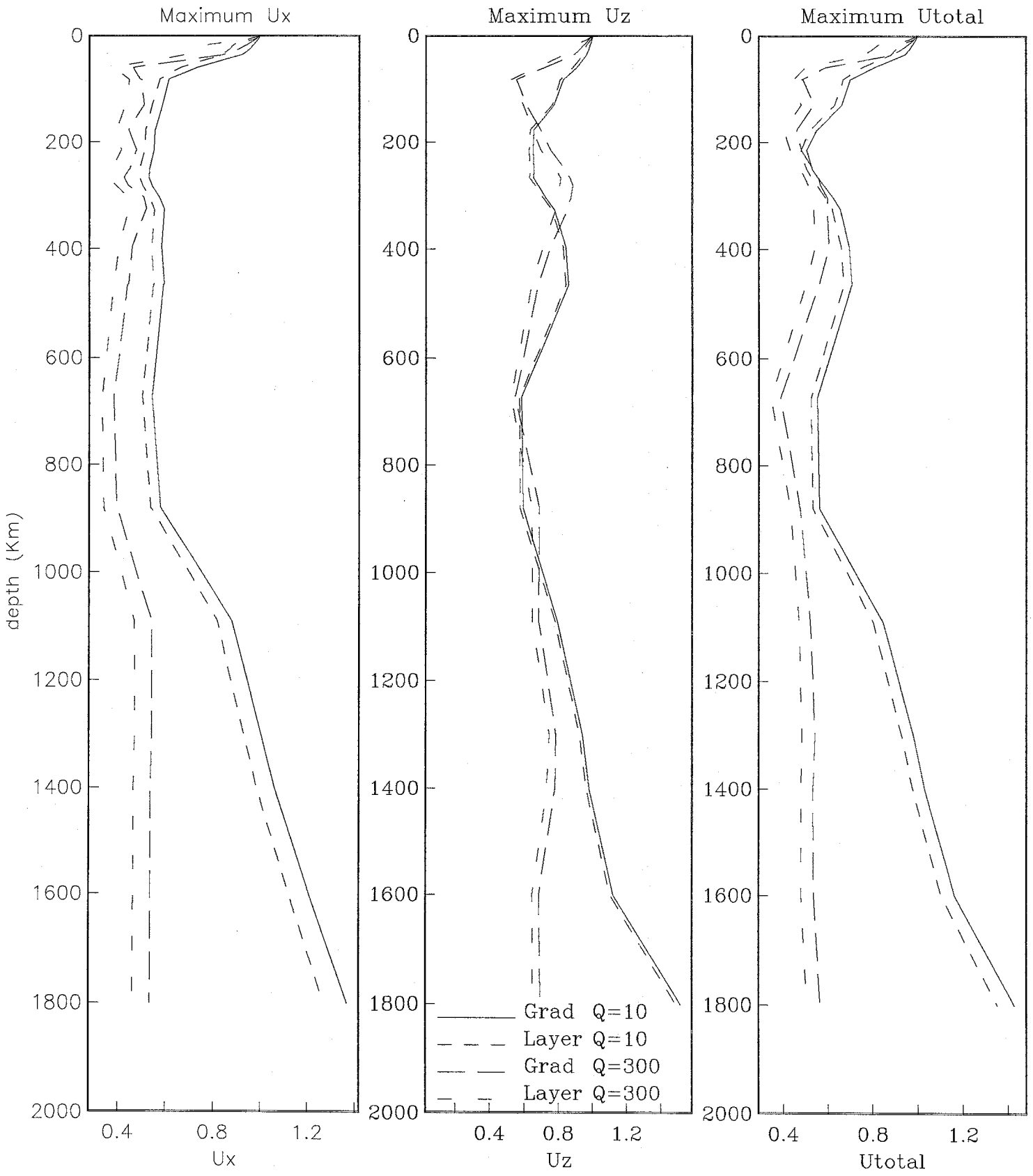

Maximum Displacement
incident angle : 20

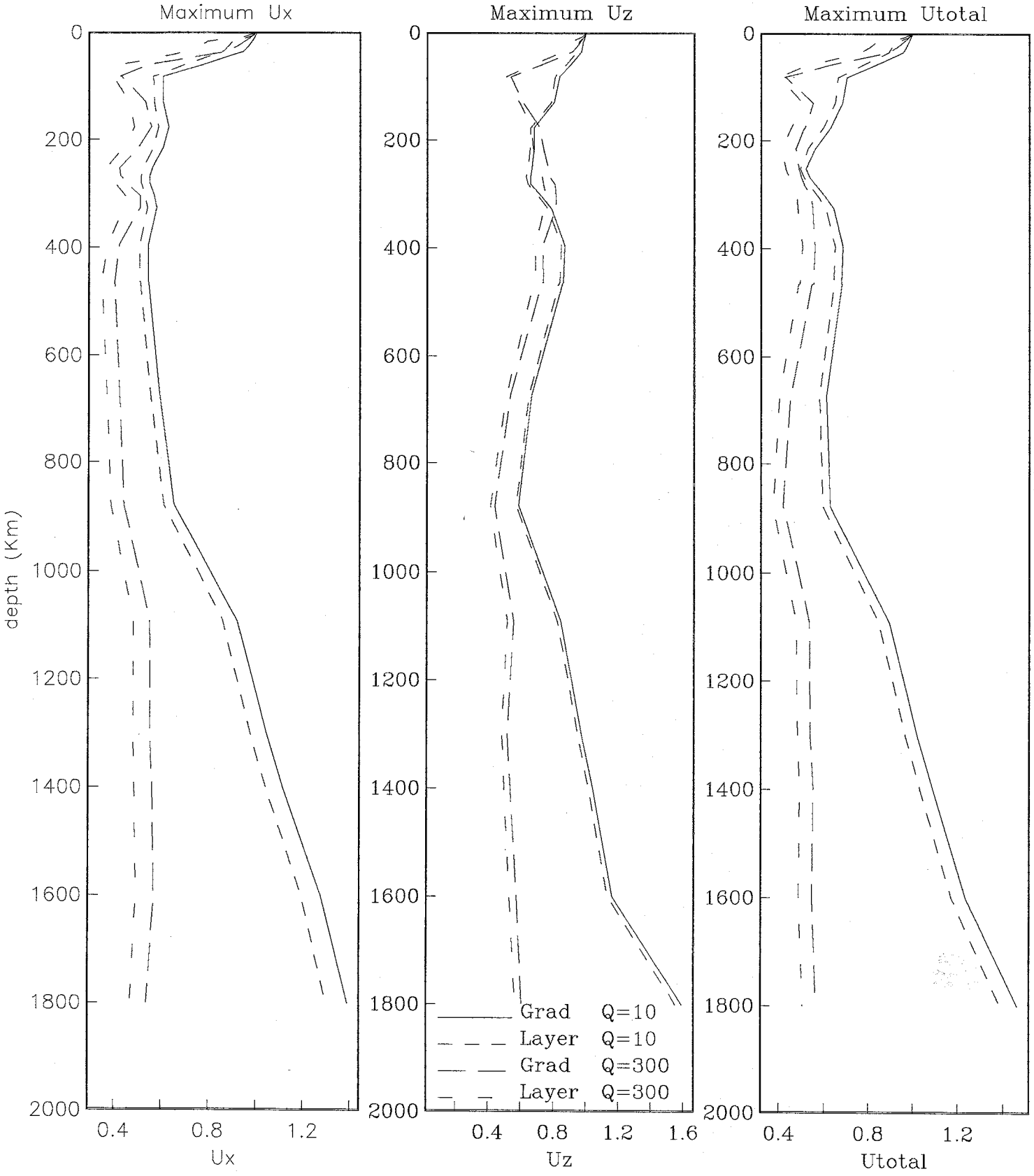

Maximum Displacement
incident angle : 30

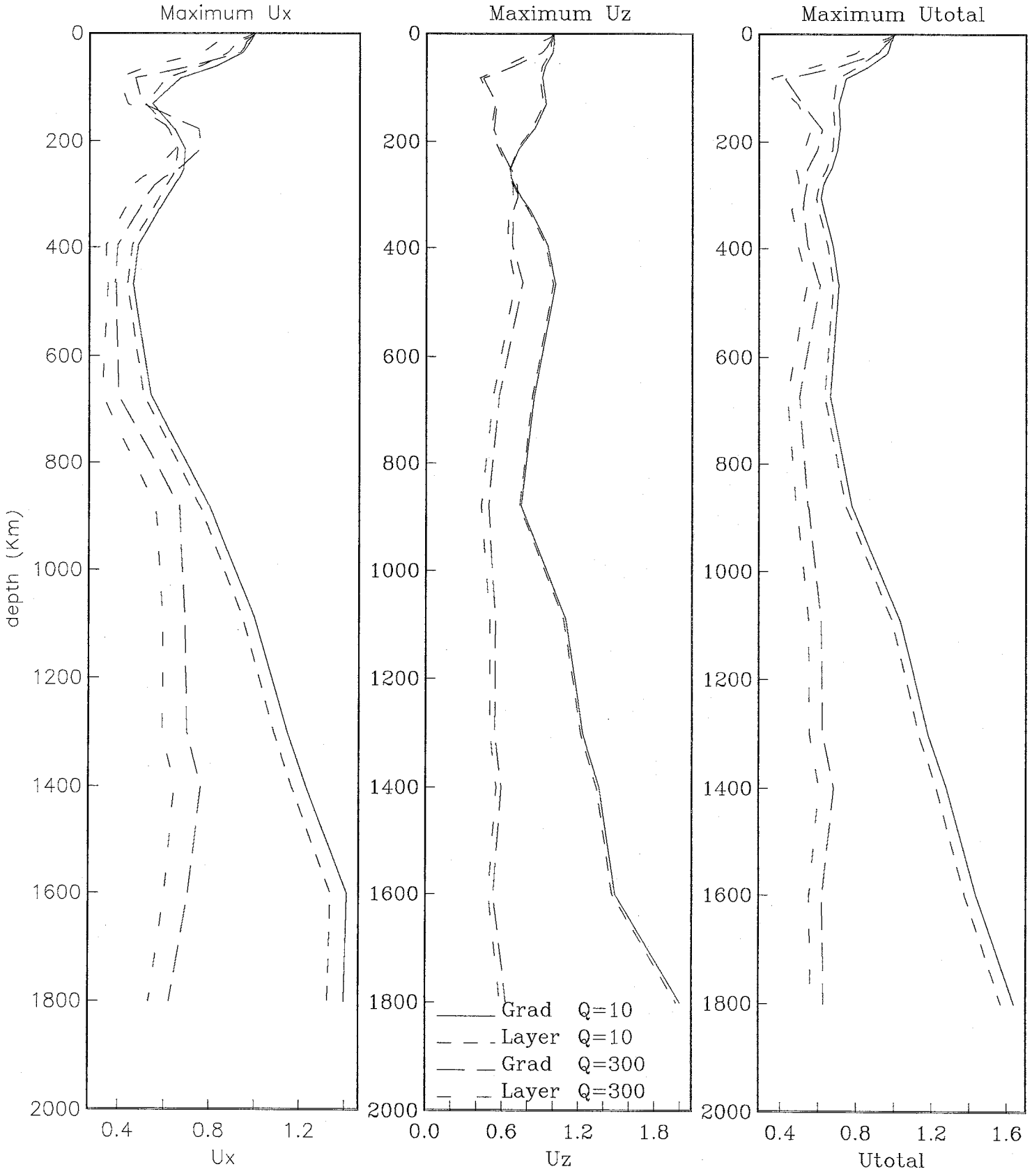

Maximum Displacement
incident angle : 40

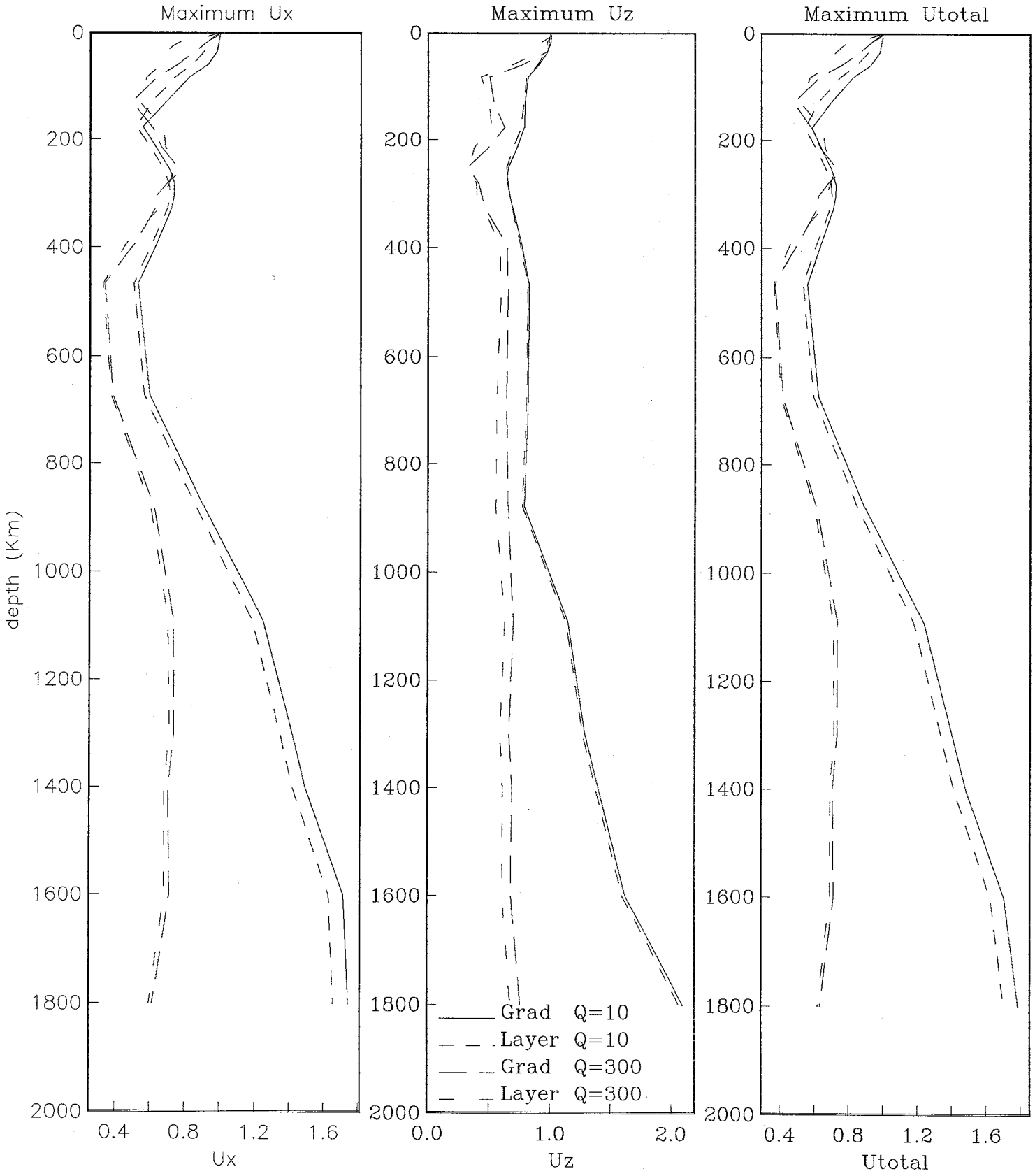

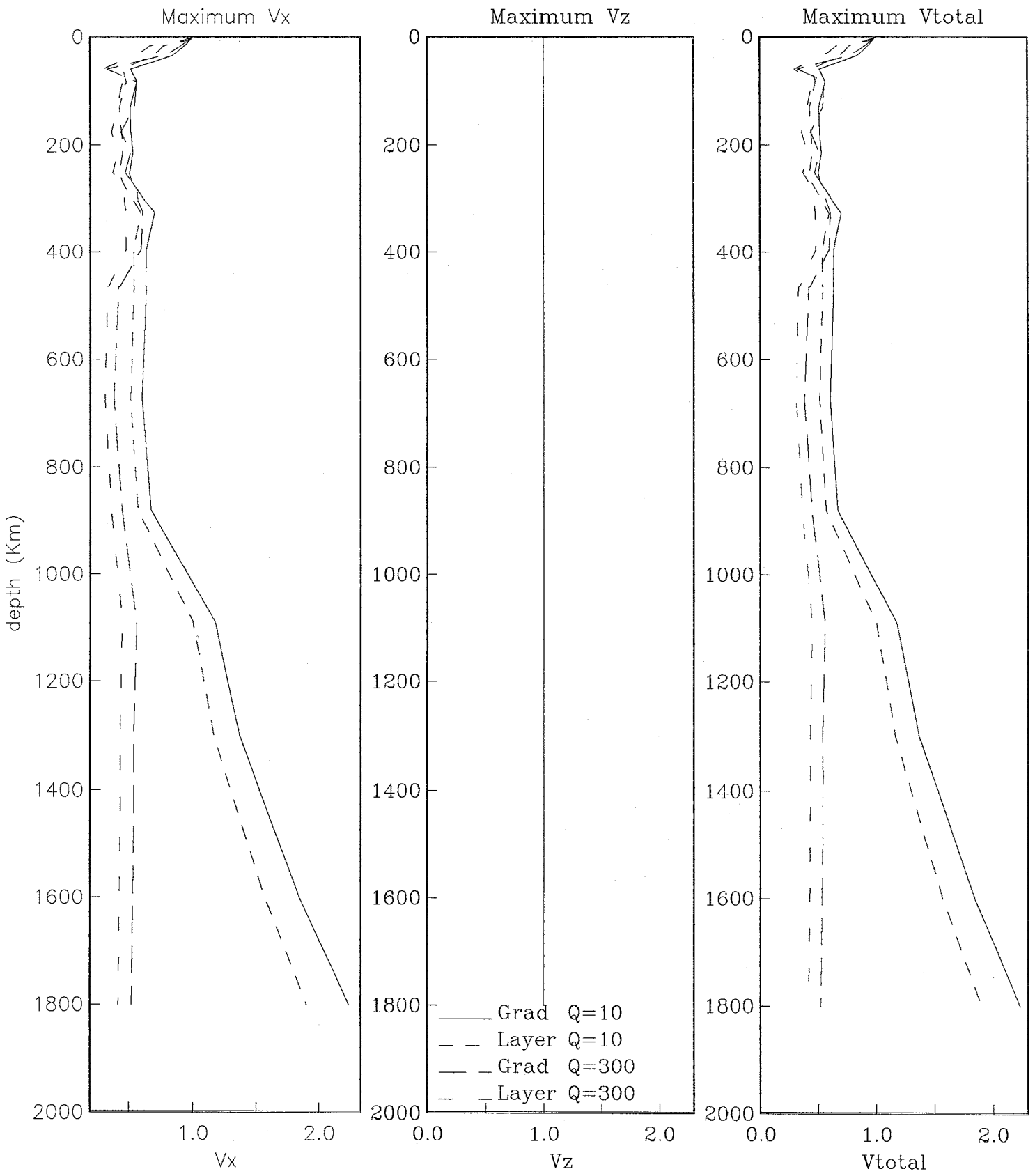
Maximum velocity
incident angle : 0
Maximum Vx
Maximum Vz
Maximum Vtotal
depth (Km)
0
200
400
600
800
1000
1200
1400
1600
1800
2000
1.0
2.0
0.0
Vx
Vz
Vtotal
Grad Q=10
Layer Q=10
Grad Q=300
Layer Q=300

Maximum velocity
incident angle : 10

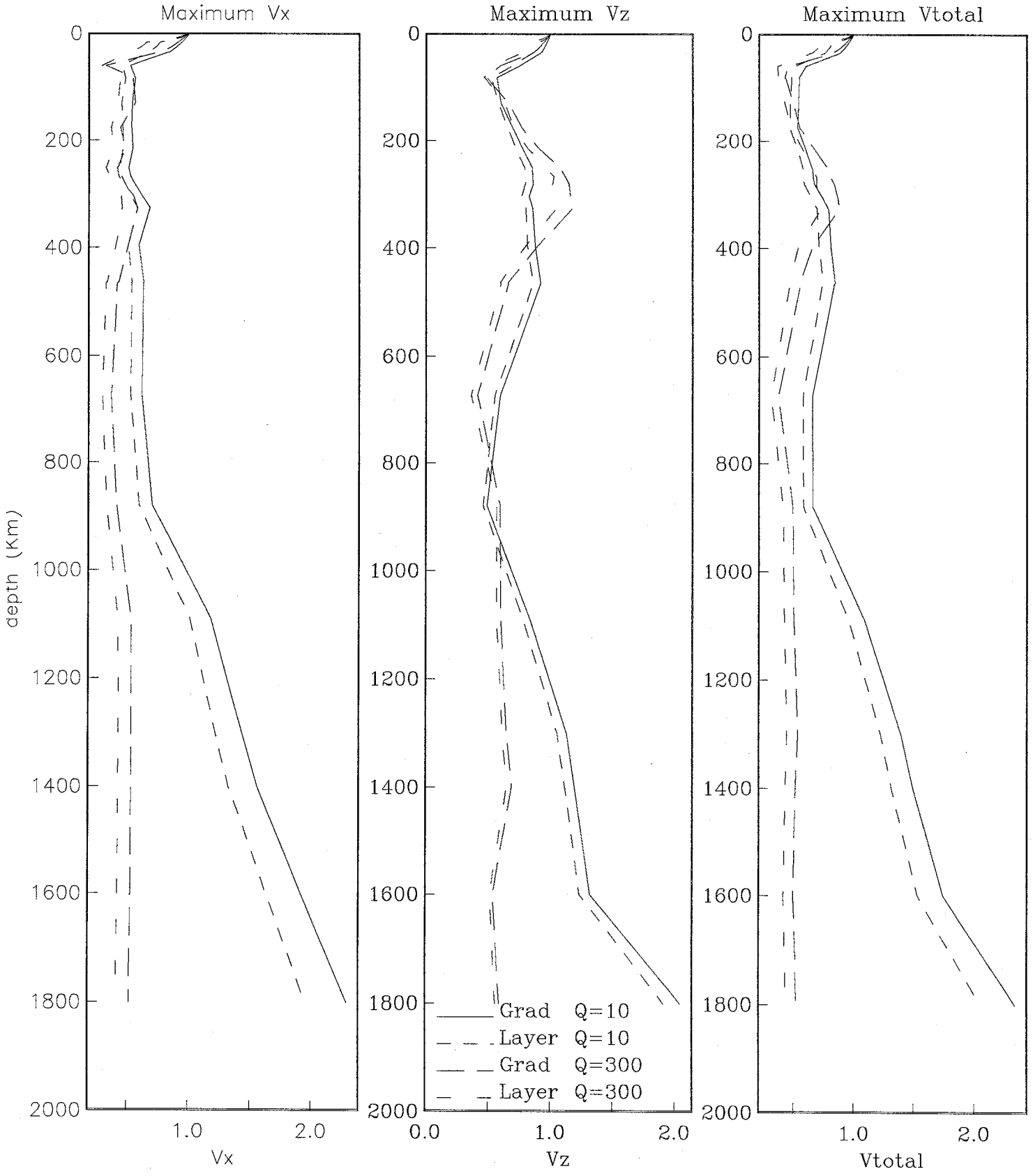

Maximum velocity
incident angle : 20

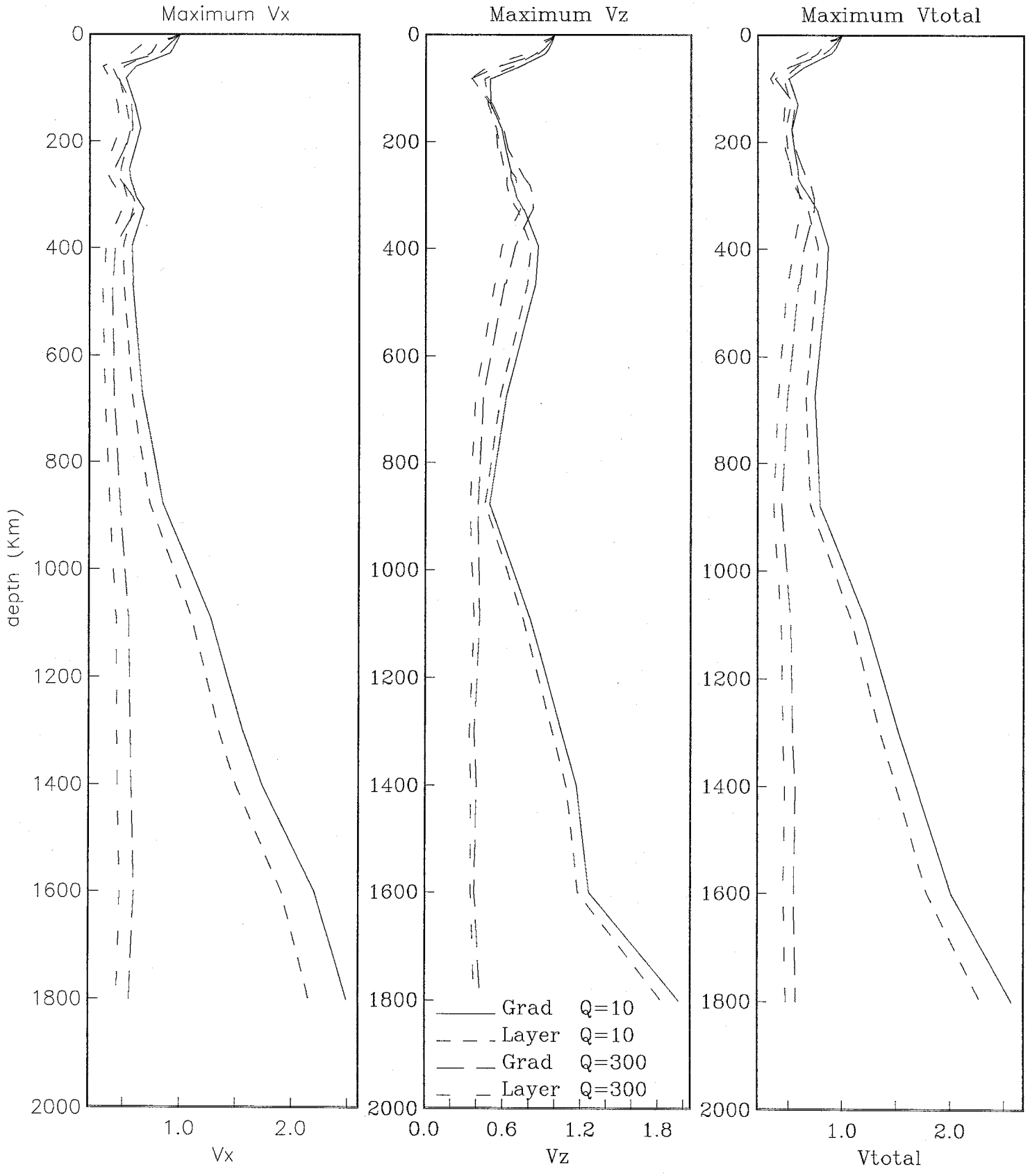

Maximum velocity
incident angle : 30

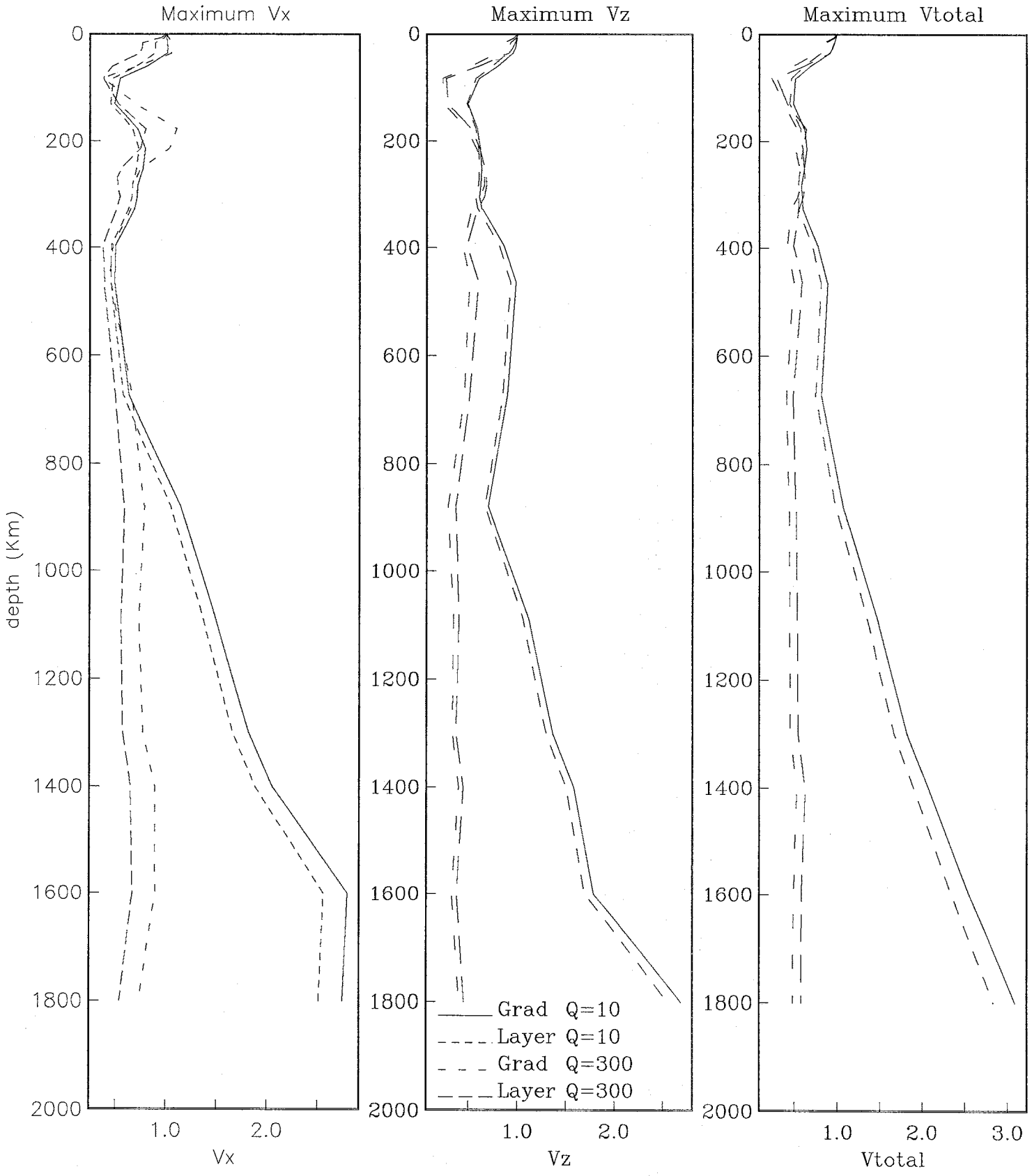

Maximum velocity
incident angle : 40

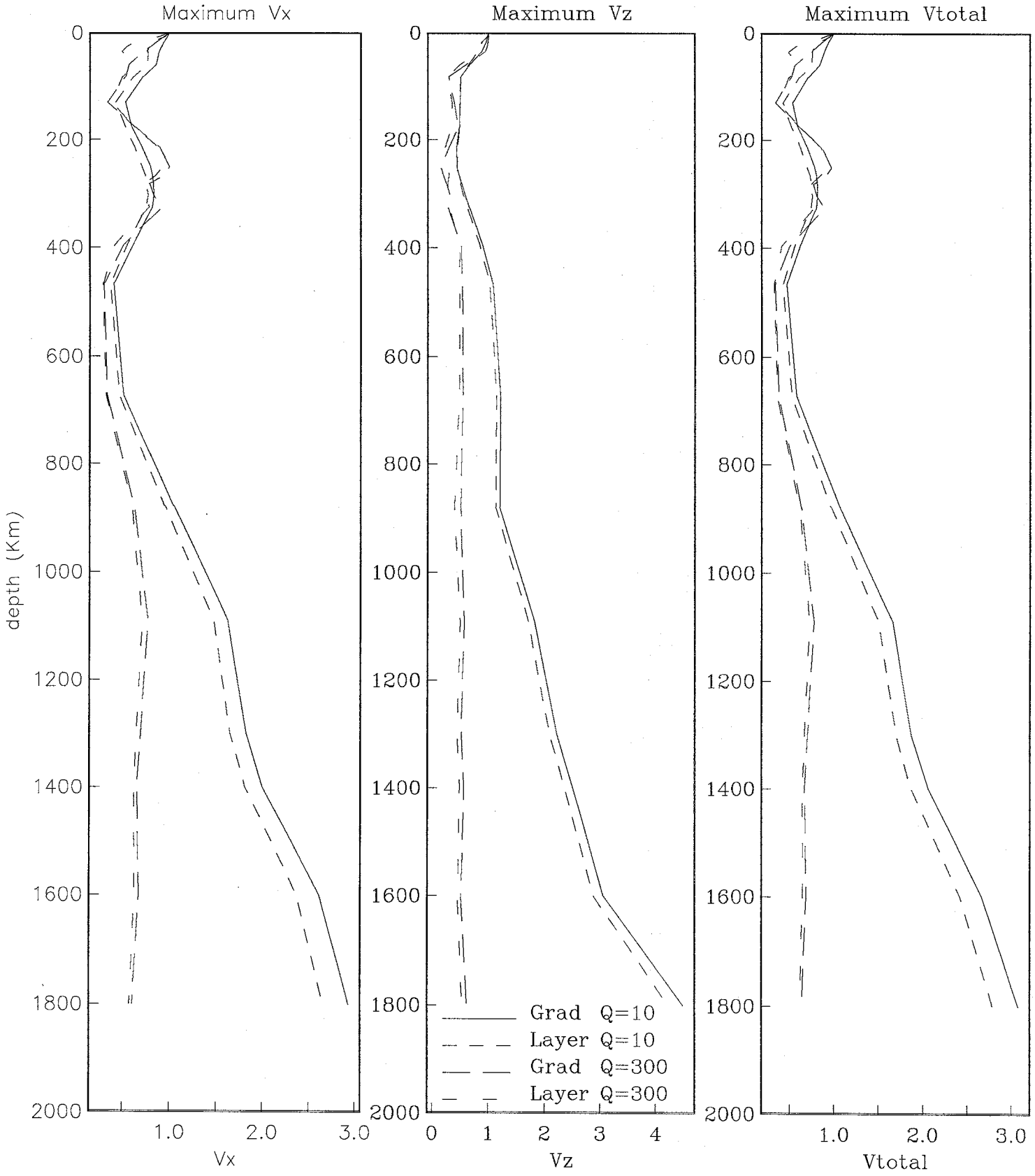

Maximum acceleration
incident angle : 0

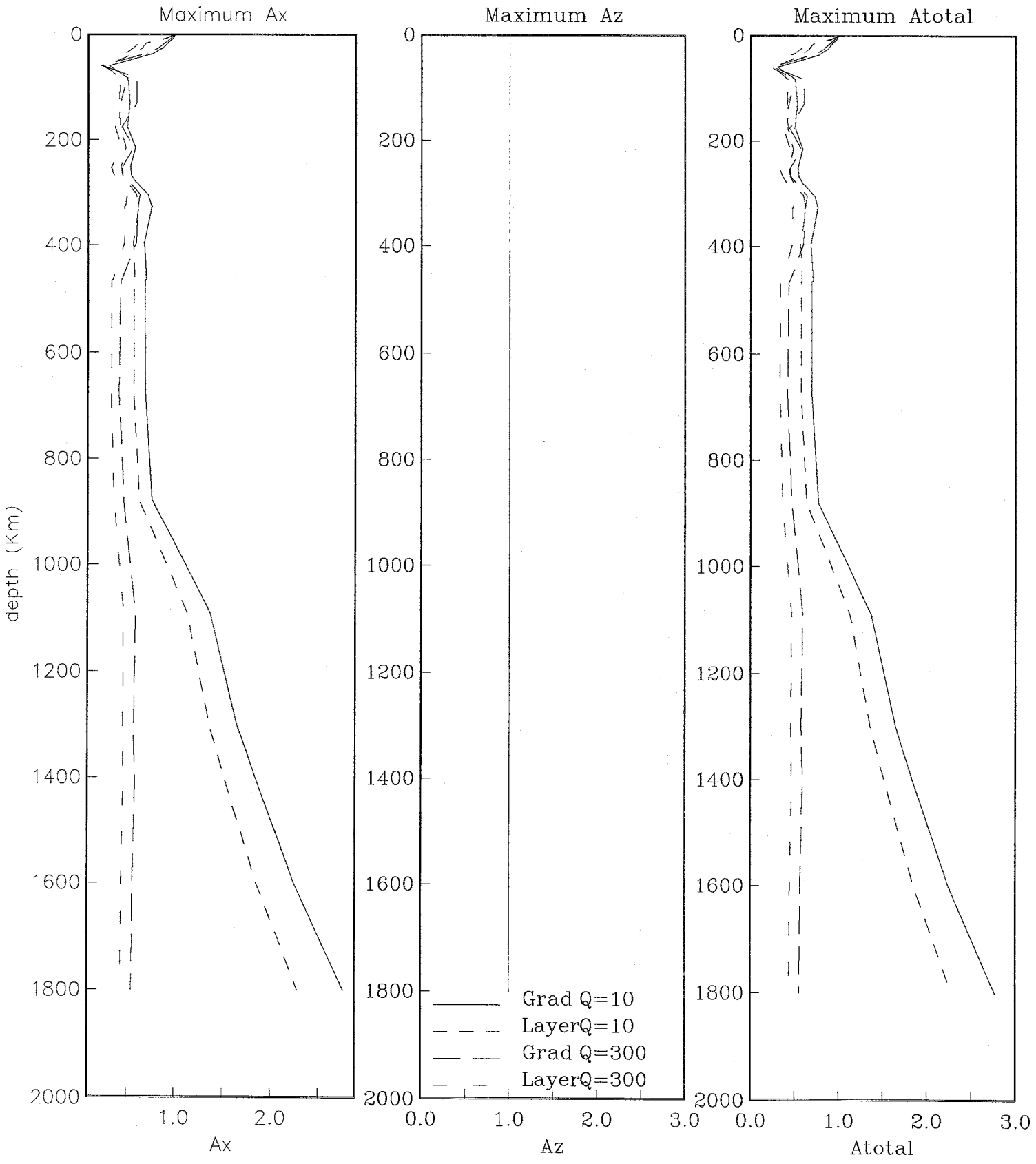

Maximum acceleration
incident angle : 10

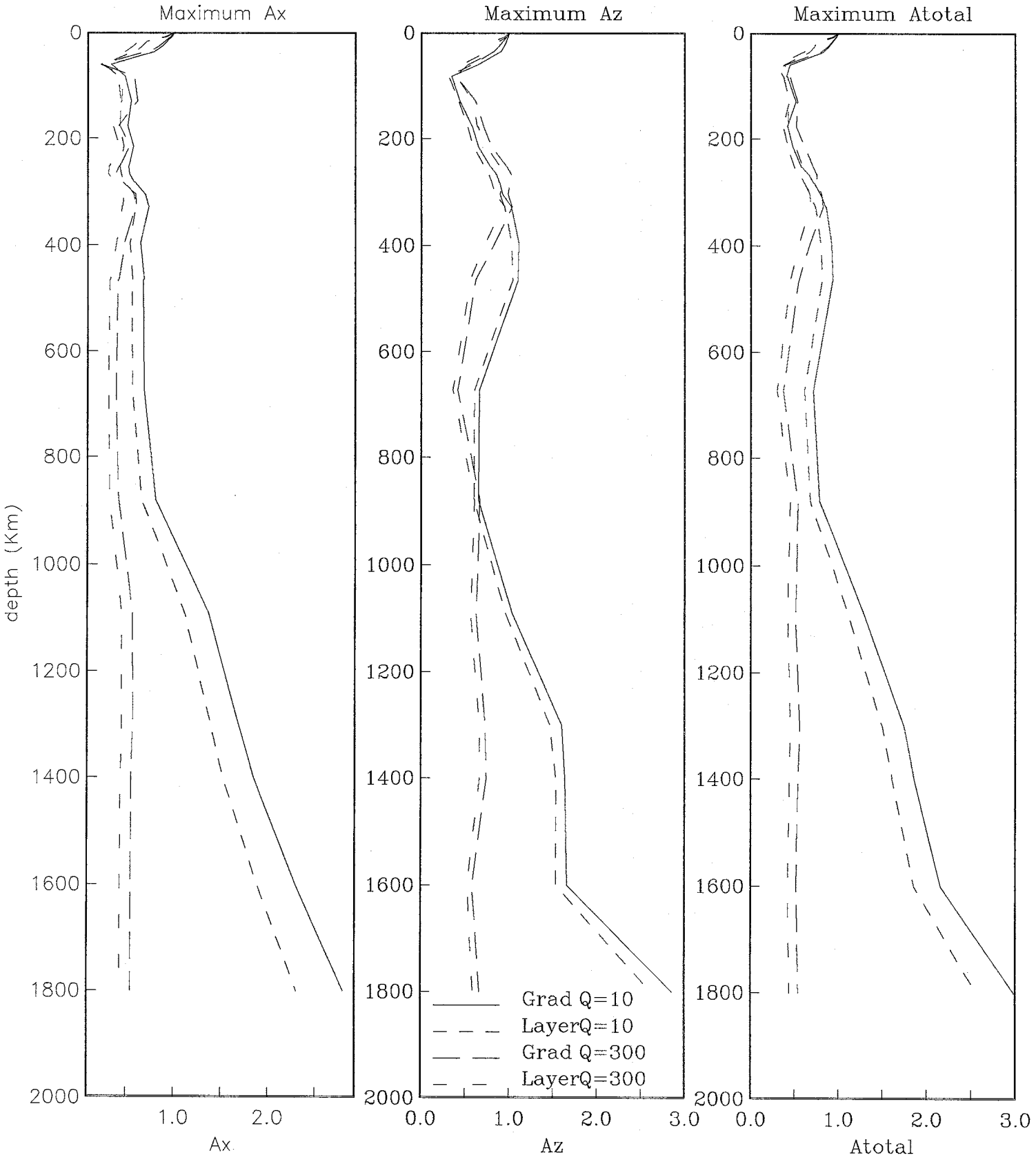

Maximum acceleration
incident angle : 20

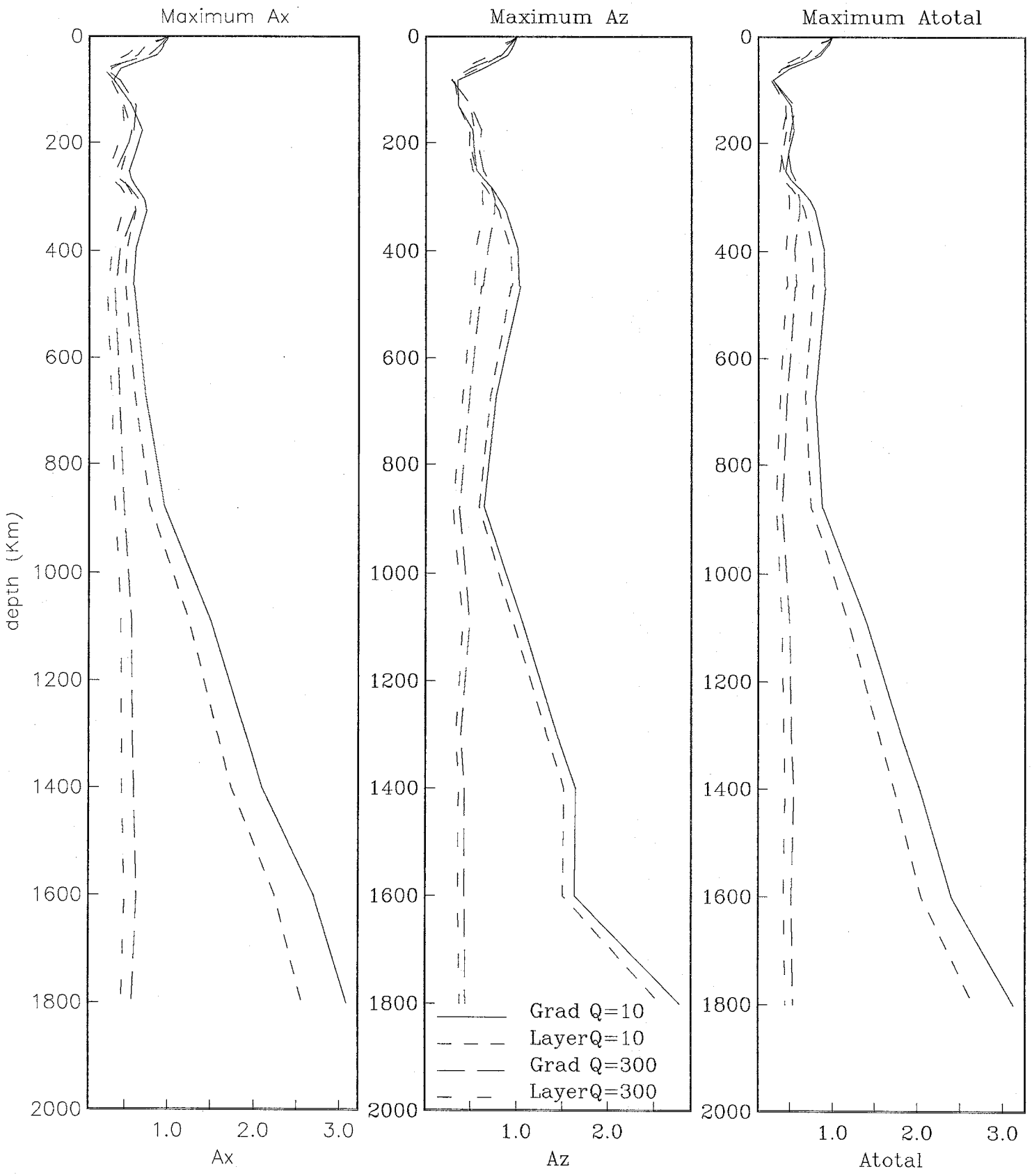

Maximum acceleration
incident angle : 30

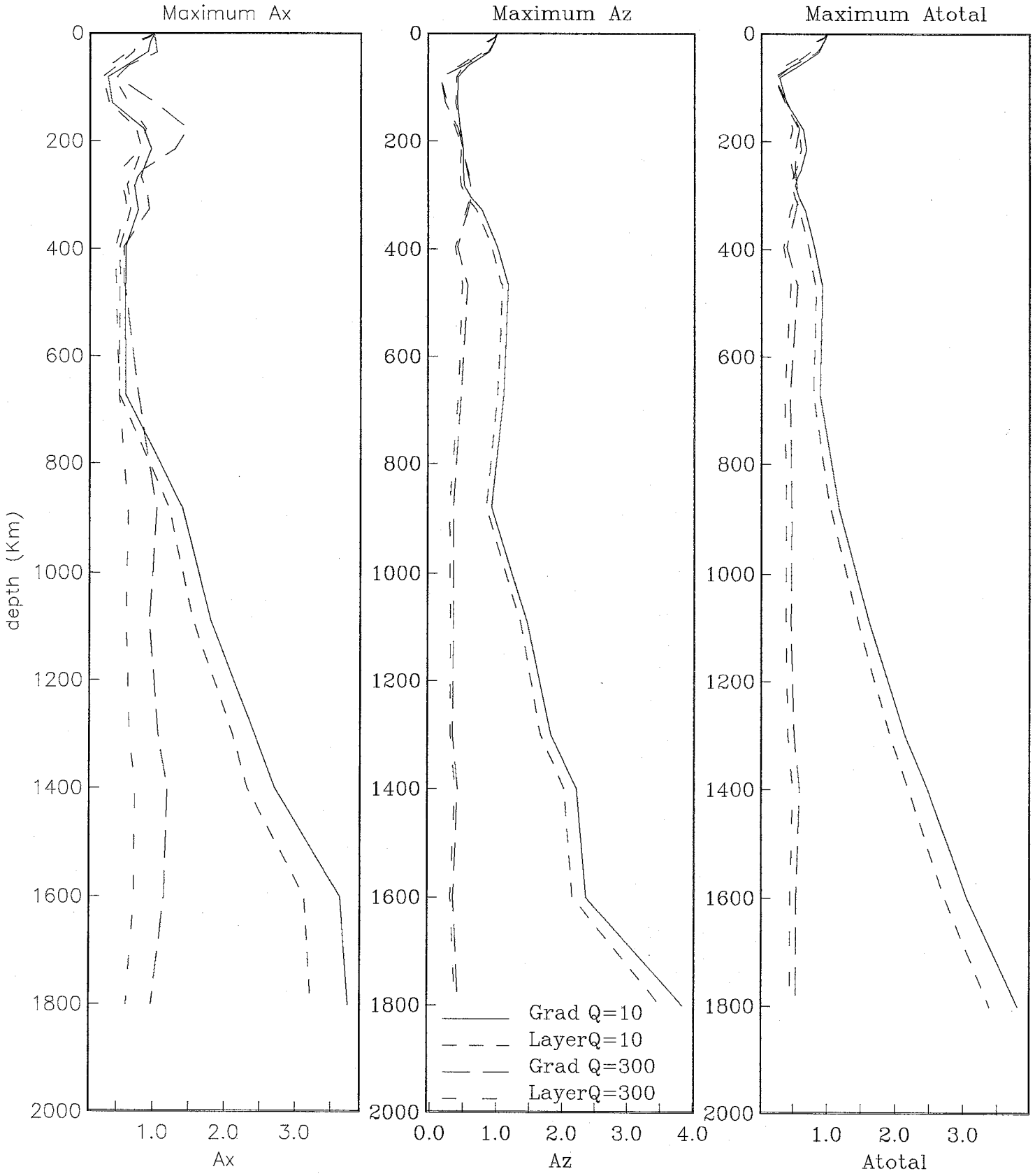

Maximum acceleration
incident angle : 40

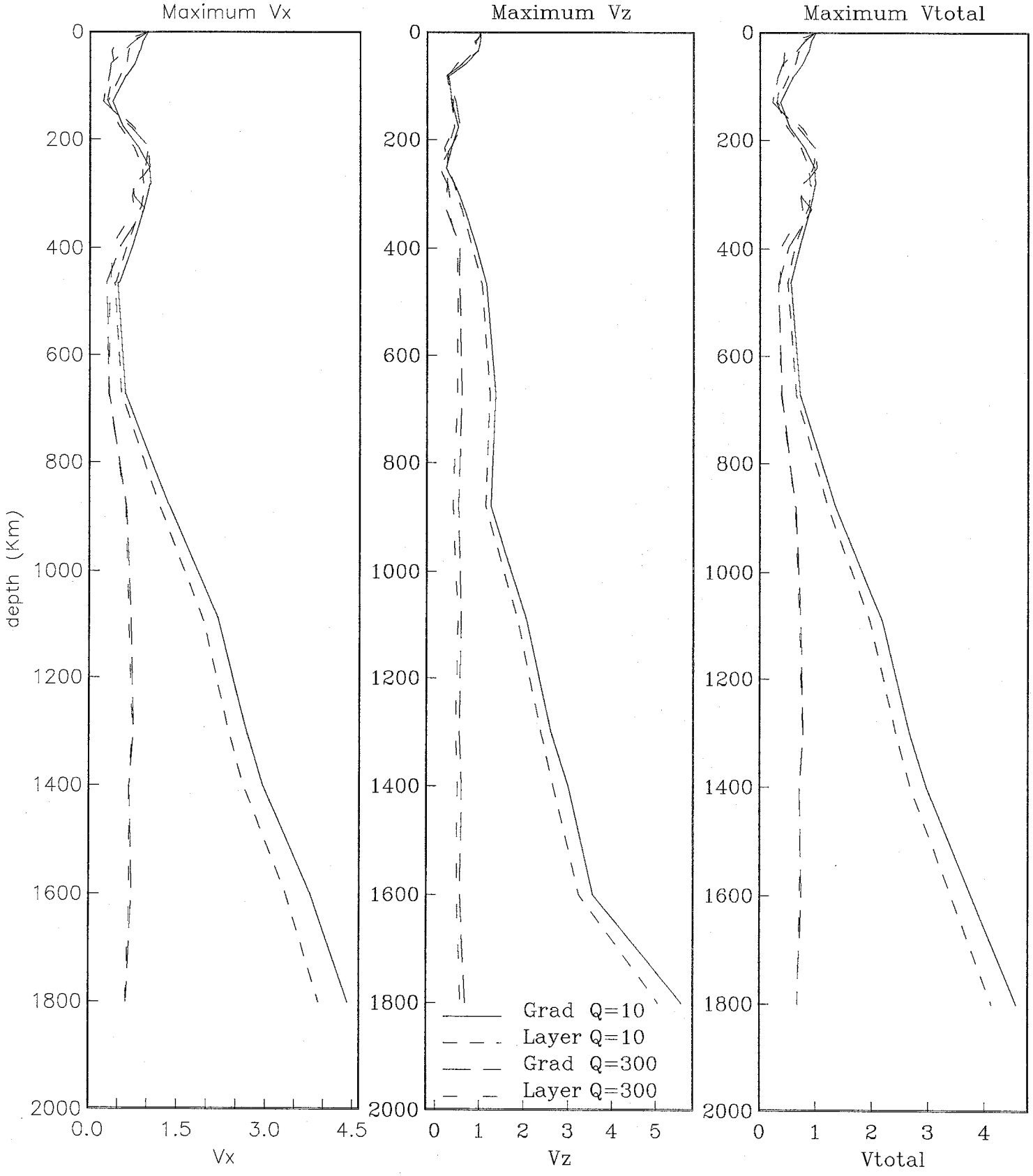

Appendix E

Content :

20 tables containing maximum displacements, velocities, accelerations for angles of incidence 0, 10, 20, 30, and 40, depths 0, 8, 16, 17, 26, 35, 37, 60, 82, 83, 130, 177, 178, 215, 252, 253, 268, 282, 283, 305, 327, 328, 296, 464, 466, 673, 879, 880, 1090, 1300 and 1600 m, gradient and homogeneous top 16.5 m of ground, Q values 10 and 300, for a frequency content 0 to 10 Hz.

Incident angle : 0

Depth	Qs= Qp	1st Layer	maximum displacement			maximum velocity			maximum acceleration		
			Ux	Uz	Ut	Vx	Vz	Vt	Ax	Az	At
0	10	G	1.0000	1.0000	1.0000	1.0000	1.0000	1.0000	1.0000	1.0000	1.0000
	10	L	1.0000	1.0000	1.0000	1.0000	1.0000	1.0000	1.0000	1.0000	1.0000
	300	G	1.0000	1.0000	1.0000	1.0000	1.0000	1.0000	1.0000	1.0000	1.0000
	300	L	1.0000	1.0000	1.0000	1.0000	1.0000	1.0000	1.0000	1.0000	1.0000
8	10	G	0.9886	1.0000	0.9886	0.9732	1.0000	0.9732	0.9787	1.0000	0.9787
	10	L	0.9729	1.0000	0.9729	0.9462	1.0000	0.9462	0.9211	1.0000	0.9211
	300	G	0.9763	1.0000	0.9763	0.9630	1.0000	0.9630	0.9557	1.0000	0.9557
	300	L	0.9472	1.0000	0.9472	0.9191	1.0000	0.9191	0.9094	1.0000	0.9094
16	10	G	0.9727	1.0000	0.9727	0.9395	1.0000	0.9395	0.9255	1.0000	0.9255
	10	L	0.8963	1.0000	0.8963	0.7932	1.0000	0.7932	0.7281	1.0000	0.7281
	300	G	0.9457	1.0000	0.9457	0.9137	1.0000	0.9137	0.8994	1.0000	0.8994
	300	L	0.7983	1.0000	0.7983	0.6906	1.0000	0.6906	0.6582	1.0000	0.6582
17	10	G	0.9708	1.0000	0.9708	0.9323	1.0000	0.9323	0.9255	1.0000	0.9255
	10	L	0.8863	1.0000	0.8863	0.7738	1.0000	0.7738	0.7018	1.0000	0.7018
	300	G	0.9414	1.0000	0.9414	0.9075	1.0000	0.9075	0.8913	1.0000	0.8913
	300	L	0.7796	1.0000	0.7796	0.6624	1.0000	0.6624	0.6264	1.0000	0.6264
26	10	G	0.9511	1.0000	0.9511	0.8927	1.0000	0.8927	0.8723	1.0000	0.8723
	10	L	0.8669	1.0000	0.8669	0.7356	1.0000	0.7356	0.6579	1.0000	0.6579
	300	G	0.9032	1.0000	0.9032	0.8467	1.0000	0.8467	0.8270	1.0000	0.8270
	300	L	0.7428	1.0000	0.7428	0.6120	1.0000	0.6120	0.5644	1.0000	0.5644
35	10	G	0.9239	1.0000	0.9239	0.8390	1.0000	0.8390	0.7872	1.0000	0.7872
	10	L	0.8410	1.0000	0.8410	0.6859	1.0000	0.6859	0.5965	1.0000	0.5965
	300	G	0.8503	1.0000	0.8503	0.7639	1.0000	0.7639	0.7324	1.0000	0.7324
	300	L	0.6954	1.0000	0.6954	0.5488	1.0000	0.5488	0.4897	1.0000	0.4897
37	10	G	0.9124	1.0000	0.9124	0.8162	1.0000	0.8162	0.7766	1.0000	0.7766
	10	L	0.8304	1.0000	0.8304	0.6651	1.0000	0.6651	0.5877	1.0000	0.5877
	300	G	0.8279	1.0000	0.8279	0.7286	1.0000	0.7286	0.6922	1.0000	0.6922
	300	L	0.6759	1.0000	0.6759	0.5228	1.0000	0.5228	0.4610	1.0000	0.4610
60	10	G	0.7195	1.0000	0.7195	0.5158	1.0000	0.5158	0.3085	1.0000	0.3085
	10	L	0.6555	1.0000	0.6555	0.4528	1.0000	0.4528	0.2605	1.0000	0.2605
	300	G	0.4533	1.0000	0.4533	0.3286	1.0000	0.3286	0.2437	1.0000	0.2437
	300	L	0.3871	1.0000	0.3871	0.2973	1.0000	0.2973	0.2300	1.0000	0.2300

Incident angle : 0

Depth	Qs= Qp	1st Layer	maximum displacement			maximum velocity			maximum acceleration		
			Ux	Uz	Ut	Vx	Vz	Vt	Ax	Az	At
82	10	G	0.6150	1.0000	0.6150	0.5615	1.0000	0.5615	0.4936	1.0000	0.4936
	10	L	0.5763	1.0000	0.5763	0.4801	1.0000	0.4801	0.4158	1.0000	0.4158
	300	G	0.5133	1.0000	0.5133	0.5535	1.0000	0.5535	0.5855	1.0000	0.5855
	300	L	0.4593	1.0000	0.4593	0.4461	1.0000	0.4461	0.4833	1.0000	0.4833
83	10	G	0.6150	1.0000	0.6150	0.5651	1.0000	0.5651	0.5053	1.0000	0.5053
	10	L	0.5761	1.0000	0.5761	0.4814	1.0000	0.4814	0.4237	1.0000	0.4237
	300	G	0.5176	1.0000	0.5176	0.5594	1.0000	0.5594	0.6016	1.0000	0.6016
	300	L	0.4624	1.0000	0.4624	0.4515	1.0000	0.4515	0.4913	1.0000	0.4913
130	10	G	0.5732	1.0000	0.5732	0.5102	1.0000	0.5102	0.5266	1.0000	0.5266
	10	L	0.5312	1.0000	0.5312	0.4266	1.0000	0.4266	0.4167	1.0000	0.4167
	300	G	0.5001	1.0000	0.5001	0.5449	1.0000	0.5449	0.6058	1.0000	0.6058
	300	L	0.4239	1.0000	0.4239	0.4098	1.0000	0.4098	0.4337	1.0000	0.4337
177	10	G	0.5352	1.0000	0.5352	0.5154	1.0000	0.5154	0.4989	1.0000	0.4989
	10	L	0.4978	1.0000	0.4978	0.4433	1.0000	0.4433	0.4211	1.0000	0.4211
	300	G	0.4356	1.0000	0.4356	0.4372	1.0000	0.4372	0.4406	1.0000	0.4406
	300	L	0.3867	1.0000	0.3867	0.3611	1.0000	0.3611	0.3720	1.0000	0.3720
178	10	G	0.5347	1.0000	0.5347	0.5174	1.0000	0.5174	0.5064	1.0000	0.5064
	10	L	0.4974	1.0000	0.4974	0.4450	1.0000	0.4450	0.4263	1.0000	0.4263
	300	G	0.4396	1.0000	0.4396	0.4442	1.0000	0.4442	0.4507	1.0000	0.4507
	300	L	0.3900	1.0000	0.3900	0.3643	1.0000	0.3643	0.3768	1.0000	0.3768
215	10	G	0.5438	1.0000	0.5438	0.5330	1.0000	0.5330	0.5883	1.0000	0.5883
	10	L	0.5050	1.0000	0.5050	0.4518	1.0000	0.4518	0.4860	1.0000	0.4860
	300	G	0.4894	1.0000	0.4894	0.5124	1.0000	0.5124	0.5734	1.0000	0.5734
	300	L	0.4241	1.0000	0.4241	0.4154	1.0000	0.4154	0.4436	1.0000	0.4436
252	10	G	0.5282	1.0000	0.5282	0.5062	1.0000	0.5062	0.5362	1.0000	0.5362
	10	L	0.4893	1.0000	0.4893	0.4293	1.0000	0.4293	0.4368	1.0000	0.4368
	300	G	0.4877	1.0000	0.4877	0.4731	1.0000	0.4731	0.4487	1.0000	0.4487
	300	L	0.4158	1.0000	0.4158	0.3719	1.0000	0.3719	0.3370	1.0000	0.3370
253	10	G	0.5286	1.0000	0.5286	0.5054	1.0000	0.5054	0.5372	1.0000	0.5372
	10	L	0.4897	1.0000	0.4897	0.4293	1.0000	0.4293	0.4377	1.0000	0.4377
	300	G	0.4874	1.0000	0.4874	0.4747	1.0000	0.4747	0.4487	1.0000	0.4487
	300	L	0.4146	1.0000	0.4146	0.3762	1.0000	0.3762	0.3339	1.0000	0.3339

Incident angle : 0

Depth	Qs= Qp	1st Layer	maximum displacement			maximum velocity			maximum acceleration		
			Ux	Uz	Ut	Vx	Vz	Vt	Ax	Az	At
268	10	G	0.5283	1.0000	0.5283	0.5226	1.0000	0.5226	0.5415	1.0000	0.5415
	10	L	0.4906	1.0000	0.4906	0.4470	1.0000	0.4470	0.4491	1.0000	0.4491
	300	G	0.4831	1.0000	0.4831	0.5219	1.0000	0.5219	0.4567	1.0000	0.4567
	300	L	0.4152	1.0000	0.4152	0.4170	1.0000	0.4170	0.3609	1.0000	0.3609
282	10	G	0.5390	1.0000	0.5390	0.5603	1.0000	0.5603	0.5936	1.0000	0.5936
	10	L	0.5013	1.0000	0.5013	0.4797	1.0000	0.4797	0.4947	1.0000	0.4947
	300	G	0.4872	1.0000	0.4872	0.5605	1.0000	0.5605	0.5231	1.0000	0.5231
	300	L	0.4266	1.0000	0.4266	0.4646	1.0000	0.4646	0.4149	1.0000	0.4149
283	10	G	0.5417	1.0000	0.5417	0.5643	1.0000	0.5643	0.6032	1.0000	0.6032
	10	L	0.5038	1.0000	0.5038	0.4831	1.0000	0.4831	0.5018	1.0000	0.5018
	300	G	0.4896	1.0000	0.4896	0.5646	1.0000	0.5646	0.5312	1.0000	0.5312
	300	L	0.4274	1.0000	0.4274	0.4665	1.0000	0.4665	0.4181	1.0000	0.4181
305	10	G	0.5796	1.0000	0.5796	0.6264	1.0000	0.6264	0.7213	1.0000	0.7213
	10	L	0.5385	1.0000	0.5385	0.5363	1.0000	0.5363	0.5974	1.0000	0.5974
	300	G	0.5255	1.0000	0.5255	0.5728	1.0000	0.5728	0.6378	1.0000	0.6378
	300	L	0.4572	1.0000	0.4572	0.4658	1.0000	0.4658	0.5024	1.0000	0.5024
327	10	G	0.6047	1.0000	0.6047	0.6972	1.0000	0.6972	0.7585	1.0000	0.7585
	10	L	0.5607	1.0000	0.5607	0.5925	1.0000	0.5925	0.6228	1.0000	0.6228
	300	G	0.5336	1.0000	0.5336	0.6096	1.0000	0.6096	0.6177	1.0000	0.6177
	300	L	0.4590	1.0000	0.4590	0.4794	1.0000	0.4794	0.4817	1.0000	0.4817
328	10	G	0.6055	1.0000	0.6055	0.7008	1.0000	0.7008	0.7606	1.0000	0.7606
	10	L	0.5614	1.0000	0.5614	0.5952	1.0000	0.5952	0.6237	1.0000	0.6237
	300	G	0.5338	1.0000	0.5338	0.6086	1.0000	0.6086	0.6157	1.0000	0.6157
	300	L	0.4593	1.0000	0.4593	0.4783	1.0000	0.4783	0.4738	1.0000	0.4738
396	10	G	0.5970	1.0000	0.5970	0.6348	1.0000	0.6348	0.6830	1.0000	0.6830
	10	L	0.5547	1.0000	0.5547	0.5397	1.0000	0.5397	0.5658	1.0000	0.5658
	300	G	0.4822	1.0000	0.4822	0.5967	1.0000	0.5967	0.5976	1.0000	0.5976
	300	L	0.4220	1.0000	0.4220	0.4809	1.0000	0.4809	0.4738	1.0000	0.4738
464	10	G	0.5964	1.0000	0.5964	0.6324	1.0000	0.6324	0.7064	1.0000	0.7064
	10	L	0.5533	1.0000	0.5533	0.5387	1.0000	0.5387	0.5807	1.0000	0.5807
	300	G	0.4549	1.0000	0.4549	0.4347	1.0000	0.4347	0.4447	1.0000	0.4447
	300	L	0.3948	1.0000	0.3948	0.3427	1.0000	0.3427	0.3498	1.0000	0.3498

Incident angle : 0

Depth	Qs= Qp	1st Layer	maximum displacement			maximum velocity			maximum acceleration		
			Ux	Uz	Ut	Vx	Vz	Vt	Ax	Az	At
464	10	G	0.5964	1.0000	0.5964	0.6324	1.0000	0.6324	0.7064	1.0000	0.7064
	10	L	0.5533	1.0000	0.5533	0.5387	1.0000	0.5387	0.5807	1.0000	0.5807
	300	G	0.4549	1.0000	0.4549	0.4347	1.0000	0.4347	0.4447	1.0000	0.4447
	300	L	0.3948	1.0000	0.3948	0.3427	1.0000	0.3427	0.3498	1.0000	0.3498
466	10	G	0.5922	1.0000	0.5922	0.6368	1.0000	0.6368	0.6926	1.0000	0.6926
	10	L	0.5497	1.0000	0.5497	0.5421	1.0000	0.5421	0.5728	1.0000	0.5728
	300	G	0.4490	1.0000	0.4490	0.4198	1.0000	0.4198	0.4346	1.0000	0.4346
	300	L	0.3898	1.0000	0.3898	0.3317	1.0000	0.3317	0.3386	1.0000	0.3386
673	10	G	0.5301	1.0000	0.5301	0.6043	1.0000	0.6043	0.6947	1.0000	0.6947
	10	L	0.4923	1.0000	0.4923	0.5145	1.0000	0.5145	0.5746	1.0000	0.5746
	300	G	0.3873	1.0000	0.3873	0.3834	1.0000	0.3834	0.4185	1.0000	0.4185
	300	L	0.3380	1.0000	0.3380	0.3119	1.0000	0.3119	0.3355	1.0000	0.3355
879	10	G	0.5567	1.0000	0.5567	0.6704	1.0000	0.6704	0.7670	1.0000	0.7670
	10	L	0.5167	1.0000	0.5167	0.5707	1.0000	0.5707	0.6333	1.0000	0.6333
	300	G	0.4308	1.0000	0.4308	0.4471	1.0000	0.4471	0.4688	1.0000	0.4688
	300	L	0.3732	1.0000	0.3732	0.3640	1.0000	0.3640	0.3641	1.0000	0.3641
880	10	G	0.5576	1.0000	0.5576	0.6708	1.0000	0.6708	0.7702	1.0000	0.7702
	10	L	0.5174	1.0000	0.5174	0.5700	1.0000	0.5700	0.6342	1.0000	0.6342
	300	G	0.4310	1.0000	0.4310	0.4472	1.0000	0.4472	0.4668	1.0000	0.4668
	300	L	0.3730	1.0000	0.3730	0.3630	1.0000	0.3630	0.3657	1.0000	0.3657
1090	10	G	0.8756	1.0000	0.8756	1.1750	1.0000	1.1750	1.3723	1.0000	1.3723
	10	L	0.8127	1.0000	0.8127	1.0000	1.0000	1.0000	1.1316	1.0000	1.1316
	300	G	0.5465	1.0000	0.5465	0.5616	1.0000	0.5616	0.5936	1.0000	0.5936
	300	L	0.4748	1.0000	0.4748	0.4493	1.0000	0.4493	0.4674	1.0000	0.4674
1300	10	G	0.9816	1.0000	0.9816	1.3696	1.0000	1.3696	1.6489	1.0000	1.6489
	10	L	0.9111	1.0000	0.9111	1.1652	1.0000	1.1652	1.3596	1.0000	1.3596
	300	G	0.5377	1.0000	0.5377	0.5400	1.0000	0.5400	0.5755	1.0000	0.5755
	300	L	0.4682	1.0000	0.4682	0.4322	1.0000	0.4322	0.4579	1.0000	0.4579
1400	10	G	1.0520	1.0000	1.0520	1.5270	1.0000	1.5270	1.8404	1.0000	1.8404
	10	L	0.9764	1.0000	0.9764	1.2995	1.0000	1.2995	1.5175	1.0000	1.5175
	300	G	0.5448	1.0000	0.5448	0.5415	1.0000	0.5415	0.5875	1.0000	0.5875
	300	L	0.4744	1.0000	0.4744	0.4323	1.0000	0.4323	0.4658	1.0000	0.4658
1600	10	G	1.1916	1.0000	1.1916	1.8426	1.0000	1.8426	2.2447	1.0000	2.2447
	10	L	1.1060	1.0000	1.1060	1.5676	1.0000	1.5676	1.8509	1.0000	1.8509
	300	G	0.5384	1.0000	0.5384	0.5327	1.0000	0.5327	0.5654	1.0000	0.5654
	300	L	0.4688	1.0000	0.4688	0.4259	1.0000	0.4259	0.4467	1.0000	0.4467

Incident angle : 10

Depth	Qs= Qp	1st Layer	maximum displacement			maximum velocity			maximum acceleration		
			Ux	Uz	Ut	Vx	Vz	Vt	Ax	Az	At
0	10	G	1.0000	1.0000	1.0000	1.0000	1.0000	1.0000	1.0000	1.0000	1.0000
	10	L	1.0000	1.0000	1.0000	1.0000	1.0000	1.0000	1.0000	1.0000	1.0000
	300	G	1.0000	1.0000	1.0000	1.0000	1.0000	1.0000	1.0000	1.0000	1.0000
	300	L	1.0000	1.0000	1.0000	1.0000	1.0000	1.0000	1.0000	1.0000	1.0000
8	10	G	0.9885	0.9944	0.9908	0.9774	0.9871	0.9817	0.9785	0.9849	0.9810
	10	L	0.9733	0.9913	0.9798	0.9440	0.9746	0.9559	0.9292	0.9710	0.9464
	300	G	0.9775	0.9778	0.9823	0.9641	0.9757	0.9724	0.9608	0.9655	0.9688
	300	L	0.9475	0.9676	0.9590	0.9195	0.9588	0.9375	0.9092	0.9490	0.9272
16	10	G	0.9732	0.9871	0.9786	0.9437	0.9717	0.9580	0.9247	0.9648	0.9361
	10	L	0.8975	0.9668	0.9230	0.7879	0.9085	0.8395	0.7345	0.8852	0.7836
	300	G	0.9477	0.9535	0.9590	0.9169	0.9470	0.9370	0.9059	0.9270	0.9271
	300	L	0.7977	0.8982	0.8407	0.6926	0.8544	0.7618	0.6585	0.8324	0.7391
17	10	G	0.9713	0.9863	0.9771	0.9412	0.9696	0.9560	0.9247	0.9610	0.9361
	10	L	0.8880	0.9636	0.9159	0.7690	0.8999	0.8248	0.7168	0.8770	0.7674
	300	G	0.9437	0.9500	0.9557	0.9108	0.9429	0.9322	0.9000	0.9229	0.9218
	300	L	0.7789	0.8892	0.8259	0.6641	0.8410	0.7402	0.6277	0.8179	0.7151
26	10	G	0.9521	0.9775	0.9620	0.8968	0.9509	0.9251	0.8710	0.9358	0.8915
	10	L	0.8684	0.9557	0.9008	0.7315	0.8824	0.7950	0.6637	0.8515	0.7233
	300	G	0.9067	0.9221	0.9267	0.8530	0.9085	0.8890	0.8353	0.8783	0.8741
	300	L	0.7430	0.8650	0.7980	0.6107	0.8102	0.7008	0.5692	0.7796	0.6678
35	10	G	0.9259	0.9662	0.9417	0.8413	0.9263	0.8854	0.7957	0.9019	0.8282
	10	L	0.8429	0.9455	0.8812	0.6839	0.8595	0.7579	0.6018	0.8202	0.6741
	300	G	0.8558	0.8913	0.8867	0.7743	0.8654	0.8302	0.7471	0.8256	0.8059
	300	L	0.6964	0.8365	0.7610	0.5427	0.7712	0.6506	0.4954	0.7341	0.6083
37	10	G	0.9151	0.9622	0.9335	0.8175	0.9164	0.8682	0.7849	0.8868	0.8160
	10	L	0.8322	0.9415	0.8731	0.6640	0.8502	0.7429	0.5752	0.8063	0.6575
	300	G	0.8340	0.8821	0.8696	0.7402	0.8486	0.8049	0.7078	0.8073	0.7768
	300	L	0.6771	0.8262	0.7457	0.5142	0.7558	0.6299	0.4662	0.7177	0.5860
60	10	G	0.7292	0.9042	0.8013	0.5253	0.7500	0.6009	0.3333	0.6440	0.4437
	10	L	0.6615	0.8806	0.7478	0.4582	0.6921	0.5109	0.2566	0.5766	0.3718
	300	G	0.4647	0.7151	0.5835	0.3248	0.5942	0.4525	0.2289	0.5233	0.3856
	300	L	0.3822	0.6685	0.4943	0.2902	0.5408	0.3654	0.2257	0.4554	0.3076

Incident angle : 10

Depth	Qs= Qp	1st Layer	maximum displacement			maximum velocity			maximum acceleration		
			Ux	Uz	Ut	Vx	Vz	Vt	Ax	Az	At
82	10	G	0.6123	0.8301	0.6993	0.5631	0.5736	0.5400	0.4753	0.3488	0.4022
	10	L	0.5739	0.8111	0.6669	0.4830	0.5294	0.4790	0.4035	0.3034	0.3607
	300	G	0.4931	0.5573	0.4822	0.5400	0.4887	0.4234	0.5647	0.3876	0.4308
	300	L	0.4443	0.5248	0.4454	0.4381	0.4623	0.3695	0.4554	0.3863	0.3631
83	10	G	0.6122	0.8269	0.6989	0.5672	0.5678	0.5432	0.4860	0.3379	0.4141
	10	L	0.5737	0.8095	0.6669	0.4855	0.5236	0.4816	0.4133	0.3055	0.3723
	300	G	0.4995	0.5552	0.4892	0.5469	0.4902	0.4320	0.5824	0.3945	0.4460
	300	L	0.4472	0.5220	0.4510	0.4421	0.4688	0.3746	0.4615	0.3916	0.3723
130	10	G	0.5864	0.7716	0.6616	0.5409	0.6011	0.5383	0.5538	0.4327	0.5125
	10	L	0.5429	0.7631	0.6297	0.4540	0.5799	0.4701	0.4398	0.4165	0.4362
	300	G	0.5092	0.6121	0.5360	0.5657	0.6602	0.4956	0.6180	0.6146	0.5324
	300	L	0.4326	0.5943	0.4778	0.4193	0.6318	0.4254	0.4477	0.5792	0.4260
177	10	G	0.5548	0.6562	0.5507	0.5351	0.6955	0.5291	0.5129	0.5698	0.4120
	10	L	0.5155	0.6351	0.5201	0.4599	0.6521	0.4683	0.4274	0.5197	0.3624
	300	G	0.4453	0.6944	0.4587	0.4431	0.7690	0.5493	0.4157	0.7039	0.5180
	300	L	0.3920	0.6484	0.4019	0.3666	0.7029	0.4760	0.3492	0.6302	0.4212
178	10	G	0.5543	0.6555	0.5474	0.5376	0.6980	0.5312	0.5129	0.5723	0.4175
	10	L	0.5151	0.6351	0.5169	0.4620	0.6537	0.4699	0.4301	0.5209	0.3685
	300	G	0.4453	0.6959	0.4582	0.4453	0.7725	0.5536	0.4275	0.7018	0.5180
	300	L	0.3924	0.6484	0.4010	0.3679	0.7035	0.4786	0.3569	0.6357	0.4261
215	10	G	0.5496	0.6506	0.5030	0.5450	0.7741	0.5967	0.5731	0.6415	0.4806
	10	L	0.5103	0.6287	0.4775	0.4624	0.7212	0.5267	0.4726	0.5847	0.4195
	300	G	0.4777	0.7516	0.4801	0.4811	0.9035	0.6713	0.5353	0.7972	0.6137
	300	L	0.4135	0.6959	0.4281	0.3841	0.8167	0.5701	0.4185	0.7413	0.5129
252	10	G	0.5313	0.6544	0.5293	0.5113	0.8502	0.6527	0.5301	0.7799	0.5744
	10	L	0.4921	0.6314	0.5030	0.4344	0.7908	0.5734	0.4292	0.7146	0.4925
	300	G	0.4482	0.8392	0.5357	0.4219	1.0754	0.7813	0.4275	0.9635	0.7080
	300	L	0.3727	0.7768	0.4773	0.3248	0.9643	0.6514	0.3185	0.8852	0.5932
253	10	G	0.5298	0.6548	0.5314	0.5117	0.8519	0.6543	0.5258	0.7836	0.5813
	10	L	0.4907	0.6315	0.5049	0.4347	0.7912	0.5740	0.4283	0.7158	0.4965
	300	G	0.4458	0.8404	0.5364	0.4161	1.0784	0.7840	0.4216	0.9696	0.7127
	300	L	0.3721	0.7807	0.4793	0.3249	0.9708	0.6518	0.3138	0.8889	0.5957

Incident angle : 10

Depth	Qs= Qp	1st Layer	maximum displacement			maximum velocity			maximum acceleration		
			Ux	Uz	Ut	Vx	Vz	Vt	Ax	Az	At
268	10	G	0.5288	0.6543	0.5552	0.5261	0.8540	0.6605	0.5355	0.8528	0.6609
	10	L	0.4905	0.6306	0.5264	0.4508	0.7972	0.5737	0.4416	0.7668	0.5651
	300	G	0.4247	0.8659	0.5562	0.4262	1.1165	0.8017	0.3843	1.0203	0.7532
	300	L	0.3625	0.8128	0.4952	0.3529	1.0247	0.6868	0.3062	0.8962	0.6009
282	10	G	0.5400	0.6791	0.5817	0.5582	0.8584	0.6711	0.5817	0.8855	0.7142
	10	L	0.5020	0.6634	0.5513	0.4788	0.7966	0.5863	0.4823	0.7970	0.6076
	300	G	0.4422	0.8821	0.5656	0.4682	1.1471	0.8359	0.4510	0.9980	0.7529
	300	L	0.3885	0.8061	0.5107	0.3962	1.0149	0.6880	0.3692	0.9035	0.6268
283	10	G	0.5402	0.6812	0.5832	0.5627	0.8582	0.6746	0.5871	0.8881	0.7211
	10	L	0.5023	0.6655	0.5527	0.4827	0.7950	0.5893	0.4885	0.7993	0.6125
	300	G	0.4434	0.8813	0.5676	0.4694	1.1464	0.8362	0.4627	0.9980	0.7600
	300	L	0.3897	0.8036	0.5107	0.3995	1.0106	0.6857	0.3769	0.9053	0.6278
305	10	G	0.5722	0.7236	0.6224	0.6219	0.8251	0.7313	0.7000	0.9220	0.7963
	10	L	0.5317	0.7081	0.5890	0.5296	0.7666	0.6412	0.5796	0.8422	0.6802
	300	G	0.5078	0.8706	0.5974	0.5534	1.1593	0.8646	0.5980	0.9838	0.8103
	300	L	0.4408	0.7952	0.5374	0.4491	1.0235	0.7101	0.4708	0.8944	0.6731
327	10	G	0.5932	0.7719	0.6544	0.6848	0.8527	0.7846	0.7323	1.0113	0.8506
	10	L	0.5499	0.7583	0.6194	0.5842	0.8009	0.6909	0.5991	0.9420	0.7345
	300	G	0.5194	0.8516	0.5961	0.5823	1.1737	0.8786	0.6039	1.0243	0.8219
	300	L	0.4472	0.7824	0.5364	0.4554	1.0464	0.7261	0.4631	0.9381	0.6805
328	10	G	0.5943	0.7746	0.6547	0.6839	0.8540	0.7875	0.7366	1.0176	0.8571
	10	L	0.5509	0.7609	0.6198	0.5831	0.8020	0.6936	0.6027	0.9455	0.7389
	300	G	0.5168	0.8522	0.5964	0.5831	1.1758	0.8797	0.5961	1.0304	0.8235
	300	L	0.4447	0.7813	0.5351	0.4550	1.0452	0.7245	0.4554	0.9417	0.6822
396	10	G	0.5815	0.8422	0.6939	0.5964	0.8752	0.8083	0.6495	1.1057	0.9210
	10	L	0.5405	0.8269	0.6581	0.5093	0.8137	0.7085	0.5389	1.0209	0.7955
	300	G	0.4600	0.7542	0.6038	0.5084	0.8996	0.6559	0.4804	0.8357	0.6727
	300	L	0.4025	0.7104	0.5426	0.4065	0.8016	0.5356	0.3908	0.7177	0.5502
464	10	G	0.5923	0.8567	0.7062	0.6354	0.9197	0.8427	0.6903	1.0943	0.9337
	10	L	0.5496	0.8419	0.6697	0.5397	0.8607	0.7416	0.5664	1.0325	0.8149
	300	G	0.4451	0.6802	0.5595	0.4287	0.6566	0.5515	0.4216	0.6126	0.5487
	300	L	0.3842	0.6420	0.5009	0.3344	0.5964	0.4646	0.3277	0.5519	0.4468

Incident angle : 10

Depth	Qs= Qp	1st Layer	maximum displacement			maximum velocity			maximum acceleration		
			Ux	Uz	Ut	Vx	Vz	Vt	Ax	Az	At
464	10	G	0.5923	0.8567	0.7062	0.6354	0.9197	0.8427	0.6903	1.0943	0.9337
	10	L	0.5496	0.8419	0.6697	0.5397	0.8607	0.7416	0.5664	1.0325	0.8149
	300	G	0.4451	0.6802	0.5595	0.4287	0.6566	0.5515	0.4216	0.6126	0.5487
	300	L	0.3842	0.6420	0.5009	0.3344	0.5964	0.4646	0.3277	0.5519	0.4468
466	10	G	0.5897	0.8575	0.7053	0.6330	0.9176	0.8370	0.6806	1.0943	0.9291
	10	L	0.5472	0.8427	0.6688	0.5373	0.8587	0.7367	0.5584	1.0325	0.8110
	300	G	0.4406	0.6811	0.5577	0.4168	0.6625	0.5538	0.4098	0.6126	0.5436
	300	L	0.3807	0.6431	0.4996	0.3253	0.6029	0.4676	0.3200	0.5537	0.4444
673	10	G	0.5416	0.5833	0.5518	0.6223	0.5965	0.6551	0.6892	0.6566	0.7139
	10	L	0.5028	0.5715	0.5228	0.5303	0.5554	0.5761	0.5681	0.6021	0.6137
	300	G	0.3821	0.5472	0.3863	0.3700	0.4130	0.3734	0.3902	0.4101	0.3699
	300	L	0.3327	0.5223	0.3442	0.2958	0.3604	0.3121	0.3092	0.3546	0.2986
879	10	G	0.5781	0.5931	0.5610	0.7061	0.4917	0.6597	0.8065	0.6491	0.7861
	10	L	0.5366	0.5759	0.5316	0.6010	0.4591	0.5795	0.6637	0.5963	0.6759
	300	G	0.3949	0.6873	0.4731	0.4138	0.5957	0.4931	0.4176	0.6633	0.5346
	300	L	0.3399	0.6451	0.4297	0.3329	0.5679	0.4133	0.3215	0.5993	0.4460
880	10	G	0.5784	0.5926	0.5612	0.7053	0.4908	0.6588	0.8065	0.6478	0.7857
	10	L	0.5369	0.5753	0.5318	0.6006	0.4587	0.5791	0.6637	0.5963	0.6759
	300	G	0.3954	0.6867	0.4747	0.4141	0.5972	0.4929	0.4196	0.6633	0.5386
	300	L	0.3395	0.6459	0.4304	0.3320	0.5676	0.4149	0.3231	0.6029	0.4484
1090	10	G	0.8799	0.7928	0.8449	1.1850	0.8365	1.0908	1.3656	1.0340	1.2919
	10	L	0.8168	0.7789	0.8011	1.0095	0.7818	0.9589	1.1150	0.9571	1.1133
	300	G	0.5417	0.6846	0.5207	0.5372	0.6021	0.5013	0.5706	0.6227	0.5108
	300	L	0.4708	0.6484	0.4688	0.4276	0.5694	0.4233	0.4538	0.5592	0.4182
1300	10	G	1.0026	0.9412	0.9793	1.4328	1.1326	1.3958	1.6882	1.5975	1.7438
	10	L	0.9306	0.9233	0.9280	1.2202	1.0560	1.2265	1.3894	1.4617	1.4964
	300	G	0.5429	0.7865	0.5412	0.5386	0.6497	0.5329	0.5745	0.7282	0.5578
	300	L	0.4712	0.7461	0.4832	0.4295	0.6163	0.4451	0.4538	0.6612	0.4513
1400	10	G	1.0600	0.9791	1.0295	1.5594	1.1984	1.4979	1.8495	1.6352	1.8618
	10	L	0.9840	0.9621	0.9762	1.3280	1.1197	1.3165	1.5221	1.5313	1.6116
	300	G	0.5372	0.7797	0.5318	0.5363	0.6912	0.5121	0.5569	0.7404	0.5413
	300	L	0.4667	0.7305	0.4780	0.4282	0.6494	0.4319	0.4415	0.6648	0.4417
1600	10	G	1.2069	1.1216	1.1626	1.9166	1.3244	1.7450	2.2903	1.6604	2.1549
	10	L	1.1203	1.1012	1.1021	1.6321	1.2363	1.5335	1.8850	1.5313	1.8549
	300	G	0.5374	0.6864	0.5349	0.5322	0.5396	0.4966	0.5529	0.5781	0.5169
	300	L	0.4654	0.6493	0.4780	0.4228	0.5158	0.4160	0.4354	0.5228	0.4188

Incident angle : 20

Depth	Qs= Qp	1st Layer	maximum displacement			maximum velocity			maximum acceleration		
			Ux	Uz	Ut	Vx	Vz	Vt	Ax	Az	At
0	10	G	1.0000	1.0000	1.0000	1.0000	1.0000	1.0000	1.0000	1.0000	1.0000
	10	L	1.0000	1.0000	1.0000	1.0000	1.0000	1.0000	1.0000	1.0000	1.0000
	300	G	1.0000	1.0000	1.0000	1.0000	1.0000	1.0000	1.0000	1.0000	1.0000
	300	L	1.0000	1.0000	1.0000	1.0000	1.0000	1.0000	1.0000	1.0000	1.0000
8	10	G	0.9915	0.9934	0.9906	0.9815	0.9882	0.9819	0.9879	0.9856	0.9734
	10	L	0.9755	0.9895	0.9806	0.9486	0.9756	0.9610	0.9200	0.9712	0.9418
	300	G	0.9791	0.9860	0.9817	0.9637	0.9800	0.9703	0.9602	0.9690	0.9681
	300	L	0.9510	0.9770	0.9603	0.9207	0.9636	0.9369	0.9130	0.9512	0.9342
16	10	G	0.9797	0.9851	0.9817	0.9613	0.9728	0.9590	0.9398	0.9675	0.9543
	10	L	0.9070	0.9612	0.9271	0.8095	0.9070	0.8431	0.7500	0.8858	0.7958
	300	G	0.9523	0.9684	0.9585	0.9180	0.9545	0.9334	0.9119	0.9307	0.9280
	300	L	0.8110	0.9106	0.8475	0.7059	0.8599	0.7692	0.6732	0.8252	0.7563
17	10	G	0.9784	0.9834	0.9805	0.9577	0.9706	0.9562	0.9518	0.9651	0.9414
	10	L	0.8984	0.9572	0.9202	0.7955	0.8982	0.8304	0.7400	0.8747	0.7795
	300	G	0.9487	0.9659	0.9554	0.9126	0.9507	0.9285	0.9057	0.9234	0.9240
	300	L	0.7935	0.9018	0.8333	0.6793	0.8463	0.7484	0.6437	0.8110	0.7339
26	10	G	0.9640	0.9776	0.9704	0.9374	0.9510	0.9311	0.9157	0.9374	0.8957
	10	L	0.8807	0.9491	0.9062	0.7694	0.8796	0.8037	0.7000	0.8503	0.7513
	300	G	0.9167	0.9441	0.9273	0.8709	0.9180	0.8854	0.8470	0.8850	0.8748
	300	L	0.7602	0.8831	0.8057	0.6274	0.8159	0.7089	0.5878	0.7717	0.6928
35	10	G	0.9443	0.9710	0.9558	0.9077	0.9247	0.8946	0.8675	0.9049	0.8562
	10	L	0.8611	0.9434	0.8920	0.7421	0.8543	0.7687	0.6500	0.8182	0.6958
	300	G	0.8767	0.9158	0.8902	0.8231	0.8745	0.8298	0.7820	0.8358	0.8146
	300	L	0.7186	0.8573	0.7703	0.5752	0.7754	0.6595	0.5205	0.7228	0.6365
37	10	G	0.9358	0.9677	0.9493	0.8924	0.9137	0.8765	0.8434	0.8905	0.8365
	10	L	0.8525	0.9402	0.8855	0.7300	0.8440	0.7555	0.6300	0.8049	0.6848
	300	G	0.8599	0.9048	0.8750	0.8002	0.8570	0.8082	0.7526	0.8193	0.7903
	300	L	0.7016	0.8468	0.7560	0.5579	0.7590	0.6402	0.4959	0.7024	0.6160
60	10	G	0.7746	0.9022	0.8270	0.6137	0.7273	0.6456	0.4458	0.6354	0.4862
	10	L	0.7013	0.8739	0.7687	0.5111	0.6677	0.5659	0.3400	0.5698	0.4037
	300	G	0.5492	0.7221	0.6156	0.3946	0.5633	0.5009	0.2631	0.4872	0.4003
	300	L	0.4300	0.6661	0.5188	0.3150	0.4842	0.4050	0.2308	0.4000	0.3350

Incident angle : 20

Depth	Qs= Qp	1st Layer	maximum displacement			maximum velocity			maximum acceleration		
			Ux	Uz	Ut	Vx	Vz	Vt	Ax	Az	At
82	10	G	0.6083	0.8333	0.7042	0.5209	0.5110	0.4988	0.3627	0.3610	0.2953
	10	L	0.5660	0.8084	0.6646	0.4593	0.4646	0.4514	0.3250	0.3226	0.2745
	300	G	0.4245	0.5397	0.4248	0.4444	0.3559	0.3732	0.4235	0.2889	0.2954
	300	L	0.3865	0.5092	0.3984	0.3725	0.3517	0.3269	0.3629	0.2906	0.2717
83	10	G	0.6047	0.8325	0.7020	0.5241	0.5024	0.5046	0.3699	0.3526	0.3027
	10	L	0.5642	0.8072	0.6626	0.4620	0.4576	0.4566	0.3330	0.3204	0.2830
	300	G	0.4308	0.5348	0.4314	0.4543	0.3602	0.3802	0.4361	0.2932	0.3050
	300	L	0.3915	0.5087	0.4041	0.3757	0.3551	0.3320	0.3711	0.2978	0.2797
130	10	G	0.6052	0.8006	0.6828	0.6006	0.5039	0.5836	0.5747	0.3610	0.5106
	10	L	0.5682	0.7836	0.6503	0.5208	0.4842	0.5182	0.4800	0.3659	0.4488
	300	G	0.5324	0.6096	0.5515	0.5734	0.5193	0.5542	0.6226	0.4982	0.5487
	300	L	0.4616	0.5872	0.5022	0.4450	0.5033	0.4630	0.4680	0.4945	0.4675
177	10	G	0.6279	0.6786	0.6278	0.6529	0.5890	0.5277	0.6964	0.5174	0.5408
	10	L	0.5859	0.6582	0.5948	0.5645	0.5492	0.4697	0.5740	0.4823	0.4557
	300	G	0.5557	0.7124	0.5125	0.5814	0.6037	0.5268	0.5975	0.6150	0.5075
	300	L	0.4840	0.6630	0.4538	0.4677	0.5463	0.4466	0.4795	0.5339	0.4142
178	10	G	0.6280	0.6790	0.6254	0.6515	0.5894	0.5251	0.6964	0.5162	0.5401
	10	L	0.5860	0.6564	0.5925	0.5633	0.5502	0.4703	0.5740	0.4823	0.4551
	300	G	0.5555	0.7133	0.5088	0.5822	0.6050	0.5279	0.5975	0.6113	0.5026
	300	L	0.4838	0.6624	0.4503	0.4681	0.5456	0.4465	0.4762	0.5354	0.4148
215	10	G	0.6056	0.6789	0.5581	0.6029	0.6215	0.5520	0.6253	0.5331	0.4849
	10	L	0.5643	0.6551	0.5275	0.5208	0.5761	0.4901	0.5150	0.4812	0.4122
	300	G	0.5008	0.7352	0.4735	0.5052	0.6359	0.5621	0.4948	0.5894	0.4736
	300	L	0.4350	0.6735	0.4130	0.3977	0.5584	0.4671	0.3892	0.5024	0.3875
252	10	G	0.5612	0.6653	0.5185	0.5543	0.6560	0.5827	0.5446	0.5596	0.4492
	10	L	0.5231	0.6393	0.4925	0.4799	0.6093	0.5179	0.4500	0.5166	0.3791
	300	G	0.4226	0.7656	0.4868	0.4216	0.7224	0.6345	0.3878	0.6332	0.5084
	300	L	0.3643	0.6984	0.4287	0.3340	0.6465	0.5270	0.2956	0.5591	0.4295
253	10	G	0.5605	0.6643	0.5192	0.5520	0.6572	0.5838	0.5422	0.5656	0.4498
	10	L	0.5225	0.6389	0.4931	0.4780	0.6090	0.5176	0.4510	0.5222	0.3792
	300	G	0.4214	0.7668	0.4871	0.4219	0.7255	0.6374	0.3857	0.6332	0.5077
	300	L	0.3635	0.6982	0.4301	0.3345	0.6509	0.5307	0.2939	0.5622	0.4320

Incident angle : 20

Depth	Qs= Qp	1st Layer	maximum displacement			maximum velocity			maximum acceleration		
			Ux	Uz	Ut	Vx	Vz	Vt	Ax	Az	At
268	10	G	0.5495	0.6568	0.5348	0.5601	0.6603	0.5880	0.5651	0.6378	0.5019
	10	L	0.5128	0.6289	0.5081	0.4854	0.6261	0.5306	0.4710	0.5854	0.4261
	300	G	0.4240	0.7732	0.4974	0.4552	0.7613	0.6650	0.4340	0.6953	0.5575
	300	L	0.3706	0.7265	0.4440	0.3702	0.6949	0.5673	0.3481	0.5858	0.4509
282	10	G	0.5493	0.6561	0.5602	0.5795	0.6768	0.6219	0.6205	0.7148	0.5915
	10	L	0.5129	0.6391	0.5314	0.5021	0.6290	0.5500	0.5180	0.6475	0.5012
	300	G	0.4534	0.8042	0.5105	0.5029	0.8042	0.7044	0.5367	0.7190	0.5768
	300	L	0.3999	0.7356	0.4463	0.4093	0.7045	0.5757	0.4368	0.6189	0.4776
283	10	G	0.5505	0.6589	0.5625	0.5817	0.6771	0.6252	0.6265	0.7196	0.6020
	10	L	0.5141	0.6417	0.5336	0.5037	0.6286	0.5528	0.5240	0.6552	0.5082
	300	G	0.4563	0.8057	0.5110	0.5091	0.8061	0.7063	0.5409	0.7208	0.5783
	300	L	0.4026	0.7350	0.4457	0.4140	0.7040	0.5754	0.4433	0.6236	0.4812
305	10	G	0.5677	0.7252	0.6073	0.6123	0.7018	0.6973	0.7253	0.8087	0.7276
	10	L	0.5300	0.7045	0.5748	0.5294	0.6498	0.6158	0.6020	0.7339	0.6143
	300	G	0.5083	0.8130	0.5431	0.5850	0.8300	0.7339	0.6583	0.7609	0.6094
	300	L	0.4451	0.7506	0.4783	0.4784	0.7341	0.6049	0.5222	0.6252	0.4874
327	10	G	0.5773	0.7823	0.6437	0.6763	0.7547	0.7618	0.7494	0.8845	0.7953
	10	L	0.5387	0.7605	0.6086	0.5851	0.7027	0.6758	0.6210	0.8071	0.6713
	300	G	0.5093	0.8133	0.5477	0.6194	0.8278	0.7368	0.6122	0.7555	0.6076
	300	L	0.4394	0.7376	0.4815	0.4901	0.7301	0.6074	0.4696	0.6362	0.4895
328	10	G	0.5772	0.7852	0.6449	0.6785	0.7598	0.7653	0.7494	0.8869	0.7961
	10	L	0.5386	0.7633	0.6098	0.5871	0.7078	0.6785	0.6200	0.8093	0.6736
	300	G	0.5085	0.8118	0.5486	0.6169	0.8258	0.7351	0.6101	0.7555	0.6077
	300	L	0.4386	0.7382	0.4822	0.4875	0.7306	0.6075	0.4663	0.6331	0.4871
396	10	G	0.5428	0.8673	0.6851	0.5777	0.8703	0.8669	0.6229	1.0072	0.8949
	10	L	0.5062	0.8464	0.6494	0.4994	0.8132	0.7719	0.5170	0.9313	0.7574
	300	G	0.4183	0.7309	0.5579	0.4274	0.6927	0.6441	0.4382	0.6843	0.5497
	300	L	0.3679	0.6871	0.5030	0.3453	0.5890	0.5433	0.3498	0.5512	0.4520
464	10	G	0.5440	0.8582	0.6790	0.5880	0.8496	0.8499	0.5952	1.0265	0.9033
	10	L	0.5087	0.8359	0.6434	0.5099	0.7884	0.7542	0.4980	0.9501	0.7740
	300	G	0.4002	0.7349	0.5537	0.4076	0.6238	0.6026	0.3941	0.6314	0.5752
	300	L	0.3453	0.6837	0.4918	0.3172	0.5491	0.4950	0.2989	0.5402	0.4697

0

Incident angle : 20

Depth	Qs= Qp	1st Layer	maximum displacement			maximum velocity			maximum acceleration		
			Ux	Uz	Ut	Vx	Vz	Vt	Ax	Az	At
464	10	G	0.5440	0.8582	0.6790	0.5880	0.8496	0.8499	0.5952	1.0265	0.9033
	10	L	0.5087	0.8359	0.6434	0.5099	0.7884	0.7542	0.4980	0.9501	0.7740
	300	G	0.4002	0.7349	0.5537	0.4076	0.6238	0.6026	0.3941	0.6314	0.5752
	300	L	0.3453	0.6837	0.4918	0.3172	0.5491	0.4950	0.2989	0.5402	0.4697
466	10	G	0.5462	0.8524	0.6805	0.5835	0.8496	0.8502	0.6036	1.0361	0.9129
	10	L	0.5107	0.8302	0.6446	0.5060	0.7884	0.7543	0.5030	0.9368	0.7679
	300	G	0.4000	0.7248	0.5456	0.4015	0.6102	0.5890	0.3795	0.6131	0.5575
	300	L	0.3469	0.6738	0.4845	0.3127	0.5370	0.4841	0.2890	0.5228	0.4546
673	10	G	0.5919	0.6643	0.6113	0.6700	0.6262	0.7433	0.7386	0.7750	0.7990
	10	L	0.5529	0.6473	0.5793	0.5801	0.5809	0.6596	0.6140	0.7118	0.6786
	300	G	0.4214	0.5333	0.4513	0.4186	0.4489	0.4903	0.4319	0.4836	0.4654
	300	L	0.3674	0.5095	0.4015	0.3346	0.3874	0.4008	0.3415	0.4094	0.3819
879	10	G	0.6529	0.5859	0.6281	0.8487	0.4988	0.7911	0.9590	0.6414	0.8779
	10	L	0.6100	0.5710	0.5953	0.7343	0.4635	0.7026	0.7950	0.5898	0.7470
	300	G	0.4411	0.4400	0.4184	0.4738	0.4081	0.4348	0.4864	0.3777	0.4052
	300	L	0.3859	0.4119	0.3744	0.3793	0.3468	0.3608	0.3842	0.3055	0.3330
880	10	G	0.6537	0.5871	0.6297	0.8523	0.5004	0.7942	0.9639	0.6462	0.8830
	10	L	0.6106	0.5721	0.5969	0.7370	0.4646	0.7049	0.8010	0.5931	0.7522
	300	G	0.4428	0.4396	0.4198	0.4736	0.4085	0.4340	0.4885	0.3759	0.4064
	300	L	0.3865	0.4122	0.3742	0.3784	0.3473	0.3597	0.3892	0.3071	0.3380
1090	10	G	0.9201	0.8458	0.8933	1.2783	0.8139	1.2215	1.5060	1.0614	1.4019
	10	L	0.8592	0.8238	0.8465	1.1067	0.7570	1.0852	1.2500	0.9612	1.1879
	300	G	0.5519	0.5564	0.5350	0.5526	0.4222	0.5207	0.5765	0.4891	0.4959
	300	L	0.4809	0.5166	0.4760	0.4394	0.3783	0.4308	0.4532	0.4126	0.4047
1300	10	G	1.0433	0.9751	1.0188	1.5642	1.0553	1.5244	1.9036	1.4440	1.8182
	10	L	0.9743	0.9507	0.9658	1.3537	0.9827	1.3549	1.5800	1.3304	1.5493
	300	G	0.5536	0.5166	0.5396	0.5680	0.3818	0.5360	0.5891	0.3923	0.5169
	300	L	0.4811	0.4837	0.4820	0.4473	0.3435	0.4495	0.4598	0.3417	0.4285
1400	10	G	1.1134	1.0448	1.0888	1.7357	1.1721	1.6891	2.0964	1.6486	2.0294
	10	L	1.0398	1.0186	1.0321	1.5014	1.0910	1.5010	1.7400	1.5188	1.7293
	300	G	0.5625	0.5354	0.5522	0.5776	0.3977	0.5618	0.6017	0.4288	0.5419
	300	L	0.4863	0.4987	0.4907	0.4527	0.3559	0.4645	0.4631	0.3669	0.4425
1600	10	G	1.2765	1.1633	1.2357	2.2049	1.2712	2.0087	2.6988	1.6366	2.4014
	10	L	1.1922	1.1342	1.1714	1.9073	1.1825	1.7872	2.2400	1.5078	2.0463
	300	G	0.5697	0.5740	0.5462	0.6005	0.3831	0.5491	0.6373	0.4343	0.5154
	300	L	0.4936	0.5299	0.4859	0.4747	0.3556	0.4531	0.4943	0.3622	0.4230

Incident angle : 30

Depth	Qs= Qp	1st Layer	maximum displacement			maximum velocity			maximum acceleration		
			Ux	Uz	Ut	Vx	Vz	Vt	Ax	Az	At
0	10	G	1.0000	1.0000	1.0000	1.0000	1.0000	1.0000	1.0000	1.0000	1.0000
	10	L	1.0000	1.0000	1.0000	1.0000	1.0000	1.0000	1.0000	1.0000	1.0000
	300	G	1.0000	1.0000	1.0000	1.0000	1.0000	1.0000	1.0000	1.0000	1.0000
	300	L	1.0000	1.0000	1.0000	1.0000	1.0000	1.0000	1.0000	1.0000	1.0000
8	10	G	0.9891	1.0010	0.9912	1.0038	0.9954	0.9865	0.9839	0.9826	0.9824
	10	L	0.9794	0.9980	0.9836	0.9835	0.9854	0.9708	0.9444	0.9725	0.9654
	300	G	0.9819	0.9866	0.9843	1.0226	0.9909	0.9861	1.0078	0.9803	0.9786
	300	L	0.9590	0.9729	0.9657	0.9495	0.9645	0.9548	0.9229	0.9577	0.9489
16	10	G	0.9768	1.0000	0.9813	1.0087	0.9872	0.9684	0.9516	0.9588	0.9543
	10	L	0.9236	0.9785	0.9372	0.8998	0.9318	0.8692	0.7917	0.8699	0.8358
	300	G	0.9606	0.9681	0.9645	1.0377	0.9753	0.9712	1.0235	0.9508	0.9482
	300	L	0.8434	0.8949	0.8685	0.7823	0.8647	0.8359	0.7214	0.8438	0.8103
17	10	G	0.9753	1.0000	0.9808	1.0093	0.9861	0.9660	0.9516	0.9540	0.9511
	10	L	0.9160	0.9763	0.9310	0.8913	0.9250	0.8585	0.7778	0.8584	0.8201
	300	G	0.9578	0.9654	0.9616	1.0398	0.9726	0.9687	1.0196	0.9459	0.9429
	300	L	0.8287	0.8846	0.8560	0.7658	0.8519	0.8207	0.6940	0.8263	0.7917
26	10	G	0.9608	0.9970	0.9737	1.0136	0.9743	0.9446	0.9355	0.9208	0.9111
	10	L	0.9002	0.9745	0.9179	0.8928	0.9119	0.8358	0.7500	0.8251	0.7854
	300	G	0.9499	0.9406	0.9374	1.0512	0.9494	0.9469	1.0314	0.9066	0.9041
	300	L	0.8000	0.8628	0.8307	0.7609	0.8258	0.7888	0.6791	0.7927	0.7553
35	10	G	0.9448	0.9910	0.9635	1.0082	0.9543	0.9153	0.9194	0.8764	0.8789
	10	L	0.8816	0.9692	0.9061	0.8873	0.8924	0.8073	0.7222	0.7832	0.7433
	300	G	0.9346	0.9068	0.9131	1.0502	0.9119	0.9122	1.0392	0.8557	0.8539
	300	L	0.7686	0.8329	0.7989	0.7433	0.7900	0.7490	0.6517	0.7474	0.7077
37	10	G	0.9390	0.9876	0.9586	1.0022	0.9450	0.9034	0.9032	0.8590	0.8637
	10	L	0.8747	0.9659	0.9014	0.8813	0.8832	0.7961	0.7083	0.7659	0.7283
	300	G	0.9262	0.8934	0.9035	1.0449	0.8957	0.8962	1.0353	0.8344	0.8328
	300	L	0.7580	0.8207	0.7863	0.7307	0.7752	0.7334	0.6343	0.7314	0.6910
60	10	G	0.8308	0.9301	0.8638	0.8129	0.7915	0.6826	0.6290	0.5689	0.5900
	10	L	0.7598	0.9068	0.8075	0.7087	0.7386	0.6068	0.5000	0.4971	0.4753
	300	G	0.7243	0.6835	0.7033	0.7236	0.5964	0.5963	0.6549	0.4967	0.4981
	300	L	0.5407	0.6132	0.5755	0.4634	0.5238	0.4775	0.3948	0.4368	0.3869

Incident angle : 30

Depth	Qs= Qp	1st Layer	maximum displacement			maximum velocity			maximum acceleration		
			Ux	Uz	Ut	Vx	Vz	Vt	Ax	Az	At
82	10	G	0.6756	0.9065	0.7466	0.5483	0.6107	0.5167	0.3677	0.4041	0.3086
	10	L	0.6124	0.8884	0.6984	0.4773	0.5764	0.4688	0.2972	0.3858	0.2707
	300	G	0.4775	0.4518	0.4337	0.3693	0.2741	0.3005	0.4882	0.1459	0.2168
	300	L	0.3968	0.4195	0.3479	0.3739	0.2385	0.2346	0.4353	0.1639	0.2239
83	10	G	0.6686	0.9081	0.7428	0.5374	0.6030	0.5100	0.3645	0.4057	0.3018
	10	L	0.6059	0.8909	0.6950	0.4693	0.5721	0.4652	0.2931	0.3858	0.2707
	300	G	0.4737	0.4449	0.4226	0.3784	0.2672	0.2976	0.5063	0.1467	0.2186
	300	L	0.3968	0.4214	0.3541	0.3743	0.2316	0.2365	0.4430	0.1549	0.2276
130	10	G	0.5446	0.9371	0.7064	0.4861	0.4874	0.4895	0.4210	0.3978	0.4047
	10	L	0.5146	0.9180	0.6756	0.4454	0.4815	0.4467	0.3806	0.3728	0.3776
	300	G	0.4997	0.5521	0.5140	0.6921	0.2834	0.4202	1.0157	0.2151	0.4188
	300	L	0.4394	0.5401	0.4897	0.5221	0.2473	0.3808	0.6493	0.2380	0.3832
177	10	G	0.6407	0.8451	0.7122	0.7130	0.5850	0.6159	0.8564	0.4422	0.6430
	10	L	0.6135	0.8252	0.6838	0.6633	0.5701	0.5701	0.7542	0.4379	0.5822
	300	G	0.7469	0.5306	0.6180	1.0992	0.5245	0.6370	1.4667	0.4115	0.5892
	300	L	0.6311	0.5047	0.5569	0.7949	0.4664	0.5317	0.8905	0.3693	0.4909
178	10	G	0.6434	0.8412	0.7116	0.7169	0.5860	0.6176	0.8645	0.4453	0.6483
	10	L	0.6160	0.8220	0.6832	0.6668	0.5721	0.5717	0.7597	0.4422	0.5856
	300	G	0.7503	0.5276	0.6177	1.1020	0.5287	0.6389	1.4706	0.4148	0.5902
	300	L	0.6343	0.5011	0.5561	0.7971	0.4713	0.5327	0.8955	0.3737	0.4900
215	10	G	0.6890	0.7203	0.6983	0.7949	0.6168	0.6448	0.9645	0.4849	0.6890
	10	L	0.6556	0.7082	0.6718	0.7297	0.5998	0.5952	0.8292	0.4552	0.6137
	300	G	0.7559	0.5832	0.5920	1.0279	0.6134	0.5989	1.2980	0.4787	0.5338
	300	L	0.6463	0.5692	0.5223	0.7433	0.5809	0.5084	0.8184	0.4715	0.4189
252	10	G	0.6813	0.6538	0.6653	0.7730	0.6297	0.6139	0.8661	0.4881	0.6123
	10	L	0.6453	0.6533	0.6400	0.7062	0.6008	0.5652	0.7361	0.4399	0.5408
	300	G	0.6627	0.6590	0.5387	0.7494	0.6594	0.6115	0.8745	0.5410	0.5291
	300	L	0.5646	0.6325	0.4797	0.5523	0.6444	0.5630	0.5572	0.5504	0.4848
253	10	G	0.6810	0.6539	0.6640	0.7709	0.6297	0.6115	0.8645	0.4897	0.6108
	10	L	0.6447	0.6533	0.6386	0.7042	0.6013	0.5629	0.7333	0.4413	0.5383
	300	G	0.6568	0.6611	0.5386	0.7486	0.6605	0.6124	0.8588	0.5410	0.5281
	300	L	0.5593	0.6342	0.4798	0.5510	0.6459	0.5642	0.5498	0.5518	0.4863

0

Incident angle : 30

Depth	Qs= Qp	1st Layer	maximum displacement			maximum velocity			maximum acceleration		
			Ux	Uz	Ut	Vx	Vz	Vt	Ax	Az	At
268	10	G	0.6661	0.6639	0.6405	0.7463	0.6251	0.5960	0.7774	0.4913	0.5524
	10	L	0.6302	0.6597	0.6164	0.6858	0.6022	0.5518	0.6639	0.4393	0.4928
	300	G	0.5986	0.6886	0.5374	0.7083	0.6737	0.6204	0.8275	0.5705	0.5386
	300	L	0.5021	0.6558	0.4896	0.5134	0.6579	0.5732	0.5080	0.5796	0.5109
282	10	G	0.6430	0.6878	0.6225	0.7223	0.6225	0.5846	0.7403	0.4976	0.5272
	10	L	0.6087	0.6788	0.5990	0.6658	0.5964	0.5433	0.6333	0.4538	0.4789
	300	G	0.5557	0.7086	0.5347	0.7158	0.6796	0.6217	0.8655	0.5918	0.5483
	300	L	0.4617	0.6738	0.4944	0.5180	0.6574	0.5711	0.5510	0.5956	0.5241
283	10	G	0.6414	0.6896	0.6220	0.7196	0.6220	0.5853	0.7323	0.4976	0.5305
	10	L	0.6072	0.6805	0.5985	0.6648	0.5959	0.5438	0.6292	0.4552	0.4802
	300	G	0.5523	0.7098	0.5342	0.7136	0.6796	0.6213	0.8694	0.5934	0.5494
	300	L	0.4585	0.6749	0.4945	0.5164	0.6571	0.5707	0.5550	0.5971	0.5252
305	10	G	0.6075	0.7405	0.6125	0.7141	0.6076	0.5880	0.7581	0.6038	0.5801
	10	L	0.5758	0.7279	0.5878	0.6584	0.5648	0.5431	0.6611	0.5332	0.5222
	300	G	0.5147	0.7163	0.5217	0.7080	0.6584	0.6003	0.9176	0.6049	0.5624
	300	L	0.4428	0.6785	0.4846	0.5376	0.6144	0.5345	0.6045	0.5912	0.5152
327	10	G	0.5778	0.8067	0.6248	0.6858	0.6297	0.5991	0.7855	0.7559	0.6675
	10	L	0.5467	0.7933	0.5968	0.6264	0.5871	0.5454	0.6764	0.6777	0.5858
	300	G	0.4912	0.6820	0.5167	0.6542	0.5913	0.5486	0.9341	0.5623	0.5389
	300	L	0.4269	0.6461	0.4550	0.5089	0.5330	0.4628	0.6169	0.5358	0.4624
328	10	G	0.5755	0.8094	0.6259	0.6852	0.6369	0.6005	0.7871	0.7639	0.6699
	10	L	0.5445	0.7961	0.5978	0.6259	0.5949	0.5466	0.6764	0.6835	0.5894
	300	G	0.4909	0.6790	0.5182	0.6475	0.5868	0.5452	0.9361	0.5590	0.5355
	300	L	0.4261	0.6436	0.4560	0.5030	0.5281	0.4585	0.6144	0.5328	0.4598
396	10	G	0.4860	0.9517	0.6761	0.4932	0.8562	0.7724	0.6129	1.0000	0.8080
	10	L	0.4585	0.9378	0.6477	0.4544	0.8121	0.7094	0.5306	0.9162	0.7250
	300	G	0.3942	0.6736	0.5414	0.4683	0.4813	0.4880	0.5851	0.3951	0.4032
	300	L	0.3412	0.6325	0.4889	0.3712	0.4390	0.4175	0.4614	0.3664	0.3564
464	10	G	0.4647	1.0109	0.7044	0.4845	0.9784	0.8807	0.6129	1.1601	0.9204
	10	L	0.4397	0.9941	0.6744	0.4489	0.9241	0.8055	0.5319	1.0607	0.8223
	300	G	0.3820	0.7575	0.6026	0.4338	0.5990	0.5897	0.5843	0.5459	0.5518
	300	L	0.3468	0.6962	0.5403	0.3871	0.5090	0.4923	0.4808	0.4745	0.4624

0

Incident angle : 30

Depth	Qs= Qp	1st Layer	maximum displacement			maximum velocity			maximum acceleration		
			Ux	Uz	Ut	Vx	Vz	Vt	Ax	Az	At
464	10	G	0.4647	1.0109	0.7044	0.4845	0.9784	0.8807	0.6129	1.1601	0.9204
	10	L	0.4397	0.9941	0.6744	0.4489	0.9241	0.8055	0.5319	1.0607	0.8223
	300	G	0.3820	0.7575	0.6026	0.4338	0.5990	0.5897	0.5843	0.5459	0.5518
	300	L	0.3468	0.6962	0.5403	0.3871	0.5090	0.4923	0.4808	0.4745	0.4624
466	10	G	0.4626	1.0149	0.7067	0.4845	0.9795	0.8838	0.6048	1.1696	0.9320
	10	L	0.4378	0.9980	0.6759	0.4484	0.9255	0.8085	0.5292	1.0838	0.8412
	300	G	0.3870	0.7534	0.6070	0.4490	0.5938	0.5851	0.6000	0.5541	0.5612
	300	L	0.3500	0.6918	0.5375	0.3806	0.5047	0.4879	0.4692	0.4701	0.4630
673	10	G	0.5375	0.8484	0.6611	0.6285	0.8942	0.8128	0.6097	1.1030	0.8975
	10	L	0.5080	0.8340	0.6320	0.5726	0.8476	0.7452	0.5222	1.0072	0.7991
	300	G	0.3977	0.5724	0.4969	0.6597	0.5079	0.4842	0.7922	0.4557	0.4576
	300	L	0.3253	0.5268	0.4339	0.4940	0.4526	0.4070	0.5246	0.4146	0.3736
879	10	G	0.7938	0.7459	0.7765	1.1364	0.6980	1.0655	1.3871	0.9192	1.1726
	10	L	0.7522	0.7341	0.7437	1.0394	0.6636	0.9787	1.2083	0.8381	1.0413
	300	G	0.6611	0.4903	0.5426	0.7809	0.3664	0.5132	1.0353	0.3459	0.4791
	300	L	0.5580	0.4336	0.4806	0.5812	0.2890	0.4347	0.6418	0.2832	0.3984
880	10	G	0.7974	0.7458	0.7799	1.1413	0.6995	1.0694	1.4032	0.9176	1.1729
	10	L	0.7557	0.7341	0.7470	1.0439	0.6646	0.9821	1.2222	0.8382	1.0525
	300	G	0.6655	0.4900	0.5463	0.7880	0.3659	0.5182	1.0471	0.3475	0.4854
	300	L	0.5617	0.4330	0.4840	0.5863	0.2882	0.4389	0.6493	0.2847	0.4013
1090	10	G	1.0000	1.0964	1.0321	1.4905	1.1166	1.4793	1.8064	1.4580	1.6250
	10	L	0.9477	1.0802	0.9890	1.3636	1.0589	1.3581	1.5556	1.3584	1.4600
	300	G	0.6909	0.5464	0.6144	0.7325	0.3979	0.5315	0.9490	0.3459	0.4699
	300	L	0.5941	0.5017	0.5481	0.5529	0.3425	0.4462	0.6244	0.2978	0.3948
1300	10	G	1.1445	1.2356	1.1800	1.8151	1.3647	1.8207	2.4193	1.8225	2.1418
	10	L	1.0853	1.2162	1.1307	1.6594	1.2936	1.6704	2.1111	1.6618	1.9233
	300	G	0.7006	0.5411	0.6222	0.7730	0.3705	0.5401	1.0667	0.3311	0.5124
	300	L	0.5934	0.5025	0.5516	0.5695	0.3341	0.4533	0.6716	0.2964	0.4253
1400	10	G	1.2280	1.3638	1.2801	2.0529	1.5819	2.0718	2.7097	2.2187	2.4781
	10	L	1.1638	1.3425	1.2262	1.8768	1.4995	1.9006	2.3194	2.0231	2.1989
	300	G	0.7628	0.5936	0.6795	0.8905	0.4427	0.6245	1.2000	0.4098	0.5977
	300	L	0.6452	0.5529	0.6026	0.6485	0.3964	0.5256	0.7512	0.3693	0.4960
1600	10	G	1.4103	1.4881	1.4359	2.8009	1.7874	2.5558	3.6290	2.3613	3.0580
	10	L	1.3365	1.4648	1.3754	2.5606	1.6943	2.3448	3.1250	2.1532	2.7230
	300	G	0.7053	0.5291	0.6188	0.8950	0.3757	0.5817	1.1529	0.3410	0.5438
	300	L	0.6016	0.4903	0.5505	0.6676	0.3268	0.4907	0.7363	0.3007	0.4540

Incident angle : 40

Depth	Qs= Qp	1st Layer	maximum displacement			maximum velocity			maximum acceleration		
			Ux	Uz	Ut	Vx	Vz	Vt	Ax	Az	At
0	10	G	1.0000	1.0000	1.0000	1.0000	1.0000	1.0000	1.0000	1.0000	1.0000
	10	L	1.0000	1.0000	1.0000	1.0000	1.0000	1.0000	1.0000	1.0000	1.0000
	300	G	1.0000	1.0000	1.0000	1.0000	1.0000	1.0000	1.0000	1.0000	1.0000
	300	L	1.0000	1.0000	1.0000	1.0000	1.0000	1.0000	1.0000	1.0000	1.0000
8	10	G	0.9967	0.9943	0.9969	0.9728	0.9826	0.9735	0.9661	1.0026	0.9682
	10	L	0.9806	0.9939	0.9819	0.9488	0.9745	0.9504	0.9098	0.9907	0.9133
	300	G	0.9674	1.0035	0.9699	0.9377	1.0019	0.9407	0.8987	1.0061	0.9013
	300	L	0.9283	0.9934	0.9325	0.8839	0.9823	0.8867	0.8386	0.9896	0.8445
16	10	G	0.9918	0.9899	0.9922	0.9438	0.9593	0.9450	0.9237	0.9948	0.9280
	10	L	0.9295	0.9757	0.9339	0.8279	0.8962	0.8328	0.7519	0.9182	0.7802
	300	G	0.9328	1.0009	0.9377	0.8714	0.9941	0.8776	0.7951	1.0012	0.8188
	300	L	0.7914	0.9381	0.8028	0.6568	0.8916	0.6658	0.5418	0.8982	0.5765
17	10	G	0.9914	0.9895	0.9918	0.9407	0.9564	0.9420	0.9153	0.9974	0.9199
	10	L	0.9229	0.9731	0.9277	0.8116	0.8852	0.8170	0.7444	0.9065	0.7726
	300	G	0.9282	1.0004	0.9334	0.8628	0.9927	0.8694	0.7811	1.0000	0.8087
	300	L	0.7741	0.9304	0.7909	0.6284	0.8789	0.6384	0.5068	0.8825	0.5438
26	10	G	0.9874	0.9841	0.9876	0.9117	0.9235	0.9158	0.8898	0.9767	0.9020
	10	L	0.9144	0.9692	0.9201	0.7791	0.8543	0.7856	0.6992	0.8925	0.7290
	300	G	0.8941	0.9918	0.9011	0.7985	0.9744	0.8080	0.6834	0.9832	0.7344
	300	L	0.7260	0.9195	0.7599	0.5495	0.8540	0.5598	0.4131	0.8642	0.4889
35	10	G	0.9821	0.9756	0.9819	0.8885	0.8790	0.8955	0.8729	0.9483	0.8838
	10	L	0.9074	0.9619	0.9131	0.7630	0.8133	0.7543	0.6692	0.8645	0.7046
	300	G	0.8594	0.9736	0.8675	0.7332	0.9398	0.7453	0.6065	0.9475	0.6608
	300	L	0.6937	0.8983	0.7283	0.4934	0.8144	0.4877	0.3849	0.8277	0.4609
37	10	G	0.9792	0.9720	0.9790	0.8834	0.8625	0.8901	0.8559	0.9354	0.8672
	10	L	0.9043	0.9585	0.9100	0.7686	0.7960	0.7586	0.6617	0.8528	0.6964
	300	G	0.8488	0.9636	0.8620	0.7141	0.9231	0.7267	0.5832	0.9292	0.6387
	300	L	0.6840	0.8882	0.7231	0.4971	0.7971	0.4914	0.3804	0.8146	0.4534
60	10	G	0.9303	0.9042	0.9268	0.8518	0.6544	0.8390	0.7797	0.6641	0.7681
	10	L	0.8428	0.8905	0.8465	0.7630	0.6403	0.7528	0.6316	0.5794	0.6363
	300	G	0.7561	0.7679	0.7562	0.5664	0.5929	0.5547	0.3667	0.5888	0.4166
	300	L	0.6627	0.6878	0.6752	0.6068	0.4836	0.6035	0.4199	0.4700	0.4308

Incident angle : 40

Depth	Qs= Qp	1st Layer	maximum displacement			maximum velocity			maximum acceleration		
			Ux	Uz	Ut	Vx	Vz	Vt	Ax	Az	At
82	10	G	0.8308	0.8175	0.8298	0.7270	0.5082	0.7159	0.6356	0.2997	0.6115
	10	L	0.7479	0.8037	0.7537	0.6242	0.4954	0.6176	0.5263	0.2430	0.5164
	300	G	0.6459	0.5115	0.6345	0.5328	0.2899	0.5213	0.3423	0.2558	0.3376
	300	L	0.5842	0.4383	0.5813	0.5047	0.2736	0.5024	0.3928	0.2705	0.3931
83	10	G	0.8254	0.8141	0.8247	0.7201	0.5073	0.7092	0.6271	0.2817	0.6031
	10	L	0.7428	0.8003	0.7489	0.6142	0.4945	0.6078	0.5263	0.2430	0.5161
	300	G	0.6399	0.5024	0.6282	0.5261	0.2893	0.5148	0.3353	0.2624	0.3304
	300	L	0.5789	0.4286	0.5757	0.4948	0.2762	0.4924	0.3860	0.2779	0.3861
130	10	G	0.6892	0.7891	0.6957	0.5306	0.4908	0.5313	0.3965	0.3566	0.3782
	10	L	0.6073	0.7799	0.6214	0.4202	0.4827	0.4243	0.3114	0.3505	0.3059
	300	G	0.4941	0.5344	0.4802	0.3347	0.3863	0.3395	0.2305	0.4452	0.2294
	300	L	0.5336	0.4925	0.5155	0.3776	0.3467	0.3733	0.3025	0.3814	0.3127
177	10	G	0.5567	0.7848	0.5855	0.5942	0.4773	0.5898	0.5716	0.4935	0.5460
	10	L	0.5186	0.7584	0.5432	0.5256	0.4763	0.5209	0.5113	0.4089	0.4995
	300	G	0.6088	0.6232	0.5834	0.6326	0.4558	0.6171	0.6915	0.5491	0.6813
	300	L	0.6701	0.5133	0.6481	0.6282	0.3334	0.6213	0.7483	0.3838	0.7483
178	10	G	0.5575	0.7834	0.5860	0.5996	0.4753	0.5950	0.5769	0.4910	0.5510
	10	L	0.5213	0.7567	0.5451	0.5300	0.4754	0.5252	0.5263	0.4065	0.5141
	300	G	0.6112	0.6215	0.5857	0.6425	0.4530	0.6268	0.7055	0.5491	0.6951
	300	L	0.6717	0.5106	0.6496	0.6363	0.3304	0.6293	0.7619	0.3786	0.7618
215	10	G	0.6317	0.7251	0.6401	0.7098	0.4269	0.7015	0.8390	0.3488	0.8050
	10	L	0.6011	0.6909	0.6090	0.6298	0.4444	0.6223	0.7594	0.2757	0.7413
	300	G	0.6621	0.4894	0.6360	0.8904	0.2862	0.8687	1.0081	0.3234	0.9932
	300	L	0.6863	0.3720	0.6646	0.8710	0.2241	0.8610	1.0090	0.1992	1.0087
252	10	G	0.6990	0.6545	0.6947	0.7946	0.4308	0.7825	1.0254	0.2351	0.9804
	10	L	0.6665	0.6404	0.6639	0.7060	0.4390	0.6963	0.9098	0.2453	0.8871
	300	G	0.7533	0.3182	0.7267	0.9961	0.1435	0.9720	1.0314	0.0894	1.0156
	300	L	0.7301	0.3339	0.7124	0.9190	0.2812	0.9086	0.9526	0.2426	0.9529
253	10	G	0.7011	0.6532	0.6964	0.7951	0.4337	0.7829	1.0254	0.2377	0.9805
	10	L	0.6685	0.6406	0.6655	0.7063	0.4399	0.6965	0.9023	0.2523	0.8797
	300	G	0.7540	0.3207	0.7274	0.9946	0.1468	0.9705	1.0233	0.0903	1.0076
	300	L	0.7307	0.3332	0.7130	0.9162	0.2827	0.9058	0.9503	0.2452	0.9507

Incident angle : 40

Depth	Qs= Qp	1st Layer	maximum displacement			maximum velocity			maximum acceleration		
			Ux	Uz	Ut	Vx	Vz	Vt	Ax	Az	At
268	10	G	0.7231	0.6441	0.7139	0.8143	0.4734	0.8028	1.0339	0.3204	0.9881
	10	L	0.6886	0.6412	0.6817	0.7393	0.4563	0.7302	0.9098	0.3294	0.8891
	300	G	0.7450	0.3677	0.7187	0.9297	0.1974	0.9074	0.9208	0.1678	0.9072
	300	L	0.7236	0.3664	0.7064	0.8504	0.2881	0.8413	0.8668	0.2624	0.8680
282	10	G	0.7341	0.6487	0.7238	0.8241	0.5150	0.8112	1.0424	0.4134	0.9981
	10	L	0.7045	0.6469	0.6967	0.7535	0.4918	0.7429	0.9248	0.4019	0.9039
	300	G	0.6986	0.4068	0.6771	0.7999	0.2437	0.7808	0.7567	0.2550	0.7459
	300	L	0.7066	0.3880	0.6929	0.7509	0.2764	0.7454	0.7754	0.2534	0.7804
283	10	G	0.7353	0.6498	0.7247	0.8254	0.5179	0.8123	1.0339	0.4160	0.9899
	10	L	0.7060	0.6481	0.6979	0.7530	0.4954	0.7423	0.9398	0.4089	0.9183
	300	G	0.6968	0.4100	0.6754	0.7861	0.2503	0.7673	0.7404	0.2617	0.7315
	300	L	0.7058	0.3888	0.6921	0.7515	0.2746	0.7459	0.7698	0.2558	0.7748
305	10	G	0.7349	0.6663	0.7242	0.8274	0.5837	0.8150	0.9831	0.5349	0.9447
	10	L	0.7115	0.6629	0.7030	0.7691	0.5528	0.7585	0.9173	0.4907	0.8991
	300	G	0.6378	0.4361	0.6220	0.8299	0.3142	0.8109	0.7590	0.3049	0.7473
	300	L	0.6769	0.3934	0.6656	0.7555	0.2655	0.7494	0.7291	0.2407	0.7341
327	10	G	0.7235	0.6880	0.7106	0.8123	0.6573	0.8010	0.9322	0.6305	0.8997
	10	L	0.7002	0.6827	0.6907	0.7495	0.6230	0.7401	0.8797	0.5631	0.8649
	300	G	0.6311	0.4582	0.6155	0.9118	0.2849	0.8919	0.9348	0.2279	0.9205
	300	L	0.6525	0.4456	0.6412	0.7788	0.2986	0.7704	0.7675	0.2611	0.7675
328	10	G	0.7210	0.6893	0.7104	0.8100	0.6621	0.7985	0.9322	0.6357	0.8995
	10	L	0.6983	0.6841	0.6902	0.7458	0.6257	0.7363	0.8647	0.5724	0.8502
	300	G	0.6311	0.4634	0.6153	0.9108	0.2825	0.8911	0.9383	0.2285	0.9240
	300	L	0.6518	0.4507	0.6403	0.7769	0.3049	0.7685	0.7630	0.2676	0.7630
396	10	G	0.6346	0.7619	0.6349	0.6094	0.8955	0.6168	0.7373	0.9070	0.7156
	10	L	0.6065	0.7518	0.6089	0.5484	0.8434	0.5553	0.6391	0.8131	0.6326
	300	G	0.5060	0.6423	0.4970	0.5073	0.5100	0.4988	0.5332	0.5339	0.5275
	300	L	0.4569	0.5830	0.4546	0.4117	0.4877	0.4104	0.3905	0.4830	0.3923
464	10	G	0.5355	0.8204	0.5624	0.4135	1.0726	0.4707	0.5170	1.1292	0.5600
	10	L	0.5105	0.8099	0.5377	0.3763	1.0173	0.4287	0.4511	1.0280	0.5069
	300	G	0.3432	0.6483	0.3740	0.3076	0.5208	0.3371	0.2980	0.5278	0.3448
	300	L	0.3338	0.5926	0.3673	0.2967	0.4761	0.3246	0.3657	0.4883	0.3698

Incident angle : 40

Depth	Qs= Qp	1st Layer	maximum displacement			maximum velocity			maximum acceleration		
			Ux	Uz	Ut	Vx	Vz	Vt	Ax	Az	At
464	10	G	0.5355	0.8204	0.5624	0.4135	1.0726	0.4707	0.5170	1.1292	0.5600
	10	L	0.5105	0.8099	0.5377	0.3763	1.0173	0.4287	0.4511	1.0280	0.5069
	300	G	0.3432	0.6483	0.3740	0.3076	0.5208	0.3371	0.2980	0.5278	0.3448
	300	L	0.3338	0.5926	0.3673	0.2967	0.4761	0.3246	0.3657	0.4883	0.3698
466	10	G	0.5302	0.8238	0.5582	0.4029	1.0755	0.4645	0.4831	1.1395	0.5647
	10	L	0.5058	0.8134	0.5337	0.3656	1.0200	0.4228	0.4361	1.0397	0.5112
	300	G	0.3364	0.6527	0.3729	0.2965	0.5293	0.3358	0.2969	0.5369	0.3414
	300	L	0.3270	0.5969	0.3656	0.2844	0.4829	0.3215	0.3488	0.4935	0.3539
673	10	G	0.5962	0.8188	0.6245	0.5108	1.2159	0.5771	0.6186	1.3540	0.7263
	10	L	0.5678	0.8048	0.5961	0.4649	1.1430	0.5243	0.5489	1.2220	0.6565
	300	G	0.3867	0.6384	0.4185	0.3317	0.5429	0.3779	0.3399	0.5857	0.4005
	300	L	0.3744	0.5609	0.4076	0.3203	0.4782	0.3608	0.3296	0.4830	0.3900
879	10	G	0.9021	0.7840	0.8906	1.0401	1.2052	1.0631	1.3559	1.2507	1.3511
	10	L	0.8575	0.7702	0.8490	0.9419	1.1311	0.9637	1.1955	1.1285	1.2148
	300	G	0.6185	0.6518	0.6120	0.6251	0.5031	0.6279	0.6333	0.5156	0.6408
	300	L	0.5993	0.5528	0.5985	0.5992	0.3954	0.6073	0.6242	0.3916	0.6396
880	10	G	0.9058	0.7852	0.8941	1.0503	1.2014	1.0733	1.3644	1.2558	1.3593
	10	L	0.8610	0.7714	0.8523	0.9535	1.1275	0.9751	1.2030	1.1332	1.2222
	300	G	0.6219	0.6522	0.6153	0.6304	0.5047	0.6330	0.6426	0.5156	0.6500
	300	L	0.6024	0.5528	0.6015	0.6044	0.3953	0.6125	0.6287	0.3916	0.6438
1090	10	G	1.2471	1.1444	1.2372	1.6256	1.8170	1.6620	2.1949	2.0517	2.1895
	10	L	1.1836	1.1263	1.1779	1.4698	1.7104	1.5050	1.9323	1.8551	1.9663
	300	G	0.7361	0.6960	0.7354	0.7729	0.5660	0.7754	0.7253	0.5796	0.7410
	300	L	0.7040	0.6259	0.7117	0.7125	0.4951	0.7261	0.6840	0.5065	0.7168
1300	10	G	1.4156	1.2884	1.4032	1.8207	2.2178	1.8694	2.6695	2.6098	2.6736
	10	L	1.3439	1.2687	1.3365	1.6512	2.0865	1.6973	2.3759	2.3832	2.4274
	300	G	0.7375	0.6622	0.7337	0.6970	0.5182	0.7044	0.7660	0.5369	0.7807
	300	L	0.7123	0.5899	0.7160	0.6520	0.4449	0.6681	0.7506	0.4569	0.7758
1400	10	G	1.4906	1.3961	1.4816	2.0005	2.5053	2.0586	2.9576	2.9974	2.9725
	10	L	1.4152	1.3737	1.4110	1.8116	2.3570	1.8667	2.6241	2.6636	2.6839
	300	G	0.7057	0.6860	0.7068	0.6558	0.5626	0.6681	0.6938	0.5918	0.7184
	300	L	0.6844	0.6085	0.6919	0.6246	0.4846	0.6433	0.6862	0.4935	0.7183
1600	10	G	1.7141	1.6210	1.7030	2.6143	3.0561	2.6652	3.7712	3.5659	3.7657
	10	L	1.6274	1.5963	1.6221	2.3674	2.8743	2.4169	3.3459	3.2477	3.4080
	300	G	0.7139	0.6786	0.7131	0.6774	0.5156	0.6876	0.7311	0.5522	0.7472
	300	L	0.6843	0.6097	0.6914	0.6294	0.4547	0.6484	0.6975	0.4830	0.7259

Appendix F

Content :

10 spectral amplitude graphs for displacement.

(The amplitudes are in dB)

Ux | Incident angle : 0

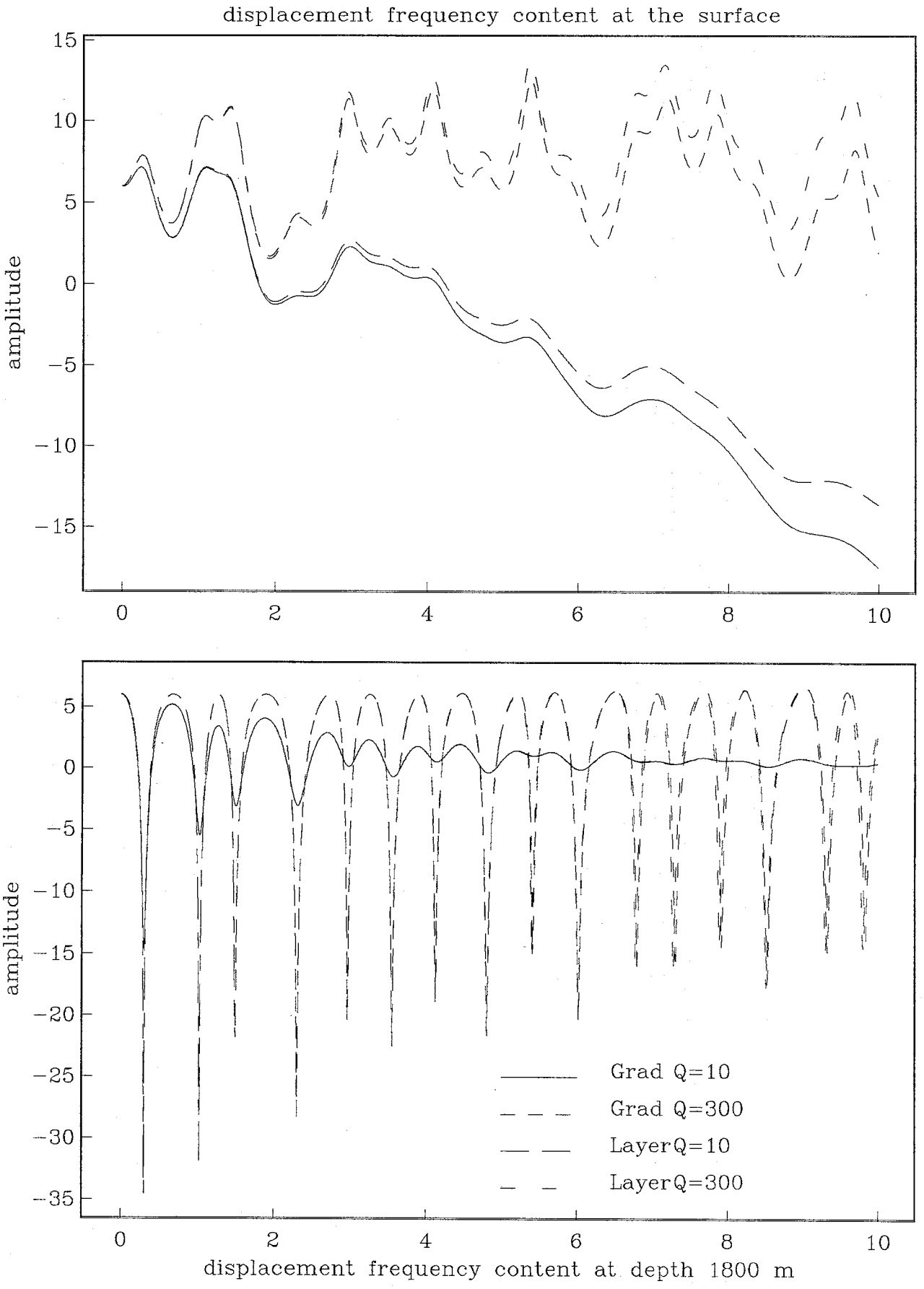

Ux | Incident angle : 10

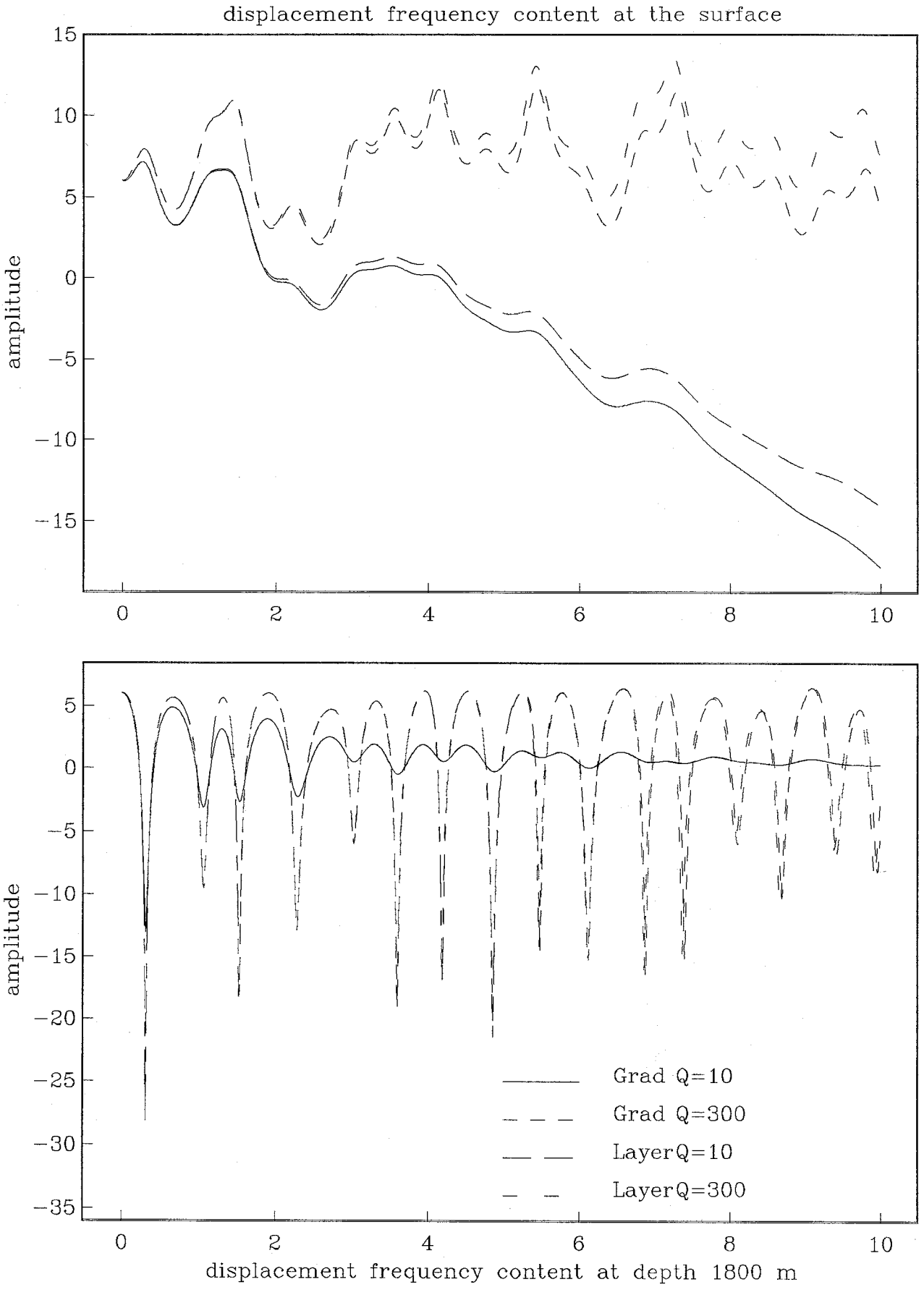

Ux | Incident angle : 20

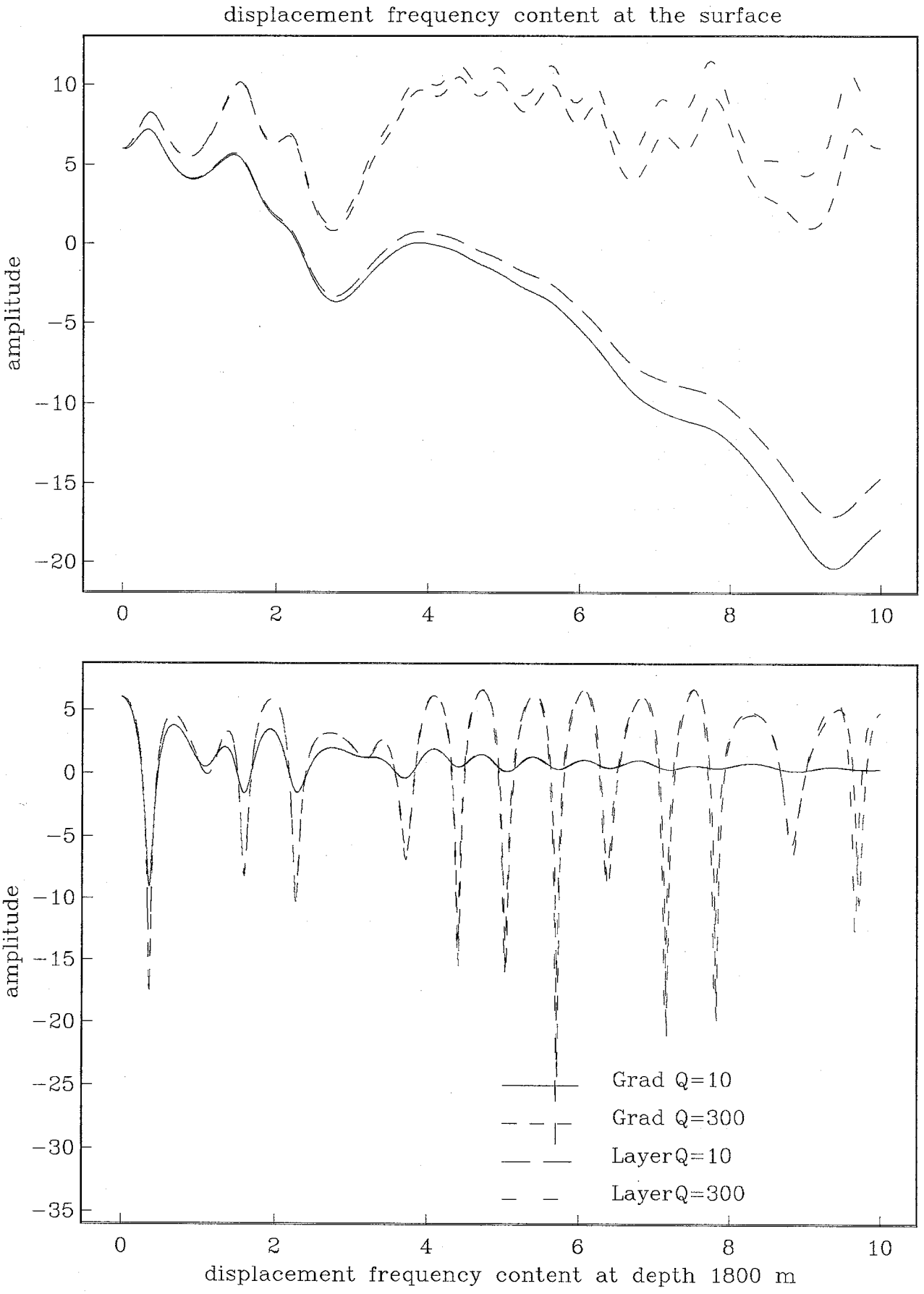

Ux | Incident angle : 40

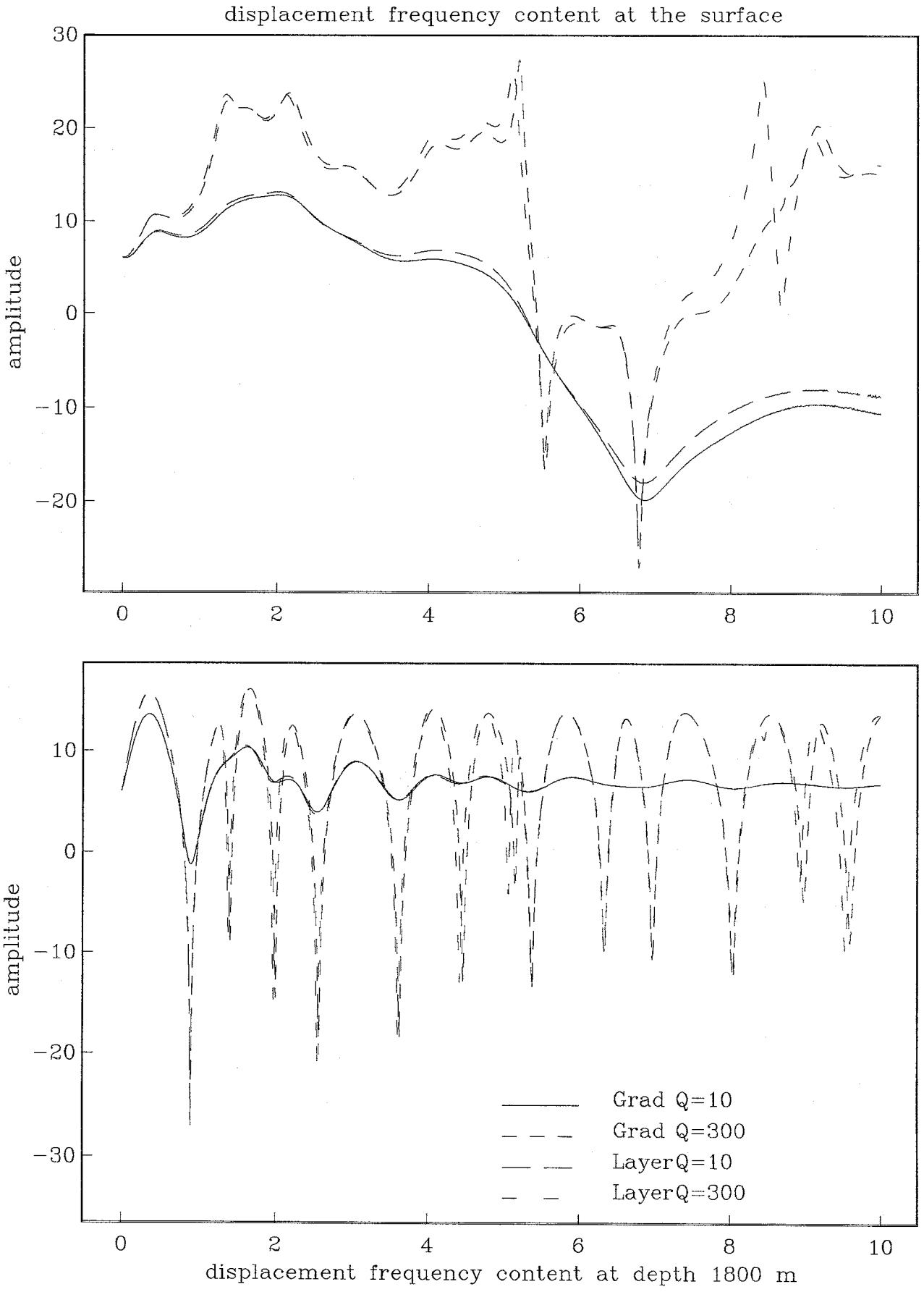

Uz | Incident angle : 10

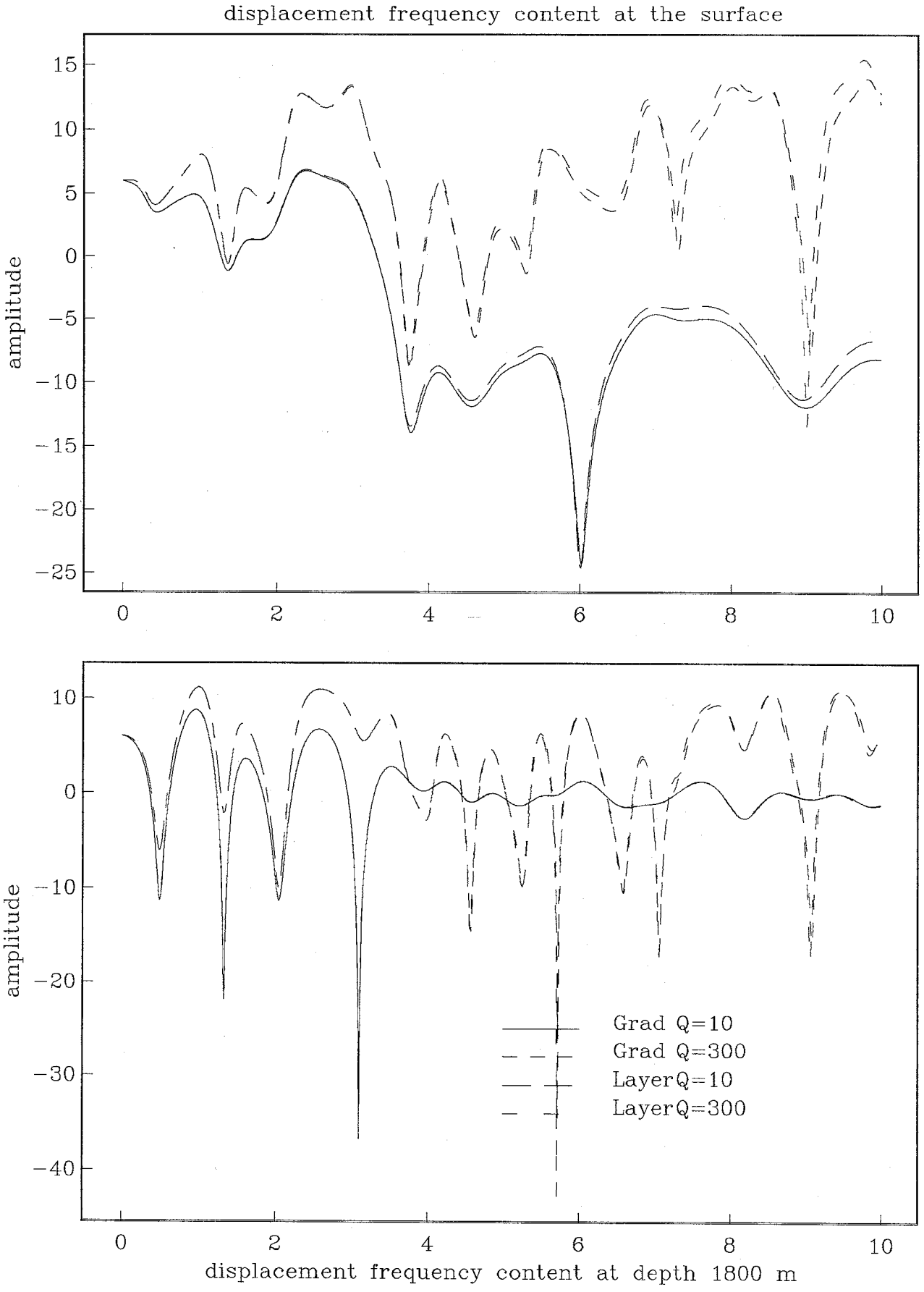

Uz | Incident angle : 20

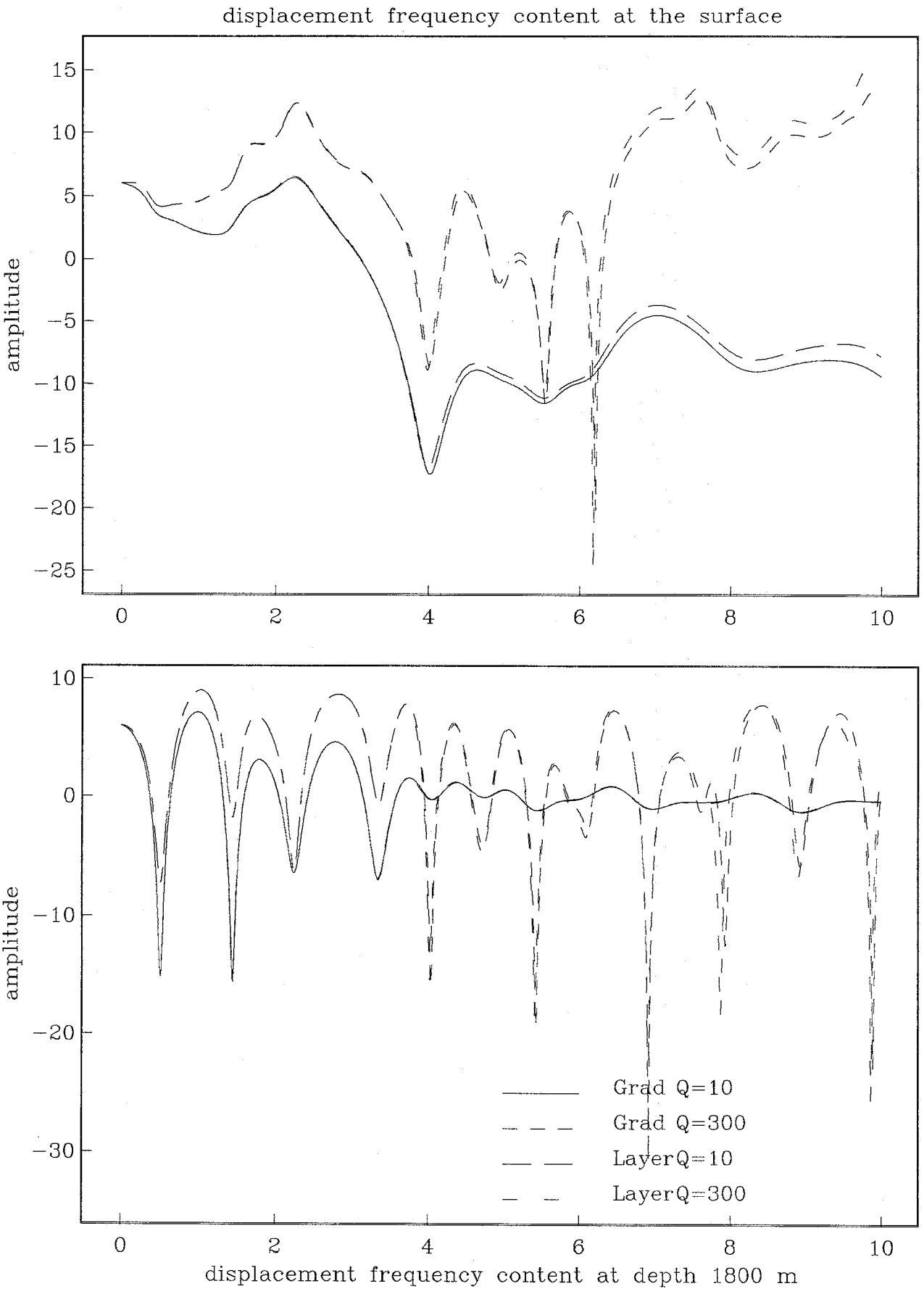

Uz | Incident angle : 30

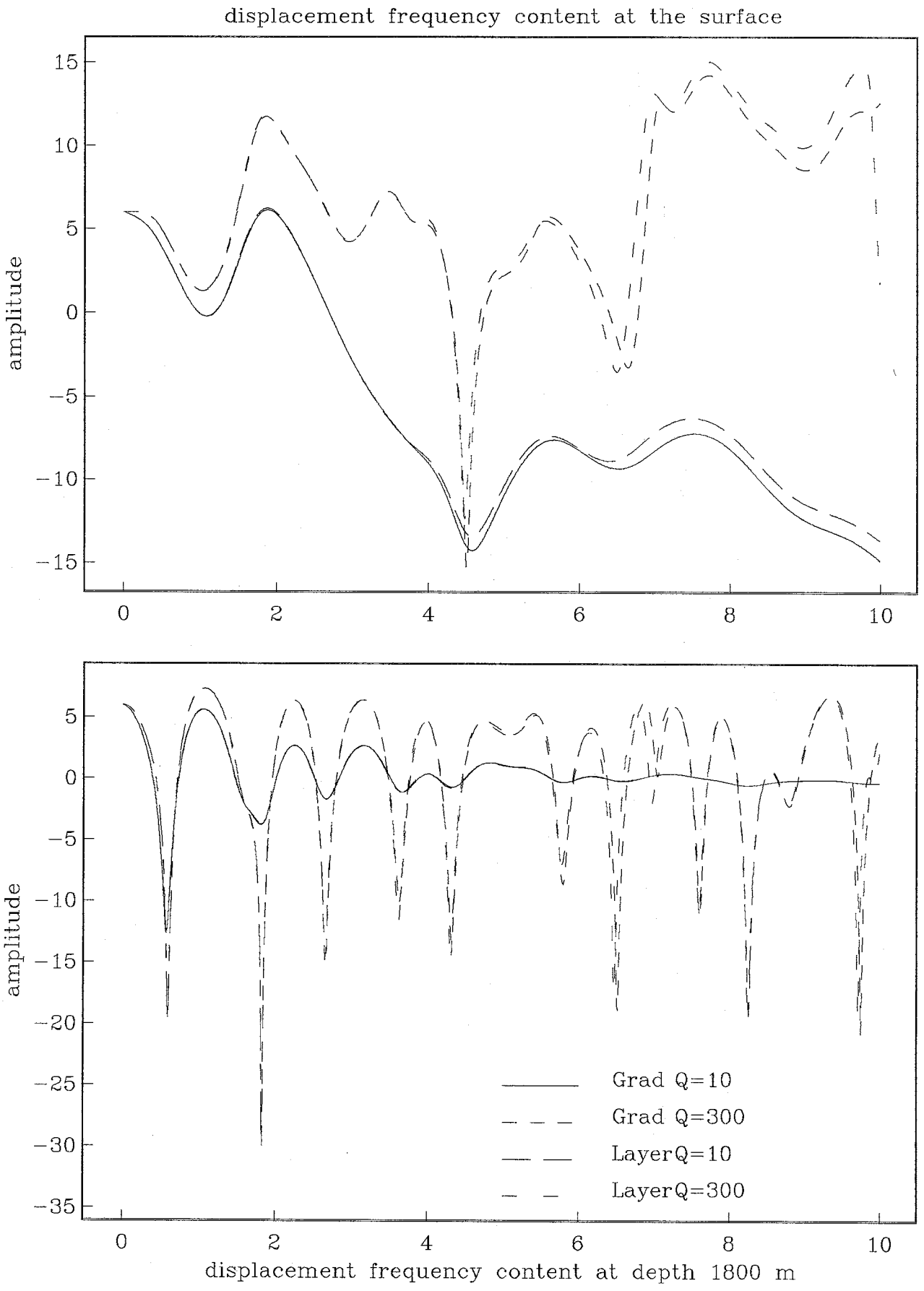

Uz | Incident angle : 40

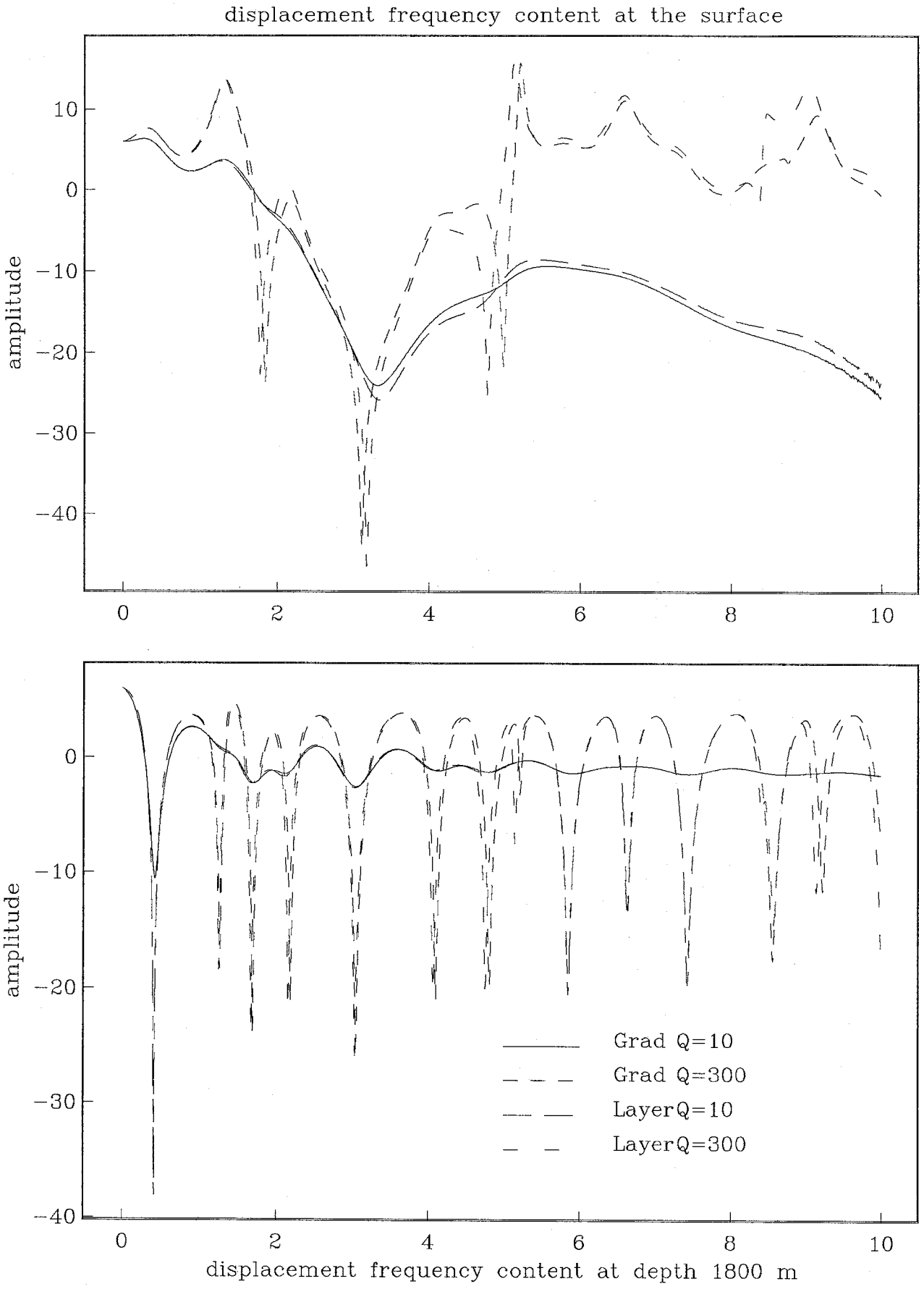

Appendix G

Content :

5 maximum strain profiles with frequency content 0 to 10 Hz

Maximum strain
incident angle : 0

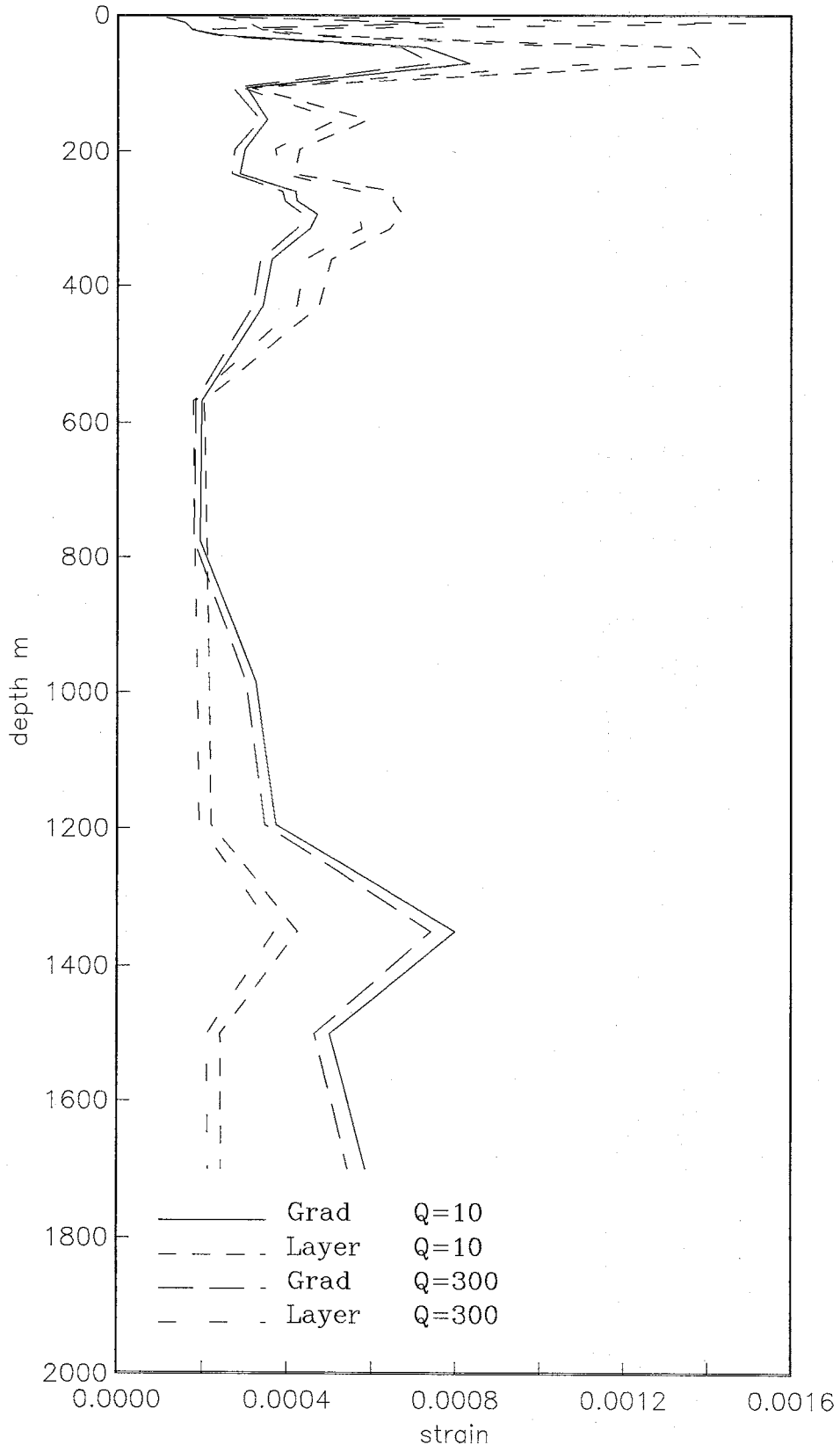

Maximum strain
incident angle : 10

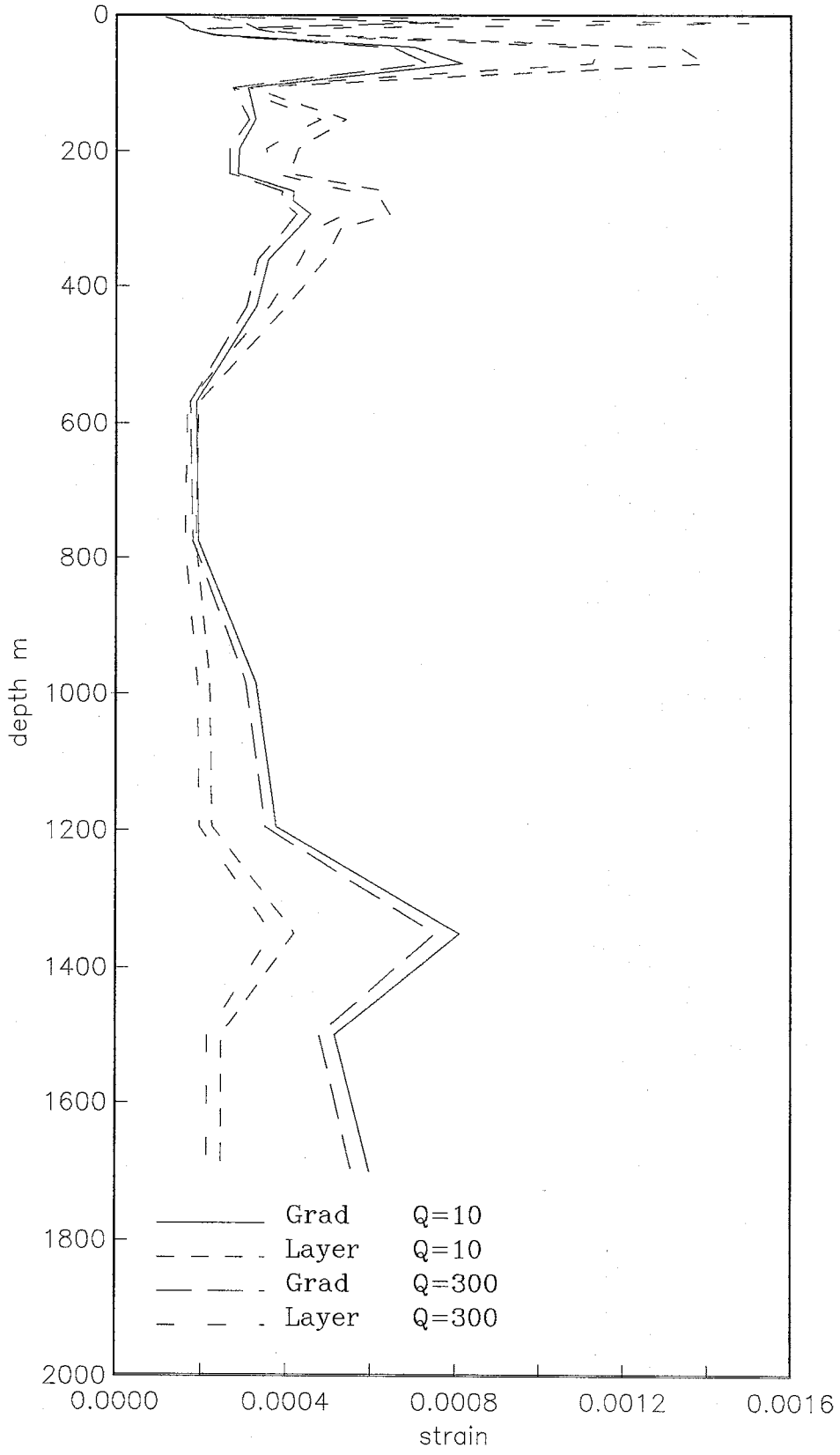

Maximum strain
incident angle : 20

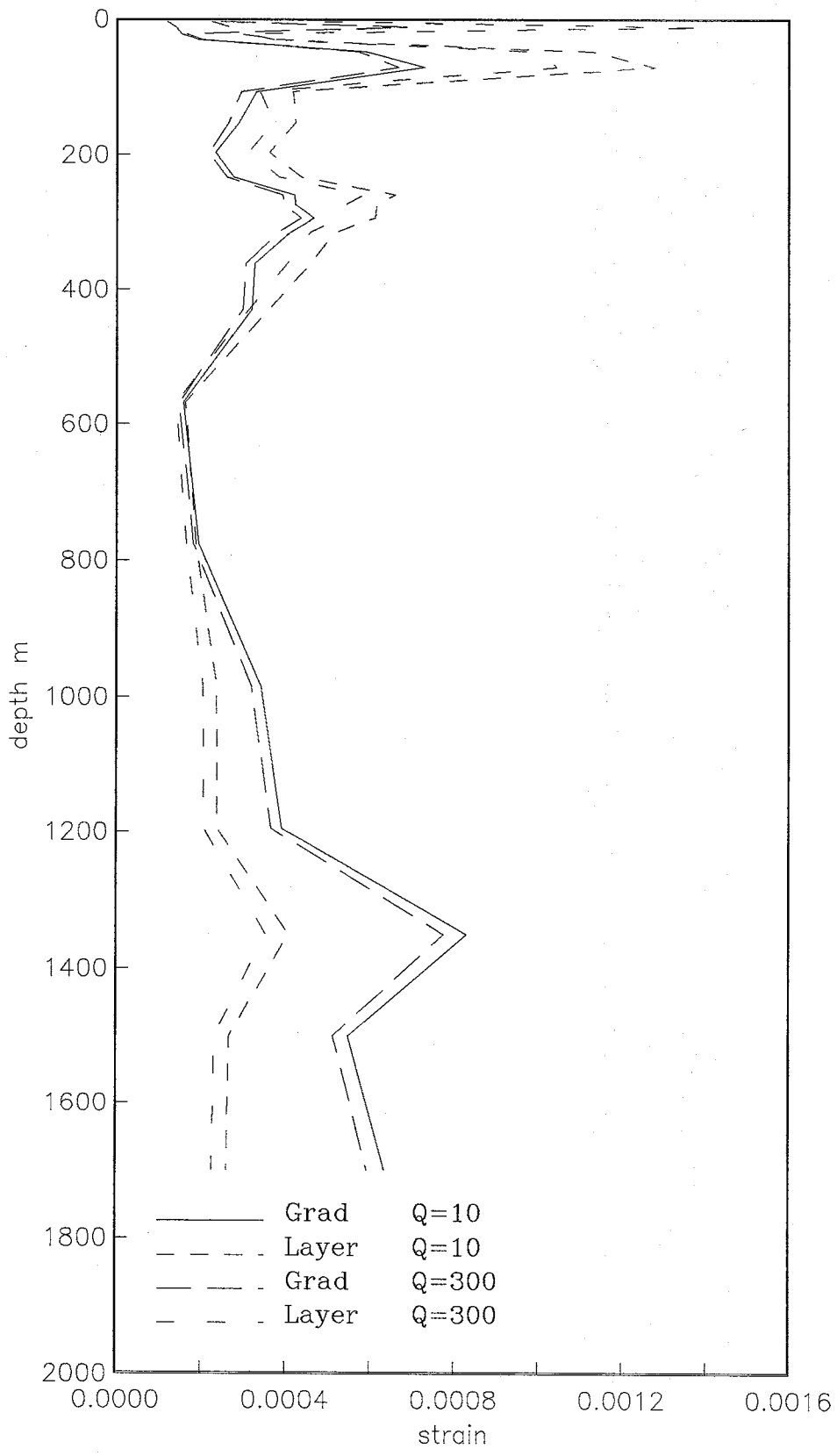

Maximum strain
incident angle : 30

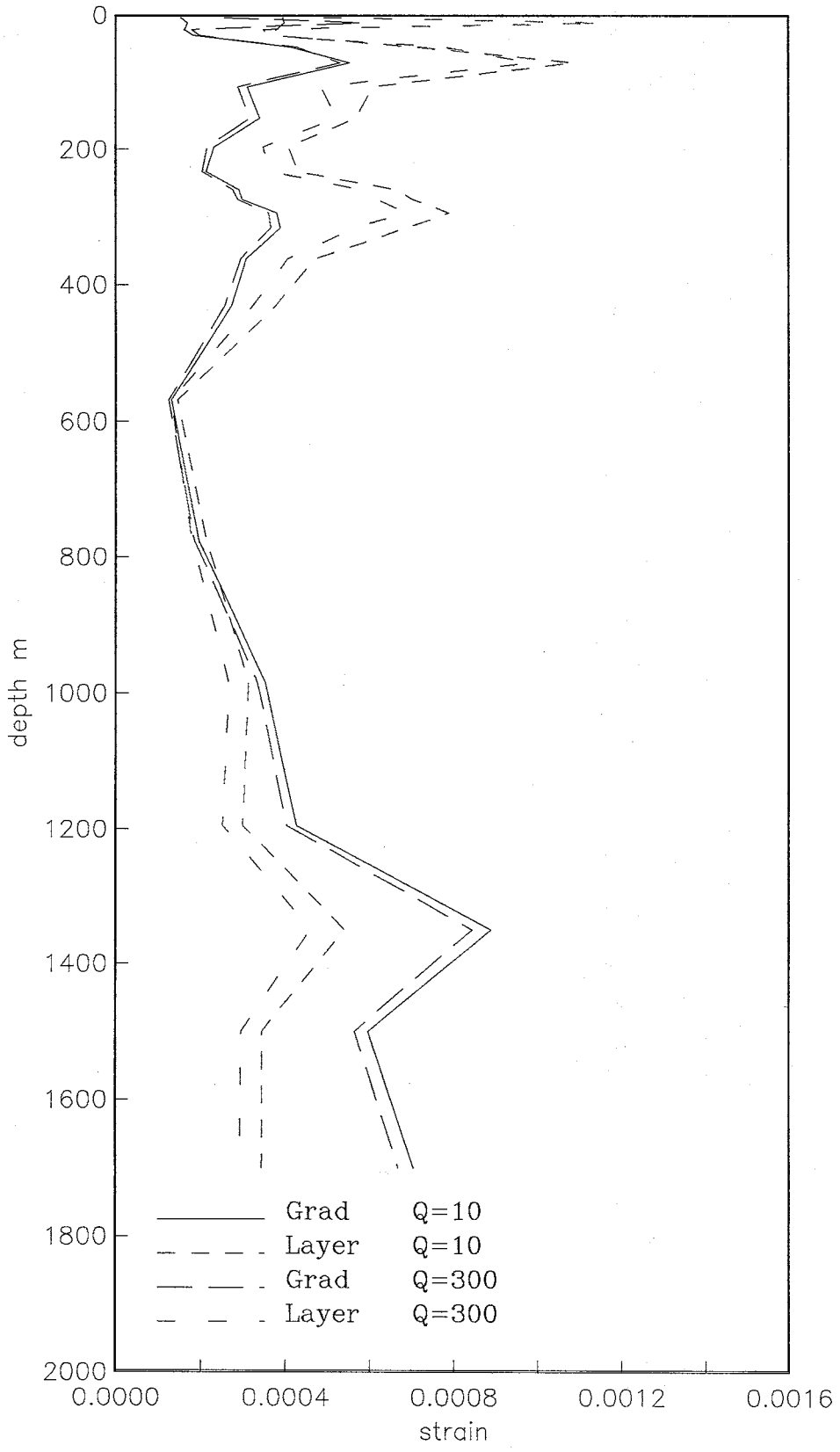

Maximum strain
incident angle : 40